

AD-756 861

STOL TRANSPORT THRUST REVERSER/
VECTERING PROGRAM. VOLUME II

John E. Petit, et al

Boeing Company

Prepared for:

Air Force Aero Propulsion Laboratory

February 1973

DISTRIBUTED BY:

NTIS

National Technical Information Service
U. S. DEPARTMENT OF COMMERCE
5285 Port Royal Road, Springfield Va. 22151

AD756861



STOL TRANSPORT THRUST REVERSER/VECTERING PROGRAM

Volume II

John E. Petit
Michael B. Scholey

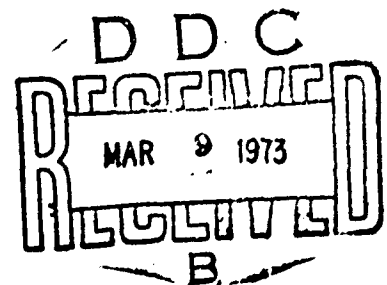
THE **BOEING** COMPANY

Technical Report AFAPL-TR-72-109, Volume II
February 1973

Reproduced by
NATIONAL TECHNICAL
INFORMATION SERVICE
U.S. Department of Commerce
NIST-72-109-1

Approved for public release; distribution unlimited

Air Force Aero Propulsion Laboratory
Air Force Systems Command
Wright-Patterson Air Force Base, Ohio



1870

NOTICE

When Government drawings, specifications, or other data are used for any purpose other than in connection with a definitely related Government procurement operation, the United States Government thereby incurs no responsibility nor any obligation whatsoever; and the fact that the government may have formulated, furnished, or in any way supplied the said drawings, specifications, or other data, is not to be regarded by implication or otherwise as in any manner licensing the holder or any other person or corporation, or conveying any rights or permission to manufacture, use, or sell any patented invention that may in any way be related thereto.

ACCESSION FOR	
NTIS	Write Section <input checked="" type="checkbox"/>
DDI	But Section <input type="checkbox"/>
UNANNOUNCED	<input type="checkbox"/>
JUSTIFICATION	
BY	
DISSEMINATION/AVAILABILITY CODES	
0101	1. 2. 3. 4. 5. 6. 7. 8. 9. 10.
A	

Copies of this report should not be returned unless return is required by security considerations, contractual obligations, or notice on a specific document.

Unclassified

Security Classification

DOCUMENT CONTROL DATA - R & D

(Security classification of title, body of abstract and indexing annotation must be entered when the overall report is classified)

1. ORIGINATING ACTIVITY (Corporate author)		2a. REPORT SECURITY CLASSIFICATION	
The Boeing Company, Box 3999, Seattle, Washington 98124		Unclassified	
3. REPORT TITLE		7b. GROUP	
STOL Transport Thrust Reverser/Vectoring Program, Volume II			
4. DESCRIPTIVE NOTES (Type of report and inclusive dates)			
July 1971 - November 1972 Final Report Volume II			
5. AUTHOR(S) (First name, include initial, last name)			
John E. Petit and Michael B. Scholey			
6. REPORT DATE	7a. TOTAL NO. OF PAGES	7b. NO. OF REFS	
December 1972	182 / 87	24	
8a. CONTRACT OR GRANT NO.	9a. ORIGINATOR'S REPORT NUMBER(S)		
F33615-71-C-1850	None		
b. PROJECT NO.	9b. OTHER REPORT NO(S) (Any other numbers that may be assigned this report)		
643A	AFAPL-TR-72-109, Volume II		
10. DISTRIBUTION STATEMENT			
11. SUPPLEMENTARY NOTES		12. SPONSORING MILITARY ACTIVITY	
Details of illustrations in this document may be better studied on microfiche.		Air Force Aero Propulsion Laboratory/TBD Wright-Patterson AFB, Ohio 45433	
13. ABSTRACT			
<p>Design studies were conducted of thrust reverser and thrust vectoring systems for STOL tactical transports to evolve systems properly integrated with the aircraft. The studies included configuration design, performance, and weight analyses of feasible thrust reverser and thrust vectoring concepts. Test plans were developed for static tests of the most promising concepts. Following Air Force approval of the test plans, test model hardware were fabricated.</p> <p>Model tests were conducted of 1) a fan thrust reverser that exhausts all of the fan flow through cascades installed in the upper 180° sector of the nacelle, and 2) an external deflector/target TR/TV system that combines the functions of thrust vectoring and reversing into a single mechanism. Scaling relationships were used to correct the data to full-scale performance, and data correlations were developed for the external/target model as a function of geometric parameters and nozzle pressure ratio.</p>			

DD FORM 1473
1 NOV 65

I-a

Security Classification

14 KEY WORDS	LINK A		LINK B		LINK C	
	ROLE	WT	ROLE	WT	ROLE	WT
Thrust Reverser						
Thrust Vectoring						
Nozzles						
Turbine Engines						
Transport Aircraft						

I-8

Unclassified

Security Classification

STOL TRANSPORT THRUST REVERSER/VECTORIZING PROGRAM

VOLUME II

John E. Petie

Michael B. Scholey

This document has been approved for public
release, its distribution is unlimited.

I-C

FOREWORD

This report was prepared by John E. Petit and Michael B. Scholey of the Research and Engineering Division, Aerospace Group, The Boeing Company, Seattle, Washington. It is the second of a two-volume final report submitted under Air Force Contract F33615-71-C-1850, "STOL Transport Thrust Reverser/Vectoring Program." Volume II covers work conducted during Design and Model Testing, from July 1971 to October 1972. Volume I covers work conducted during Part IA - Data Review and Analysis from July 1971 to April 1972. The contract was initiated under Project 643A, "Tactical Airlift Technology," Task 63205F, "Flight Vehicle Subsystem Concepts" and was administered by the Air Force Aero Propulsion Laboratory with Captain J. W. Schuman, and Mr. R. J. Krabal as Project Engineers. Subcontract support was provided by Pratt & Whitney Aircraft with H. Kozlowski as Program Manager. The final report was submitted to the Air Force in November 1972.

The authors wish to acknowledge the following Boeing personnel for their assistance during the design and model testing phases of the contract: T. W. Wainwright, Airbreathing Propulsion; L. J. Kimes and R. L. Wilson, Propulsion Project; and K. Ikeda and W. J. Stamm, Propulsion/Noise Laboratories. A special acknowledgement is due M. E. Brazier, Chief, Propulsion Technology, for his continuing interest and significant contributions made during the program.

This technical report has been reviewed and approved.



E. C. Simpson
Director, Turbine Engine Division
Air Force Aero-Propulsion
Laboratory

TABLE OF CONTENTS

	Page
I. INTRODUCTION AND SUMMARY	1
II. PART IB - DESIGN	5
2.1 Task 2.1 - Conduct Design Studies of TR/TV Concepts	5
2.1.1 Baseline Airplane Configuration	5
2.1.2 Engine Selection and Scaling	9
2.1.3 Baseline Nacelle Design	13
2.1.4 Thrust Reverser and Thrust Vectoring System Design Concepts	31
2.1.5 Fan Cascade Thrust Reverser Detailed Design	84
2.2 Task 2.2 - Analyze Performance of TR/TV Systems	94
2.2.1 Externally Blown Flap Systems	96
2.2.2 Mechanical Flap and Vectored Thrust Systems	96
2.2.3 Upper Surface Blowing Systems	102
2.2.4 Conclusions	105
2.3 Task 2.3 - Select Designs for Part IC	105
2.4 Task 2.4 - Test Plan Preparation	107
2.5 Task 2.5 - Fabricate Hardware for Part IC	107
III. PART IC - MODEL TESTING	108
3.1 Task 3.1 - Conduct Static Performance Test	108
3.1.1 Fan Cascade Thrust Reverser Model Tests	108
3.1.2 External Deflector/Target TR/TV Tests	125
3.1.3 Overwing Target Thrust Reverser Data Review	146

TABLE OF CONTENTS (Continued)

3.2	Task 3.2 - Correct Data to Full Scale Performance	151
3.3	Task 3.3 - Correlate with Existing Model Data	166
IV.	CONCLUSIONS AND RECOMMENDATIONS	175
4.1	Part IB - Design	175
4.2	Part IC - Model Testing	178
	REFERENCES	180

LIST OF ILLUSTRATIONS

<u>Figure Number</u>	<u>Title</u>	<u>Page</u>
1	Baseline Airplane Configuration 953-258	7
2	Thrust vs. Mach Number STF 342D, 342B, and 344 Engines 2500 ft, Standard Day Conditions	10
3	Thrust vs. Mach Number STF 342D, 342B, and 344 Engines Sea Level Static Conditions	11
4	STF 342 Scaling Characteristics	14
5	STF 344 Scaling Characteristics	15
6	Basic Nacelle Installation - BPR 3.0 Engine, Unmixed Flow, 2-2541-PD-194	19
7	Basic Nacelle Installation - BPR 6.0 Engine, Unmixed Flow, 2-2541-PD-198	21
8	Basic Nacelle Installation - BPR 12.0 Engine, Unmixed Flow, 2-2541-PD-193	23
9	Basic Nacelle Installation - BPR 3.0 Engine, Mixed Flow, 2-2541-PD-200	25
10	Basic Nacelle Installation - BPR 6.0 Engine, Mixed Flow, 2-2541-PD-199	27
11	Basic Nacelle Installation - BPR 3.0 Engine, Mixed Flow (Double Pod)	29
12	Intake Geometry	32
13	Basic Nacelle Weight vs. Mass Flow	34
14	Thrust Reverser Flow Control Requirements	36
15	Effect of Primary Reverse Thrust Mode on Reverser Effectiveness (η_R) _{basic} = 50%	38

LIST OF ILLUSTRATIONS (Continued)

<u>Figure Number</u>	<u>Title</u>	<u>Page</u>
16	Mixed Flow Thrust Reversal Options	39
17	STF 402 Reverser Mode	41
18	Effect of Engine Overspeed STF 402 Reverser Mode	42
19	STF 402 Part-Power Characteristics	43
20	Reverser Effectiveness STF 402 "Cycle Spoiling"	45
21	Fan/Primary Thrust Ratio Parametric Unmixed Flow Engine Results	46
22	Estimated Reverser Effectiveness for "Cycle Spoiling"	47
23	Landing Roll Distance, $M = .10$	49
24	Landing Roll Distance, $M = .30$	51
25	Landing Roll Distance, $M = .40$	53
26	Effect of Vertical Force Component On Landing Roll Distance	56
27	Effect of Airplane Gross Weight on Landing Roll Distance	57
28	Thrust Reverser Concept BPR 6.0 Engine, Unmixed Flow, TR/TV-PP-02	58
29	Thrust Reverser and EBF Concept BPR 6.0 Engine, Mixed Flow, TR/TV-PP-03	59
30	Clamshell Thrust Reverser and EBF Concept, BPR 6.0 Mixed Flow Engine, TR/TV-PP-14	61
31	Translating Sleeve Thrust Reverser and EBF Concept BPR 6.0 Mixed Flow Engine, TR/TV-PP-16	62

LIST OF ILLUSTRATIONS (Continued)

<u>Figure Number</u>	<u>Title</u>	<u>Page</u>
32	Thrust Reverser/Thrust Vectoring Concept - BPR 3.0 Engine, Mixed Flow TR/TV-PP-05	63
33	Thrust Reversing/Thrust Vectoring System Rotating Valve Selector, 2-2541-PD-211	65
34	External Deflector TR/TV Concept - BPR 6.0, Mixed Flow Engine, TR/TV-PP-19	67
35	Common Hinge External Deflector TR/TV System	69
36	Thrust Reverser/Multibearing Thrust Vectoring Concept, BPR 6.0 Mixed Flow Engine, TR/TV-PP-06	71
37	Multibearing Thrust Reverser/Thrust Vectoring Concept, BPR 6.0 Mixed Flow Engine, TR/TV-PP-13	72
38	Thrust Reverser/Lobster Tail Thrust Vectoring Concept, BPR 6.0 Mixed Flow Engine, TR/TV-PP-07	73
39	Thrust Reverser/Two Dimensional Thrust Vectoring Concept, BPR 6.0 Mixed Flow Engine, TR/TV-PP-08	75
40	Thrust Reversing/Thrust Vectoring Rotating Nozzle Concept, BPR 6.0 Engine, Unmixed Flow TR/TV-PP-10	76
41	Thrust Reverser/Multibearing Thrust Vectoring Concept, BPR 12.0 Engine, Unmixed Flow, TR/TV-PP-09	77
42	Thrust Reverser/Lobster Tail Thrust Vectoring Concept, BPR 12.0 Engine Unmixed Flow, TR/TV-PP-12	78

LIST OF ILLUSTRATIONS (Continued)

<u>Figure Number</u>	<u>Title</u>	<u>Page</u>
43	Effect of Vectoring Fan Flow, BPR 12.0	80
44	Dual Pod, External Deflector TR/TV Concept, BPR 3.0 Mixed Flow Engine TR/TV-PP-15	81
45	Overwing TR Concept, BPR 6.0 Engine, Unmixed Flow, TR/TV-PP-04	82
46	Overwing TR Concept, BPR 6.0 Engine, Mixed Flow, TR/TV-PP-18	83
47	Overwing Thrust Reverser Installation, LO-953-035	85
48	Fan Reverser, Upper 180° Sector, BPR 6.0 Engine, Mixed Flow	89
49	Area Plot Fan Duct and/or Cascades vs. Blocker Door Opening	91
50	Bifold Blocker Door Concept	92
51	Alternate Bifold Blocker Door Concept	93
52	TR/TV Nacelle Weight vs. Mass Flow	95
53	Stability and Control Engine Location Envelope	103
54	Fan Cascade Reverser Installation Schematic	110
55	Fan Cascade Reverser Model Installation	111
56	Annular Duct and Cascade Geometry	112
57	Internal Duct Static Pressure Tap Locations	114
58	Fan Cascade Reverser Model - Exit Total Pressure Rake Installation	115

LIST OF ILLUSTRATIONS (Continued)

<u>Figure Number</u>	<u>Title</u>	<u>Page</u>
59	Fan Cascade Thrust Reverser Exit Total Pressure Rake Installations	116
60	Fan Cascade Thrust Reverser, Reverser Efficiency, Corrected Reverser Efficiency	117
61	Fan Cascade Thrust Reverser Velocity Coefficient	118
62	Fan Cascade Thrust Reverser Discharge Coefficient, Airflow Match	119
63	Duct Static Pressure Distribution $P_{TAVG}/P = 1.575$	120
64	Cascade Exit Total Pressure Survey, Blocker Door Angle = 90°	122
65	External Deflector TR/TV Model Installation Schematic	127
66	External Deflector Geometry, Vector Mode	129
67	External Deflector Geometry, Section A-A	130
68	External Deflector Geometry, Reverse Mode	131
69	External Deflector TR/TV Model $S/D = 1.0$ $\theta = 7^\circ$	132
70	External Deflector TR/TV Model $S/D = 1.03$ $\theta = 36^\circ$	133
71	External Deflector Thrust Reverser Model	134
72	Vector Efficiency, η_v , Airflow Match ϕ , $D_n/D = 1.225$, $S/D = 1.033$, $Y/D = .50$	136
73	Effect of Setback Ratio on Vector Efficiency and Airflow Match, $D_n/D = 1.0$	137

LIST OF ILLUSTRATIONS (Continued)

<u>Figure Number</u>	<u>Title</u>	<u>Page</u>
74	Effect of Setback Ratio on Airflow Match $D_n/D = 1.225$, $Y/D = .50$	138
75	Effect of Setback Ratio on Vector Efficiency $D_n/D = 1.225$, $Y/D = .50$	139
76	Effect of Deflector Position on Airflow Match, $P_T/P_\infty = 1.60$	140
77	Effect of Deflector Position on Vector Efficiency, $P_T/P_\infty = 1.60$	141
78	Effect of Deflector Position on Effective Vector Angle	142
79	Effect of Entrance Mach Number on Corrected Vector Efficiency	143
80	Reverser Efficiency η_R , Airflow Match \diamond , $D_n/D = 1.225$, $S/D = 1.03$	144
81	Thrust Reverser Performance Characteristics	145
82	Overwing Target Thrust Reverser Model Schematic	147
83	Target Thrust Reverser Model, Front View	148
84	Target Thrust Reverser Model, Aft View	149
85	Reverser Efficiency Correlation	150
86	Primary Nozzle Airflow Match Data	152
87	Primary Nozzle Airflow Match Correlation	153
88	Fan Airflow Match Correlation	154
89	Scaling Effects of Reynolds Number on Velocity Coefficient	156
90	Comparison of Theoretical and Experimental Effects of Reynolds Number on Velocity Coefficient	157

LIST OF ILLUSTRATIONS (Continued)

<u>Figure Number</u>	<u>Title</u>	<u>Page</u>
91	ASME Discharge Coefficient vs Thrust Reynolds Number	158
92	Comparison of Model and Full Scale Corrected Reverser Efficiency Data for a Cascade Thrust Reverser	159
93	Comparison of Model and Full Scale Corrected Reverser Efficiency Data for the C-5A Fan Cascade Reverser	160
94	Comparison of Model and Full Scale Corrected Reverser Efficiency Data for a Hemispherical Target Reverser	161
95	Comparison of Model and Full Scale Corrected Reverser Efficiency Data for a Target Thrust Reverser	162
96	Comparison of Model and Full Scale Corrected Reverser Efficiency Data for the 737 Target Thrust Reverser	163
97	Comparison of Model and Full Scale Airflow Match Data for the 737 Target Thrust Reverser	164
98	Comparison of Model and Full Scale Perform- ance for Spherical Eyeball Nozzle	165
99	Discharge Coefficient Correlation for Hinged External Deflector $P_T/P_\infty = 1.2$	168
100	Discharge Coefficient Correlation of Hinged External Deflector Nozzle $P_T/P_\infty = 1.6$	169
101	Discharge Coefficient Correlation of Hinged External Deflector Nozzle $P_T/P_\infty = 2.2$	170
102	Corrected Vector Efficiency Correlation for Hinged External Deflector Nozzles, $P_T/P_\infty = 1.2$	171

LIST OF ILLUSTRATIONS (Continued)

<u>Figure Number</u>	<u>Title</u>	<u>Page</u>
103	Corrected Vector Efficiency Correlation for Hinged External Deflector Nozzle, $P_T/P_\infty = 1.6$	172
104	Corrected Vector Efficiency Correlation for Hinged External Deflector Nozzles, $P_T/P_\infty = 2.2$	173
105	Comparison of Discharge Coefficient Ratio Data Corrections	174

LIST OF TABLES

<u>Table Number</u>	<u>Title</u>	<u>Page</u>
I	Mixed Flow STF 342 Simulation Performance Data	12
II	Installation Dimensions STF 342D Engine (BPR 3.0)	16
III	Installation Dimensions STF 342B Engine (BPR 6.0)	17
IV	Installation Dimensions STF 344 Engine (BPR 12.0)	18
V	Baseline Nacelle Configurations	13
VI	Baseline Engine and Nacelle Design Characteristics	33
VII	Thrust Reverser Concept Evaluation for Externally Blown Flap Lift Systems	37
VIII	Thrust Vectoring and Reversing Concept Evaluation for Mechanical Flap and Vectored Thrust Lift Systems	99
IX	Thrust Reverser Concept Evaluation for Upper Surface Blowing Lift Systems	104
X	Evaluation Summary	106
XI	External Deflector Test Configurations	128

List of Nomenclature

ALT.	-	altitude
A_8	-	nozzle throat area
A_{JD}	-	effective fan duct flow area
A_{JD}^*	-	effective fan duct flow area during mixed flow operation
A_{JE}	-	effective primary exhaust flow area
A_{JE}^*	-	effective primary exhaust flow area during mixed flow operation
BPR	-	engine bypass ratio
\bar{c}	-	mean chord length
C_V	-	nozzle velocity coefficient
C_D	-	nozzle discharge coefficient
D_{RAM}	-	intake ram drag
		$D_{RAM} = \frac{WAT}{g} (V_\infty^2)$
F_x	-	Axial thrust component
F_y	-	lateral thrust component
F_z	-	vertical thrust component
F_G	-	gross thrust
FNT	-	total net thrust
		$FNT = F_{GROSS} - D_{RAM}$
FN_{DUCT}	-	fan duct net thrust
GW	-	gross weight
KTAS	-	true air speed, knots
LRD	-	landing roll distance
M	-	Mach number

List of Nomenclature (Continued)

N_1	-	low rotor speed
T_{TS}	-	turbine inlet temperature
V_∞	-	freestream velocity
WAT	-	total engine mass flow rate

Greek Symbols

η_R	-	reverser efficiency
η_{Reff}	-	reverser effectiveness
μ	-	braking coefficient
σ_{eff}	-	effective vector angle. $\sigma_{eff} = \tan^{-1} \left[\frac{F_z}{F_x} \right]$
ϕ	-	airflow match

SECTION I

INTRODUCTION AND SUMMARY

An essential requirement of military STOL tactical transports planned for the 1980 time period will be to operate from airfields of 2500 feet or less. These aircraft will use thrust reversers as primary braking devices throughout the landing ground roll. Also, some STOL concepts will use thrust vectoring systems to help control the flight-path of the airplane and reduce takeoff and landing speeds. Consequently, emphasis must be placed on designing efficient and reliable thrust reverser/vectoring systems to achieve the field length objective.

Commercial jet aircraft have used thrust reversers as secondary braking devices since the beginning of their operation. However, the complex problems caused by the interactions between reverser exhaust and aircraft flowfields have limited their usefulness. These problems include exhaust gas recirculation which can lead to engine surge, impingement of exhaust gases on the ground or adjacent aircraft surfaces, and engine mass flow matching. Also, the reverser flow can cause blanking out of aerodynamic control surfaces leading to a loss in aircraft directional stability and control, buoyancy effects that decrease the efficiency of the ground braking systems, and changes in airplane drag. All of these problems have been experienced during the development of existing commercial aircraft. However, the availability of long runways has made it unnecessary to completely resolve the interactions between the reverser and aircraft flowfields.

To avoid the limitations of existing systems on future STOL aircraft, attention must be given to the following technical areas:

- o TR/TV performance
- o Exhaust gas flowfield
- o Aerodynamic interference
- o Engine operation
- o TR/TV system design including weights and structures

The above considerations have significant influence on nacelle placement, thrust reverser and vectoring system geometry, and operating envelope.

The Boeing Company, with subcontract support from Pratt & Whitney Aircraft, conducted an 18-month research program to study the above technical areas. The program was administered by the Air Force Aero Propulsion Laboratory, Wright-Patterson Air Force Base, Ohio. Program objectives are:

1. To develop methods to predict thrust reverser and thrust vectoring system performance.
2. To establish design criteria for high efficiency, lightweight thrust reversers or thrust vectoring systems for STOL aircraft.

The program has three parts:

Part IA - Data Review and Analysis
Part IB - Design
Part IC - Model Testing

This volume of the report describes the results of Part IB and IC. Detailed results of Part IA are contained in Volume I.

Analytical models for predicting TR and TV nozzle performance and evaluating TR and TV influence on the total airplane system were developed during Part IA. Three computer programs were developed to predict jet trajectory and spreading, reingestion, and TR and TV system performance. The models were developed using analysis and data correlations, based on the results of an extensive literature survey. Supplemental static tests were conducted to fill data voids discovered in the literature.

Part IB consists of the following tasks:

- Task 2.1 -- Conduct Design Studies of TR/TV Systems
- Task 2.2 -- Analyze Performance of TR/TV Systems
- Task 2.3 -- Select Designs for Part IC
- Task 2.4 -- Test Plan Preparation
- Task 2.5 -- Fabricate Hardware for Part IC

The objective was to conduct design studies of thrust reversers and thrust vectoring systems for STOL tactical transport aircraft to evolve concepts that are properly integrated with the airplane. During Task 2.1, TR/TV concepts were designed in sufficient depth to define the TR/TV system and nacelle geometry, formulate actuation requirements, define materials, and allow performance

and weight estimates to be made. Three view layouts were completed for each system studied. The design study evolved into studies of TR and TV systems for externally blown flap (EBF), mechanical flap and vectored thrust (MF + VT), and upper surface blowing (USB) lift systems for STOL transports.

The TR and TV concepts were analyzed and evaluated during Task 2.2 on the basis of TR and TV performance and weight with the objective of obtaining the best TR/TV performance for the lightest weight system. The impact of the TR/TV system on the aircraft aerodynamic characteristics was also included in the evaluation.

The following conclusions were made based on the evaluation results for the TR/TV systems considered:

1. The thrust reverser system for externally blown flap lift systems will probably involve the use of a fan cascade thrust reverser.
2. Mechanical flap and vectored thrust lift systems could use either
 - a. rotating nozzles
 - b. multibearing vectoring nozzles
 - c. external deflector/target thrust vectoring/reversing systems

depending on the type of engine cycle (mixed or unmixed flow).

The rotating nozzle vectoring system would be applied to unmixed flow engines and would utilize the rotating nozzles for thrust vectoring and thrust reversing. However, the required nacelle position (forward of the wing leading edge) to avoid reingestion and exhaust flow/airframe interference during reverse operation results in an adverse pitching moment during vectoring operation. The external deflector/target TR/TV system would also pose pitching moment problems but to a lesser degree. Multibearing vectoring nozzle installations would present no pitching moment problems, because the installation allows the thrust vector to be placed nearer the airplane center of gravity. Combining the multibearing nozzle with a reverser system is difficult, primarily because of the weight of the separate thrust reverser and thrust vectoring systems.

The use of a fan reverser and "cycle spoiling" of primary thrust would minimize the weight of the reverser system but would result in lower reverser performance.

3. Upper surface blowing lift systems will utilize an external target thrust reverser system installed with a mixed flow engine.

On the basis of the concept performance evaluations, the following TR/TV systems representing the various STOL lift systems were considered for Part IC tests:

1. Fan cascade thrust reverser system (EBF, MF+VT)
2. External deflector/target TR/TV system (MF+VT)
3. Multibearing vectoring nozzle (MF+VT)
4. External target thrust reverser (USB)

Existing data was considered sufficient to define the performance characteristics of the multibearing nozzle and external target thrust reverser systems. Therefore, test plans were prepared during Task 2.4 for static testing of the external deflector/target and fan cascade thrust reverser systems. Following Air Force approval of the test plans, the test models were designed and fabricated during Task 2.5.

Part IC has three primary tasks:

- Task 3.1 -- Conduct Static Performance Tests
- Task 3.2 -- Correct to Full Scale Performance
- Task 3.3 -- Correlate with Existing Data and Analytical Models

The fan cascade reverser model and the external deflector TR/TV model were tested during Task 3.1. Also, the existing data for multibearing nozzles and overwing external target thrust reversers were compiled and reviewed. Task 3.2 consisted of correcting the scale model performance data obtained during Task 3.1 to full scale performance. The scaling method was also added to the TR and TV System Performance Program, TEM-357 as an option. Data correlations were developed during Task 3.3 for the external deflector/target TR/TV model performance. The correlations were compared with correlations of other external deflector thrust vectoring concepts developed during Part IA.

SECTION II

PART IB - DESIGN

The objective of Part IB - Design, was to conduct design studies of thrust reversers and thrust vectoring systems for STOL tactical transport aircraft to evolve concepts that are properly integrated with the airplane. The studies included:

- o Configuration design of feasible TR and TV concepts.
- o Performance analysis.
- o Selection of TR and TV designs that meet the design objectives.
- o Planning of static tests to establish the reverser and vectoring characteristics of the concepts.
- o Fabrication of model hardware for Part IC tests.

The following paragraphs discuss the results of Part IB.

2.1 Task 2.1---Conduct Design Studies of TR/TV Systems

2.1.1 Baseline Airplane Configuration

The thrust reverser and thrust vectoring nozzle design studies were conducted using a baseline STOL transport airplane configuration to provide a basis on which to judge variations in TR/TV system performance and weight. The baseline configuration, designated Model 953-258 and shown in Figure 1, was selected from a series of Boeing in-house STOL transport studies, Reference 1. The 953-258 configuration meets the mission requirements of a medium STOL transport.

The fuselage shape is dictated primarily by the cargo box, which is 138 inches wide by 135/148 inches high by 540 inches long. The nose shape is a minimum drag fairing consistent with crew station requirements. Similarly, the aft body shape is a minimum drag fairing consistent with aft body loading, air drop, and takeoff rotation requirements. The landing gear and fairing are configured to provide a minimum stowed frontal area consistent with flotation and runway roughness requirements.

MODEL 953-258

AERODYNAMIC DATA

		WING	HORIZ TAIL	VERT TAIL
AREA	FT ²	1450.0	349.0	300.0
SPAN	FT	107.70	37.33	17.33
ASPECT RATIO		8.0	4.0	1.0
SWEEP C/4		10°	10°	35°
DIHEDRAL		0°	-4°	—
INCIDENCE		2°	+4°-15°	—
TAPER RATIO		.3	.5	.8
THICKNESS RATIO	BODY SIDE	.152	.13	.13
	.55 b/2	.132	.13	.13
	TIP	.132	.13	.13
MAC	FT	14.76	9.72	17.39
VOLUME COEFFICIENT		—	1.08	.11

POWER PLANT

4 BY-PASS 30 TURBOFANS WITH THRUST REVERSERS 14,300 LB THRUST

LANDING GEAR LEVER SUSPENSION

MAIN 4 50x200-20 TIRES
NOSE 2 29x11.0-10 TIRES

CARGO COMPARTMENT

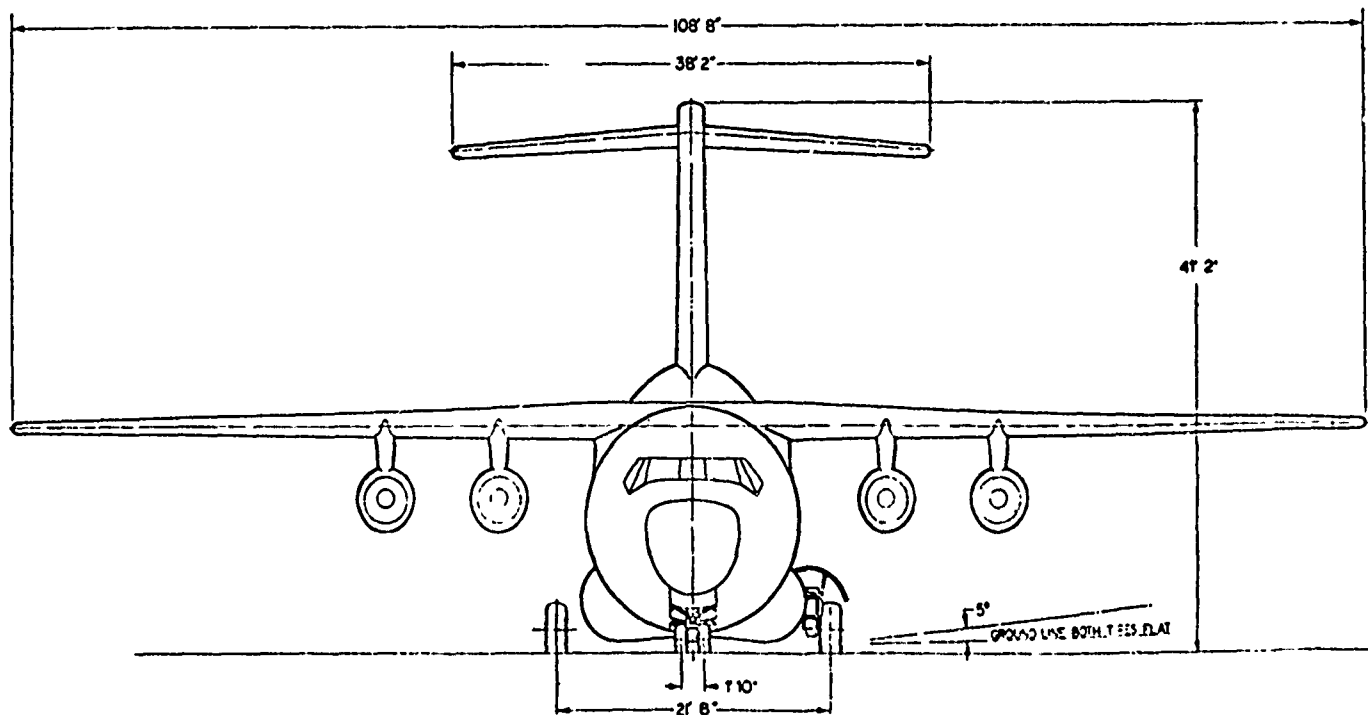
138"W 135/148"H 540"L

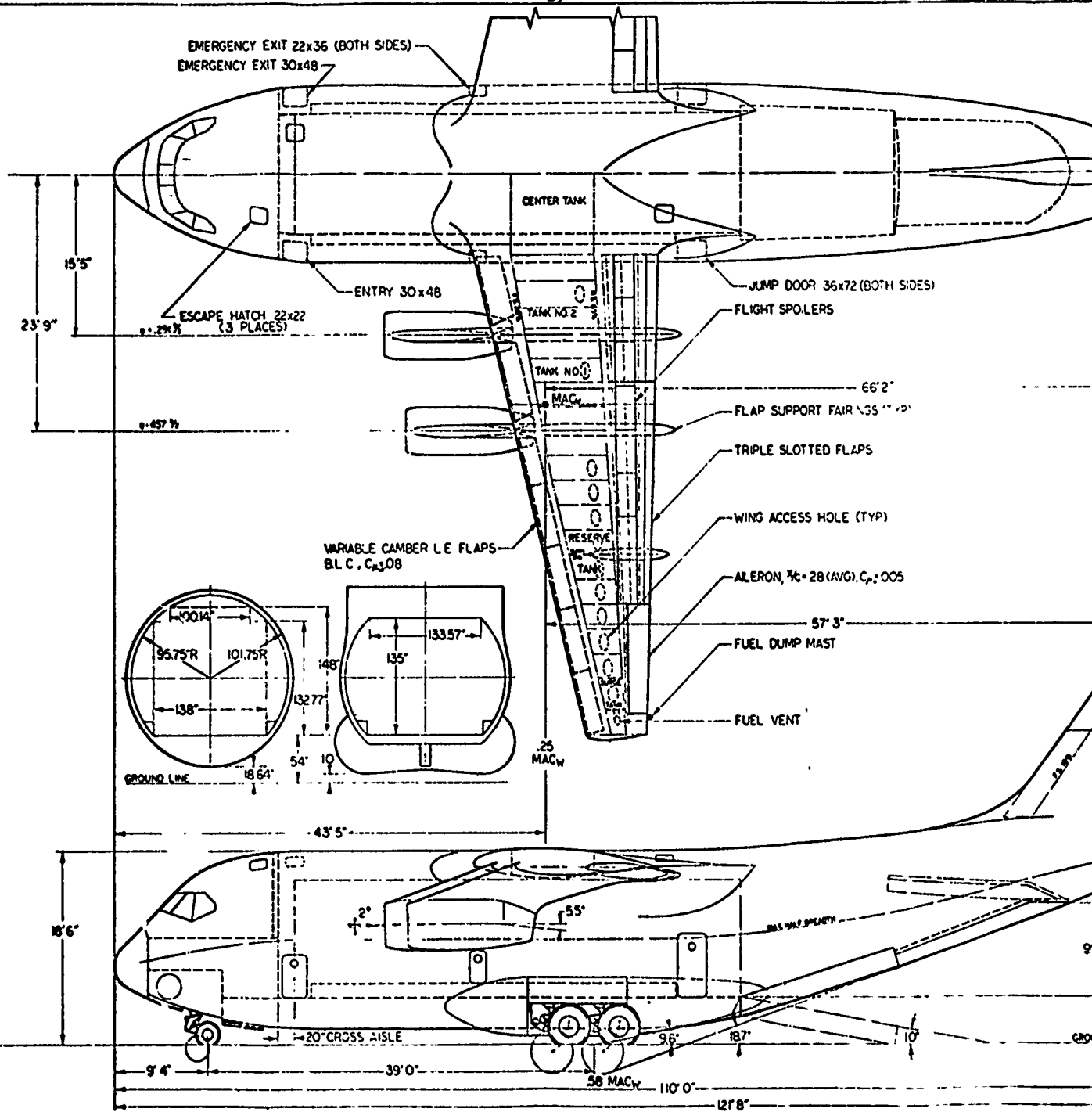
WEIGHTS

DESIGN GROSS	135,000 LB	} ASSAULT MISSION
DESIGN STOL	122,000 LB	
STOL PAYLOAD	28,000 LB	
O.E.W	77,500 LB	} CTOL MISSION
DESIGN GROSS	160,000 LB	
MAX. PAYLOAD	56,000 LB	

FUEL VOLUME

RESERVE TANKS	12,800 LB
TANK NO 1	10,300 LB
TANK NO 2	13,200 LB
TOTAL	36,300 LB
CENTER SECTION	14,900 LB
TOTAL	51,200 LB





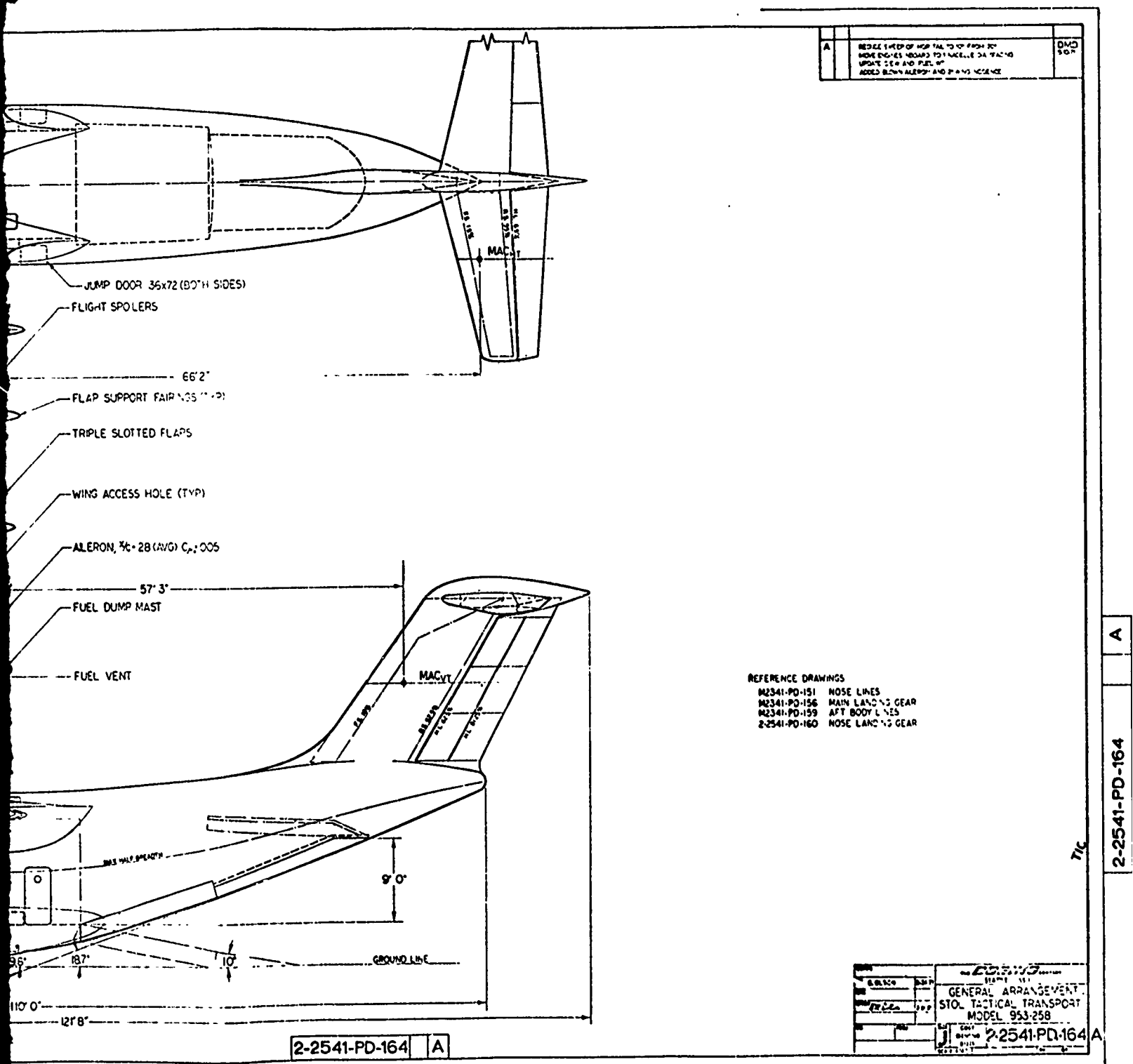


Figure 1: GENERAL ARRANGEMENT, STOL TACTICAL TRANSPORT, MODEL 953-258

The high wing configuration provides adequate cargo loading truck bed height and minimizes adverse ground effect. The wing has an aspect ratio of 8 and a quarter chord sweep angle of 10 degrees with a taper ratio of 0.3. Four nacelles are single-pod-mounted located to minimize wing-nacelle drag interference and flutter penalties. The wing area was determined by field length requirements, lift system capability, and deployment-mission fuel volume requirements.

The vertical tail is sized to provide adequate stability and control. It is equipped with a serially hinged rudder for maximum effectiveness. The horizontal tail is also sized to provide adequate stability and control. It is located on top of the vertical tail to minimize the required tail size and weight. This location also provides an end plate effect that helps to reduce the vertical tail size and weight.

2.1.2 Engine Selection and Scaling

The design study used engine performance and design data provided by Pratt & Whitney Aircraft STOL transport study engines. A review of the available study engines showed that the STF 342 series (Reference 2) and the STF 344 (Reference 3), covered the range of bypass ratios from 3.0 to 12.0 and provides a consistent level of technology. The component technologies of these engines is characteristic of the generation of high bypass ratio turbofans which will be entering service in the 1975-1980 time period. Although the study was originally intended to include bypass ratio 2.0 turbofans, these engines will adequately cover the bypass ratio range currently being considered for medium STOL transport aircraft. Also, it is expected that the results of the design studies may be extrapolated to bypass ratio 2.0 if required. The study engines are listed below:

<u>Bypass Ratio</u>	<u>Engine Designation</u>
3.0	STF 342D
6.0	STF 342B
12.0	STF 344

The study engines are dual rotor, unaugmented axial flow turbofans designed to operate with separate exhaust nozzles. Since this study includes mixed flow systems as well as unmixed flow systems, mixed flow engine data was required. This data was obtained by simulating mixed flow in the STF 342D and STF 342B engines on a Boeing parametric engine performance computer program. (Reference 4).

Engine performance data for the STF 342 and 344 engines are shown in Figures 2 and 3. The results of the mixed flow STF 342 simulation are shown in Table I.

▴ P&WA TDM-2190 REF 3
 ▴ P&WA TDM-2177 REF 2
 MODIFIED TO HAVE SIMILAR
 LAPSE RATE AS TDM-2190

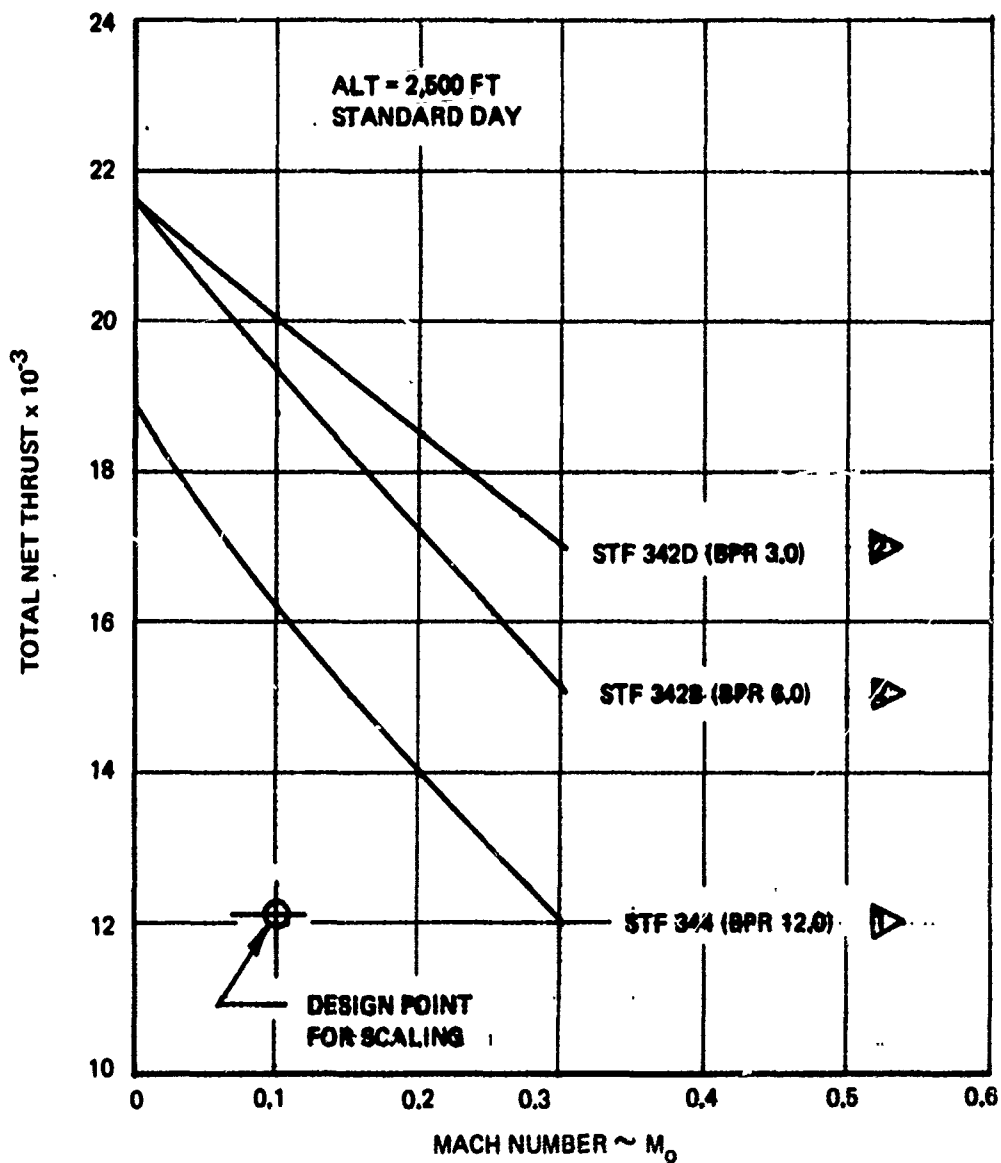


Figure 2: TOTAL NET THRUST VS MACH STF 344, 342B, 342D – 2500 FT.

▷ P&WA TDM-2190 REF 3
 ▷ P&WA TDM-2177 REF 2
 MODIFIED TO HAVE SIMILAR
 LAPSE RATE AS TDM-2190

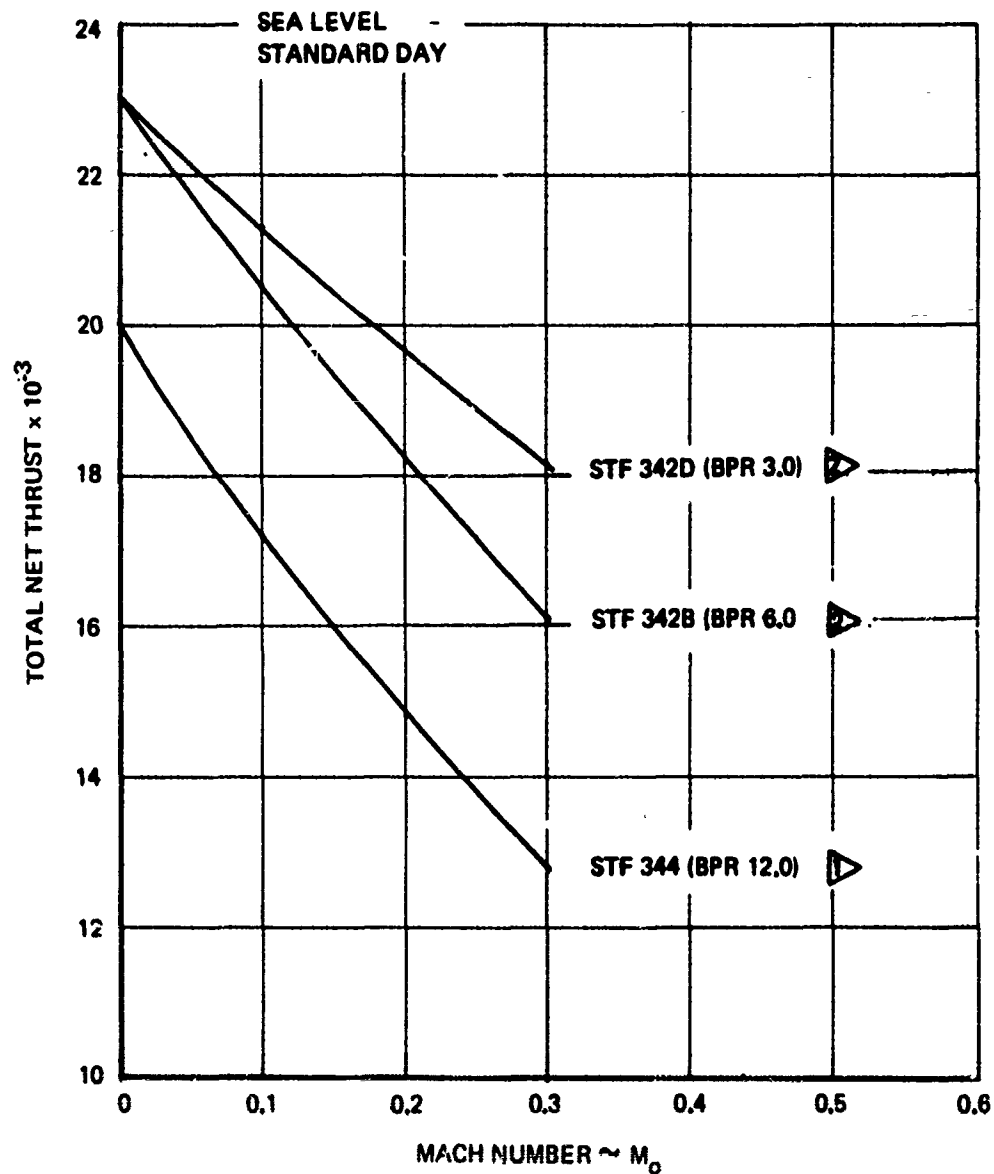


Figure 3: TOTAL NET THRUST VS MACH NO. STF 344, 342B, 342D – SEA LEVEL

TABLE I

STF 342 MIXED FLOW SIMULATION*

	BPR	ALT	M _N	FNT (lb)	WAT (lb/sec)	A _g (Ft ²)
STF 342D	3.0	0	0	14200	352.	4.955
STF 342B	6.0	0	0	14625	486.7	8.034

*PRODUCES 12100 lb TOTAL NET THRUST AT
70 KTS, 2500 Ft, 93°F DAY.

Scaling data was provided by Pratt & Whitney Aircraft to scale the engines to the required thrust size for the Model 953-258 baseline airplane, Figures 4 and 5. The scaling rule selected was to provide the thrust required for operation at 93°F, 2500 ft altitude, and 70 knots. This equates to the design point thrust of the engines on the baseline airplane. The resulting scaled engine thrust, weight and dimensions are shown in Tables II, III, and IV for the STF 342D, STF 342B, and STF 344 engines respectively.

2.1.3 Baseline Nacelle Design

The baseline nacelle designs provide a basis to evaluate nacelle weight and performance with the thrust reverser and thrust vectoring systems installed. Baseline nacelle configurations were developed for the various engines and engine pod installations to be considered in the study. The following table summarizes the basic nacelles used in the design studies:

NACELLE CONFIGURATIONS	BYPASS RATIO		
	3.0	6.0	12.0
Single pod, unmixed flow	Fig. 6	Fig. 7	Fig. 8
Single pod, mixed flow	Fig. 9	Fig. 10	
Double pod, unmixed flow	Fig. 11		

TABLE V BASELINE NACELLE CONFIGURATIONS

The basic nacelles are designed in sufficient detail to define the intake, nacelle contours, cruise nozzle design, engine accessories, and engine mounting arrangement.

The following design criterion was used to establish intake geometry:

1. The intake was sized to pass the engine design airflow at sea level takeoff thrust power setting.
2. The intake throat airflow per unit area is 0.289 lb/sec/in².
3. The engine face airflow per unit area is 0.292 lb/sec/in².
4. The intake highlight to throat area ratio, A_{hl}/A_{th} , is 1.30.
5. The cowl exit radius, R_E , is greater than 4.0 times the throat radius.
6. The intake diffuser half angle, $\beta/2$, is less than 5°.
7. The intake lip radius is 5% of the highlight radius.
8. External geometry established by an assumed cowl thickness of 5.00 inches at the fan face.

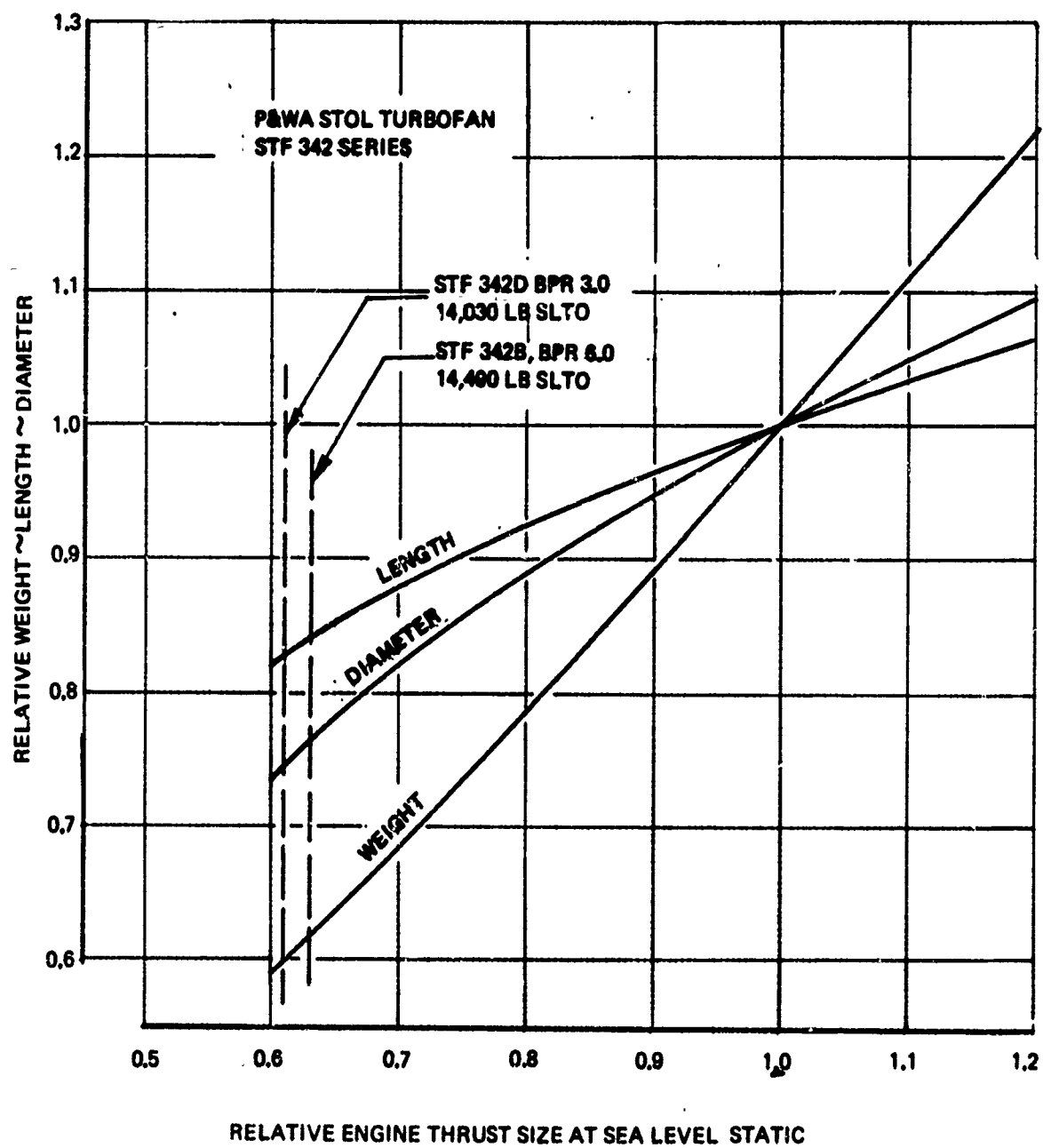


Figure 4: STF 342 SCALING CHARACTERISTICS

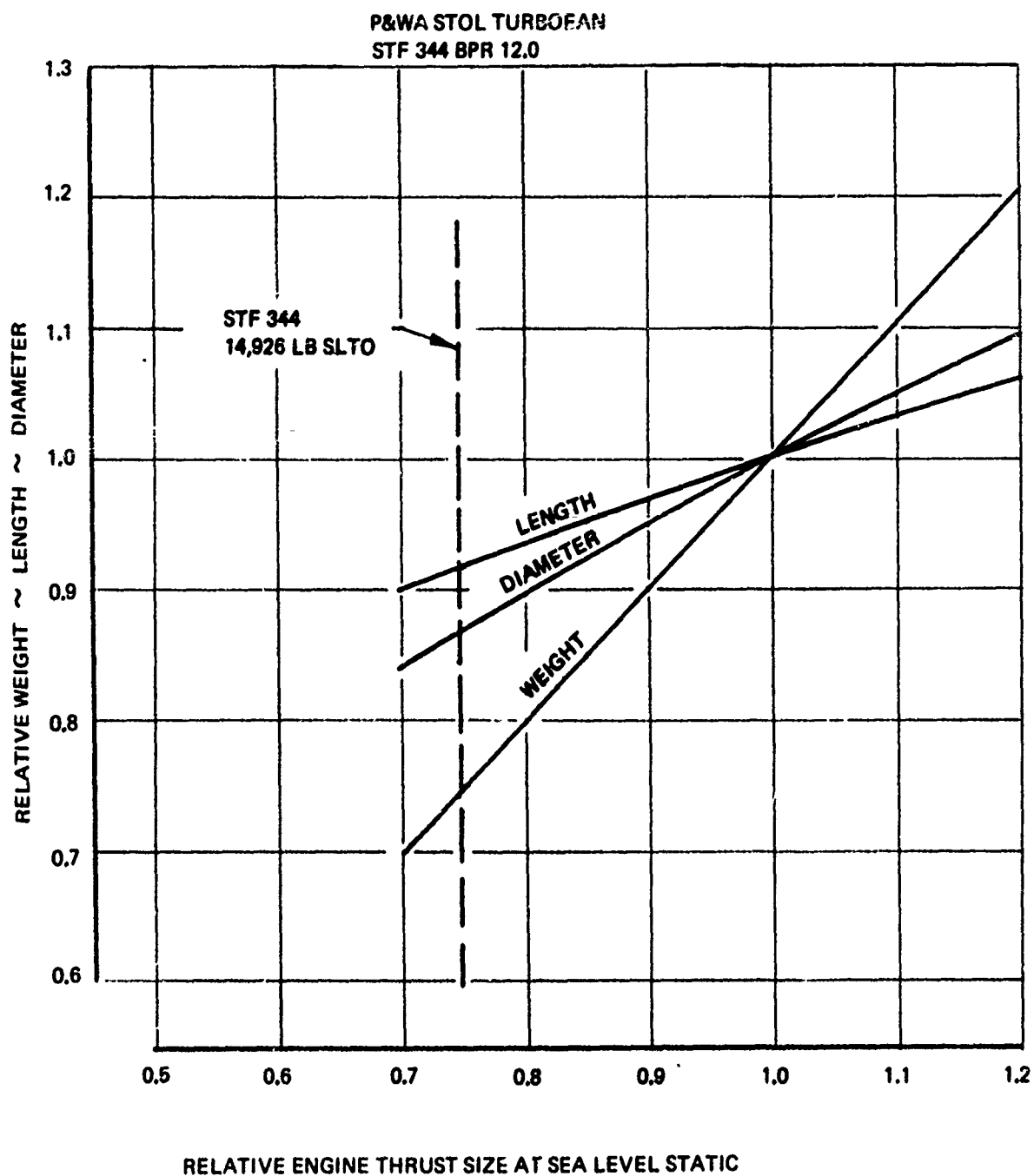
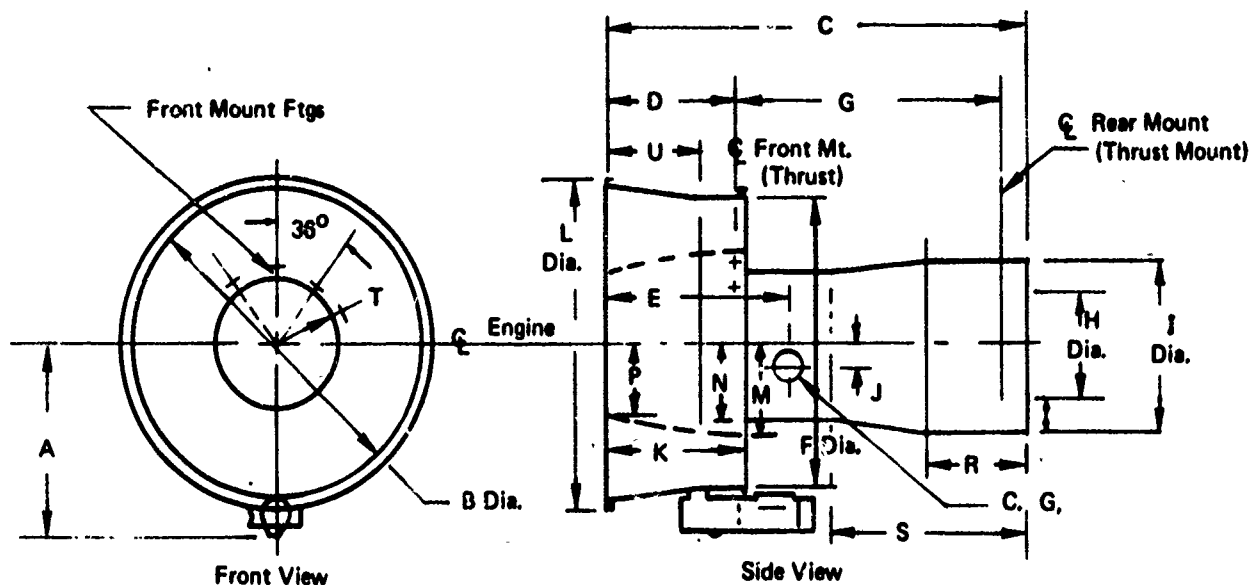


Figure 5: STF 344 SCALING CHARACTERISTICS

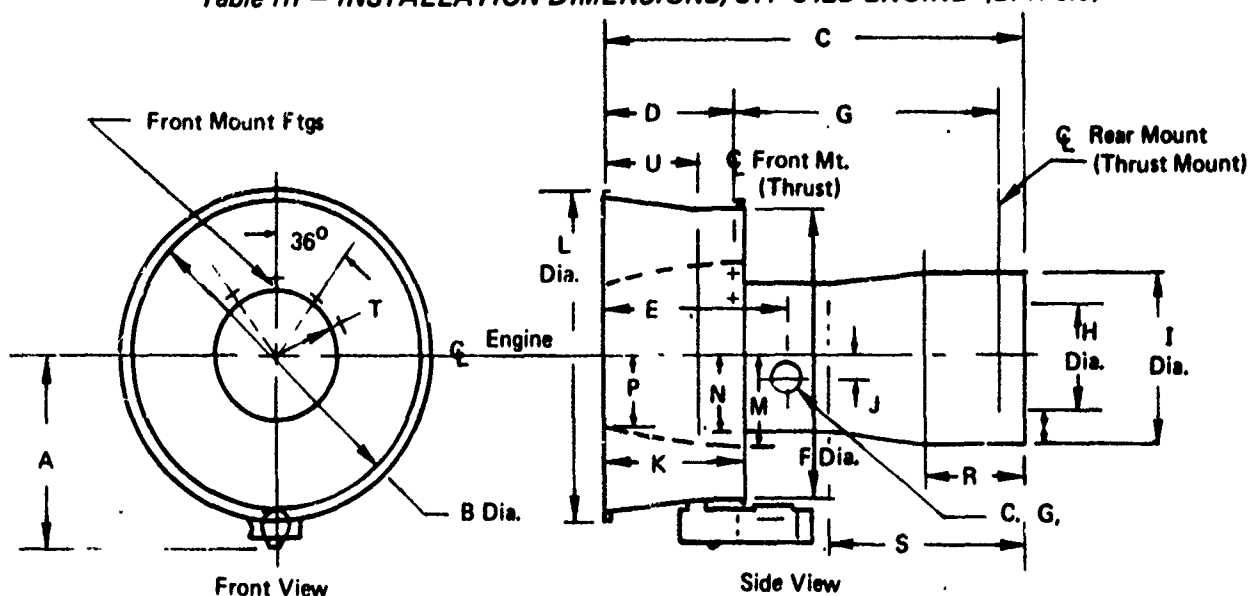
Table II: INSTALLATION DIMENSIONS - STF 342D ENGINE (BPR 3.0)



Installation Dimensions for STF 342D BPR 3.0 Engine Scaled from Basic 23,000 Lbs SLTO Thrust to 14,030 Lbs SLTO Thrust (Equivalent to 12,100 Lbs Thrust @ 2500 Ft, 93° F, 70 kts, 100% Ram Recovery, no Bleed or Power Extraction)

Parameter or Dimension (Inches)		Basic Engine	Scale Factor	Scaled Engine
SLTO Thrust	Lbs	23,000	0.610	14,030
Weight	Lbs	3,310	0.500	1,986
Primary Exit Area	F_t^2	2.48	0.610	1.51
Fan Exit Area	F_t^2	5.78	0.610	3.53
A		34.3	0.745	25.6
B		58.5	0.745	42.1
C		95.3	0.830	79.1
D		23.6	0.830	19.6
E		34.5	0.830	28.6
F		52.1	0.745	38.3
G		66.7	0.830	55.4
H		23.8	0.745	17.7
I		35.1	0.745	26.1
J		0	0.745	0
K		24.6	0.830	20.4
L		58.9	0.745	43.9
M		18.2	0.745	13.6
N		12.3	0.745	13.6
P		8.75	0.745	6.51
R		23.6	0.830	19.6
S		47.3	0.830	39.2
T		15.3	0.745	11.4
U		16.4	0.830	13.6

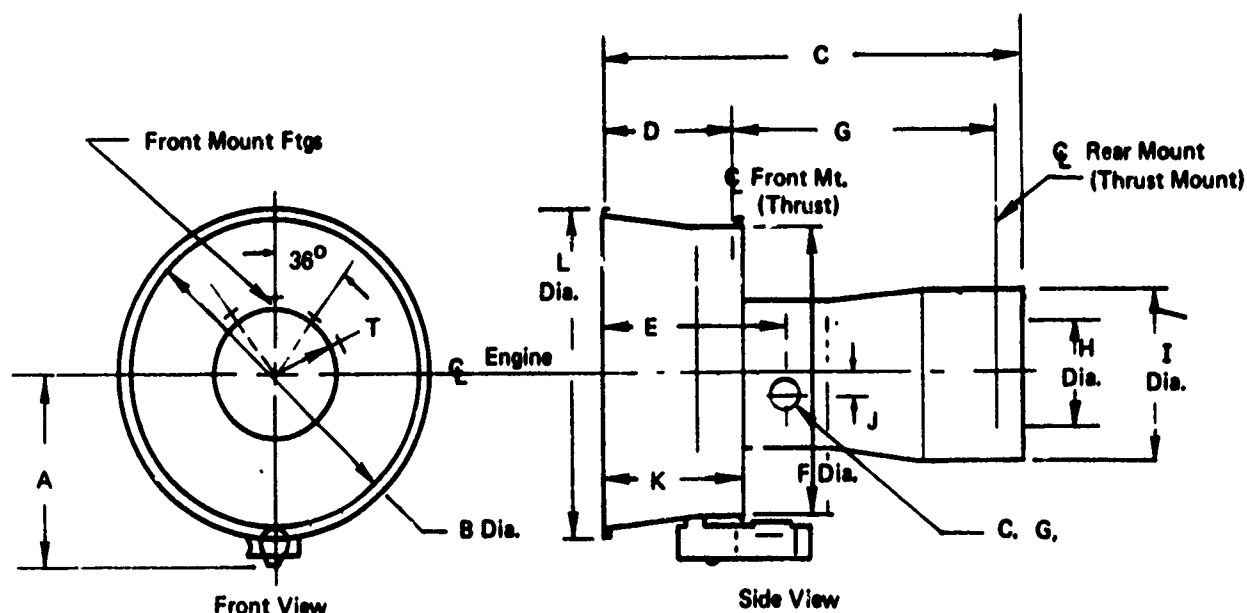
Table III – INSTALLATION DIMENSIONS, STF 342B ENGINE (BPR 6.0)



Installation Dimensions for STF 342B BPR 6.0 Engine Scaled from Basic 23,000 Lbs SLTO Thrust to 14,490 Lbs SLTO Thrust (Equivalent to 12,100 Lbs Thrust @ 2500 Ft, 93°F, 70 Kts, 100% Ram Recovery, No Bleed or Power Extraction).

Parameter or Dimension (Inches)		Basic Engine	Scale Factor	Scaled Engine
SLTO Thrust	Lbs	23,000	0.630	14,490
Weight	Lbs	3,230	0.620	2,003
Primary Exit Area	Ft ²	2.63	0.630	1.66
Fan Exit Area	Ft ²	9.79	0.630	6.17
A		38.8	0.764	29.6
B		65.4	0.764	50.0
C		89.0	0.842	74.9
D		20.5	0.842	17.3
E		39.8	0.842	33.5
F		59.7	0.764	45.6
G		64.0	0.842	53.9
H		22.3	0.764	17.0
I		34.9	0.764	26.7
J		0	0.764	0
K		21.5	0.842	18.1
L		67.8	0.764	51.8
M		18.0	0.764	13.7
N		12.1	0.764	9.2
P		11.86	0.764	9.06
R		18.5	0.842	15.6
S		37.0	0.842	31.2
T		14.9	0.764	11.4
U		14.3	0.842	12.0

Table IV: INSTALLATION DIMENSIONS – STF 344 ENGINE (BPR 12.0)

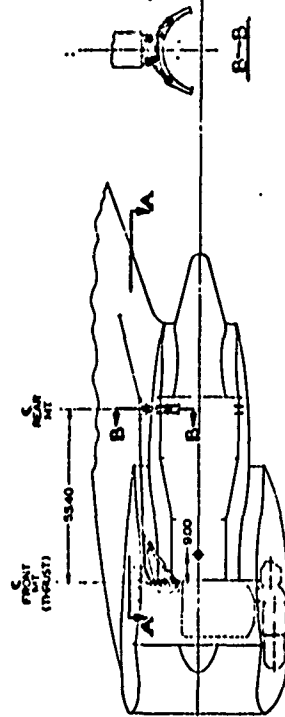
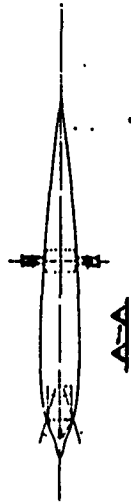


Installation Dimensions for STF 344 BPR 12.0 Engine Scaled from Basic 20,000 Lbs SLTO Thrust to 14,926 Lbs SLTO Thrust (Equivalent to 12,100 Lbs Thrust @ 2500 Ft, 93°F, 70 kts, 100% Ram Recovery, no Bleed or Power Extraction).

Parameter or Dimension (Inches)		Basic Engine	Scale Factor	Scaled Engine
SLTO Thrust	Lbs	20,000	0.746	14,926
Weight	Lbs	3,370	0.742	2,500
Primary Exit Area	Ft ²	3.30 T.O. 3.30 Cruise	0.746	2.46 T.O. 2.46 Cruise
Fan Exit Area	Ft ²	17.73 T.O. 15.07 Cruise	0.746	8.23 T.O. 11.24 Cruise
A		45.80	0.865	39.62
B		73.25	0.865	63.36
C		89.23	0.915	81.65
D		24.06	0.915	22.01
E		37.00	0.915	33.86
F		72.60	0.865	62.80
G		61.54	0.915	56.31
H		17.90	0.865	15.48
I		30.50	0.865	26.38
J		4.90	0.865	4.24
K		25.06	0.915	22.93
L		75.65	0.865	65.44

NOTES

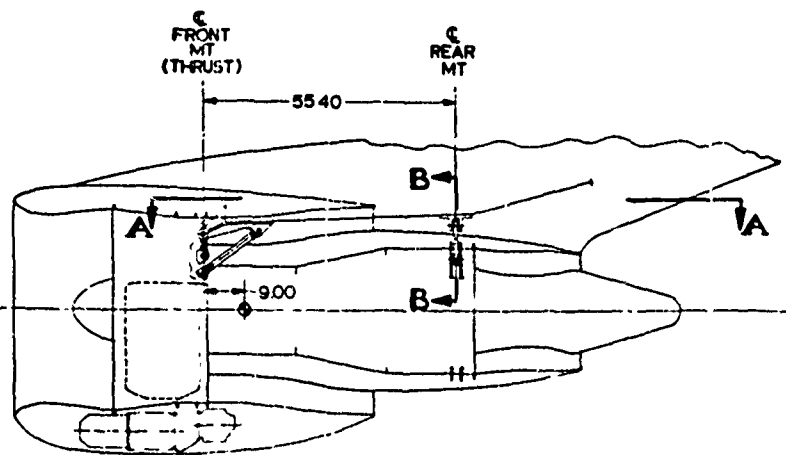
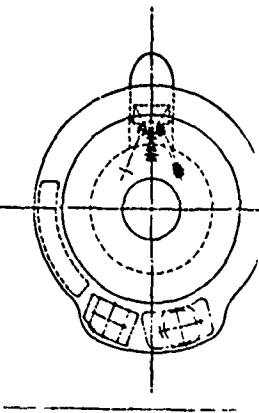
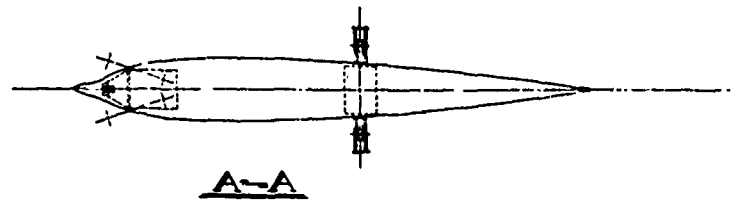
1. BASIC DATA FOR DESIGN OF THE ENGINE POD:
 TOTAL WEIGHT 400 LBS (181.4 KG)
 SUSPENSION POINTS TO BE LOCATED AT 10% OF THE TOTAL WEIGHT
 TO BE LOCATED AT 10% OF THE TOTAL WEIGHT
2. AIR INTAKE DESIGN REQUIREMENTS:
 AIRFLOW 100 CFM (2.83 M³/MIN)
 AIRFLOW VELOCITY 100 FT/MIN (30.48 M/MIN)
 EFFECTIVE AREA 100 IN² (6451.6 CM²)
3. EXHAUST SYSTEM REQUIREMENTS:
 EXHAUST VELOCITY 100 FT/MIN (30.48 M/MIN)
 EXHAUST AREA 100 IN² (6451.6 CM²)
4. CENTER OF GRAVITY LOCATION: 10% OF THE TOTAL WEIGHT
 WEIGHT ONLY, AND DOES NOT INCLUDE INHALE, EXHAUST, DUCTS,
 NOZZLES, OR AIRFRAME ACCESSORIES
5. PRIMARY NOZZLE 30-DEGREE CONE ANGLE 60°
 PLUG NOZZLE HALF ANGLE 15°, 60° CONE HALF ANGLE 60°



0 10 20 30 40 50
SCALE IN INCHES

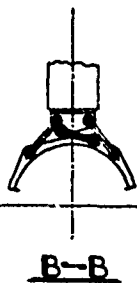
See the following pages
for greater detail.

Figure 6: BASIC NACELLE INSTALLATION -
BPR 3 ENGINE SINGLE POD, UNMIXED FLOW



NOTES:

1. ENGINE: P&WA STF 3420 ENGINE TYPE PER P&WA REPORT
TDM-2177 DATED 4/11/69 SCALED FROM BASIC 23,000 POUNDS
SLSTO THRUST TO PROVIDE 14,030 POUNDS TAKEOFF THRUST FLAT RATED
TO 93 DEGREES F AT SEA LEVEL.
SLSTO THRUST 14,030 POUNDS
WEIGHT (NO DUCTS) 1,986 POUNDS
PRIMARY NOZZLE EXIT AREA 1.51 FL²
FAN NOZZLE EXIT AREA 3.53 FL²
2. AIR INTAKE DESIGN REQUIREMENTS:
THROAT MACH NO. = 0.60 AT SLSTO THRUST DESIGN
AIRFLOW 395 POUNDS/SECOND
HIGHLIGHT AREA/THROAT AREA = 1.30
EFFECTIVE $\beta/2 = 5^\circ$ (ANGLE FROM THROAT TO COMPRESSOR FACE
MEASURED ALONG A STRAIGHT LINE)
3. REVERSER SYSTEMS: TO BE DEVELOPED ON DETAIL DRAWINGS.
NOZZLES SHOWN IN TAKEOFF POSITION.
4. CENTER OF GRAVITY LOCATION SHOWN IS FOR BASIC DRY ENGINE
WEIGHT ONLY, AND DOES NOT INCLUDE INTAKE, COWLING, EXHAUST
NOZZLES, OR AIRFRAME ACCESSORIES.
5. PRIMARY NOZZLE BOATTAIL CHORD ANGLE 6° .
PLUG NOZZLE HALF ANGLE 15° , COWL EXIT HALF ANGLE 8° .



0 10 20 30 40 50
SCALE IN INCHES

Figure 6: BASIC NACELLE INSTALLATION -
BPR 3 ENGINE SINGLE POD, UNMIXED FLOW

BASIC NACELLE INSTL -	
BPR 3 ENG - SINGLE POD	
UNMIXED FLOW	
J	22541-PD-194

2-2541-PD-194

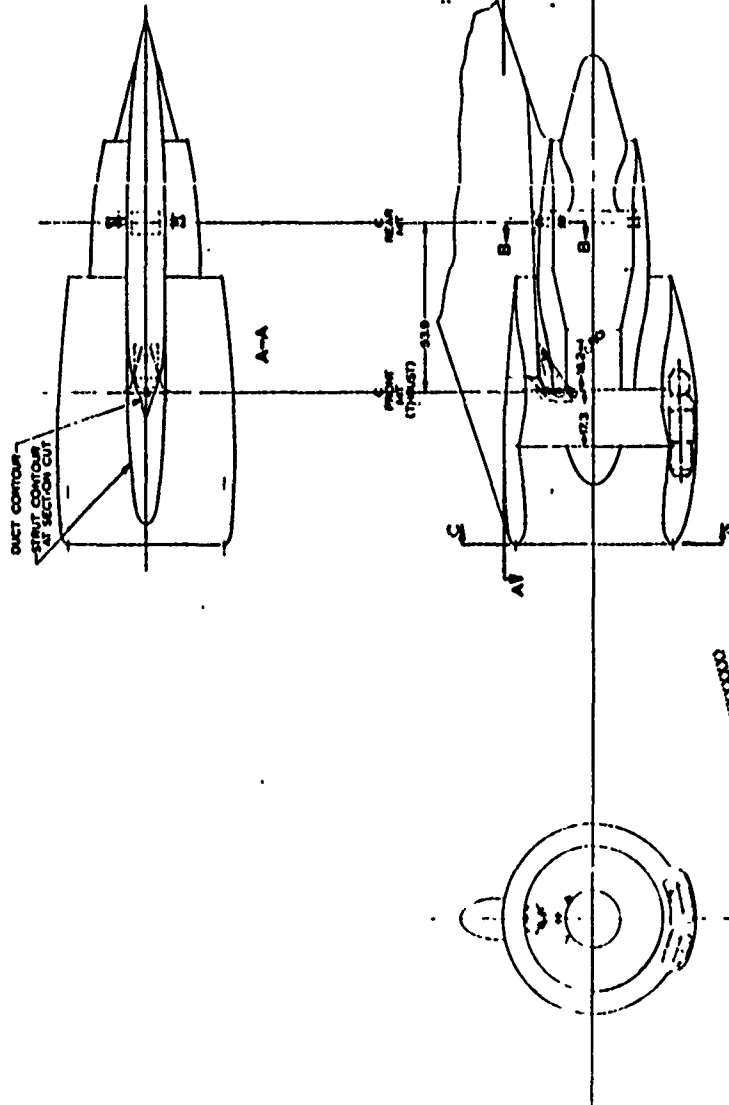
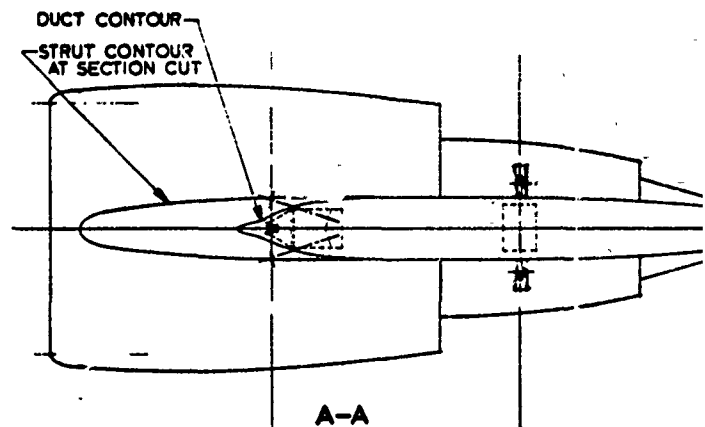


Figure 7: BASIC NACELLE INSTALLATION -
BPR S ENGINE SINGLE POD, UNMIXED FLOW

1. ENGINE, FAMA 515 MBE ENGINE TYPE PER DATA REPORT TOW 2177
BATED 411199 SCALED FROM BASIS 21,000 POUNDS LBS TO 104,251
TO PROVIDE 1A AND POUNDS WEIGHT THE WEIGHT ESTIMATED TO 10
EXCEEDS FAN SEA LEVEL
2. AIR INTAKE SECTION REQUIREMENTS
- THROAT RADIUS NO. = 6.6 AT 515 TO THROAT
DESIGN AIRFLOW 100 POUNDS PER SECOND
NEGATIVE PRESSURE LOSS = 2.10
DIRECTION OF FLOW = FLOW FROM THROAT TO COMPRESSOR FACE
MAINTAINED ALONG A STRAIGHT LINE
3. REVERSE SYSTEMS TO BE LOCATED ON THE 104,251 POUNDS
NOZZLES SHOWN IN FIGURE 104,251 POUNDS
4. CENTER OF GRAVITY LOCATED ON SPAN 1A FOR BALANCE OF ENGINE
WEIGHT ONLY, AND DOES NOT INCLUDE WEIGHT OF ENGINE DOWNST
NOZZLES OR AIRFRAME ACCESSORIES IS
5. PRIMARY NOZZLE DOWNST AIRFLOW ANGLE = 0°
PLUG ANGLE = 15°
CONC. OUT ANGLE = 0°
- 1A AND POUNDS
FAN NOZZLES
2.00 POUNDS
1.00 FT
6.17 FT

XXXXXXXXXXXXXXXXXXXXXXXXXXXX
See the following pages
for greater detail.
XXXXXXXXXXXXXXXXXXXXXXXXXXXX

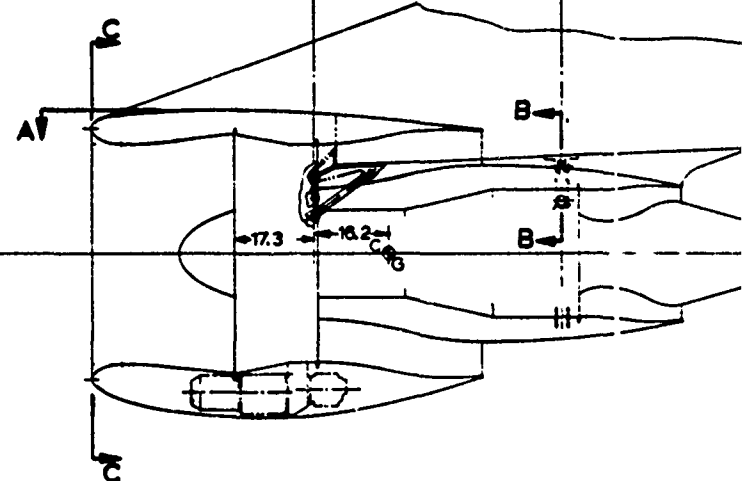


A-A

C FRONT
MT (THRUST)

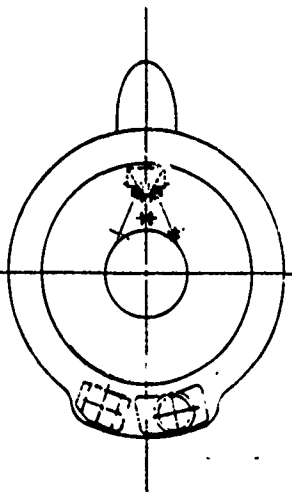
C REAR
MT

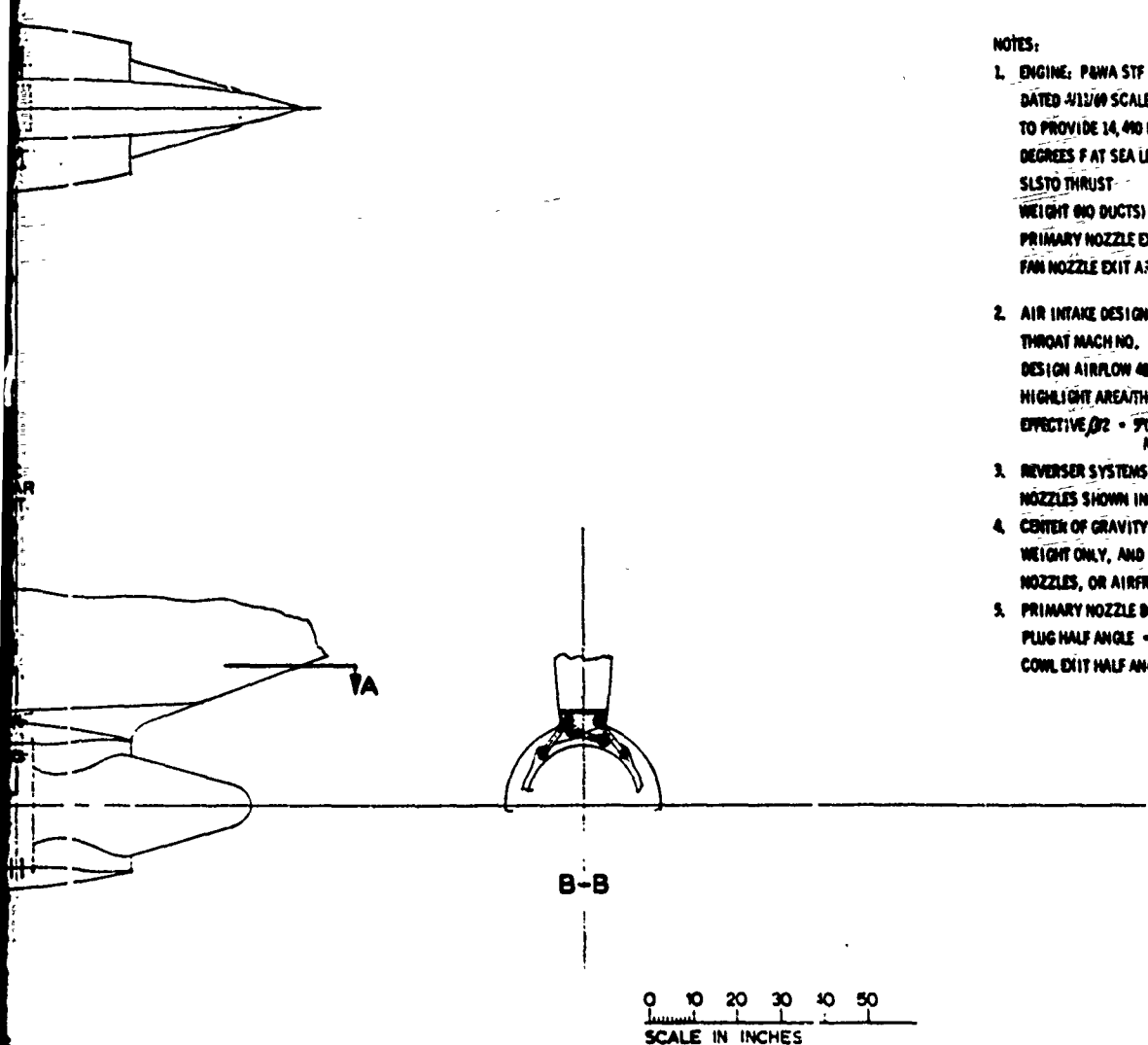
53.9



17.3 16.2

C-C





NOTES:

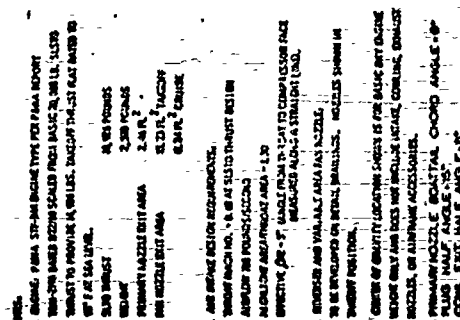
- ENGINE: P&WA STF 3428 ENGINE TYPE PER P&WA REPORT TDM 2177 DATED 4/13/69 SCALED FROM BASIC 23,000 POUND SLSTO THRUST TO PROVIDE 14,400 POUNDS TAKEOFF THRUST FLAT RATED TO 93 DEGREES F AT SEA LEVEL.

SLSTO THRUST	14,400 POUNDS
WEIGHT (NO DUCTS)	2,003 POUNDS
PRIMARY NOZZLE EXIT AREA	1.66 FT ²
FAN NOZZLE EXIT AREA	6.17 FT ²

- AIR INTAKE DESIGN REQUIREMENTS:
THROAT MACH NO. = 0.60 AT SLSTO THRUST
DESIGN AIRFLOW 481 POUNDS/SECOND
HIGH/LIGHT AREA/THROAT AREA = 1.30
EFFECTIVE $\theta/2$ = θ ANGLE FROM THROAT TO COMPRESSOR FACE MEASURED ALONG A STRAIGHT LINE
- REVERSER SYSTEMS: TO BE DEVELOPED ON DETAIL DRAWINGS. NOZZLES SHOWN IN TAKEOFF POSITION.
- CENTER OF GRAVITY LOCATION SHOWN IS FOR BASIC DRY ENGINE WEIGHT ONLY, AND DOES NOT INCLUDE INTAKE, COWLING, EXHAUST NOZZLES, OR AIRFRAME ACCESSORIES.
- PRIMARY NOZZLE BOATTAIL CHORD ANGLE = 6°
PLUG HALF ANGLE = 13°
COWL EXIT HALF ANGLE = 8°

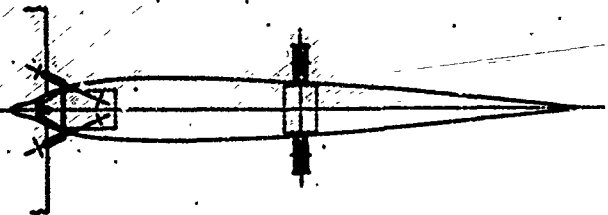
Figure 7: BASIC NACELLE INSTALLATION –
BPR 6 ENGINE SINGLE POD, UNMIXED FLOW

BASIC NACELLE INSTL	
BPR 6 ENG SINGLE POD	
UNMIXED FLOW	
2-2541-PD-198	

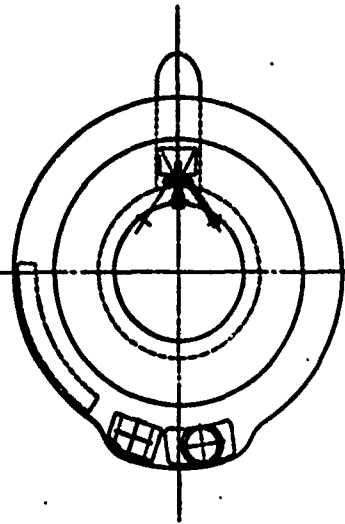
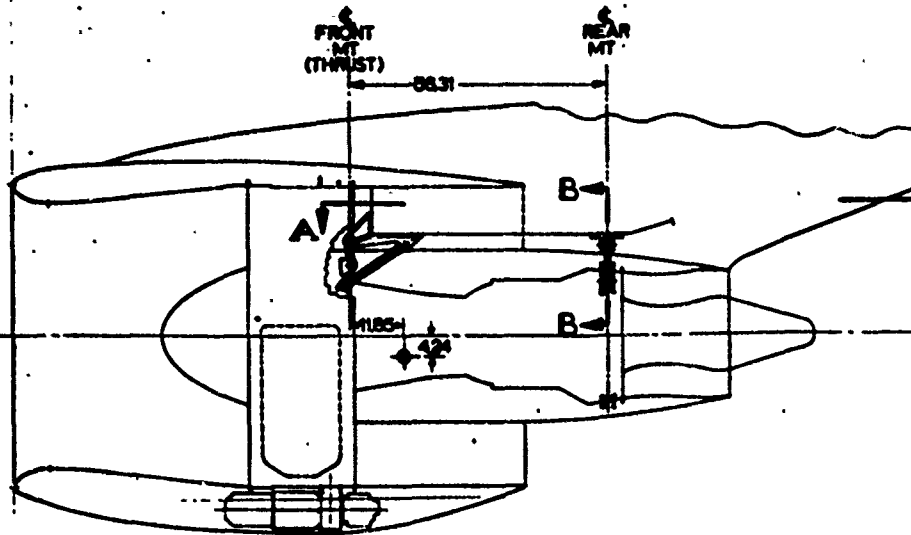
[illegible]

BASIC INCELL	
BIO D ENGINE	
SINGLE AGO	
NO.	2254FC-100

**Figure 8: BASIC NACELLE INSTALLATION --
BPR 12 ENGINE SINGLE POD**



A-A



NOTES:

1. ENGINE: PANA STF-344 ENGINE TYPE PER PANA REPORT
 TEM-870 DATED 8/22/69 SCALED FROM BASIC 28,000 L.B. SLSTO
 THRUST TO PROVIDE 14,926 LBS. TAKEOFF THRUST PLAT RATED TO
 80° F AT SEA LEVEL.

SLSTO THRUST	14,926 POUNDS
WEIGHT	2,500 POUNDS
PRIMARY NOZZLE EXIT AREA	2.46 PL ²
FAN NOZZLE EXIT AREA	13.23 PL ² TAKEOFF
	11.34 PL ² CRUISE

2. AIR INTAKE DESIGN REQUIREMENTS:

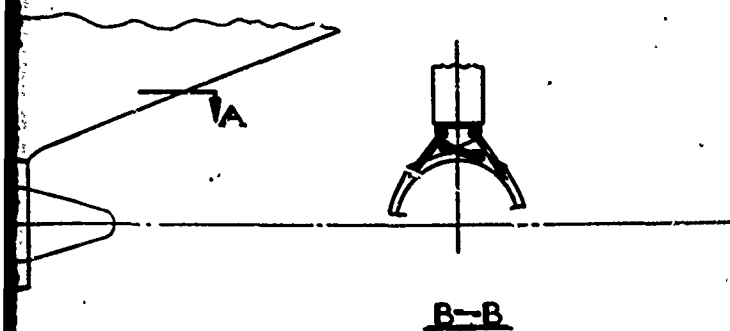
- THROAT MACH NO. = 0.80 AT SLSTO THRUST DESIGN
 AIRFLOW 785 POUNDS/SECOND
 INLET/INT AREA/THROAT AREA = 1.30
 EFFECTIVE β = 5° (ANGLE FROM THROAT TO COMPRESSOR FACE
 MEASURED ALONG A STRAIGHT LINE).

3. REVERSE AND VARIABLE AREA FAN NOZZLE:

- TO BE DEVELOPED ON DETAIL DRAWINGS. NOZZLES SHOWN IN
 TAKEOFF POSITION.

**4. CENTER OF GRAVITY LOCATION SHOWN IS FOR BASIC DRY ENGINE
 WEIGHT ONLY AND DOES NOT INCLUDE INTAKE, COWLING, EXHAUST
 NOZZLES, OR AIRFRAME ACCESSORIES.**

**5. PRIMARY NOZZLE BOATTAIL CHORD ANGLE = 6°
 PLUG HALF ANGLE = 15°
 COWL EXIT HALF ANGLE = 8°**



0 10 20 30 40 50
 SCALE IN INCHES

**Figure 8: BASIC NACELLE INSTALLATION –
 BPR 12 ENGINE SINGLE POD**

DATE	2-2541-PC-193
REVISION	
DESCRIPTION	BASIC NACELLE INSTL- BPR 12 ENGINE SINGLE POD
DATE	2-2541-PC-193

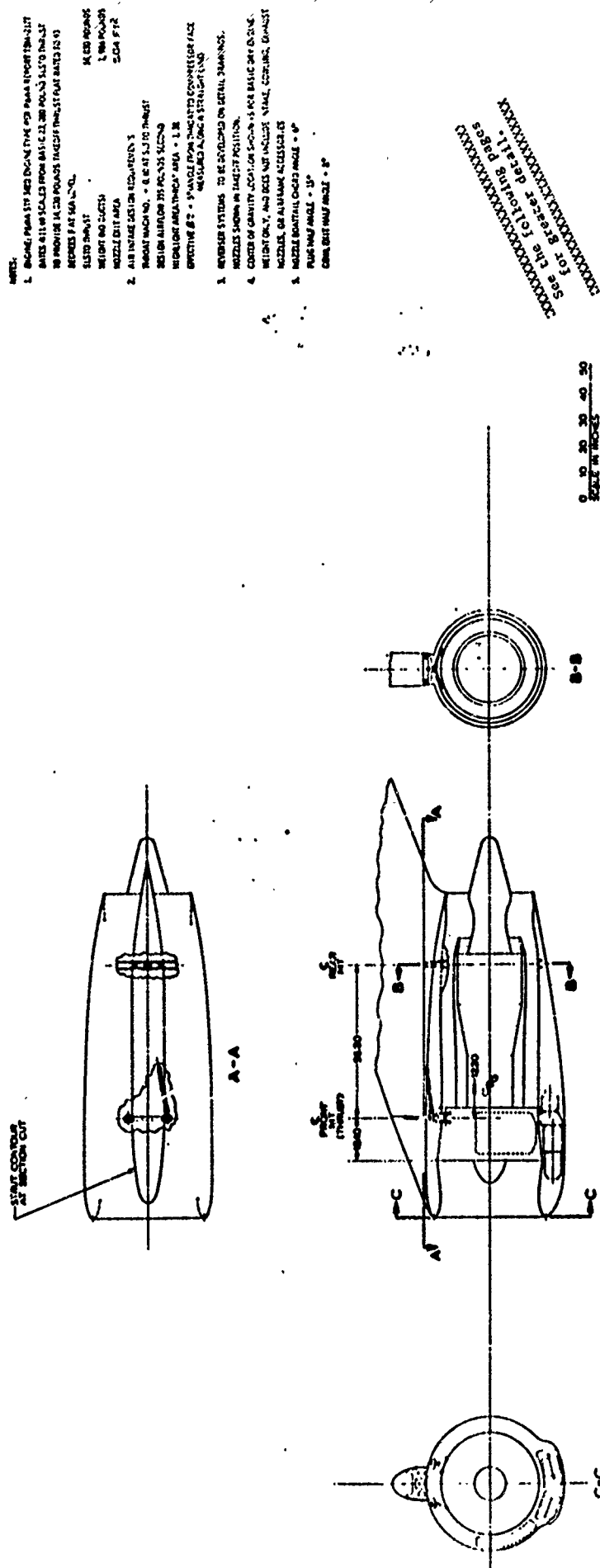
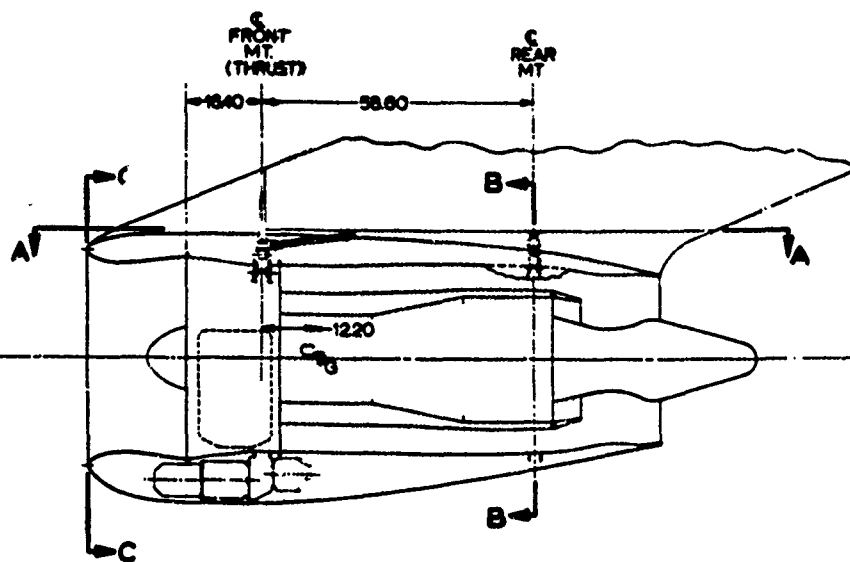
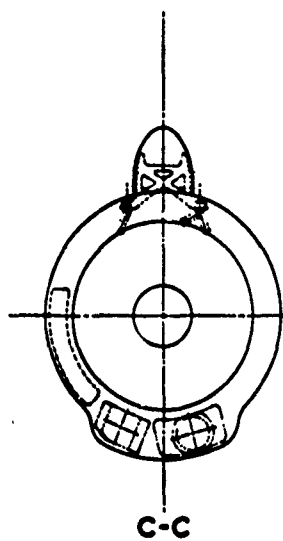
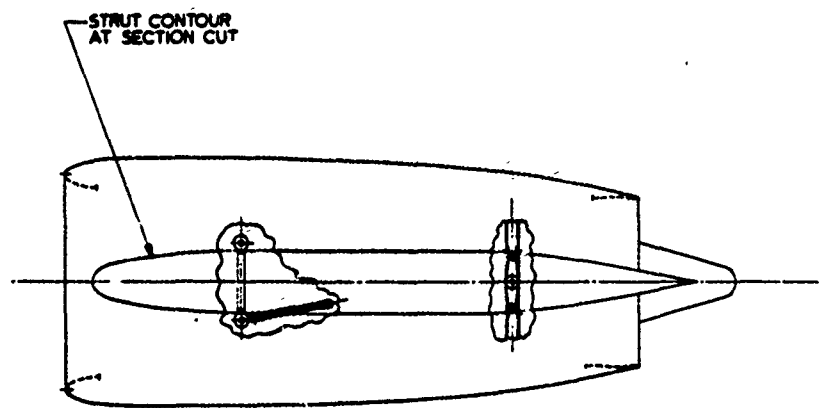
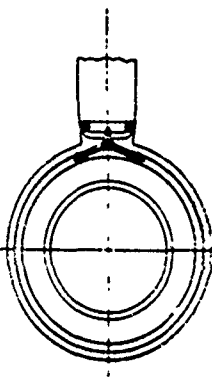


Figure 9: BASIC NACELLE INSTALLATION - BPR 3 ENGINE SINGLE POD, MIXED FLOW



NOTES:

1. ENGINE: P&WA STF 3420 ENGINE TYPE PER P&WA REPORT TDM-2177
 DATES 4/11/69 SCALED FROM BASIC 23,000 POUND SLSTO THRUST
 TO PROVIDE 14,030 POUNDS TAKEOFF THRUST FLAT RATED TO 93
 DEGREES F AT SEA LEVEL.
 SLSTO THRUST 14,030 POUNDS
 WEIGHT (NO DUCTS) 1,986 POUNDS
 NOZZLE EXIT AREA 504 FT²
2. AIR INTAKE DESIGN REQUIREMENTS:
 THROAT MACH NO. • 0.60 AT SLSTO THRUST
 DESIGN AIRFLOW 355 POUNDS/SECOND
 HIGHLIGHT AREA/THROAT AREA • 1.36
 EFFECTIVE A/R • 5° ANGLE FROM THROAT TO COMPRESSOR FACE
 MEASURED ALONG A STRAIGHT LINE
3. REVERSER SYSTEMS: TO BE DEVELOPED ON DETAIL DRAWINGS.
 NOZZLES SHOWN IN TAKEOFF POSITION.
4. CENTER OF GRAVITY LOCATION SHOWN IS FOR BASIC DRY ENGINE
 WEIGHT ONLY, AND DOES NOT INCLUDE INTAKE, COWLING, EXHAUST
 NOZZLES, OR AIRFRAME ACCESSORIES.
5. NOZZLE BOATTAIL CHORD ANGLE • 6°
 PLUG HALF ANGLE • 15°
 CONE EXIT HALF ANGLE • 8°



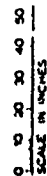
B-B

0 10 20 30 40 50
 SCALE IN INCHES

Figure 9: BASIC NACELLE INSTALLATION –
 BPR 3 ENGINE SINGLE POD, MIXED FLOW

2-2541-PD-200	
BASIC NACELLE INSTL -	
BPR 3 ENG-SINGLE POD,	
MIXED FLOW	
2-2541-PD-200	

2-2541-PD-200



**Figure 10: BASIC NACELLE INSTALLATION -
BPR 6 ENGINE SINGLE POD, MIXED FLOW**

3 - FROM THE SHOP

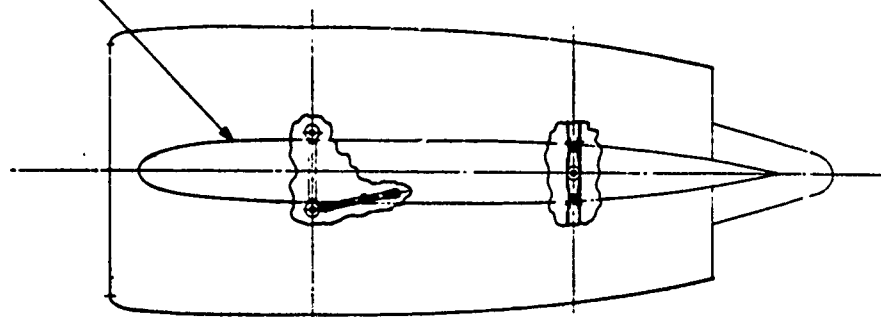
XXXXXXXXXXXXXXXXXXXX
for greater details
see the following pages
XXXXXXXXXXXXXXXXXXXX

Conclusion

7 (28 blank)

[Illegible handwritten text]

STRUT CONTOUR
AT SECTION CUT



A-A

FRONT
MIT
(THRUST)

REAR
MIT

56.8

B

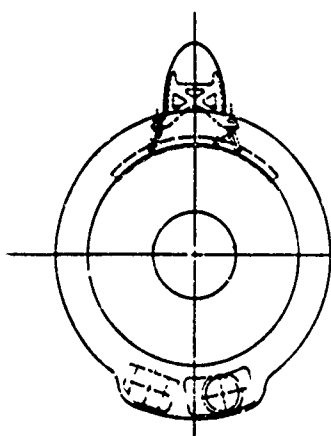
A

14.4

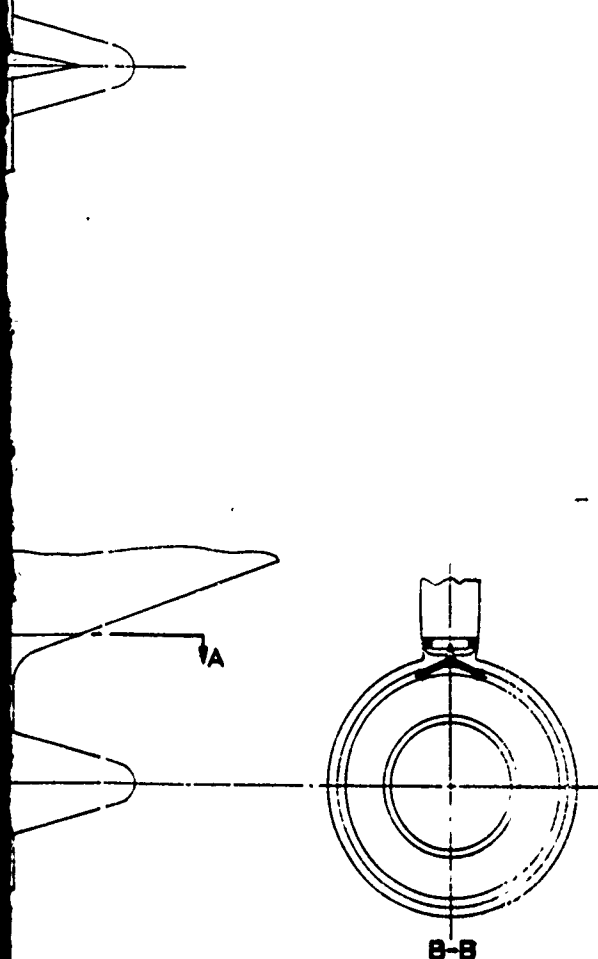
33.5

B

C



C-C



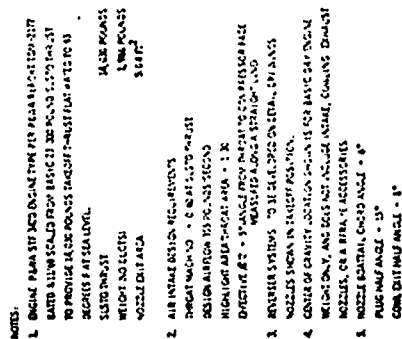
0 10 20 30 40 50
SCALE IN INCHES

NOTES:

1. ENGINE: P&WA 3TF 3428 ENGINE TYPE PER P&WA REPORT TDM-2177 DATED 4/11/69 SCALED FROM BASIC 23,000 POUNDS SLSTO THRUST TO PROVIDE 14,490 POUNDS TAKEOFF THRUST FLAT RATED TO 93 DEGREES F AT SEA LEVEL.
 SLSTO THRUST 14,490 POUNDS
 WEIGHT (NO DUCTS) 2,003 POUNDS
 NOZZLE EXIT AREA 7.83 FT²
2. AIR INTAKE DESIGN REQUIREMENTS:
 THROAT MACH NO. = 0.60 AT SLSTO THRUST
 DESIGN AIRFLOW 481 POUNDS/SECOND
 HIGHLIGHT AREA/THROAT AREA = 1.30
 EFFECTIVE $\beta/2 = 5^\circ$ (ANGLE FROM THROAT TO COMPRESSOR FACE MEASURED ALONG A STRAIGHT LINE)
3. REVERSER SYSTEMS: TO BE DEVELOPED ON DETAIL DRAWINGS.
 NOZZLES SHOWN IN TAKEOFF POSITION.
4. CENTER OF GRAVITY LOCATION SHOWN IS FOR BASIC DRY ENGINE WEIGHT ONLY, AND DOES NOT INCLUDE INTAKE, COWLING, EXHAUST NOZZLES, OR AIRFRAME ACCESSORIES.
5. NOZZLE BOATTAIL CHORD ANGLE = 6°
 PLUG HALF ANGLE = 15°
 COWL EXIT HALF ANGLE = 8°

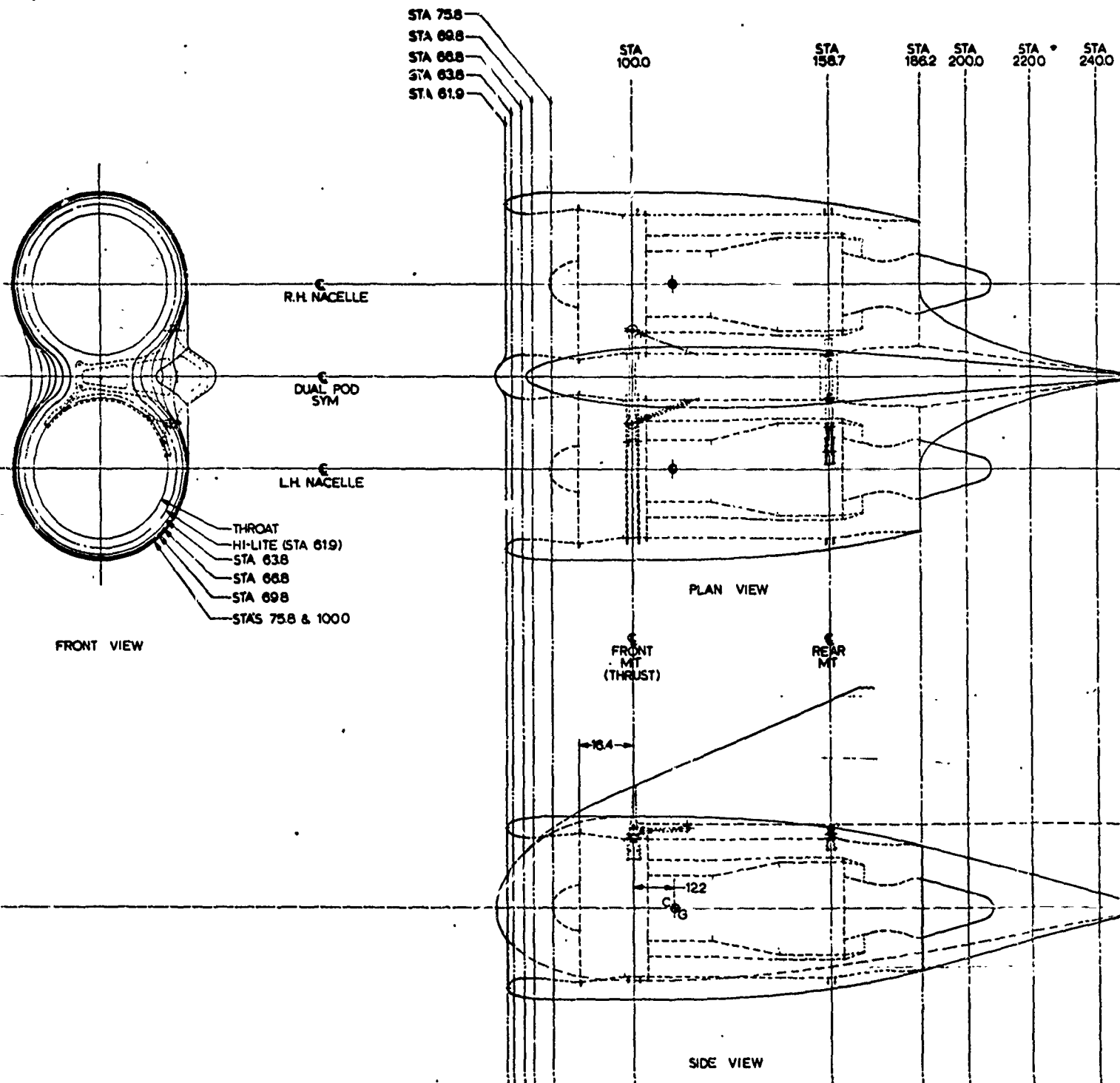
Figure 10: BASIC NACELLE INSTALLATION -
BPR 6 ENGINE SINGLE POD, MIXED FLOW

NO. 10	
DATE	11-11-69
BY	J. KINGS
CHKD	J. KINGS
BASIC NACELLE INSTL	
BPR 6 ENG SINGLE POD	
MIXED FLOW	
2-2541-PD-199	

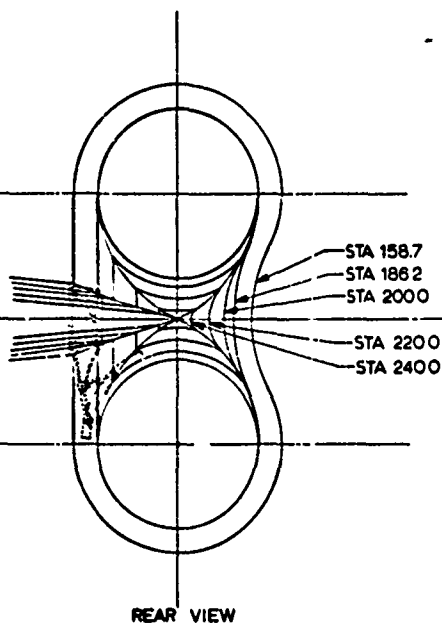


See the following pages
for greater detail.

**Figure 11: BASIC NACELLE INSTALLATION -
BPR 3 ENGINE, DOUPLE POD, MIXED FLOW**



STA 1000 STA 2200 STA 2400 STA 256.1



0 10 20 30 40 50
SCALE IN INCHES

NOTES:

1. ENGINE: P&WA STF 3420 ENGINE TYPE PER P&WA REPORT TDM-2177 DATED 4/11/69 SCALED FROM BASIC 23,000 POUND SLSTO THRUST TO PROVIDE 14,030 POUNDS TAKEOFF THRUST FLAT RATED TO 93 DEGREES F AT SEA LEVEL.
SLSTO THRUST 14,030 POUNDS
WEIGHT (NO DUCTS) 1,986 POUNDS
NOZZLE EXIT AREA 5.04 FT²
2. AIR INTAKE DESIGN REQUIREMENTS:
THROAT MACH NO. = 0.60 AT SLSTO THRUST
DESIGN AIRFLOW 355 POUNDS/SECOND
HIGH/LIGHT AREA/THROAT AREA = 1.30
EFFECTIVE $\theta/2$ = 5° (ANGLE FROM THROAT TO COMPRESSOR FACE MEASURED ALONG A STRAIGHT LINE)
3. REVERSER SYSTEMS: TO BE DEVELOPED ON DETAIL DRAWINGS.
NOZZLES SHOWN IN TAKEOFF POSITION.
4. CENTER OF GRAVITY LOCATION SHOWN IS FOR BASIC DRY ENGINE. WEIGHT ONLY, AND DOES NOT INCLUDE INTAKE, COWLING, EXHAUST NOZZLES, OR AIRFRAME ACCESSORIES.
5. NOZZLE BOATTAIL CHORD ANGLE = 6°
PLUG HALF ANGLE = 15°
COWL EXIT HALF ANGLE = 8°

Figure 11: BASIC NACELLE INSTALLATION -
BPR 3 ENGINE, DOUBLE POD, MIXED FLOW

BPR 3 ENGINE	
DATE	11/11/69
BY	J. J. B. / J. J. B.
CHKD	J. J. B. / J. J. B.
APP'D	J. J. B. / J. J. B.
REV	1
DESCRIPTION	BASIC NACELLE INSTL - BPR 3 ENG, DOUBLE POD MIXED FLOW
FIG. NO.	22541-PD-201

The resulting intake designs for each nacelle are shown in Figure 12.

The nacelle structure consists of aluminum sheet exterior attached to conventional "Z" shaped stiffening rings. The stiffening rings are secured to acoustically treated honeycomb panels on the inside surfaces. Engine loads are distributed between front and rear engine mounts. On the unmixed flow engines the front mount carries vertical, side, and thrust forces. The rear mount carries vertical, side, and torsion loads. For the mixed flow nacelle configurations the load distribution is the same except the torsional loads are carried by the front mount. Engine accessories and gear box are located on the lower side of the engine fan case for engine maintenance and safety considerations.

The exhaust nozzles are designed to provide maximum thrust minus boattail drag consistent with the nacelle maximum diameter and nozzle flow area. The plug nozzles were selected for the baseline nacelles because installations utilizing convergent nozzles would have excessive nacelle drag due to steep boattail angles.

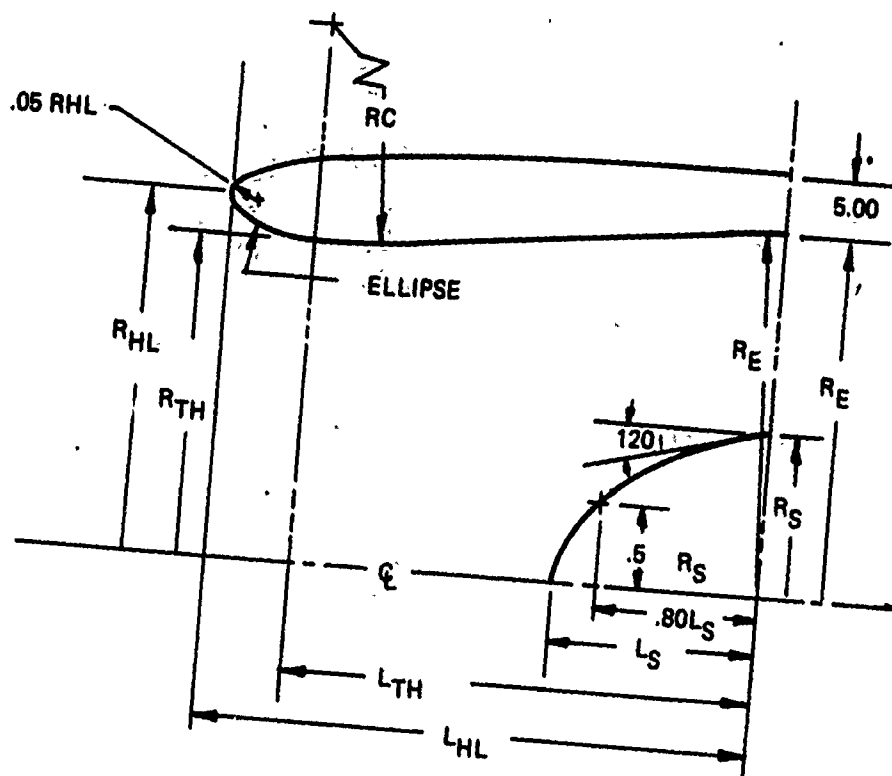
A summary of the baseline engine and nacelle design characteristics are shown in Table VI, including weight estimates. The weight estimates are accurate to ± 10 percent and do not include weight required for a quiet nacelle installation or flutter. The range of weights for the basic nacelle configurations are shown in Figure 13.

2.1.4 Thrust Reverser and Thrust Vectoring System Design Concepts

The design study was conducted in sufficient depth to:

1. define the fundamental geometry required.
2. define the fundamental requirements of the TR/TV nacelle installation on the baseline airplane configuration.
3. formulate the basic requirements for the actuation mechanisms, actuators and systems.
4. define materials selection.
5. allow estimates of TR or TV internal performance, weights, and aerodynamic effects to be made.

The design study resulted in three view layouts of each system with sufficient detail to define internal and external nacelle contours and accessories locations.



PARAMETER OR DIMENSION	STF 342D	STF 342B	STF 344
DESIGN AIRFLOW LBS/SEC	355	481	705
THROAT AREA IN ²	1228	1664	2440
HIGH-LIGHT AREA IN ²	1597	2164	3172
ENGINE FACE AREA, GROSS IN ²	1392	1964	3153
ENGINE FACE AREA, NET IN ²	1259	1706	2502
THROAT RADIUS R_{TH}	19.77	23.01	27.87
HIGH-LIGHT RADIUS R_{TH}	22.55	26.24	31.78
THROAT EXIT RADIUS R_C	79.08	92.04	111.48
ENGINE FACE RADIUS R_E	21.05	25.00	31.68
SPINNER RADIUS R_S	6.51	9.06	14.40
THROAT LENGTH L_{TH}	14.63	24.20	43.55
INTAKE LENGTH L_{HL}	20.19	30.66	51.37
SPINNER LENGTH L_S	8.60	11.97	19.03

Figure 12: INTAKE GEOMETRY

Table VI: BASELINE ENGINE & NACELLE DESIGN PARAMETERS

DRAWING NUMBER	BYPASS RATIO	MIXED OR UNMIXED FLOW	ENGINE DERIVATION	ENGINE & AIRCRAFT ACCESSORY LOCATION	ENGINE MOUNT LOADING		NACELLE STRUC- TURE	ESTIMATED WEIGHT LBS			
					FRONT	REAR		NACELLE	STRUT	ENGINE	
2-2541- PD-194	3	UNMIXED	SCALED FROM P&W STF-342D 23,000 LB THRUST ENGINE, TO 14,030 LB THRUST	GEARBOX MOUNTED ON THE LOWER SIDE OF THE ENGINE FAN CASE	VERT- ICAL SIDE THRUST	VERT- ICAL SIDE TOR- SION	ALUMINUM SHEET EXTERIOR ATTACHED TO CONVEN- TIONAL "Z" SHAPED STIFFENING RINGS THAT ARE SECURED TO ACOUSTICALLY TREATED HONEYCOMB PANELS ON THE INSIDE	440	190	1986	
-200	3	MIXED			VERT- ICAL SIDE THRUST TORSION	VERT- ICAL SIDE		610	210	1986	
-201	3	MIXED (DUAL POD)						1260	340	1986 (EACH)	
-199	6	MIXED	SCALED FROM P&W STF-342B 23,000 LB THRUST ENGINE, TO 14,490 LB THRUST					710	220	2003	
-198	6	UNMIXED			VERT- ICAL SIDE THRUST	VERT- ICAL SIDE TOR- SION		530	200	2003	
-193	12	UNMIXED	SCALED FROM P&W STF-344 20,000 LB THRUST ENGINE, TO 14,926 LB THRUST							700	240

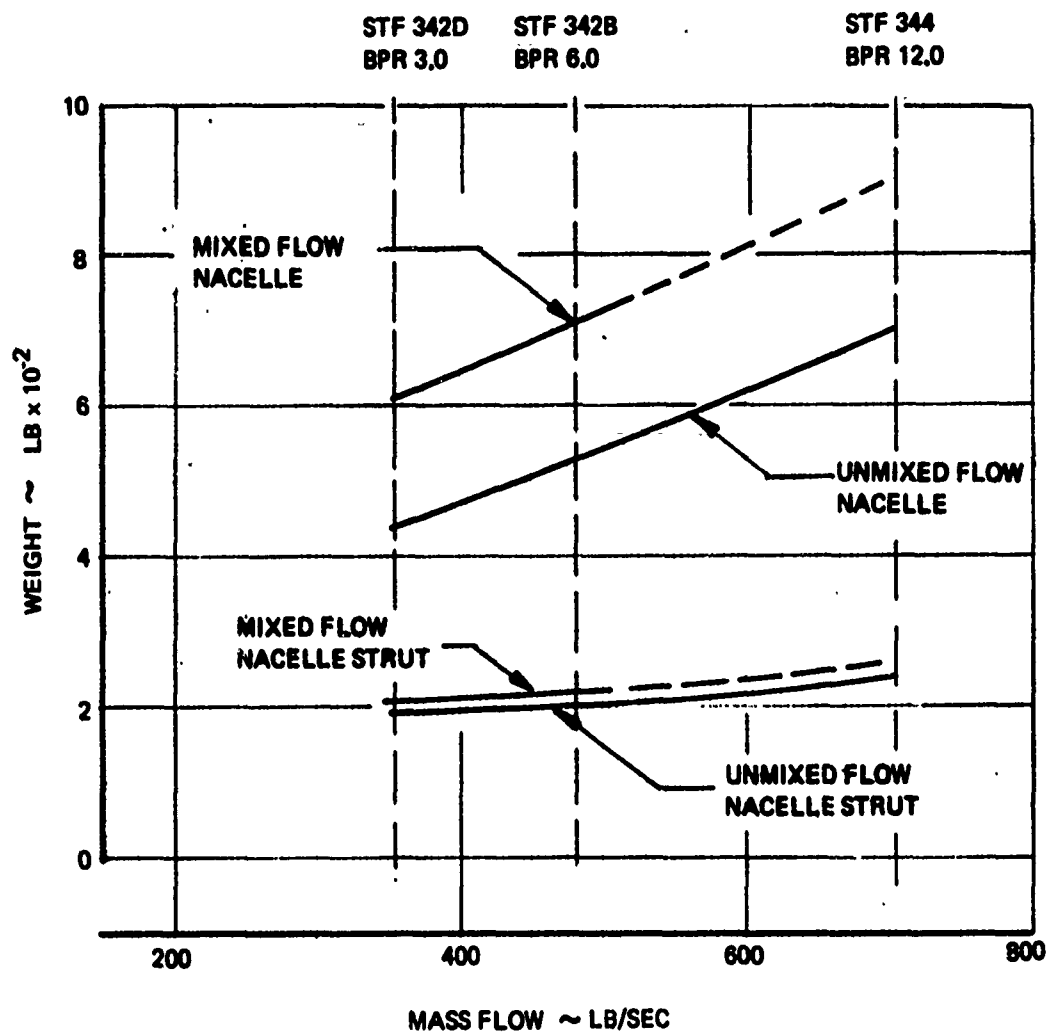


Figure 13: BASIC NACELLE WEIGHT VS MASS FLOW

It was recognized early in the study that the aircraft high lift system would have a strong influence on the TR or TV system design. Consequently, the design study evolved into studies of TR and TV systems for the following lift systems for STOL transports:

1. externally blown flap (EBF)
2. mechanical flap + vectored thrust (MF + VT)
3. upper surface blowing (USB)

The various TR and TV systems for the high lift systems are discussed in the following sections.

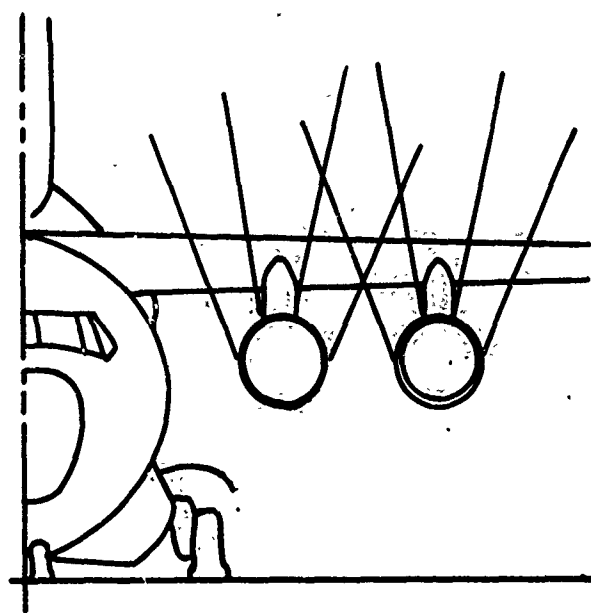
2.1.4.1 Flow Directional Control for STOL Transport Thrust Reverser Systems

STOL transports will operate on short, unimproved runways and will require thrust reversers as primary braking systems. Landing roll studies have shown that the reverser cutoff velocity, i.e. the velocity at which the engine must be shut down during reverse mode, has a strong influence on the airplane stopping distance. These studies have also shown that satisfactory stopping distance is achieved when the reversers are operated continuously at full rated takeoff power down to a rolling speed of at least 20 knots. In contrast, most commercial airplanes today must cut off the reverser or modulate the engine power setting below 60 knots. The cutoff velocity is determined primarily by engine tolerance to reverser exhaust reingestion and foreign object ingestion (dust and rocks from an unimproved field).

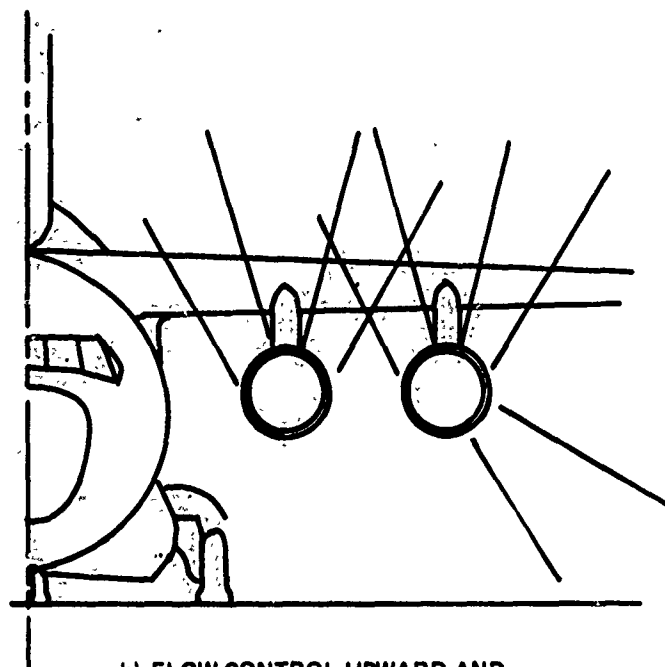
To avoid the problems of reingestion and foreign object damage at low ground roll speed, the thrust reverser must be designed to control the direction of the reverser exhaust away from the engine inlet, ground surfaces, and adjacent aircraft surfaces.

There are few regions in which the exhaust flow can be directed:

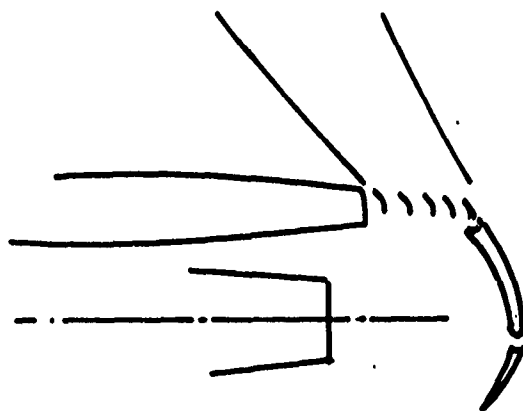
- 1) Upward and forward above the nacelle forward of the wing leading edge (Figure 14a) - - - This requires asymmetric exhaust flow with the corresponding problems of internal pressure losses, unsymmetrical structural loads and for a fan thrust reverser potential pressure distortion at the fan exit. An advantage to this type of flow control, however, is the additional gear loading obtained from the vertical thrust component of the exhaust flow which increases the braking forces.
- 2) Outboard side of outboard nacelle (Figure 14b) - - - Impingement on the ground outboard of the outboard nacelle may be allowable. For a two engine STOL aircraft this could be a



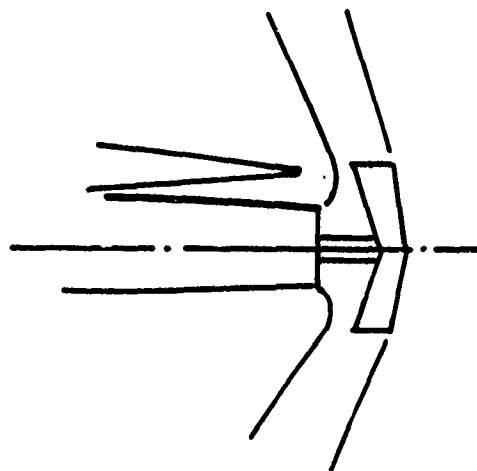
a) FLOW CONTROL UPWARD



b) FLOW CONTROL UPWARD AND
OUTBOARD (OUTBOARD NACELLE
ONLY)



c) UPWARD AFT OF WING
LEADING EDGE



d) AFT OF WING TRAILING EDGE

Figure 14: POSSIBLE REVERSER EXHAUST FLOW REGIONS TO MINIMIZE REINGESTION

satisfactory approach. However, left and right hand reverser designs would be required for either two or four engine aircraft.

3) All flow above the wing aft of leading edge (Figure 14c) - - - This requires apertures in the wing to direct the reverser flow upward and forward.

4) All flow aft of the wing trailing edge (Figure 14d) - - - This installation is ideally suited for a target thrust reverser. However, it will require removal of wing trailing edge flap sections to accommodate the extended nacelle.

The thrust reverser concepts were configured to meet the above flow directional control requirements.

2.1.4.2 Primary Thrust Reversing and Spoiling Options

Unmixed Flow Engines

It is well known that as the bypass ratio of a turbofan engine increases and the corresponding primary thrust decreases, the benefits derived from reversing the primary thrust diminish (Reference 5). This is shown in Figure 15. The curves were derived from engine data for the Pratt & Whitney Aircraft STF 342B (BPR 6.0), STF 342D (BPR 3.0) and STF 344 (BPR 12.0) unmixed flow engines (References 2 and 3).

Based on these results, the following guidelines were established for thrust reverser concepts for unmixed flow engines:

1. Bypass ratio 3.0 unmixed flow engines require thrust reverser systems for both the fan and primary flows.
2. A mechanical spoiler may be used to spoil the primary thrust of bypass ratio 6.0 unmixed flow engines.
3. A mechanical spoiler is recommended to spoil the primary of bypass ratio 12.0 engine. The spoiler may be eliminated provided fan reverser efficiency of at least 50 percent can be achieved.

"Cycle Spoiling" of Primary Thrust for Mixed Flow Engines

Thrust reverser systems for mixed flow engines present special design problems especially for high bypass ratio turbofan engines with the flow directional control requirements for a STOL transport. The major difficulty encountered is concerned with the design requirements of the blocker door mechanism. Because the exhaust duct for such engines is relatively large, the mechanism to block and turn the mixed exhaust flow becomes large and, therefore, is heavy. Also, the nacelle length must be extended to accommodate the reverser system for a mixed flow engine as shown in Figure 16a.

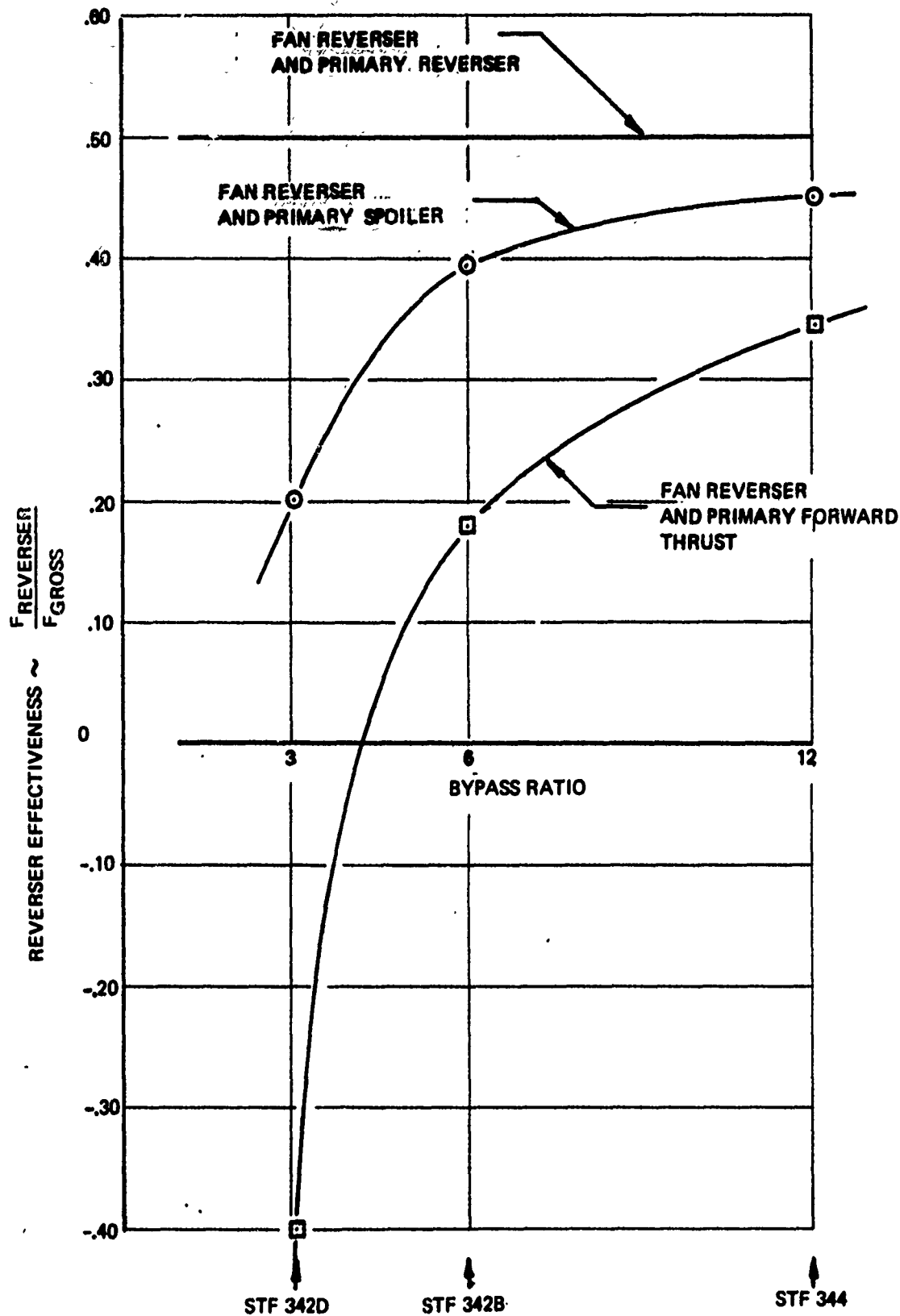


Figure 15: EFFECT OF PRIMARY REVERSE THRUST MODE ON REVERSER EFFECTIVENESS (η_R) BASIC = 50%

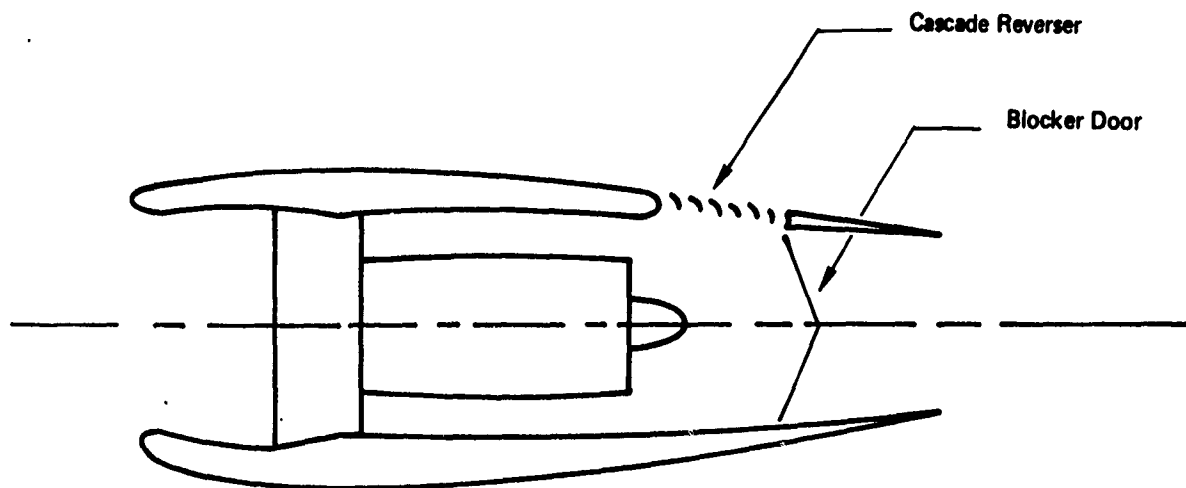


Figure 16-A: MIXED FLOW THRUST REVERSER

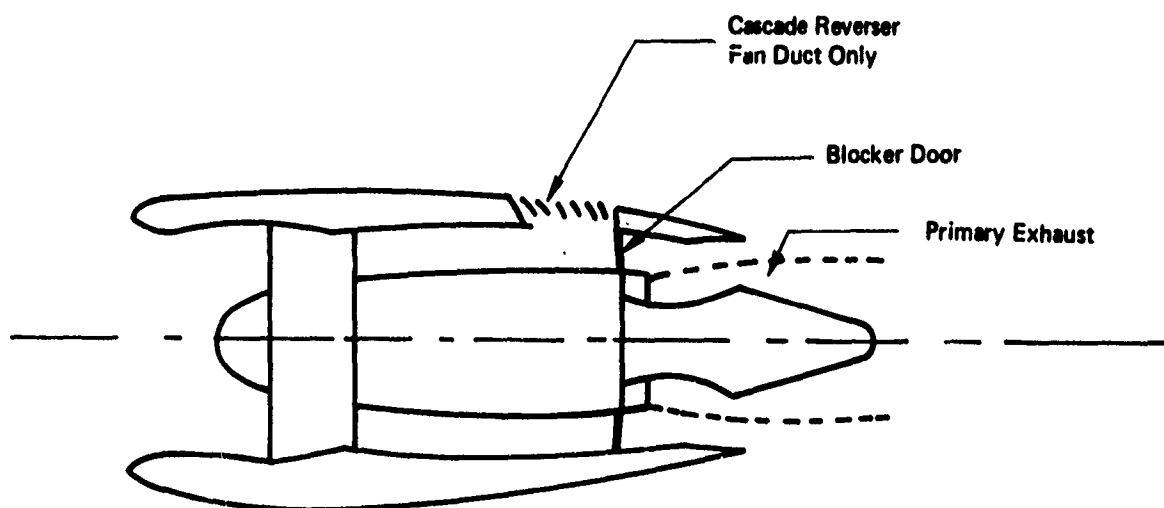


Figure 16-B: MIXED FLOW WITH FAN THRUST REVERSER AND CYCLE SPOILING OF PRIMARY THRUST

One method to reduce the nacelle length and weight involves reversing only the fan exhaust flow and allowing the primary flow to exhaust from the nozzle. This method is called "cycle spoiling" and is illustrated in Figure 16b. The effect of this operation is to cause the primary flow to be "over area" which spoils the primary thrust. A study of "cycle spoiling" was made by Pratt & Whitney Aircraft to assess the effects on engine performance and also to identify engine problem areas during reverse mode.

As a typical commercial mixed flow turbofan engine, the STF 402 is a fan-low-high, 2400°F T.I.T., BPR 5.0, 1.57 FPR mixed flow engine utilizing an advanced high spool core. Figure 17 shows STF 402 "cycle spoiling" operation in the reverse mode (separate streams) for various primary stream jet areas, and two values of fan duct exhaust area. A value of $A_{JE}/A_{JE}^* = 1.4$ is the size of the primary splitter area. It is believed that for most installations the primary flow will be controlled by the area of the primary splitter, A_{JS} splitter, and the remainder of the nozzle will fill up with ambient air. However, this will depend on the duct length between the splitter and the nozzle exit. If the duct is sufficiently long the controlling area could occur at the nozzle exit. Note that for $A_{JE}/A_{JE}^* = 1.10$ and $A_{JD}/A_{JD}^* = 1.0$, the separate stream engine cycle and performance coincides with the mixed flow engine. The engine must be throttled as primary area is increased to avoid low rotor overspeed. Note that the total thrust is dropping off as fan thrust remains about constant, indicating the primary thrust is being spoiled.

During the reverse operation the fan, low and high compressor may need more surge margin than during sea level takeoff steady state operation as inlet distortion is allowed to increase. Thus, the loss in low compressor surge margin shown in Figures 17 may be intolerable and would have to be rectified, probably with interstage bleed. There is no loss in fan or high compressor surge margin for the case where fan duct area is held constant. When the fan area is increased, the fan gains considerable surge margin.

The results shown in Figure 18 indicate that low rotor overspeed capability may be desirable. A comparison of the effect on performance during reverse if fan overspeed were designed for, and if fan overspeed is not allowed. This overspeed capability would have to be designed into the engine or reverse thrust would have to be applied at a reduced power setting such that $SLTO N_1$ would not be exceeded. If the overspeed capability were included it would be accompanied by a weight increase. Figure 19 shows the STF 402 sea level static low rotor speed characteristics at part throttle.

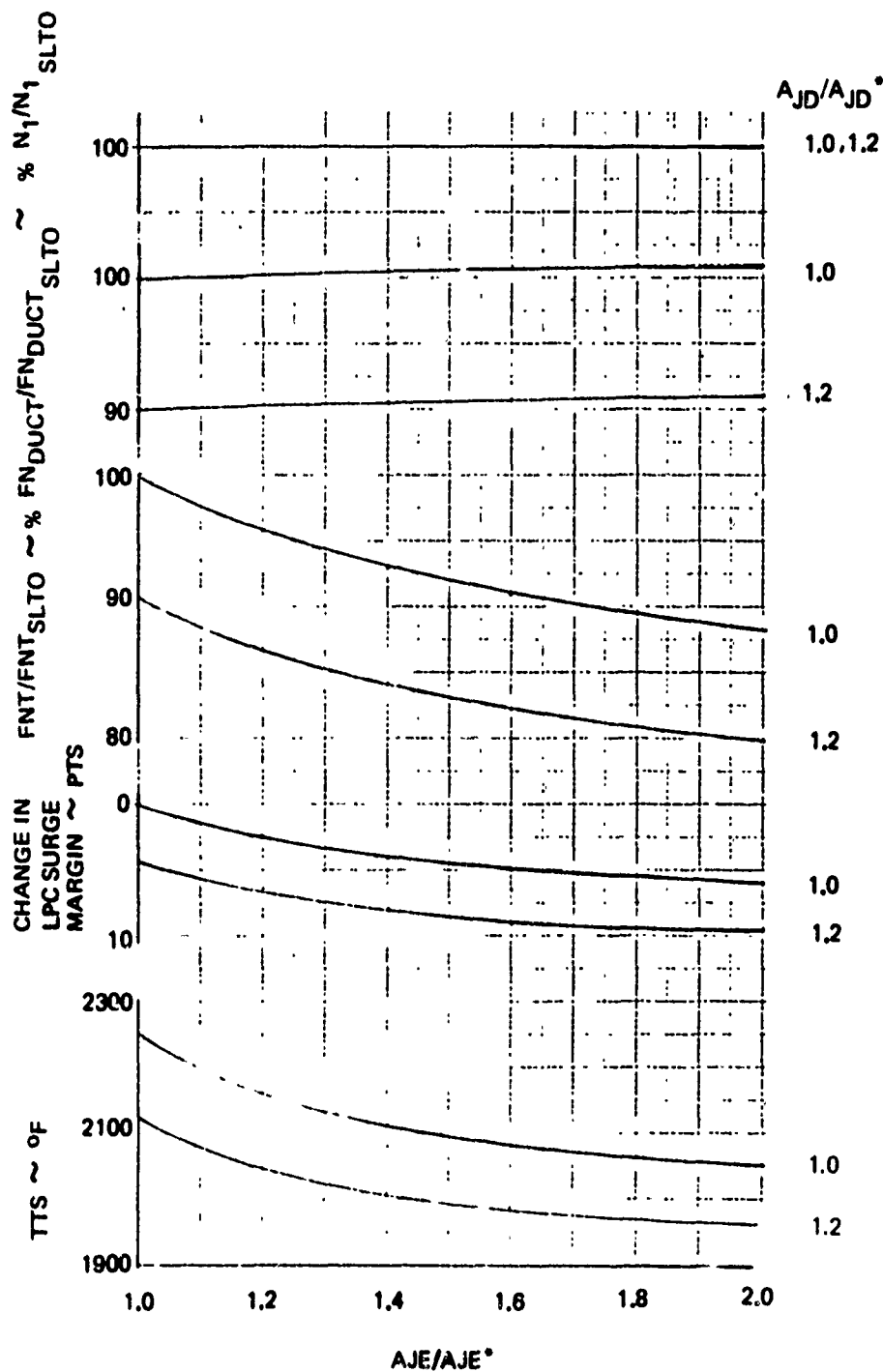
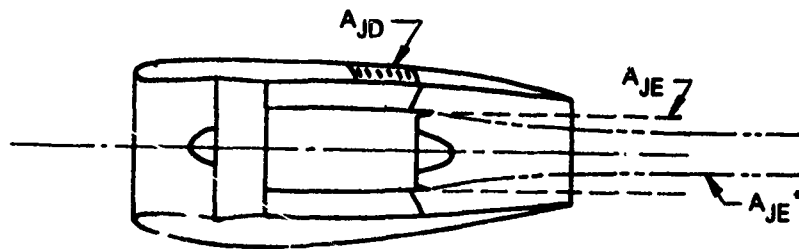


Figure 17: STF 402 REVERSE MODE

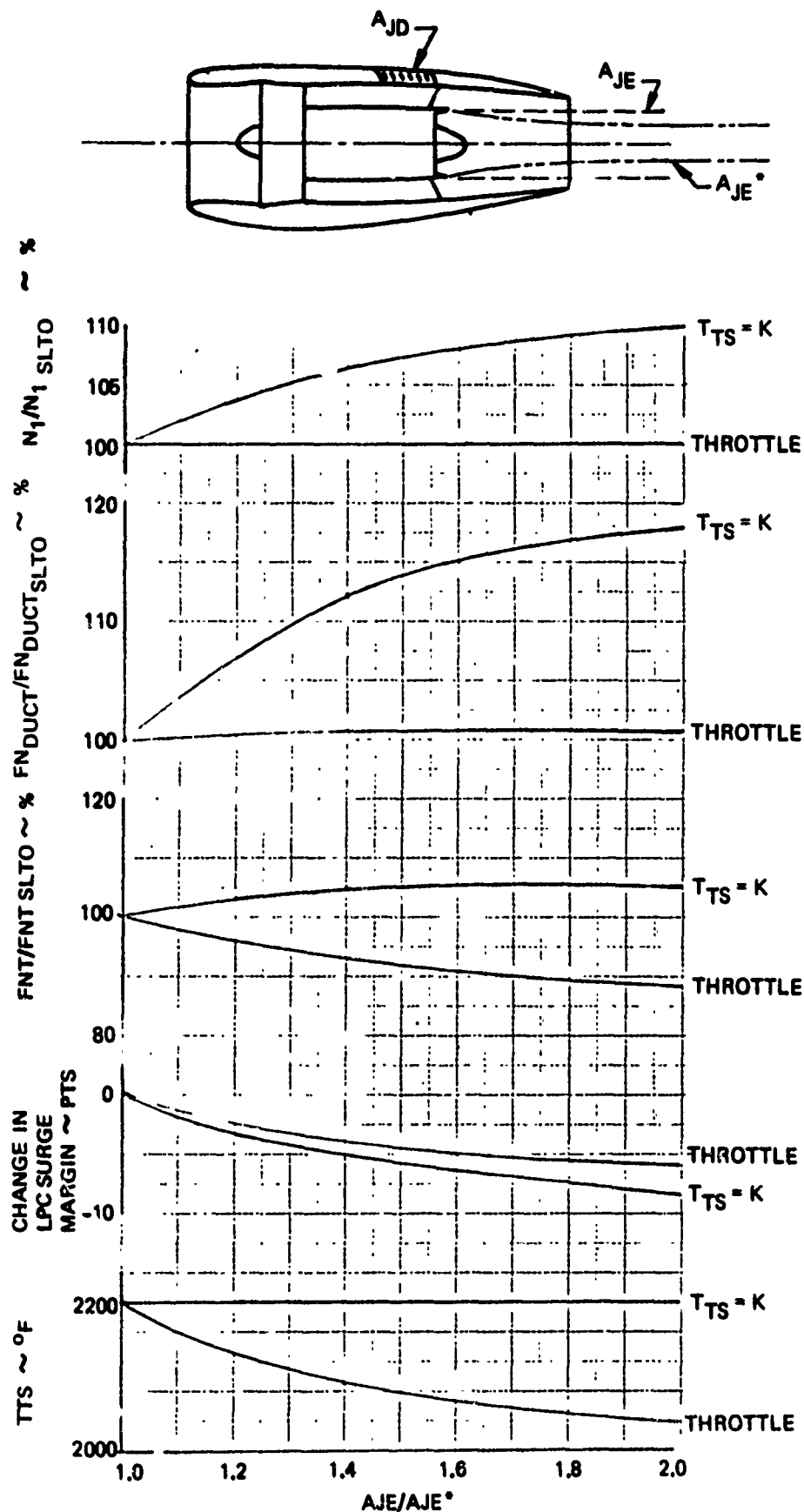


Figure 18: EFFECT OF ENGINE OVERSPEED STF 402 REVERSE MODE

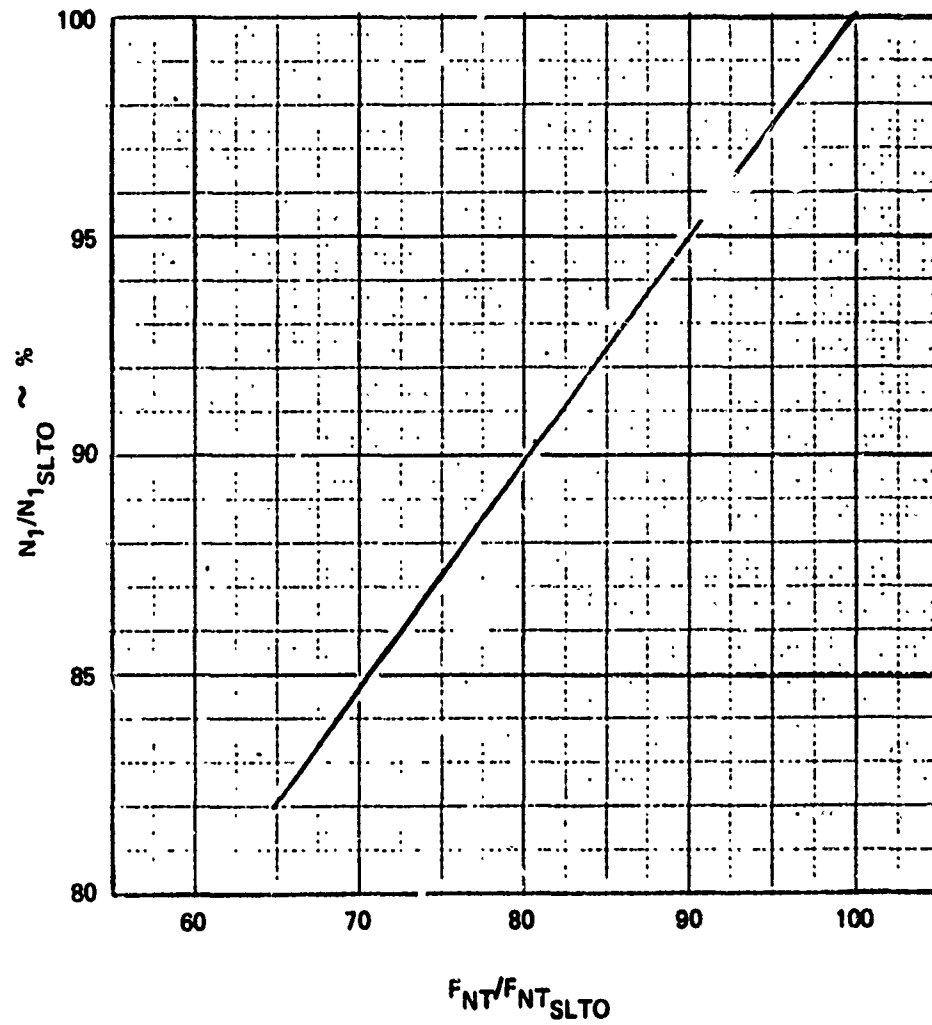


Figure 19: STF 402 LOW SPEED ROTOR CHARACTERISTICS, SEA LEVEL STATIC

Reverser effectiveness as a function of primary stream exhaust area is shown in Figure 20. If the primary flow matches to the primary splitter area, the reverser effectiveness is 23.8 percent and 24.1 percent for throttled and overspeed reverse modes, respectively, assuming the efficiency of the fan reverser is 50 percent. This reverser effectiveness is not sufficient to meet the landing field length for a STOL transport. Therefore, it appears that "cycle spoiling" would not be suitable for a BPR 5.0 engine.

Potential reverser effectiveness available using "cycle spoiling" for a BPR 6.0 engine was studied using a Boeing parametric engine computer program (References 5). An unmixed flow engine was used where the primary area was varied over a range of 0.85 to 1.70 of the equivalent primary flow area of a mixed flow engine. The results of the study are shown in Figures 21 and 22. As shown in Figure 22 reverser effectiveness of 32 percent could be expected for a bypass ratio 6.0 engine assuming the basic efficiency of the fan reverser is 50 percent. The operating point shown was determined for a mixed flow simulation of the STF 342B engine for which the area of the primary flow at the mixer was 4.163 ft². This area was assumed to be the controlling area of the primary stream during fan thrust reversing.

2.1.4.3 Landing Roll Analysis

A landing field study was conducted to assess the influence of reverser efficiency, cutoff speed, actuation delay time, and runway condition on landing roll distance. In addition, the effect of having a vertical thrust component during thrust reversing, and the affect of airplane gross weight on the landing roll distance was investigated. An existing Boeing computer program, TEM-036D (REference 6) was used for this purpose.

The analysis was based on the Model 953-758 baseline configuration and the STF 342B bypass ratio 6.0 engine performance.

Figures 23, 24 and 25 show the landing roll distance as a function of reverser efficiency, η_R , cutoff velocity, and delay time for icy field ($\mu = .10$), and wet field ($\mu = .30$) and dry field ($\mu = .40$) conditions respectively. The important parameters that effect the landing roll distance are the delay time and the reverser cutoff velocity. Significant gains in landing roll distance occur when the reverser cutoff speed is reduced from 40 to 20 knots. Below 20 knots, the gains in landing roll distance have less significance. Also, there are significant improvements obtained when the delay time is reduced to instantaneous actuation at touchdown. Each second of delay means approximately 100 feet of runway length required

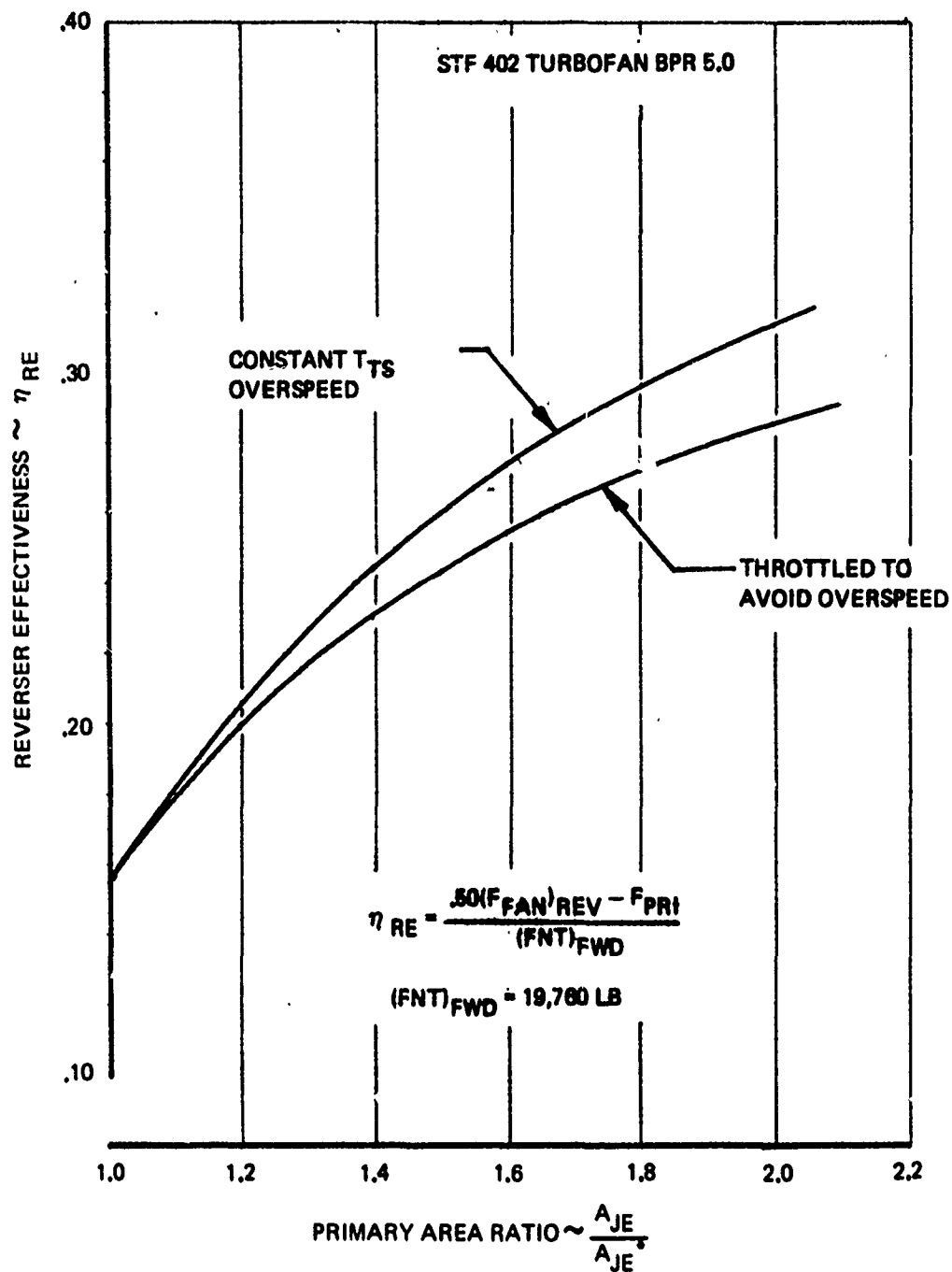


Figure 20: REVERSER EFFECTIVENESS STF 402 "CYCLE SPOILING"

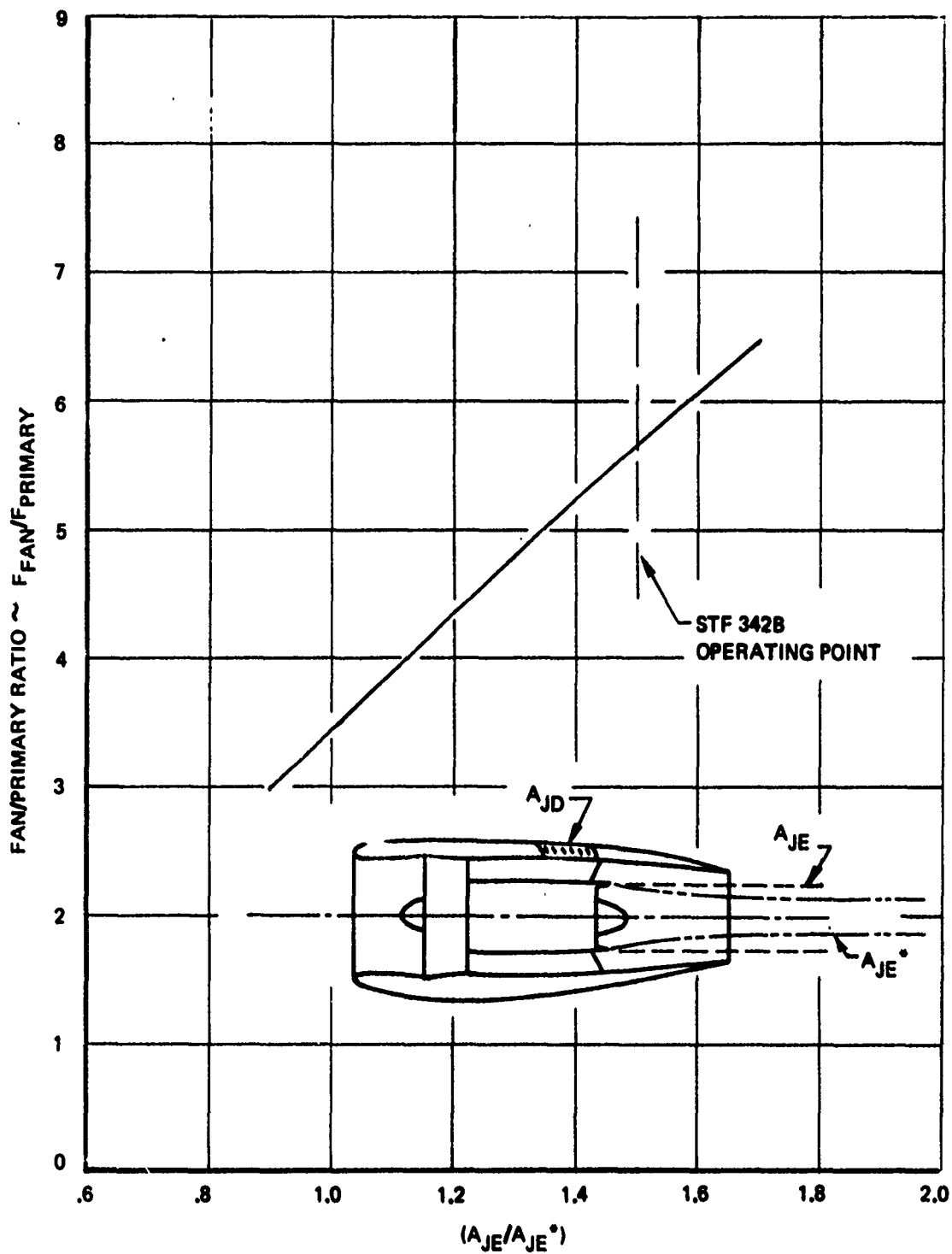


Figure 21: FAN/PRIMARY THRUST RATIO – PARAMETRIC UNMIXED FLOW ENGINE RESULTS

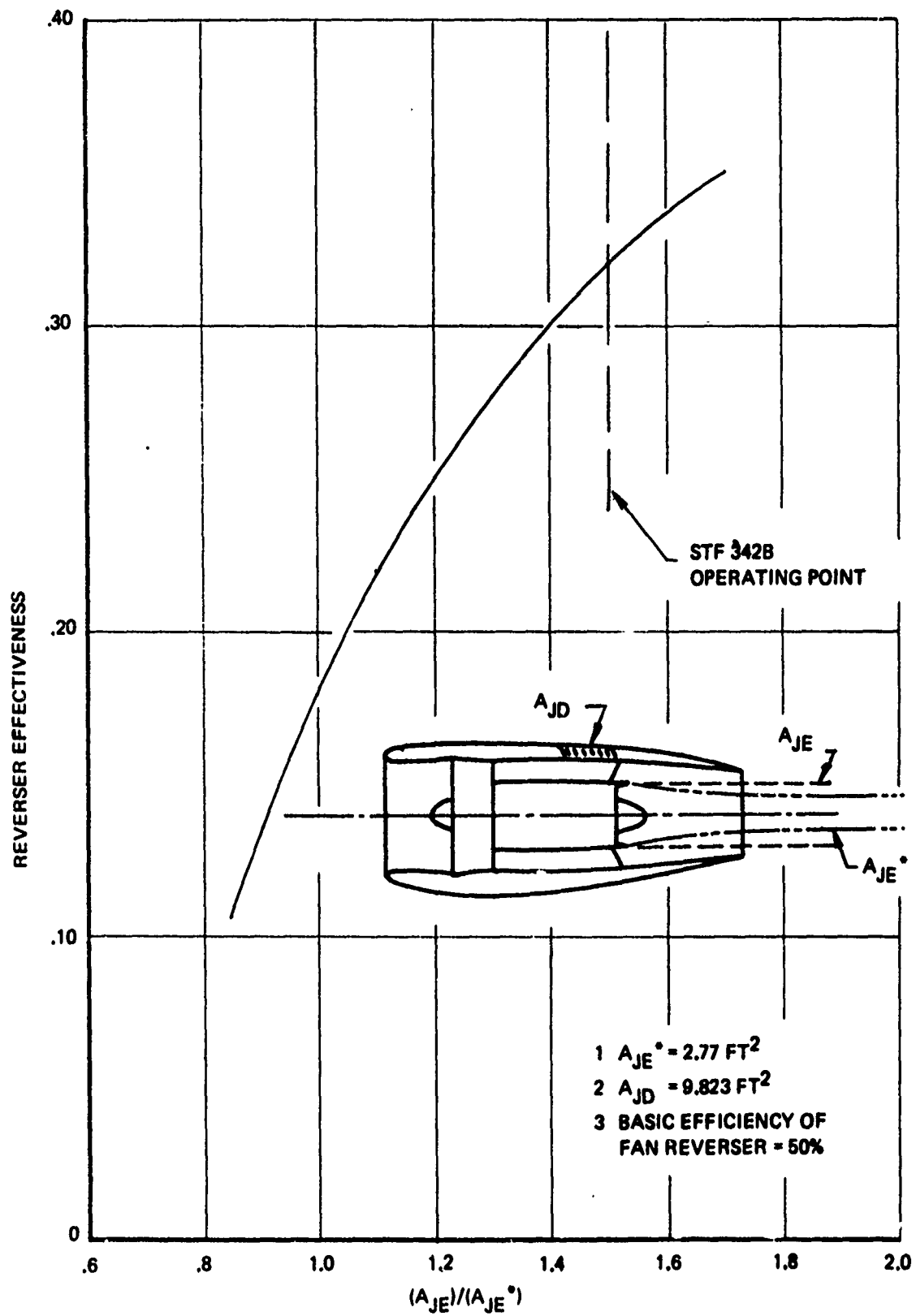
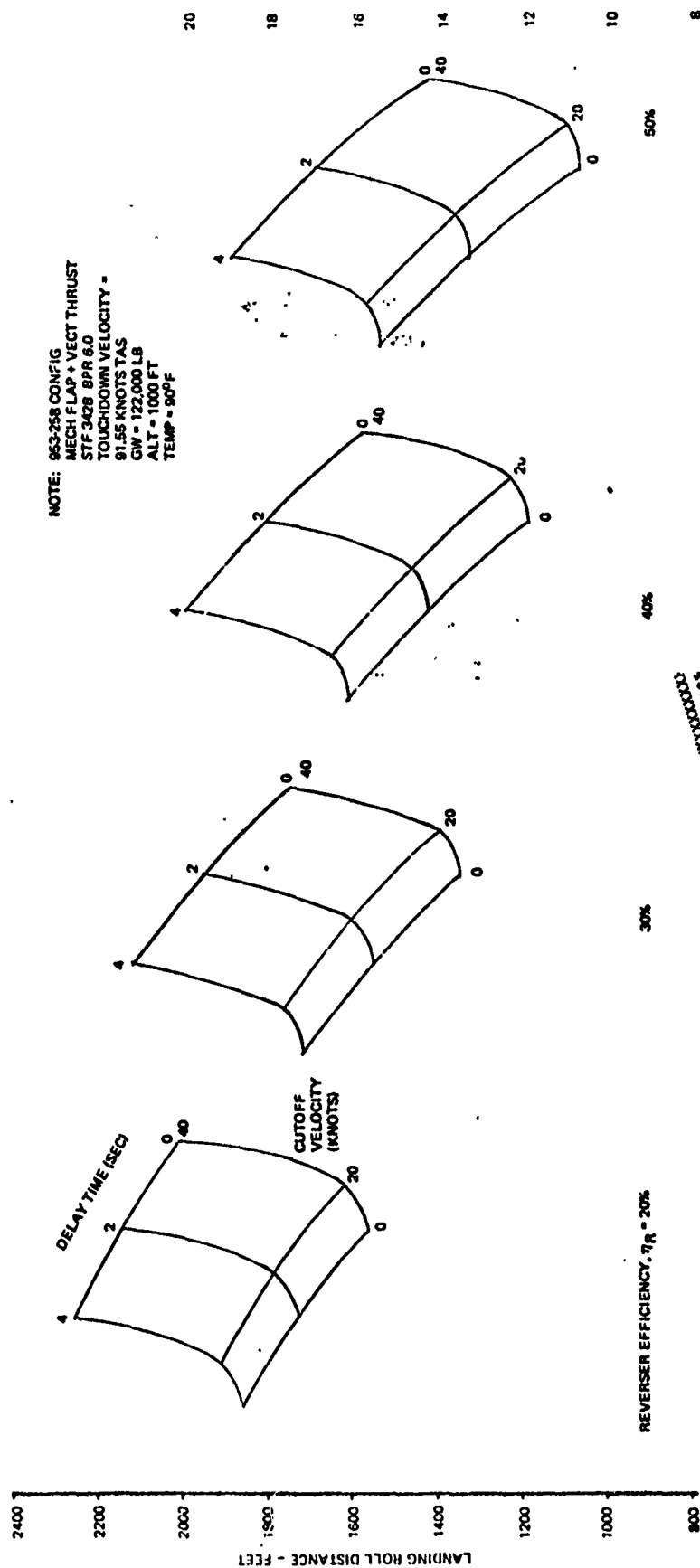


Figure 22: ESTIMATED REVERSER EFFICIENCY FOR "CYCLE SPOILING"



**Figure 23: LANDING ROLL DISTANCE
BRAKING COEFFICIENT, $\mu \leq .10$**

Mar 19 25 67

LANDING ROLL DISTANCE - FEET

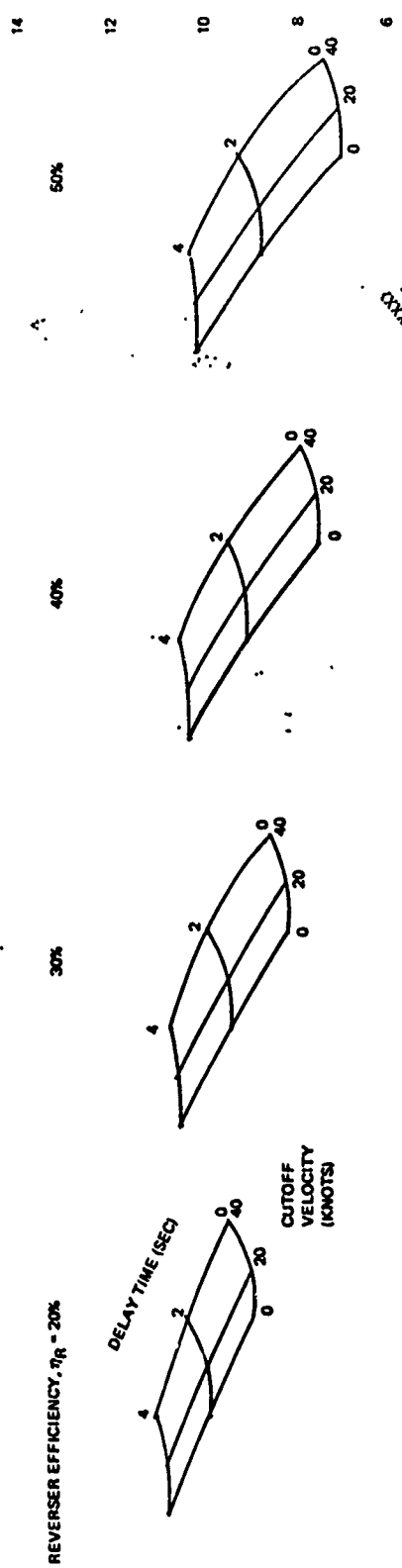
2000
1800
1600
1400
1200
1000
800
600

NOTE: 953-258 CONFIG.
MECH. FLAP + VECT. THRU
STF 3428 BPR 6.0
TOUCHDOWN VELOCITY =
91.55 KNOTS TAS
G.W. = 122,000 LB.
ALT. = 1000 FT.
TEMP. = 90° F

REVERSE EFFICIENCY, $\eta_R = 20\%$

DELAY TIME (SEC)

CUTOFF
VELOCITY
(KNOTS)



See the following pages
for greater detail.
XXXXXXXXXXXXXXXXXXXX

Figure 24: LANDING ROLL DISTANCE
BRAKING COEFFICIENT, $\mu = .30$

LANDING ROLL DISTANCE - FEET

NOTE: 953-258 CONFIG
MECH FLAP + VECT THRUST
STF 3428 BPR 6.0
TOUCHDOWN VELOCITY =
91.55 KNOTS TAS
GW = 122,000 LB
ALT = 1000 FT
TEMP = 90°F

REVERSE EFFICIENCY, $\eta_R = 20\%$

DELAY TIME (SEC)

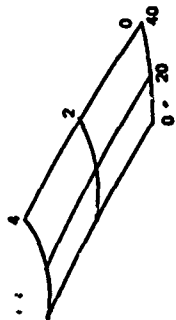


CUTOFF VELOCITY (KNOTS)

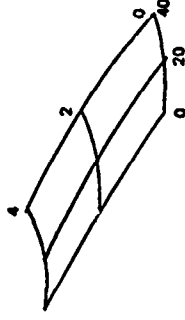
30%



40%



50%



See the following pages for greater detail.

Figure 25: LANDING ROLL DISTANCE
BRAKING COEFFICIENT, $\mu = .40$

to stop the airplane. Reverser efficiency has a lesser effect depending on the value of μ .

Based on these results, an optimum reverser system for STOL applications would have zero delay time, less than 20 knots cutoff speed, and an efficiency greater than 30 percent. It should be noted that this study assumes the fan and primary thrust is reversed. However, the results can be applied to spoiled primary thrust and fan thrust reverser systems by interchanging the reverser effectiveness for the system and reverser efficiency in the Figures.

As discussed in Section 2.1.4.1; flow directional control requirements for some reverser system will result in vertical force components during thrust reversal. The vertical component will place additional loads on the landing gear and will increase the braking forces. The effect of the vertical force component on landing roll distance is shown in Figure 26. Approximately 5 percent improvement in landing roll distance can be obtained with icy runway conditions and up to 10 percent improvements can be obtained under wet or dry field conditions.

The effect of airplane gross weight on landing roll distance is shown in Figures 27 for various runway conditions. These curves show that gross weight has a significant effect on landing roll distance.

2.1.4.4 Thrust Reverser Concepts for EBF Lift Systems

A total of four thrust reverser concepts were considered for an EBF system, each utilizing cascade thrust reversers for flow control. The concepts are shown in Figures 28 through 31.

An unmixed flow engine installation is shown in Figure 28. Thrust reversing is accomplished using a fan cascade thrust reverser and a mechanical primary thrust spoiler. The primary spoiler mechanism shown is similar to the spoiler used on the General Electric CF6-6 engine. It must be noted that other types of spoiler systems can be configured for the unmixed flow engine including target and blocker/deflector systems. A disadvantage of the primary thrust spoiler concept for high wing, four engine aircraft installation is that the primary flow would be directed to the side of the nacelle, which could result in impingement of the exhaust flow on the airplane fuselage and adjacent nacelles. This could result in higher reverser cutoff speed due to possible surface heating and reingestion problems.

A concept for a mixed flow engine installation is shown in Figure 29. This concept also uses a fan cascade thrust reverser to obtain the required flow directional control. "Cycle spoiling" is used to spoil the thrust of the primary flow.

953 - 258 CONFIG
 GW = 122,000 LB
 TOUCHDOWN VEL = 91.5 KTAS
 ALT = 1,000 FT
 TEMP = 90°F
 STF 342B BPR 6.0
 EFFECTIVE VERTICAL THRUST
 ANGLE = 50°

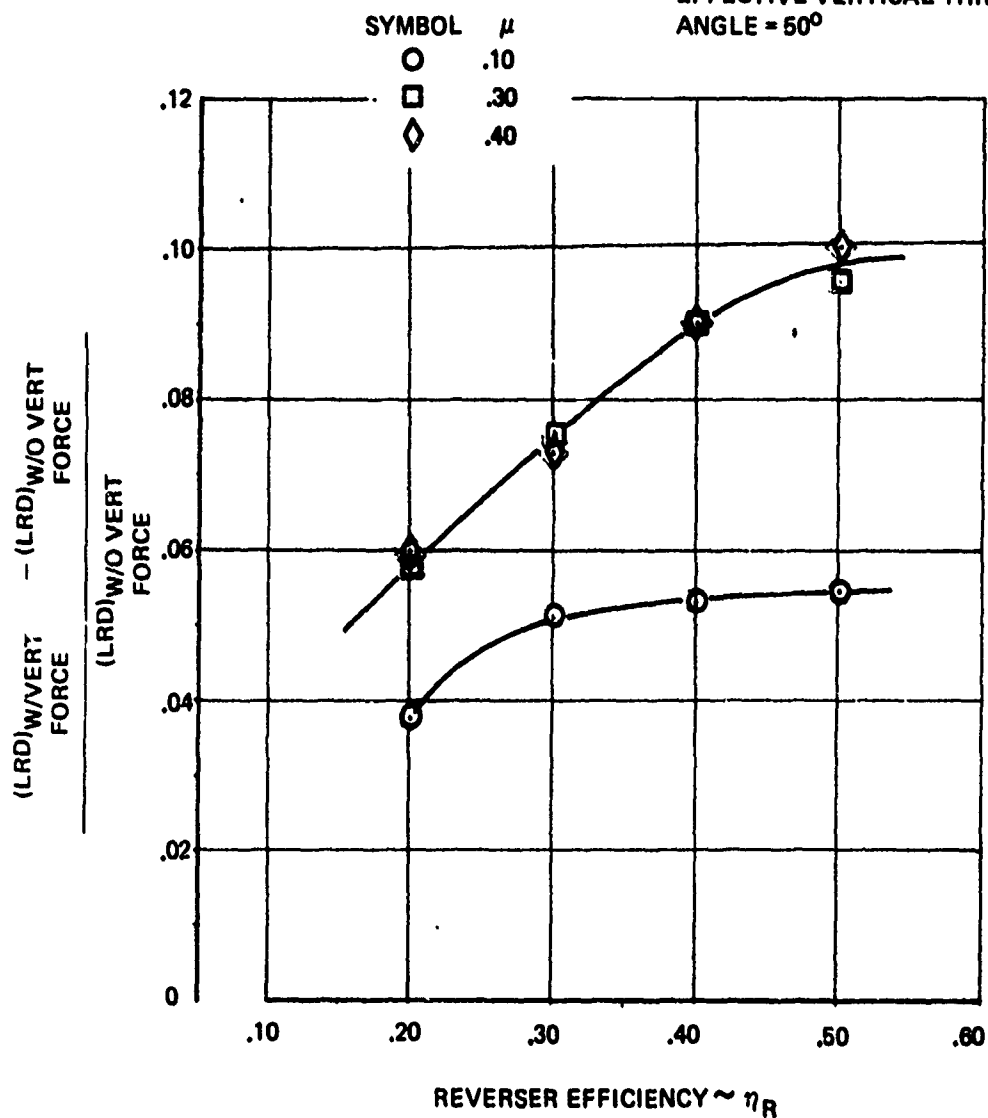


Figure 26: EFFECT OF VERTICAL FORCE COMPONENT ON LANDING ROLL DISTANCE

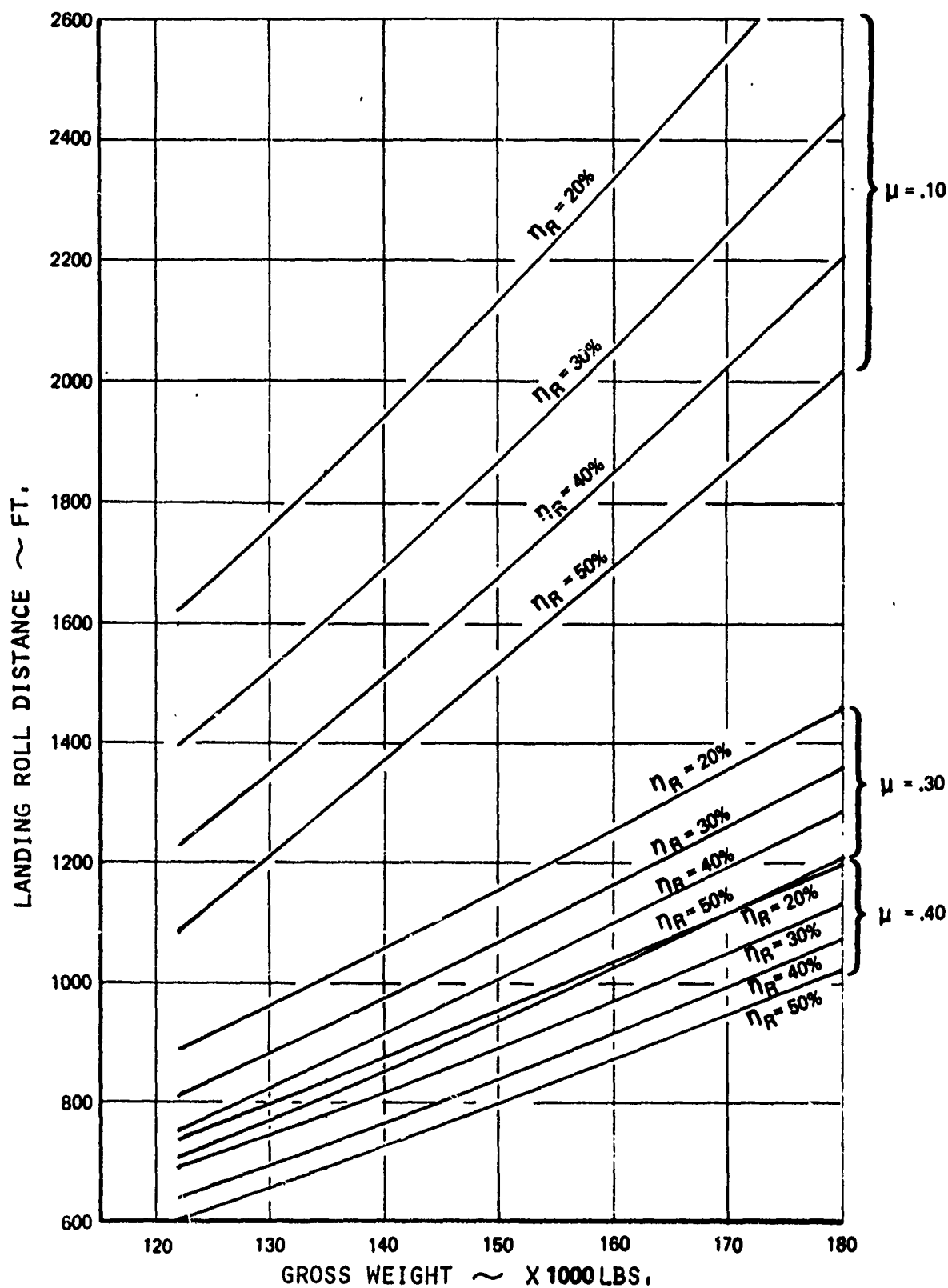


Figure 27: EFFECT OF AIRPLANE GROSS WEIGHT ON LANDING DISTANCE

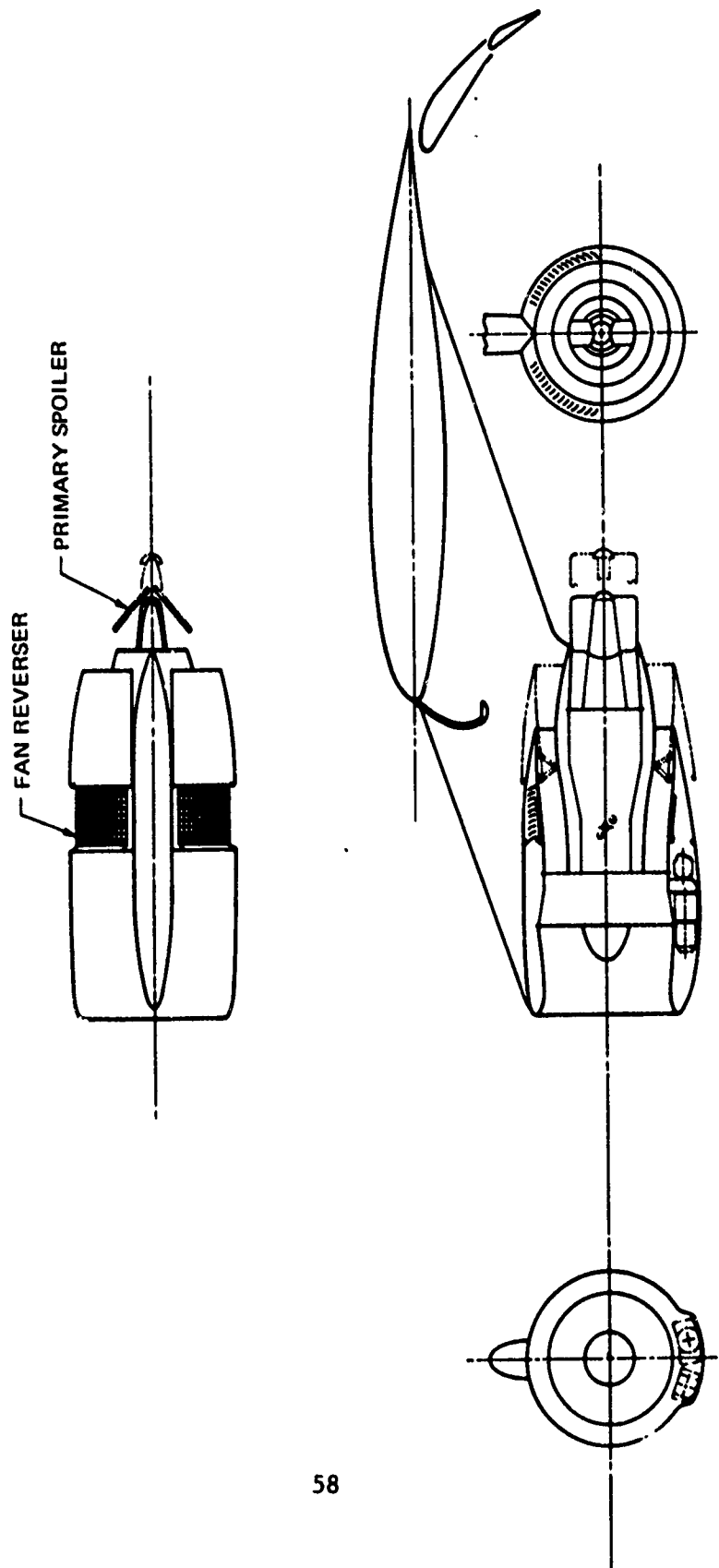


Figure 28: THRUST REVERSER CONCEPT – BPR 6 ENGINE UNIMIXED FLOW

R. L. WILSON	W/16/71	THRUST REVERSER CONCEPT – BPR 6 ENGINE UNIMIXED FLOW
		TR/TV-PP-02

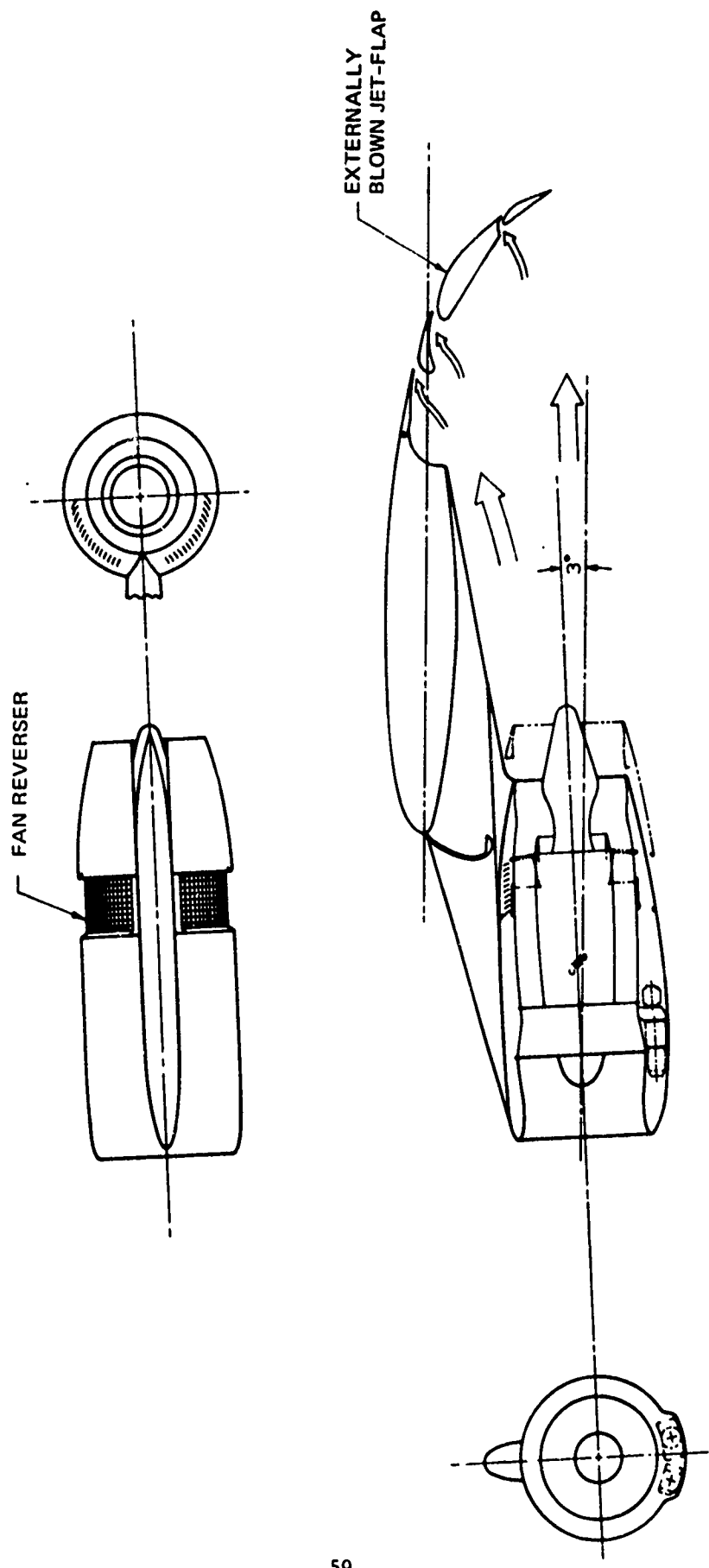


Figure 29: THRUST REV & EBF CONCEPT - BPR 6 ENGINE MIXED FLOW

R. L. WILSON	11/19/71	THRUST REV & EBF CONCEPT -
		BPR 6 ENGINE
		MIXED FLOW
		TR/TV-PP-03

The thrust reverser concept shown in Figures 28 and 29 utilize a translating cowl and blocker door mechanism similar to the mechanism used on the Boeing 747/JT9D primary flow thrust reverser (Reference 7). The cascades are fixed in the upper 180° sector of the nacelle and the cascade strongbacks are skewed to provide the required flow control upward. Air driven ball-screw actuators are used to translate the fan cowl aft exposing the cascade vanes. As the cowl translates, a drag link mechanism deploys the blocker doors. The reverser cascades are constructed of cast aluminum vanes and the blocker doors are constructed of aluminum honeycomb panels.

The difficulties of designing a thrust reverser system for mixed flow turbofan engines that reverse the total fan and primary flows are demonstrated by the concepts shown in Figures 30 and 31. Concept-14, shown in Figure 30 uses a conventional clamshell blocker door mechanism similar to the type used on the Boeing 727/JT8D and Boeing 707/JT3D thrust reverser systems. Two clamshell blocker doors with a central pivot block the engine and fan exhaust flow and divert the flow through the upper portion of the nacelle. Fixed cascades are exposed when the clamshell is deployed. This technique is not compatible with the reverser exhaust flow control requirement because the cascade aperture is too long and the clamshell cannot seal the entire cascade during cruise mode. Also, during reverse mode the clamshell blocks a portion of the available cascade flow area. An alternate design for a mixed flow engine is shown in Figure 31. A translating sleeve and fixed plug block the mixed flow and primary flows during thrust reversing. Fixed cascades provide the required flow directional control. Air driven ball-screw actuators are used to translate the cowl sleeve. The thrust reverser cascade vanes, inner surface of the translating sleeve and fixed plug are constructed of steel. This concept eliminates blocker doors and linkages and also eliminates the problems encountered with the clamshell mechanism.

2.1.4.5 Thrust Reverser and Thrust Vectoring Systems for MF+VT Lift Systems

Thrust reverser and thrust vectoring concepts for mechanical flap and vectored thrust lift systems included single pod concepts for BPR 3.0, 6.0, and 12.0 engines, and dual pod concepts for BPR 3.0 engines. Eleven concepts were evaluated, Figures 32 through 44.

Mixed Flow Engines --- Single Pod

The design options available to the designer are basically either to combine the functions of the thrust vectoring and thrust reversing system into a single mechanism or to separate

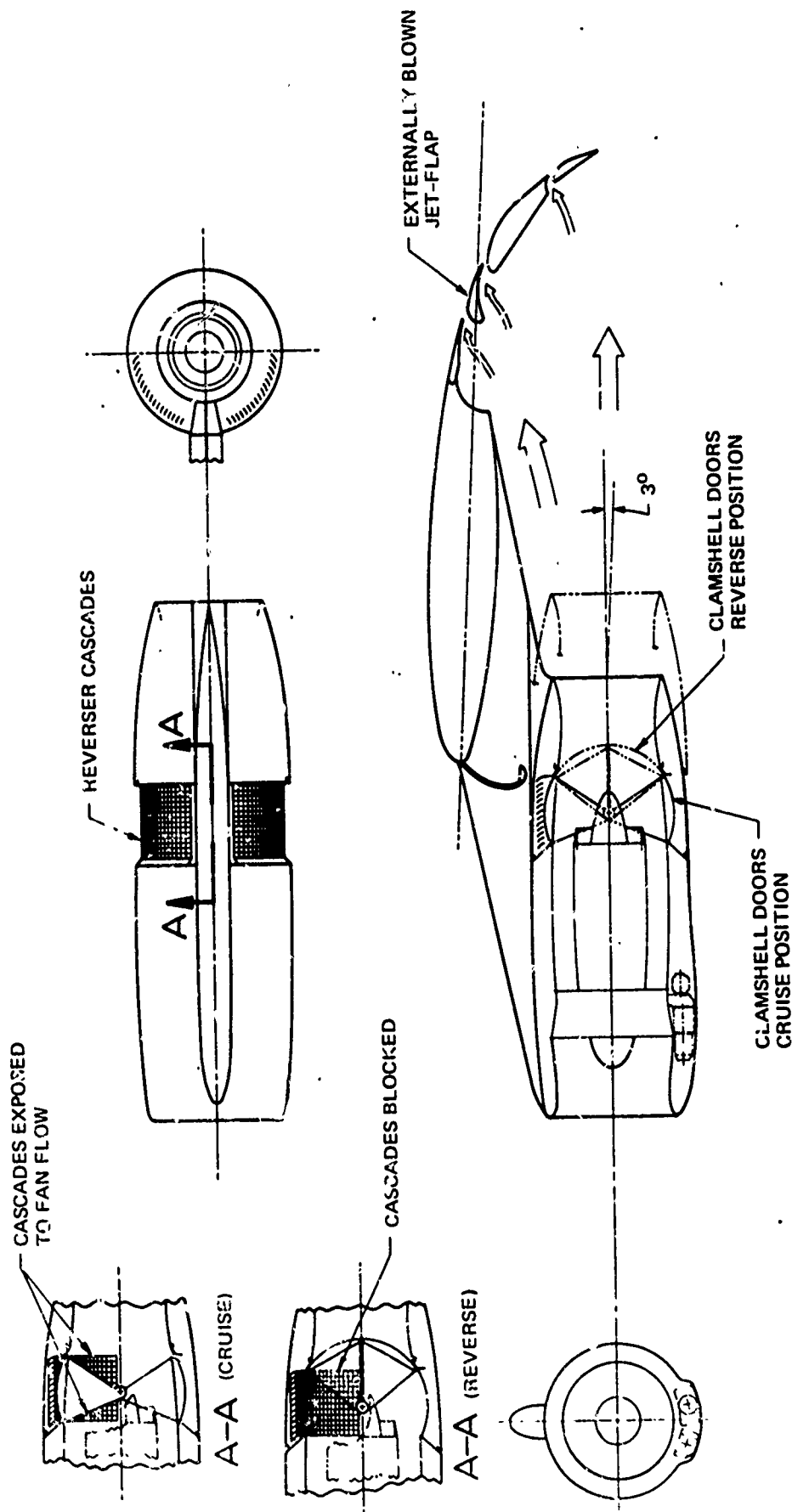


Figure 30: CLAMSHELL THRUST REVERSER & EBF CONCEPT —
BPR 6 MIXED FLOW ENGINE

R.L. Wilson	2/11/72	CLAMSHELL THRUST REVERSER & EBF CONCEPT — BPR 6 MIXED FLOW ENGINE
SCALE: 1/40		TR/TV — PP-14

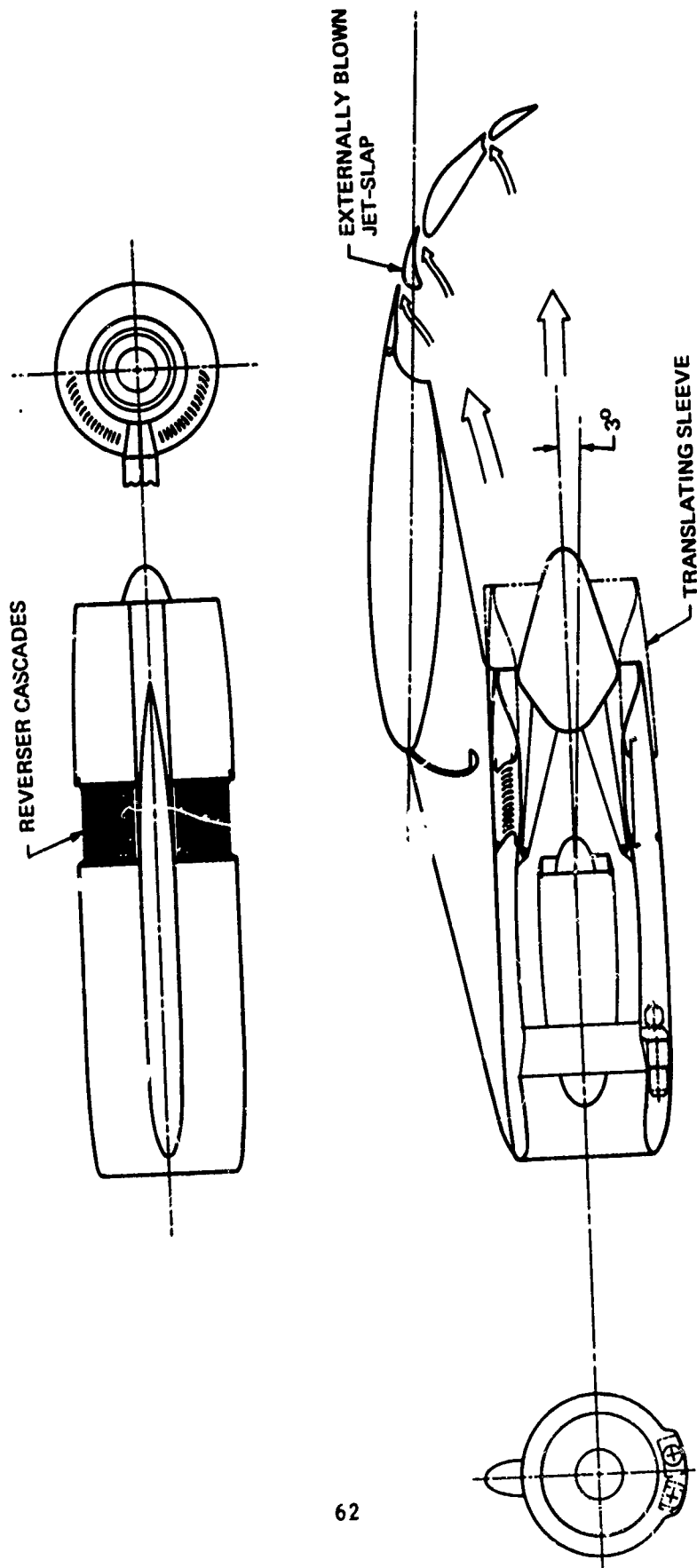
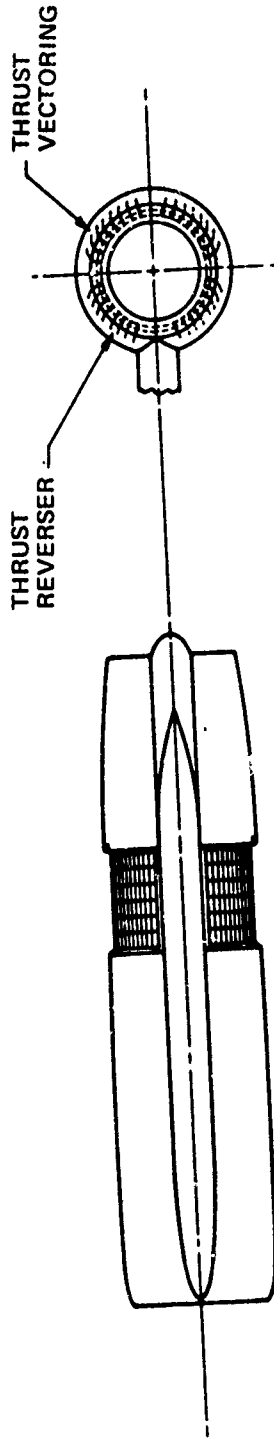


Figure 31: TRANSLATING SLEEVE T/R & EBF CONCEPT -
BPR 6 MIXED FLOW ENGINE

R.L. Wilson	3/22/74	TRANSLATING SLEEVE T/R
		& EBF CONCEPT
		B.P.R. 6 MIXED FLOW ENGINE
SCALE: 1/40		TR/TV-PP-16



ROTATING VALVE FOR
SELECTING T/R OR T/V MODE

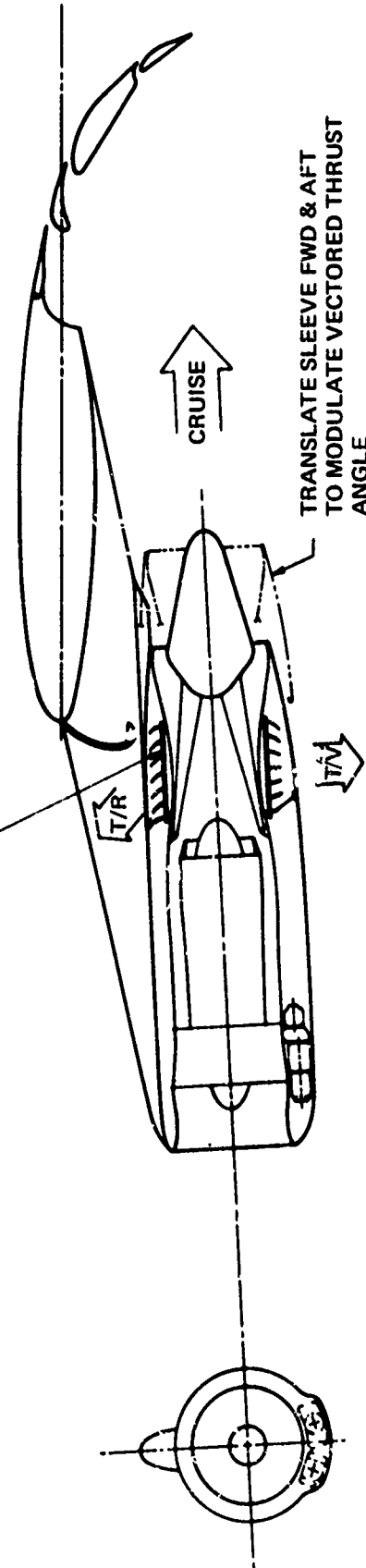
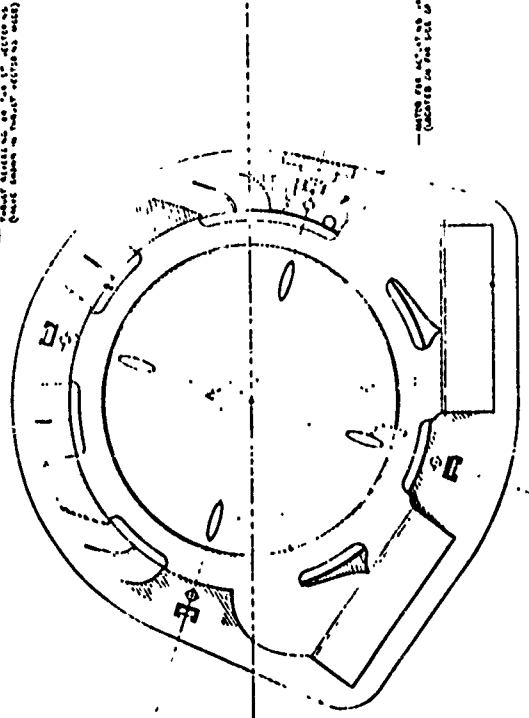
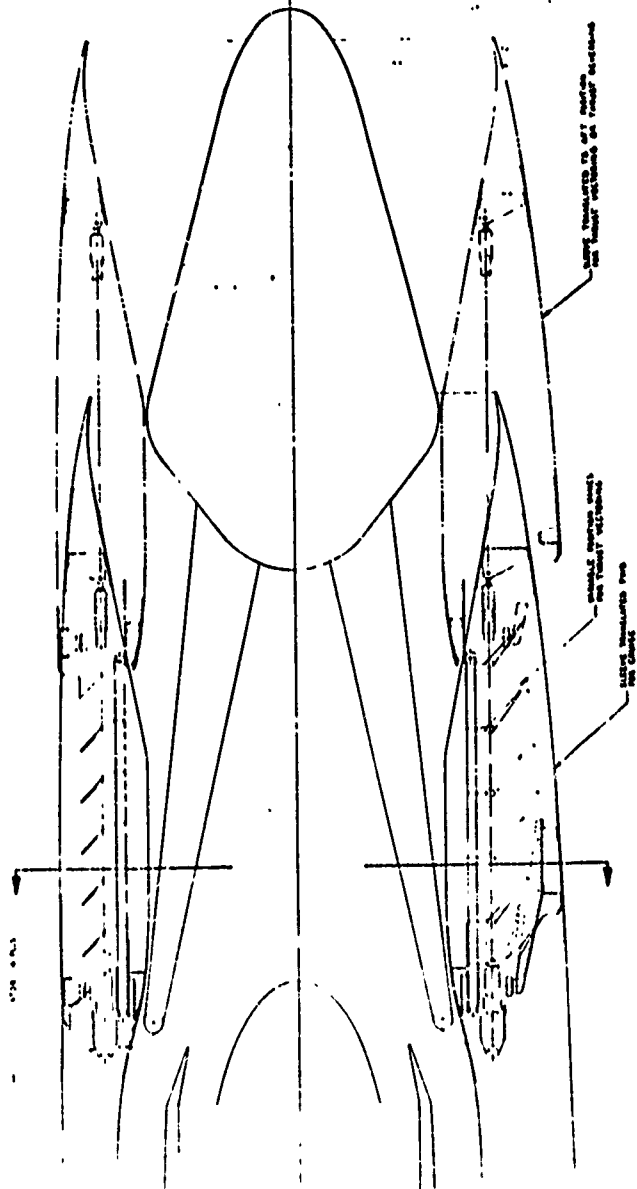


Figure 32: THRUST REV/THRUST VECTORING CONCEPT -
BPR 3 ENGINE MIXED FLOW

R. L. WILSON	11/29/71	THRUST REV/THRUST VECTORING CONCEPT - BPR 3 ENGINE MIXED FLOW
		TR/1 v-PP-05



section A-A

Figure 33: THRUST REVERSING/THRUST VECTORING SYSTEM
ROTATING VALVE SELECTOR

See the following pages
for greater detail.

REVISED	DATE	BY	REASON
1	10-1-66	J. H. P.	THRUST REVERSING/THRUST VECTORING SYSTEM
2	10-1-66	J. H. P.	ROTATING VALVE SELECTOR
3	10-1-66	J. H. P.	ROTATING VALVE SELECTOR

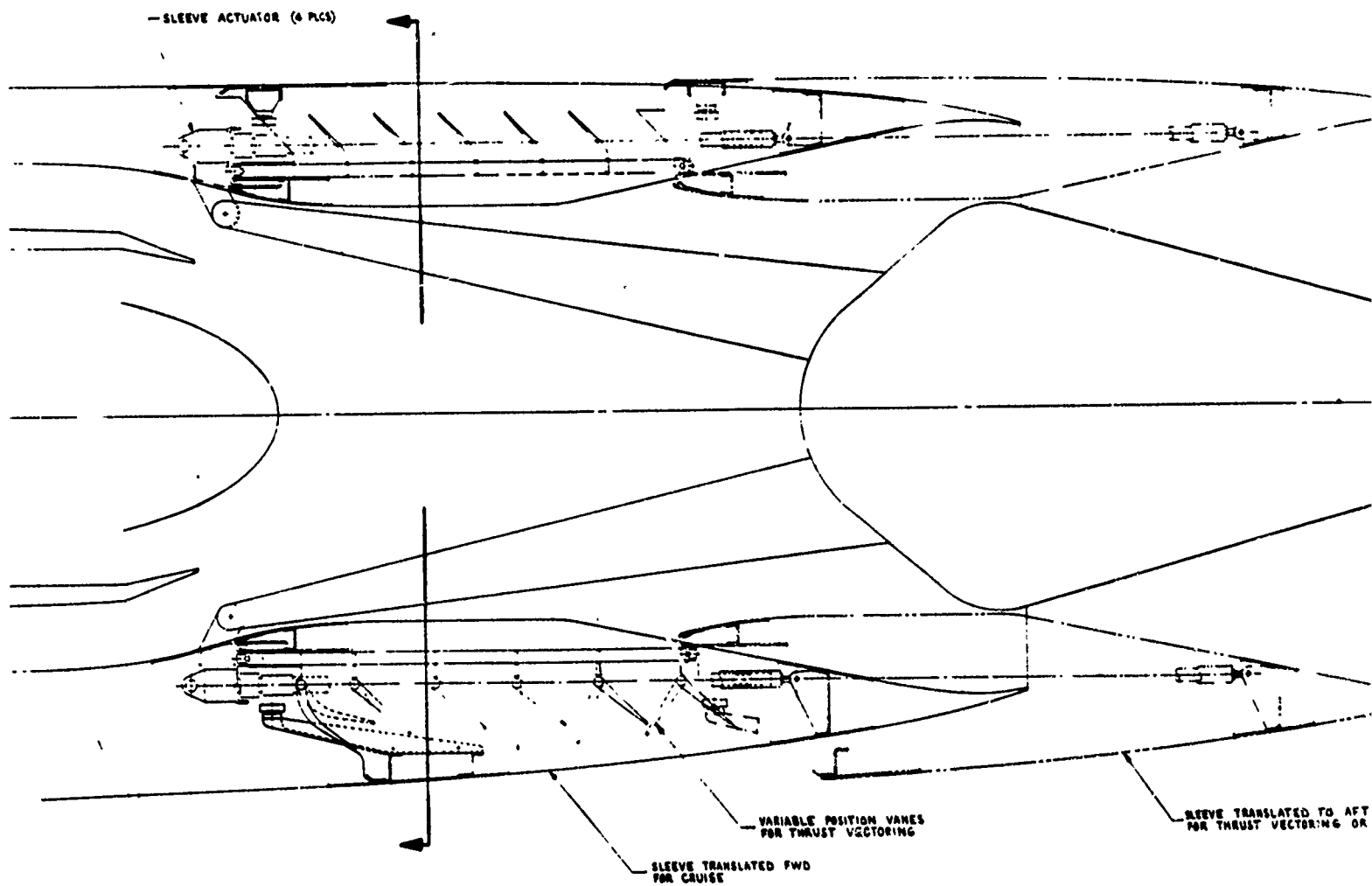


Figure 3.

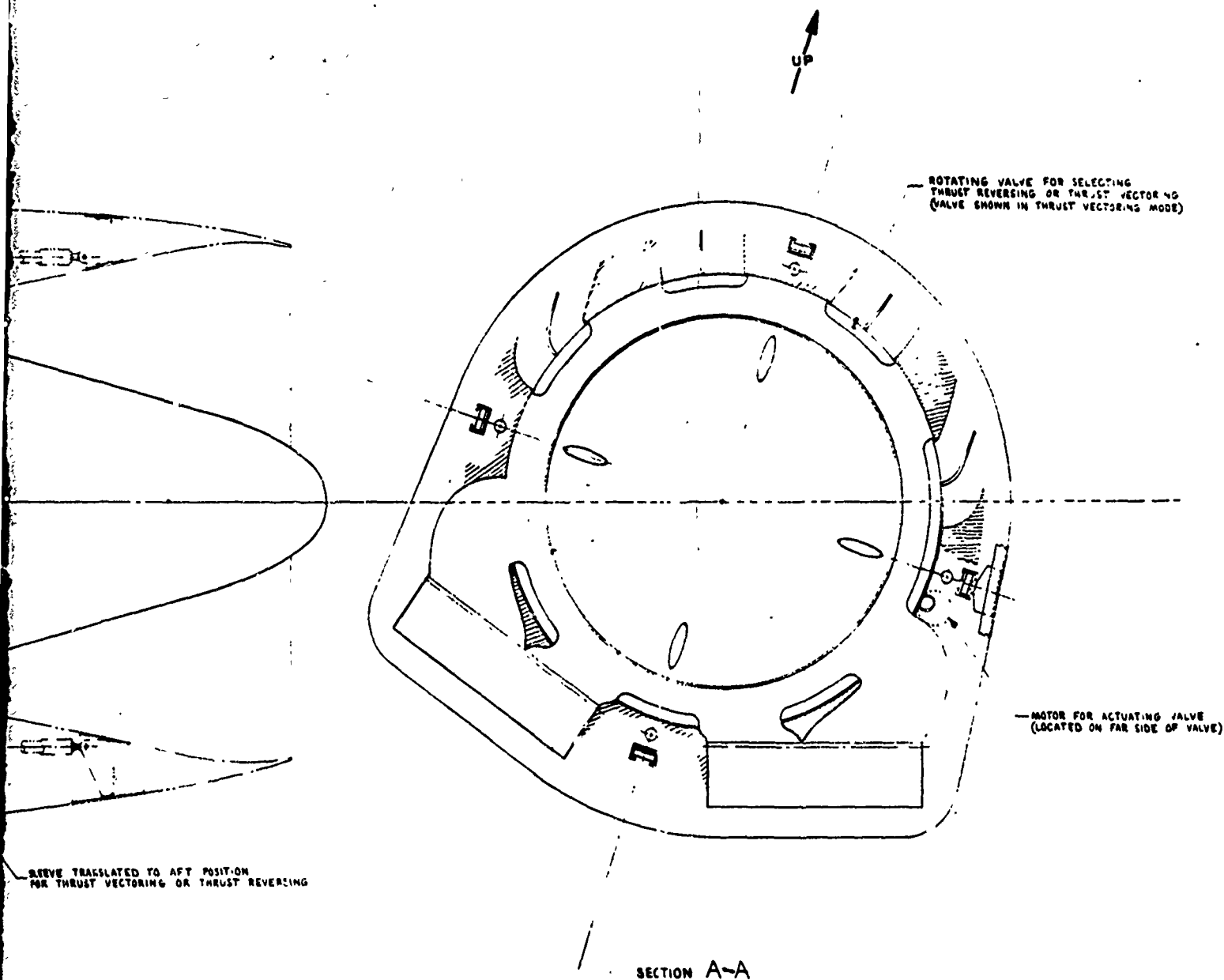
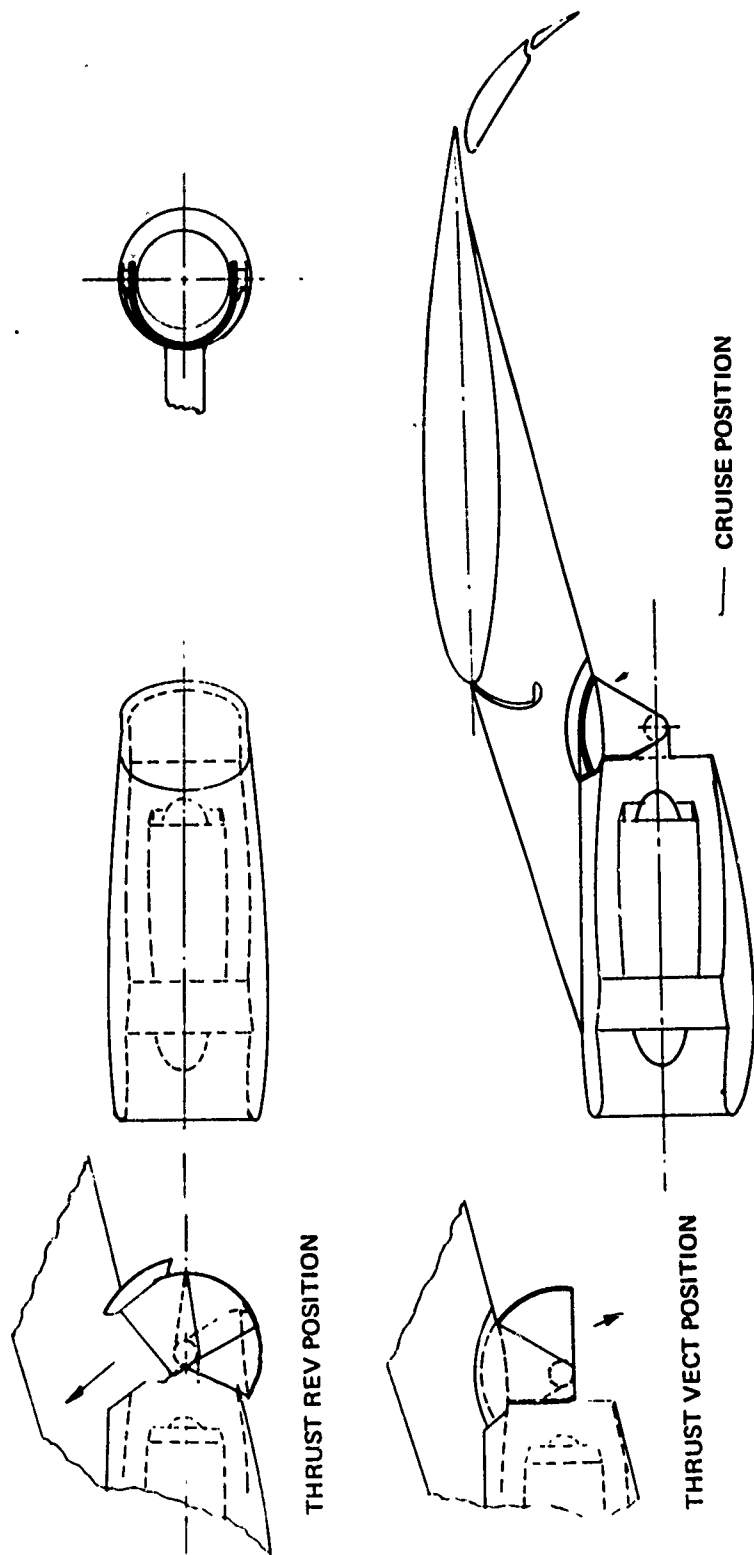


Figure 33: THRUST REVERSING/THRUST VECTORING SYSTEM ROTATING VALVE SELECTOR

DESIGNER		DATE	
E.L. WILSON (11-71)		11/11/71	
CHECKED		DATE	
E.L. WILSON (11/11/71)		11/11/71	
APPROVED		DATE	
E.L. WILSON (11/11/71)		11/11/71	
PROJECT NO.		PROJECT NO.	
2-2541-PD-211		2-2541-PD-211	



J.E. Perry	2/24/71	EXTERNAL DEFLECTOR TR/TV CONCEPT - BPR 6 MIXED FLOW ENGINE
		TR/TV - PP - 19
	SCALE 1/40	

Figure 34: EXTERNAL DEFLECTOR TR/TV CONCEPT -
BPR 6 MIXED FLOW ENGINE

the thrust reversing and vectoring function and provide a complete design for each system. The combined TR/TV is perhaps the most desirable approach primarily because of the potential weight savings and reduced mechanical systems required. For example, a single actuation system and control may be utilized for a combined TR/TV system where two actuation and control systems are required for separate TR and TV installations. However, it is probable that the combined TR/TV system will require more mechanical complexity to include both functions.

Separate thrust reverser and thrust vectoring systems that require a common exhaust duct will require additional nacelle length, and will result in a high weight installation. An alternate to separate thrust reverser and vectoring system is the "cycle spoiling" thrust reverser technique. "Cycle spoiling" allows satisfactory flow directional control to be achieved with a shorter overall nacelle and less weight. This technique was utilized on several of the concepts to obtain the lightest weight system possible.

A combined thrust reverser and vectoring concept for a BPR 3.0 mixed flow engine is shown in Figure 32. Cascades apertures in the upper half of the nacelle direct the flow upward and forward for thrust reversing. Cascades on the bottom of the nacelle direct the flow down and aft for thrust vectoring. Continuous thrust vector angle modulation between 45 and 90 degrees is provided by variable angle cascades. Area match is maintained by a mechanism that opens additional blade rows in the 45 degree position. The TR or TV mode is selected by an annular rotating valve. A translating sleeve covers the TR and TV apertures during the cruise mode and also blocks the flow by contacting the fixed position plug during the TR and TV mode. A detailed design of the concept is shown in Figure 33. The thrust reverser and thrust vectoring cascade vanes and the rotating selector valve are constructed of steel. Air driven ball-screw actuators are used to translate the sleeve fore and aft. An electric motor and linkage is used to actuate the rotating selector valve.

Another combined thrust reverser and vectoring system concept is shown in Figure 34. The system consists of three deflector doors (inner, middle, and outer) mounted aft of the exhaust nozzle and utilizing common hinge points. The inner and outer doors are geared together through a hub mounted planetary gear train (3:1 ratio). The middle and outer doors are linked together through a dwell mechanism to allow the middle door to rotate 75° before the outer door moves. A detailed schematic of the mechanism and deflector door position is shown in Figure 35. The middle door is driven by two ball screw jacks and the first 75° rotation produces 0 through 75° vectored thrust. The next

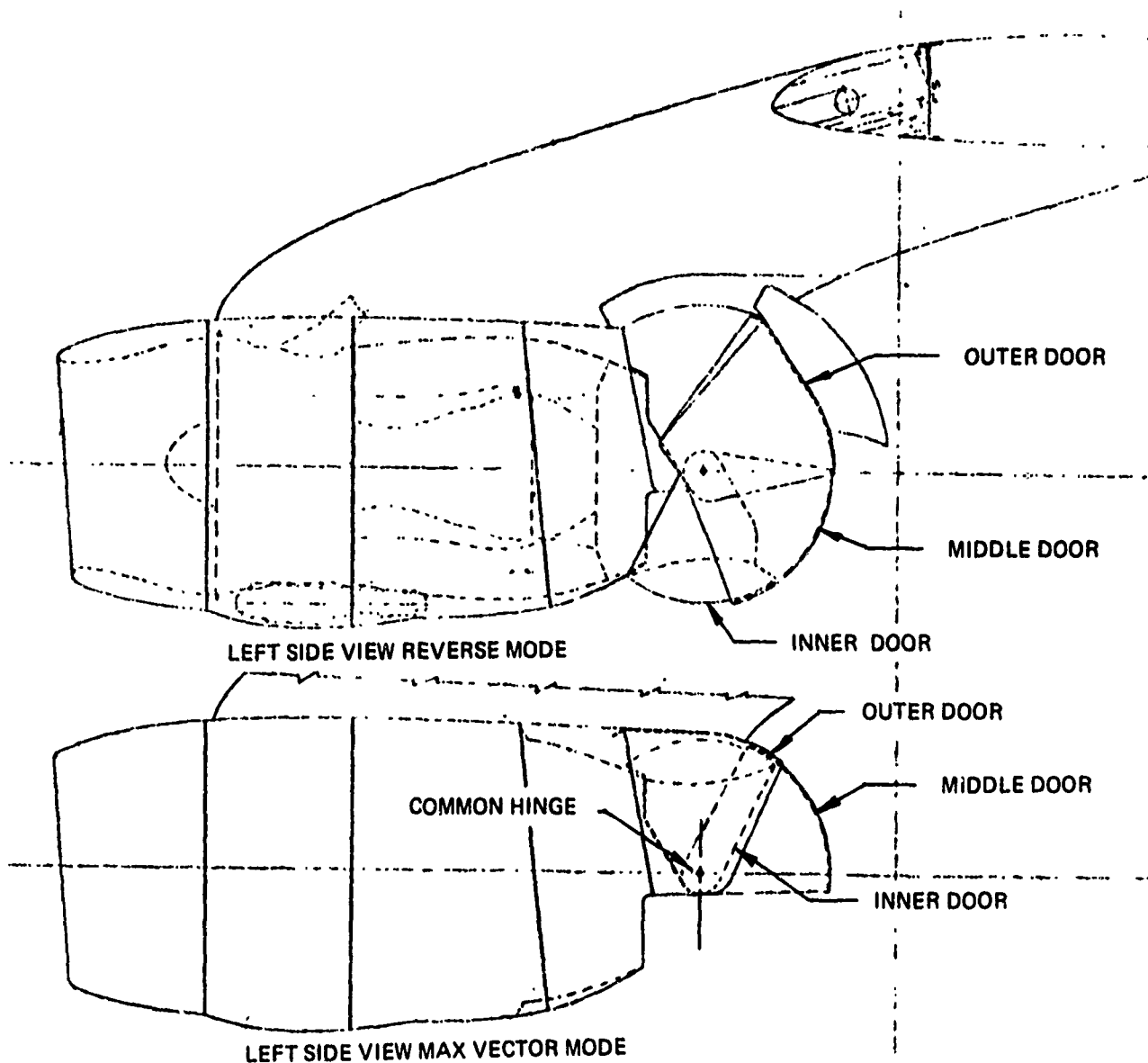


Figure 35: COMMON HINGE EXTERNAL DEFLECTION TR/TV SYSTEM

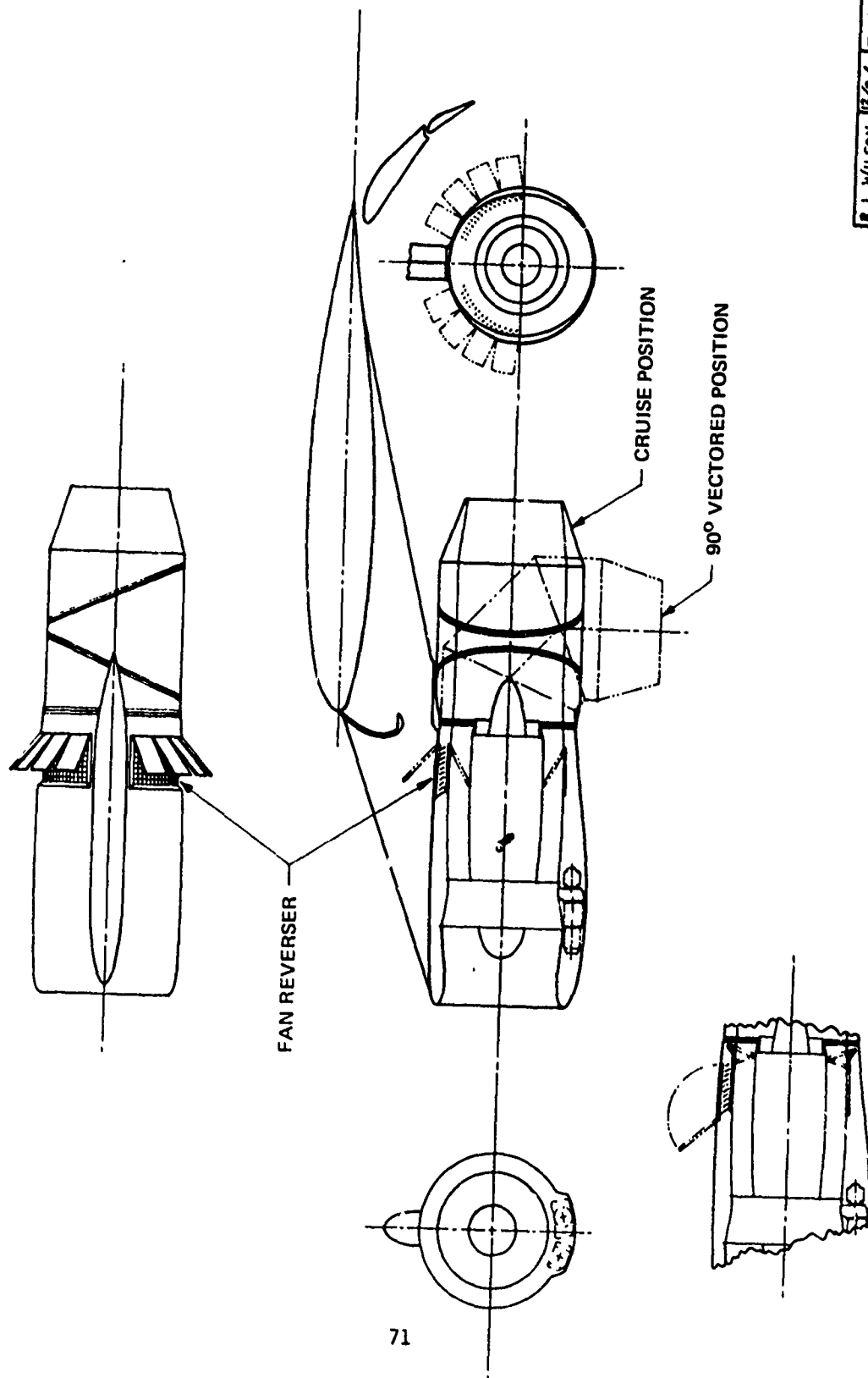
50° rotation of the middle door moves the outer door 60° and the inner door rotates 180° (through the 3:1 gear ratio, inner to outer door). This puts the three doors into reverse thrust position. The deflector doors are constructed of steel honeycomb sandwich panels. A variable geometry nozzle will be required to reduce the Mach number of the flow entering the deflector during thrust vectoring. Engine flow control must be maintained at the deflector exit in order to avoid the losses associated with high Mach number turning.

Figure 36 shows a concept that separates the thrust vectoring and thrust reverser functions. A three bearing nozzle is utilized for thrust vector modulation from horizontal to a maximum of 90° depending on the bearing plane angle. The use of multiple counter rotating duct segments eliminates side forces during vectoring. An electric or hydraulic drive system with gears on each segment are used to rotate the segments. Steel honeycomb sandwich panels are used to fabricate the duct segments.

The thrust reverser system consists of a fan cascade thrust reverser and "cycle-spoiling" of primary thrust. The reverser concept shown consists of internal and external doors with fixed cascades in the upper 180° sector of the nacelle. Hydraulic or pneumatic actuators deploy the doors. The cascades, and internal and external doors are made of aluminum.

A multibearing nozzle may also be used as a combined thrust reverser and vectoring system as shown in Figure 37. With a bearing angle of 60°, the nozzle may be deflected to a maximum of 120°. During approach and landing the nozzle deflection angle would be at approximately 75°. At touchdown the nozzle would simultaneously move to the maximum deflection position and rotate 90° to direct the exhaust flow outboard. Because of the possibility of cross flow ingestion by an adjacent nacelle inlet, this concept will probably be applicable to aircraft with one engine under each wing.

The concept shown in Figure 38 employs a lobstertail-type external deflector vectoring system consisting of three hemispherical panels deployed aft of the nacelle. The deflector doors have a common hinge and are deployed using an air driven ball-screw actuator with incremental position capability to obtain the desired vectored thrust angle. Engine flow control must be maintained at the deflector exit utilizing a variable geometry nozzle to avoid the losses associated with high Mach number turning. The thrust reverser system consists of a fan cascade thrust reverser and "cycle-spoiling" of the primary thrust. It is the same system discussed previously for the multibearing vectoring nozzle concept.



ALTERNATE THRUST REV SCHEME

Figure 36: THRUST REV/MULTIBEARING THRUST VECTORIZING
CONCEPT - BPR 6 MIXED FLOW ENGINE

R. L. Wilson	13/2/71	THRUST REV/MULTI-BEARING THRUST VECTORIZING CONCEPT - BPR 6 MIXED FLOW ENGINE
		TR/TV-PP-06

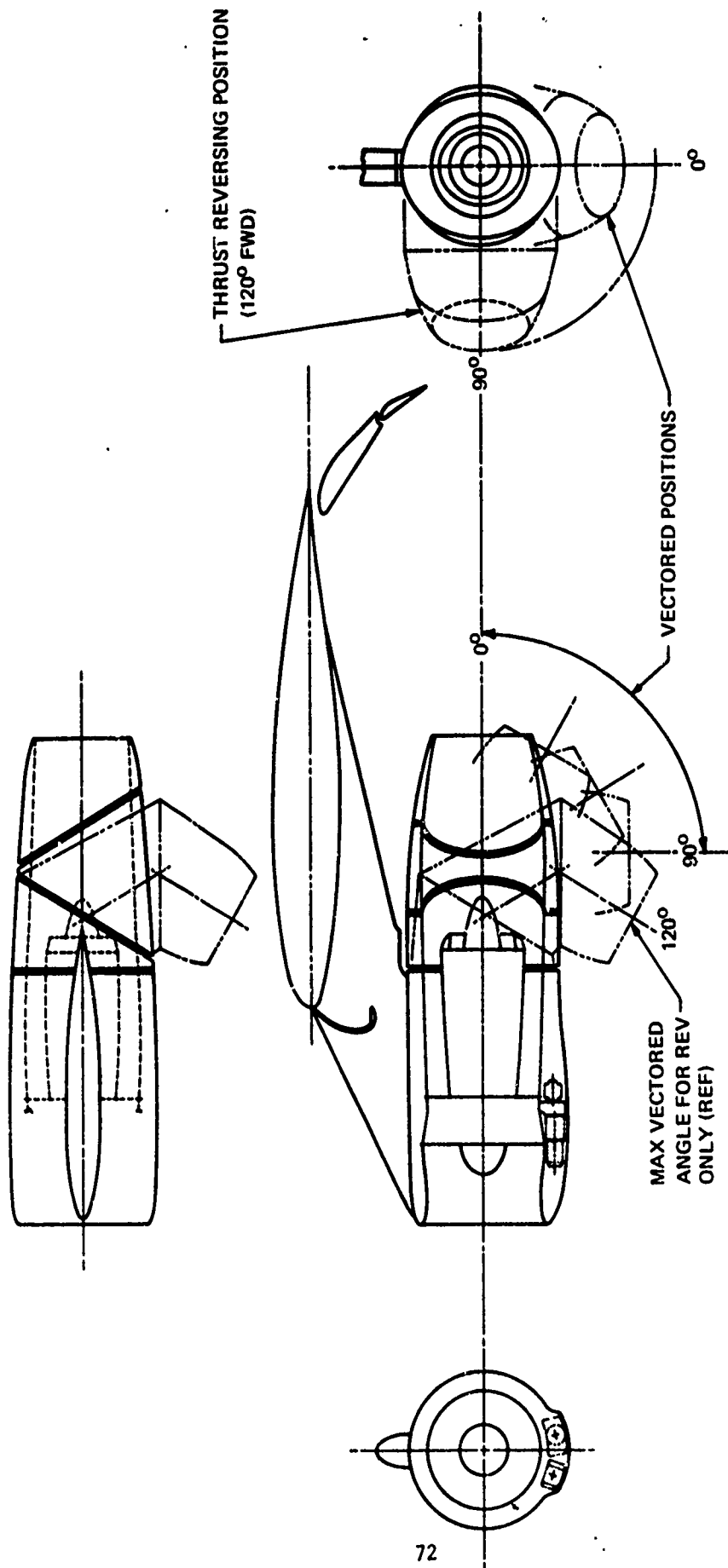


Figure 37: MULTIBEARING THRUST REV/THRUST VECTORIZING
CONCEPT - BPR 6 MIXED FLOW ENGINE

R.L. WILSON	1/22/72	MULTI-BEARING THRUST REV./
		THRUST VECTORIZING CONCEPT -
		BPR. 6 MIXED FLOW ENGINE
SCALE: 1/40		TR/TV-PP-13

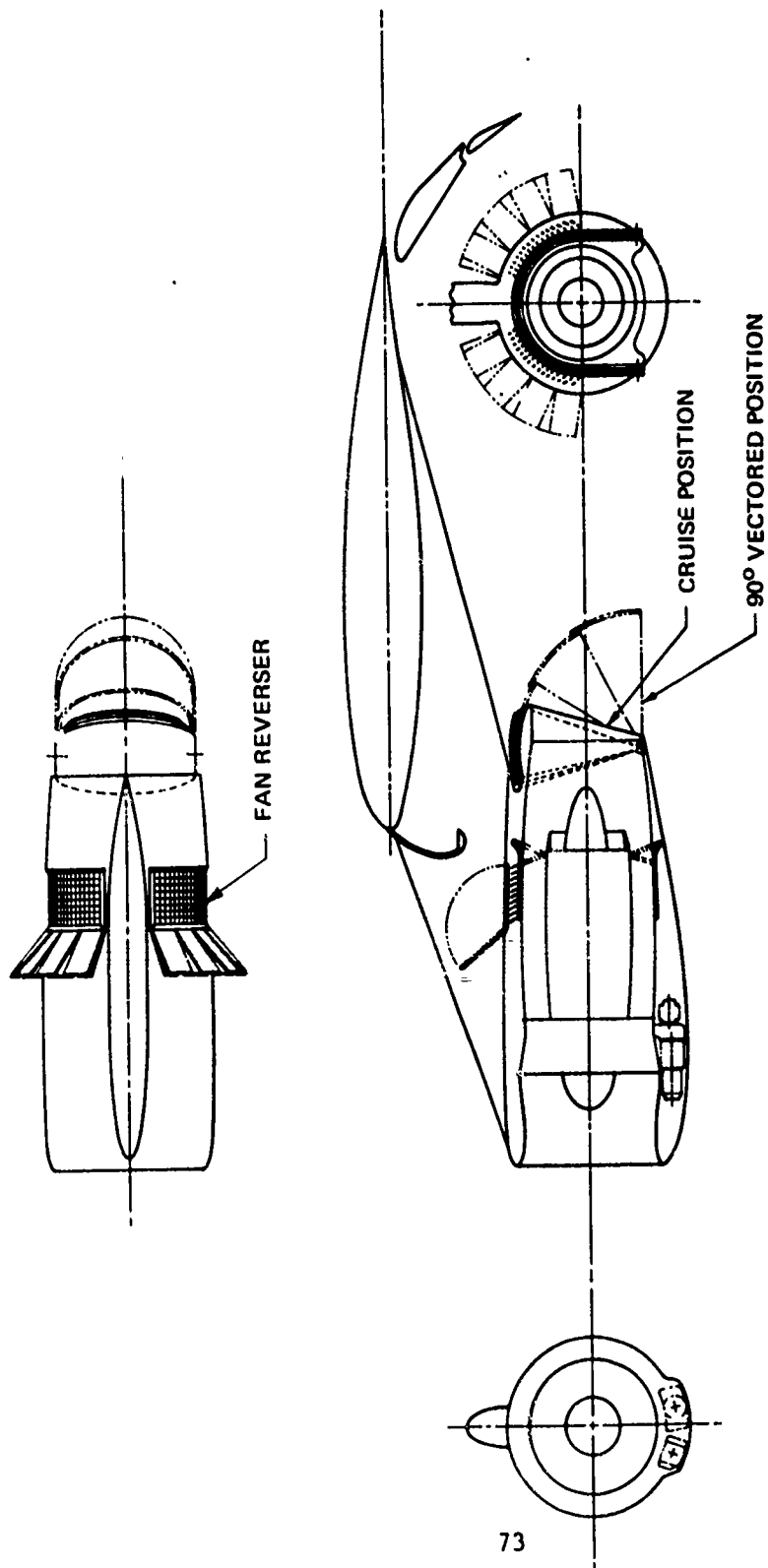


Figure 38: THRUST REV/LOBSTER TAIL THRUST VECTORING
CONCEPT - BPR 6 MIXED FLOW ENGINE

R. L. WILSON	12/9/71	THRUST REV/LOBSTER TAIL THRUST VECTORING CONCEPT - BPR 6 MIXED FLOW ENGINE
		TR/TV-PP-07

Figure 39 shows a vectoring concept consisting of a rectangular nozzle with fixed vertical side walls and hinged horizontal panels. During thrust vectoring, the horizontal panel at the bottom of the nacelle is translated forward using an electric or hydraulic motor and a rack and pinion drive mechanism. The upper hinged panels are slaved to the motion of the bottom panel using linkages not shown in the schematic. The thrust vectoring nozzle and side walls are constructed of steel honeycomb sandwich panels. The degree of mechanical complexity of this device is equivalent to other vectoring concepts. The primary design problems are concerned with sealing the side walls to prevent leakage and maintaining a good aerodynamic shape to minimize nacelle drag. The thrust reverser system consists of a fan cascade thrust reverser system and "cycle-spoiling" of the primary thrust.

Unmixed Flow Engines - Single Pod

The rotating nozzle concept shown in Figure 40 is believed to be the simplest system to provide thrust vectoring and thrust reversing of unmixed engine exhaust flows. The vectoring nozzles are rotatable from $+90^\circ$ for vectored thrust to -135° for reversed thrust. The nozzles would probably be rotated forward during reverser deployment without serious risk of reingestion. Satisfactory reverse thrust can be obtained at the -135° rotation angle position. The rotation rates during reverse mode deployment must be high, approximately $180^\circ/\text{second}$ which is twice the rate of the current Pegasus nozzles used on the Harrier V/STOL Fighter aircraft. A hydraulic motor connected to a gearbox and chain drive mechanism is used to rotate the nozzles. The fan nozzles are made of aluminum and the primary nozzles are made of steel.

There are few vectoring system concepts that are applicable to bypass ratio 12.0 unmixed flow engines. The single bearing nozzle concept discussed above is limited to engines with bypass ratios of approximately 6.0 or less. When scaled to larger bypass ratios engine size (i.e. BPR 12.0), the fbw area required for the fan nozzle increases the frontal area of the nacelle which would substantially increase nacelle drag. Two concepts for BPR 12.0 unmixed flow engines are shown in Figures 41 and 42. The multibearing vectoring concept (Figure 41) best illustrates the many difficulties of designing a satisfactory thrust vectoring arrangement for BPR 12.0 engines. The large size required for the fan duct results in a long nacelle that does not have good aerodynamic contours. Also, the weight of the ducts and vectoring nozzle is prohibitive. The external deflector concept shown in Figure 42 utilizes a lobstertail deflector to achieve thrust vectoring. The deflector is deployed using air driven ball screw actuators with incremental adjustment capability. The primary problem with this concept is the ability to maintain air flow match of the primary stream during

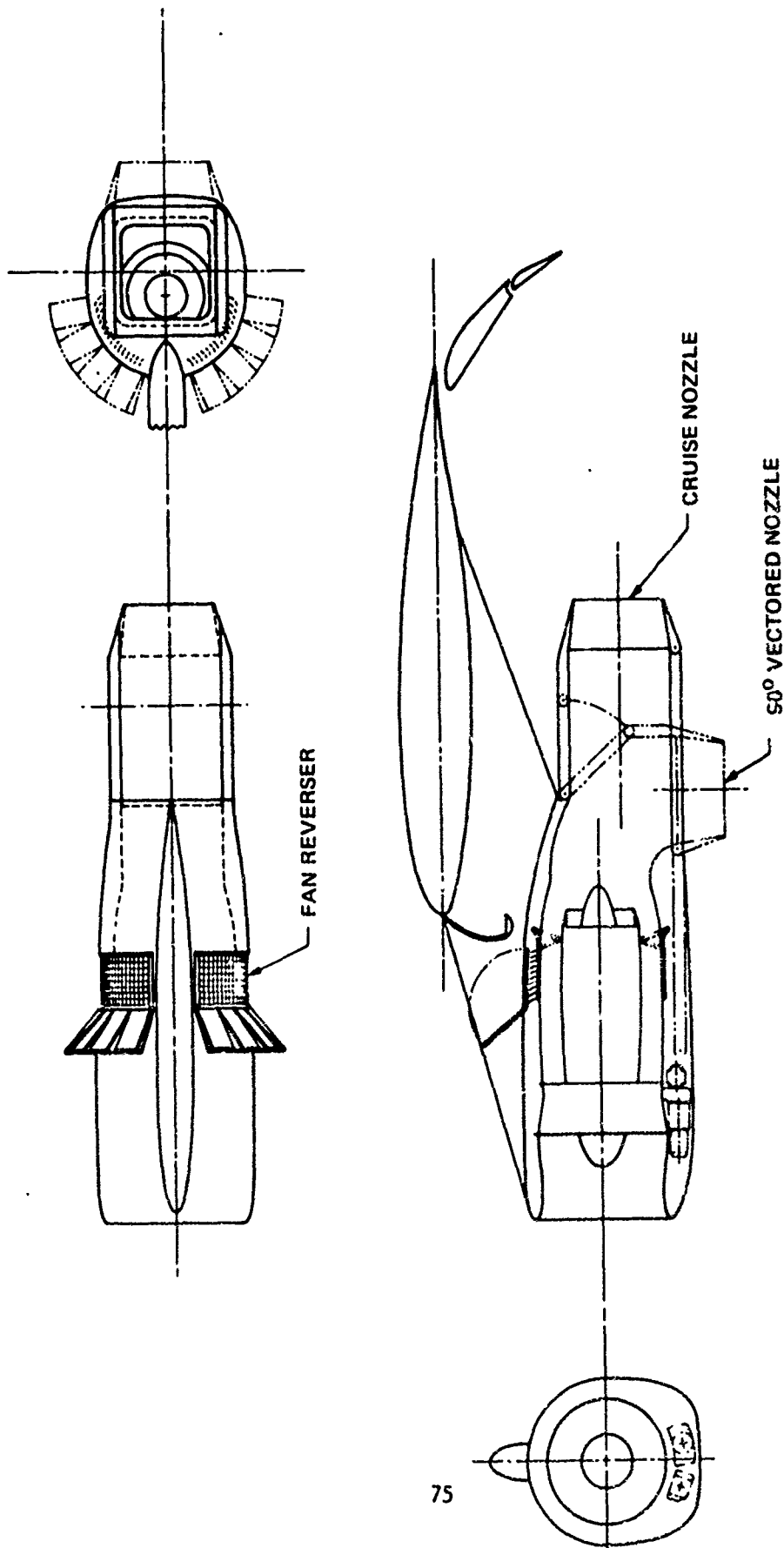


Figure 39: THRUST REV./TWO-DIMENSIONAL THRUST VECTORING
CONCEPT - BPR 6 MIXED FLOW ENGINE

R. L. WILSON	12/13/77	THRUST REV./TWO-DIMENSIONAL THRUST VECTORING CONCEPT - BPR 6 MIXED FLOW ENGINE	TR/TV-PP-08

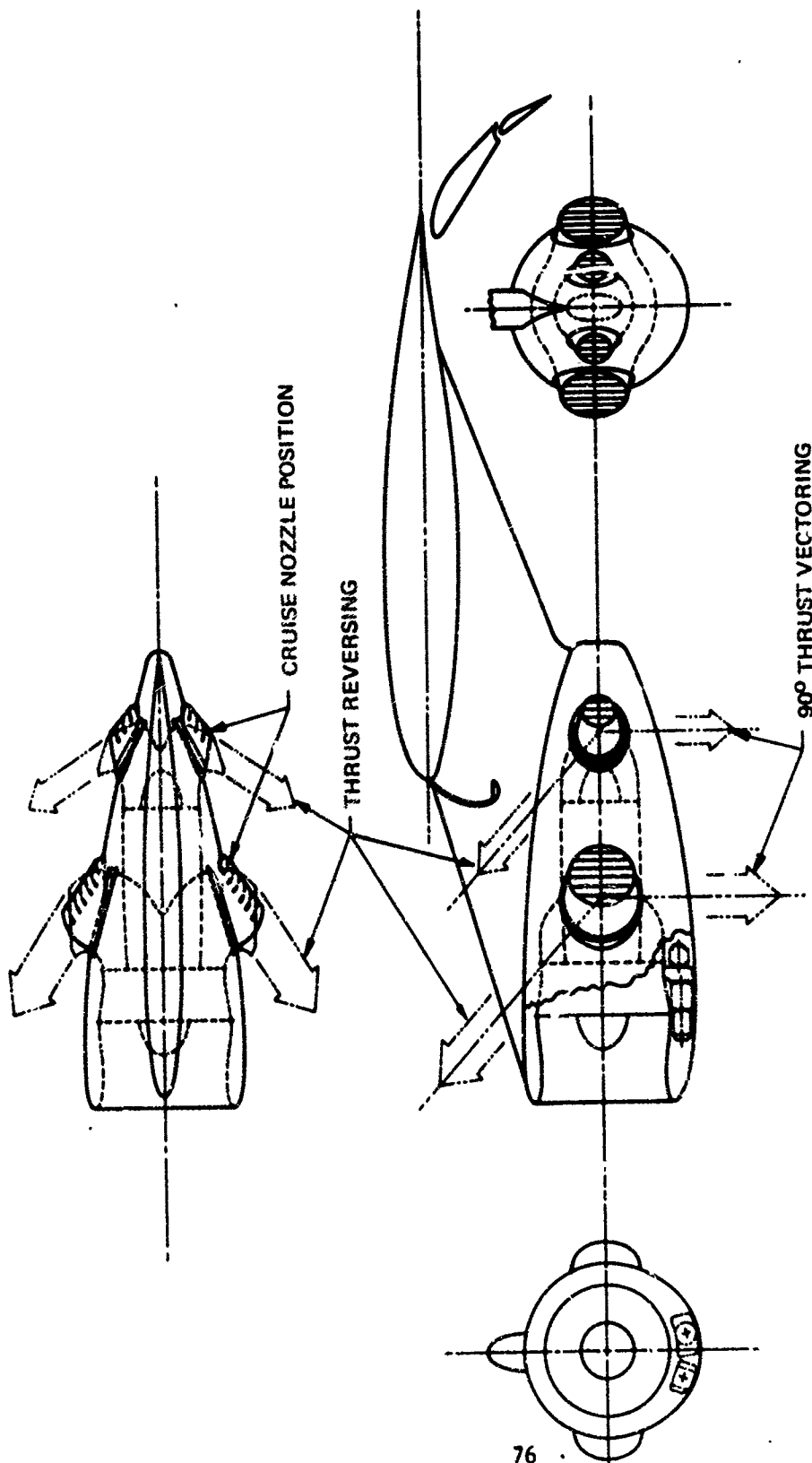
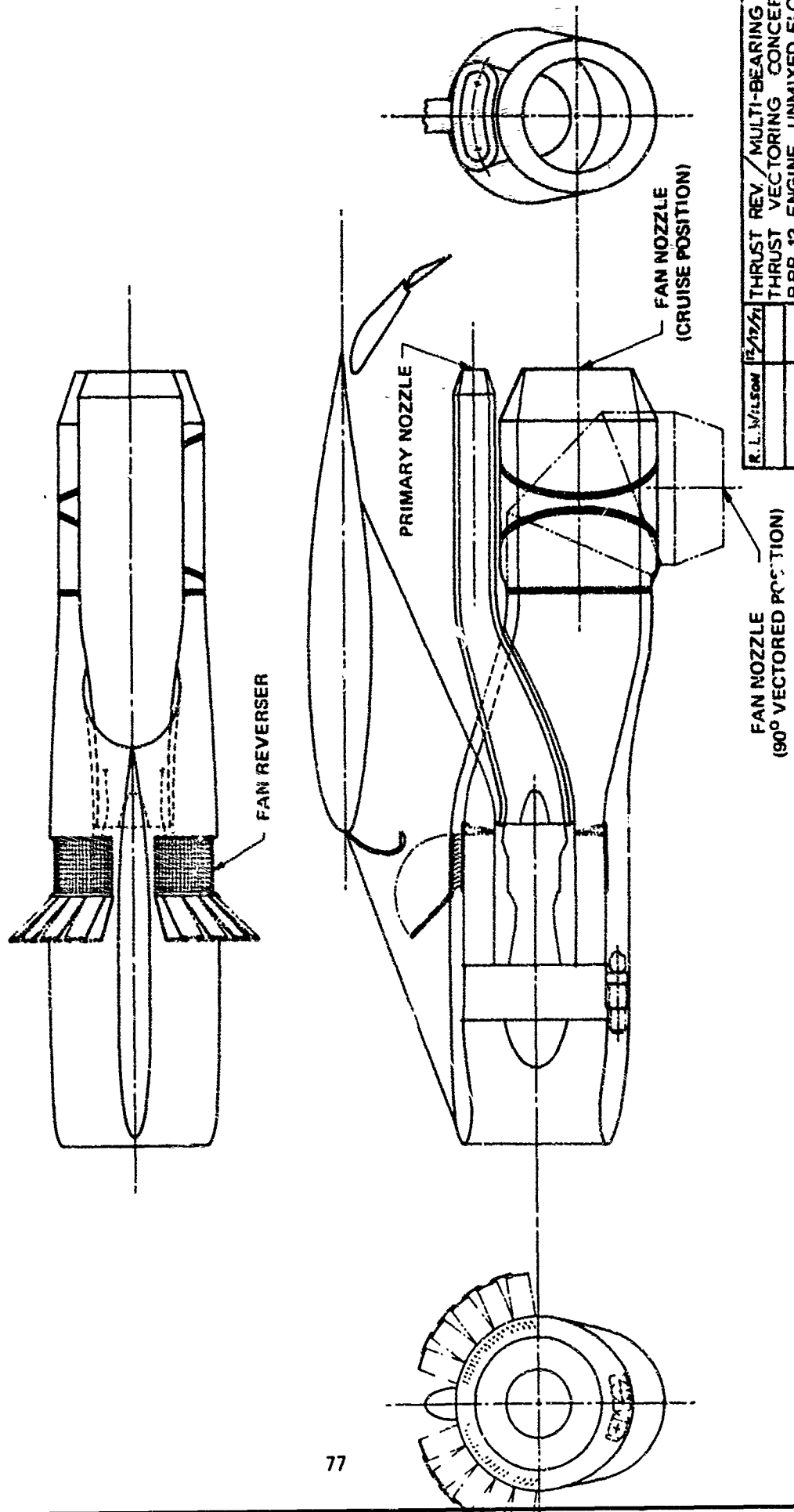


Figure 40: THRUST REV./THRUST VECT ROTATING NOZZLE
CONCEPT - BPR 6 ENGINE, UNMIXED FLOW

R. L. Wilson	1/11/71	THRUST REV./THRUST VECT.
		ROTATING NOZZLE CONCEPT -
		BPR 6 ENGINE, UNMIXED FLOW
SCALE: 1/40		TR/TV-PP-10



R. L. WILSON	12/12/71	THRUST REV. / MULTI-BEARING
		THRUST VECTURING CONCEPT-
		BPR 12 ENGINE, UNMIXED FLOW
		TR/TV-PP-09

Figure 41: THRUST REV./MULTIBEARING THRUST VECTURING
CONCEPT - BPR 12 ENGINE, UNMIXED FLOW

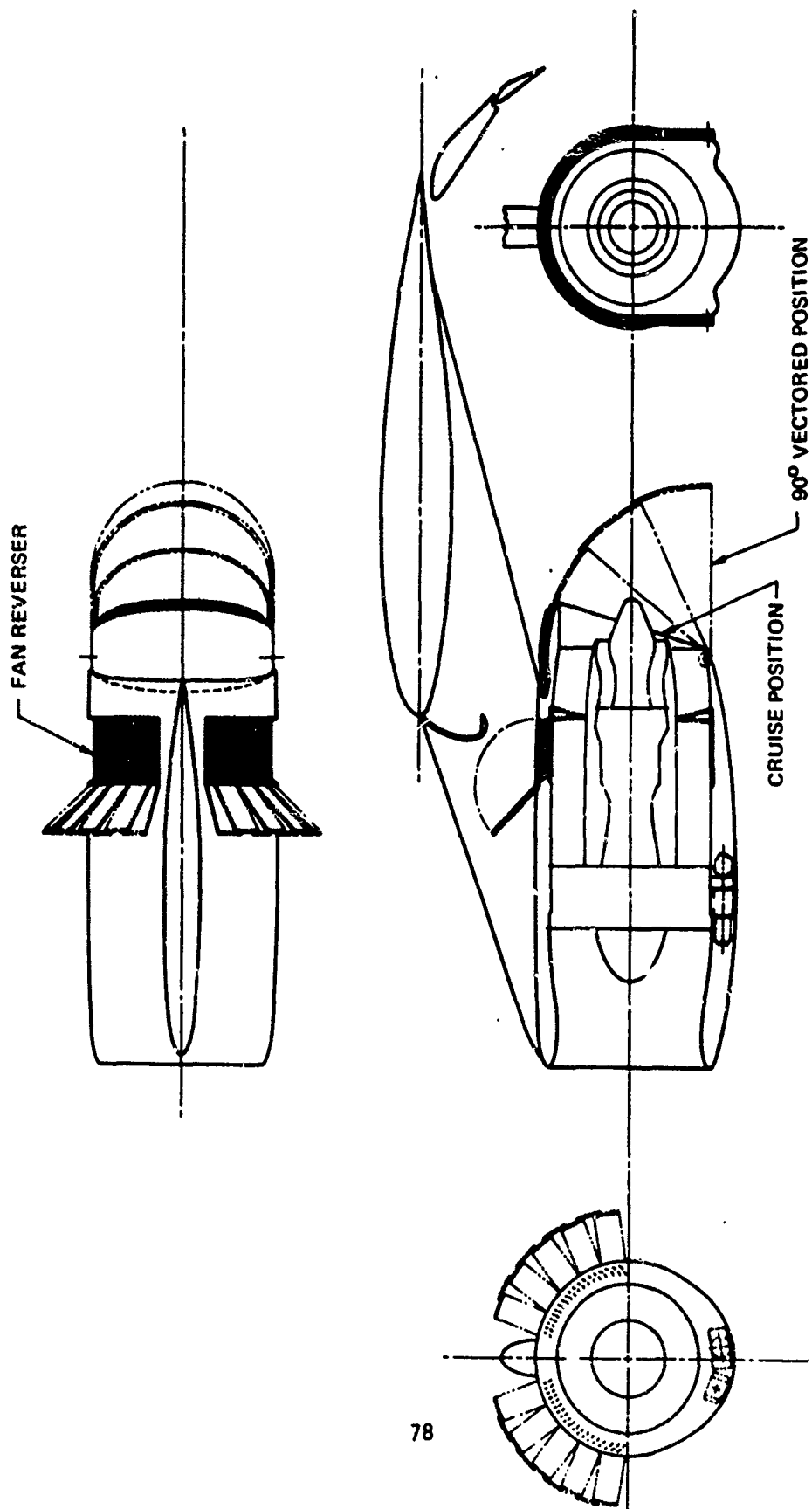


Figure 42: THRUST REV./LOBSTER TAIL THRUST VECTORING
CONCEPT - BPR 12 ENGINE, UNMIXED FLOW

R. L. Wilsey	1/21/78	THRUST REV./LOBSTER TAIL THRUST VECTORING CONCEPT - BPR 12 ENGINE, UNMIXED FLOW
SCALE: 1/40		TR/TV-PP-12

vectoring mode. The local pressure field surrounding the primary nozzle will change when the fan flow is deflected and the primary mass flow will change. Because the fan nozzle pressure ratio is relatively low it may be possible to maintain the controlling area at the fan nozzle and avoid the necessity of a variable geometry nozzle. This would probably help maintain primary air flow match. Thrust reversing on the BPR 12.0 concept is achieved using a fan cascade thrust reverser.

It should be noted that it is possible to vector only the fan flow of a BPR 12.0 engine and obtain satisfactory vectoring performance. Since the fan thrust is much greater than the primary thrust there may be a favorable trade between the savings in system weight and complexity and the loss in available vectored thrust. As shown in Figure 43, to achieve an effective vector angle of 75°, the fan thrust will require a mechanical deflection angle of 82° and will produce a vectored thrust ratio of $F_{\text{RESULTANT}} / F_{\text{GROSS}} = .92$.

VECTORED

Mixed Flow Engines --- Dual Pods

The design study included dual pod engine installations using BPR 3.0 mixed flow engines. BPR 3.0 mixed flow engines necessitate vectoring and reversing all of the engine flow (as discussed in Section 2.1.4.2) to achieve satisfactory performance. Therefore, the available design options are separate thrust vectoring and reversing systems or a combined thrust vectoring/reversing system. Because of the potential weight advantage, a combined thrust reverser and vectoring system is probably the best option for a BPR 3.0 mixed flow engine.

Of the two combined TR/TV concepts considered for the single pod mixed flow engine installation, the external deflector/target thrust reverser/vectoring system shown in Figure 34 was selected for the dual pod installation. A schematic is shown in Figure 44. This installation is relatively simple, lightweight, and provides good thrust vectoring and thrust reversing performance.

2.1.4.6 Thrust Reverser Concepts for USB Lift Systems

Two thrust reverser concepts are shown in Figure 45 and 46 for an overwing USB installation. The BPR 6.0 unmixed flow installation, Figure 45, utilizes a fan cascade thrust reverser and a mechanical primary thrust spoiler. The fixed cascades direct the flow upward above the wing surface. The BPR 6.0 mixed flow engine concept, Figure 46, utilizes a target thrust reverser consisting of two hinged doors, actuated by one centrally located hydraulic actuator. The target

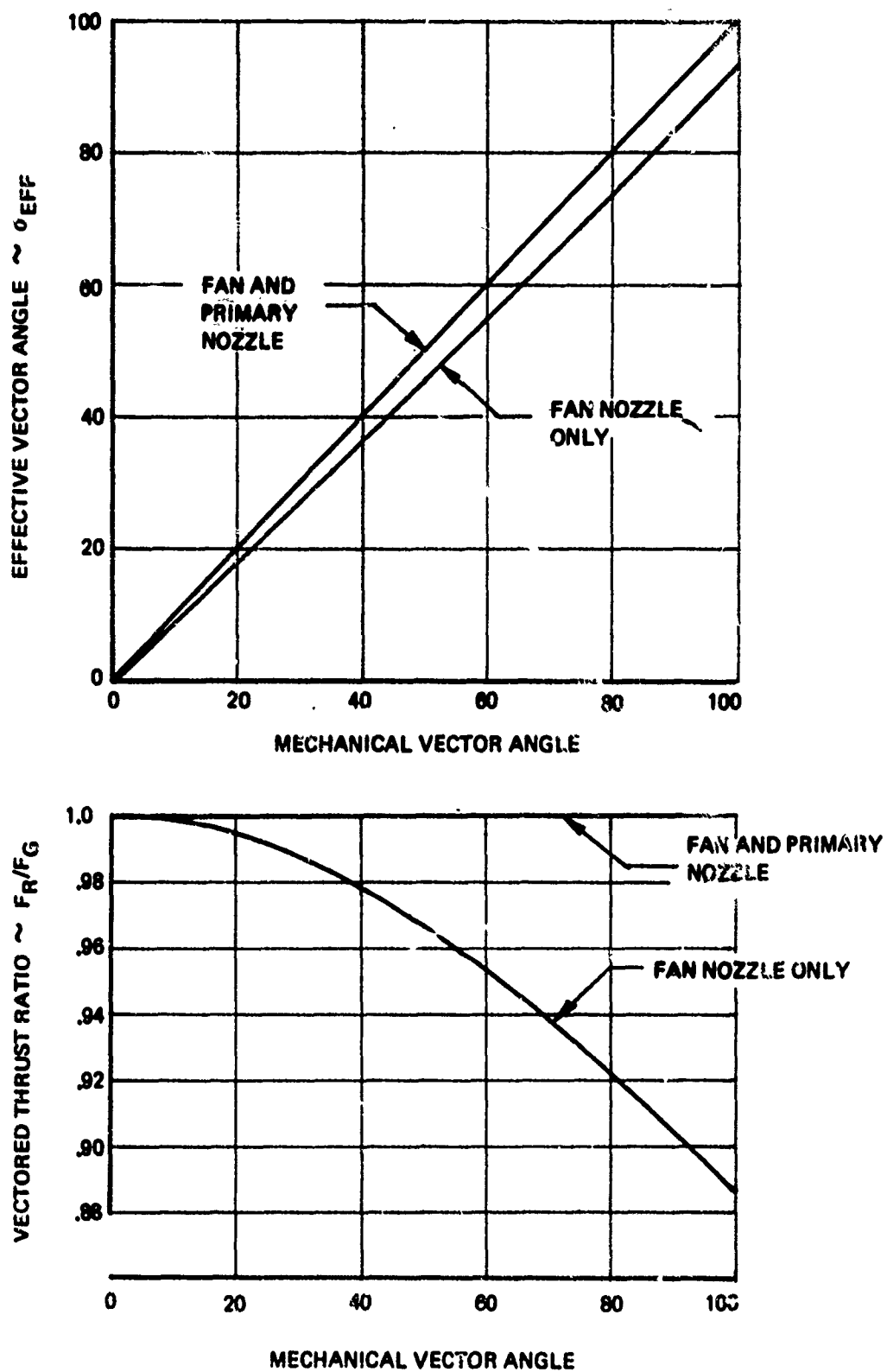


Figure 43: EFFECT OF VECTORING FAN FLOW – BPR 12

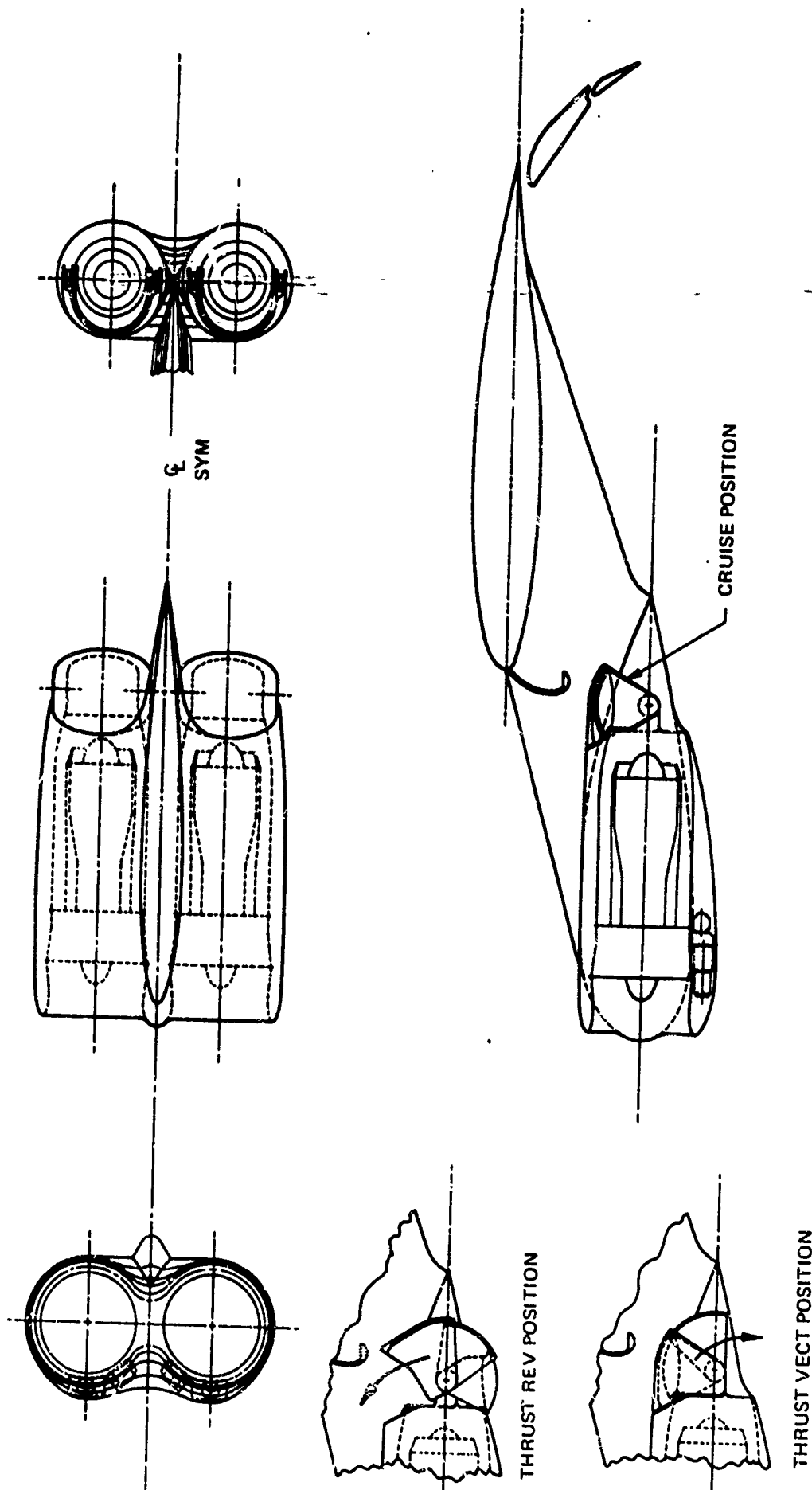


Figure 44: DUAL POD, LOBSTER TAIL, TR/TV CONCEPT -
BPR 3 MIXED FLOW ENGINE

R.L. WILSON	2/21/73	DUAL POD, LOBSTER TAIL, TR/TV CONCEPT -
		BPR 3 MIXED FLOW ENGINE
SCALE: 1/40		TR/TV-PP-15

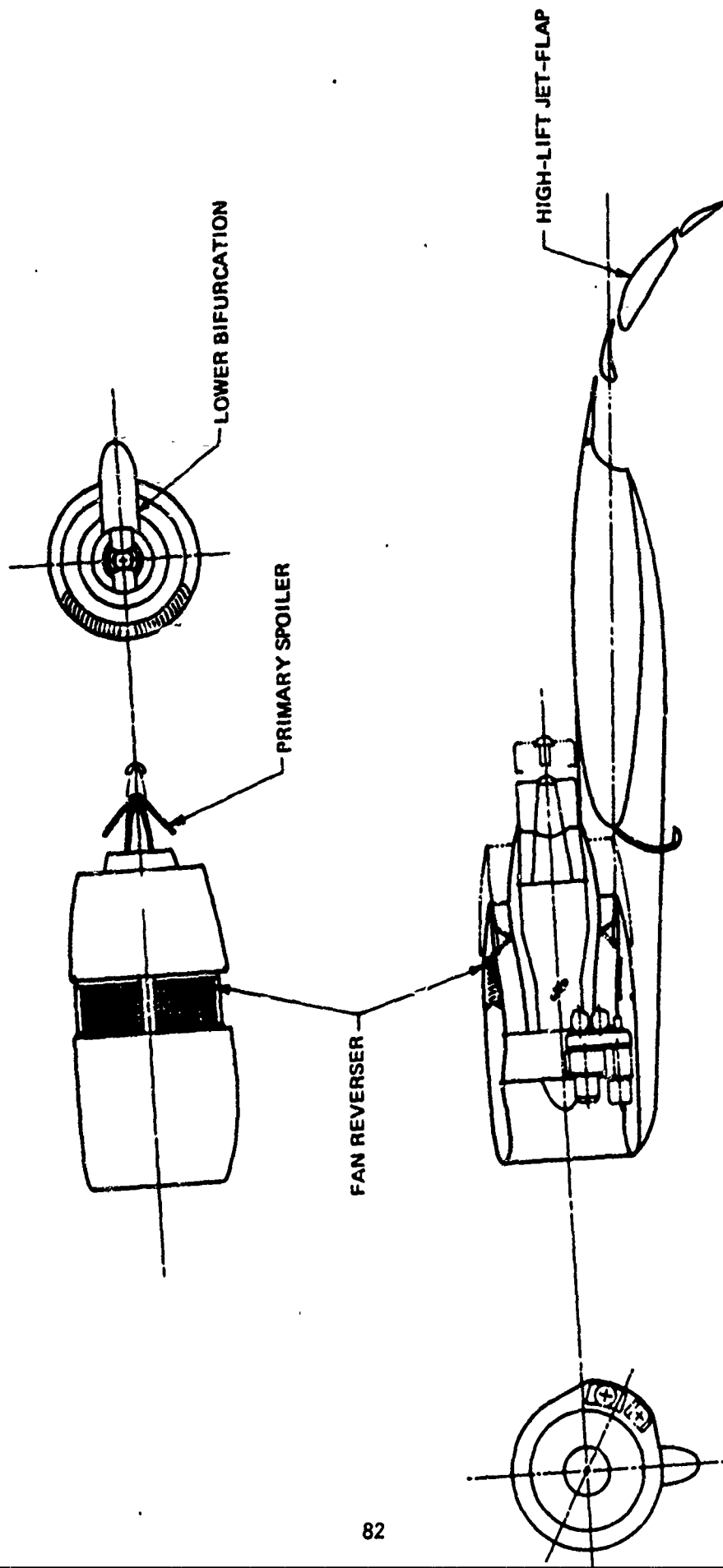
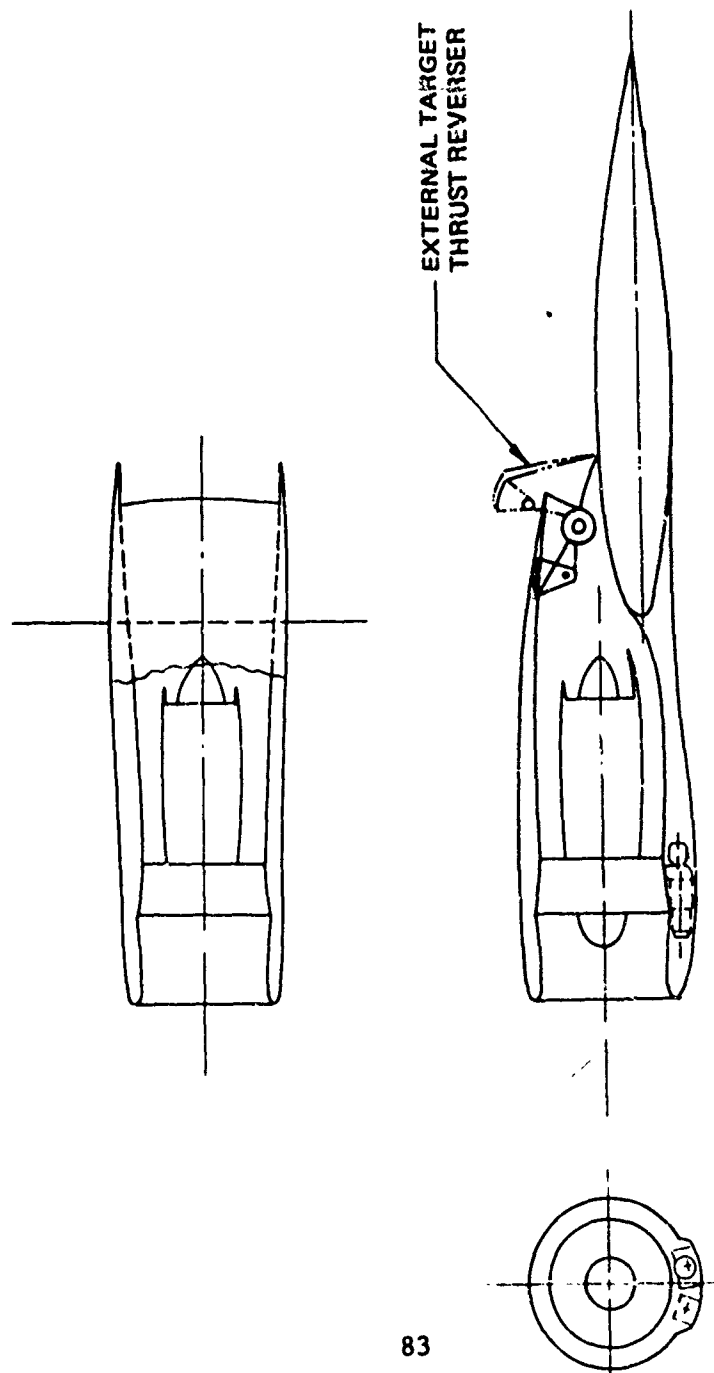


Figure 45: OVERWING T/R CONCEPT - BPR 6 ENGINE
UNMIXED FLOW

R.L. WILSON	7/19/70	OVERWING T/R CONCEPT -
		BPR 6 ENGINE
		UNMIXED FLOW
		TR/TV-PP-04



J.E. Pett	2/5/51	THRUST REVERSER CONCEPT - BPR 6 MIXED FLOW ENGINE
SCALE 1/40		TR/TV - PP - 18

Figure 45: THRUST REVERSER CONCEPT - BPR 6 MIXED FLOW ENGINE

deflector door is hinged to the nacelle structure. The deflector door is hinged to the main deflector door. As the target deflector is deployed the lip door is slaved into position using mechanical linkages. The deflector doors are constructed of stainless steel. A more detailed schematic of the reverser installation is shown in Figure 47.

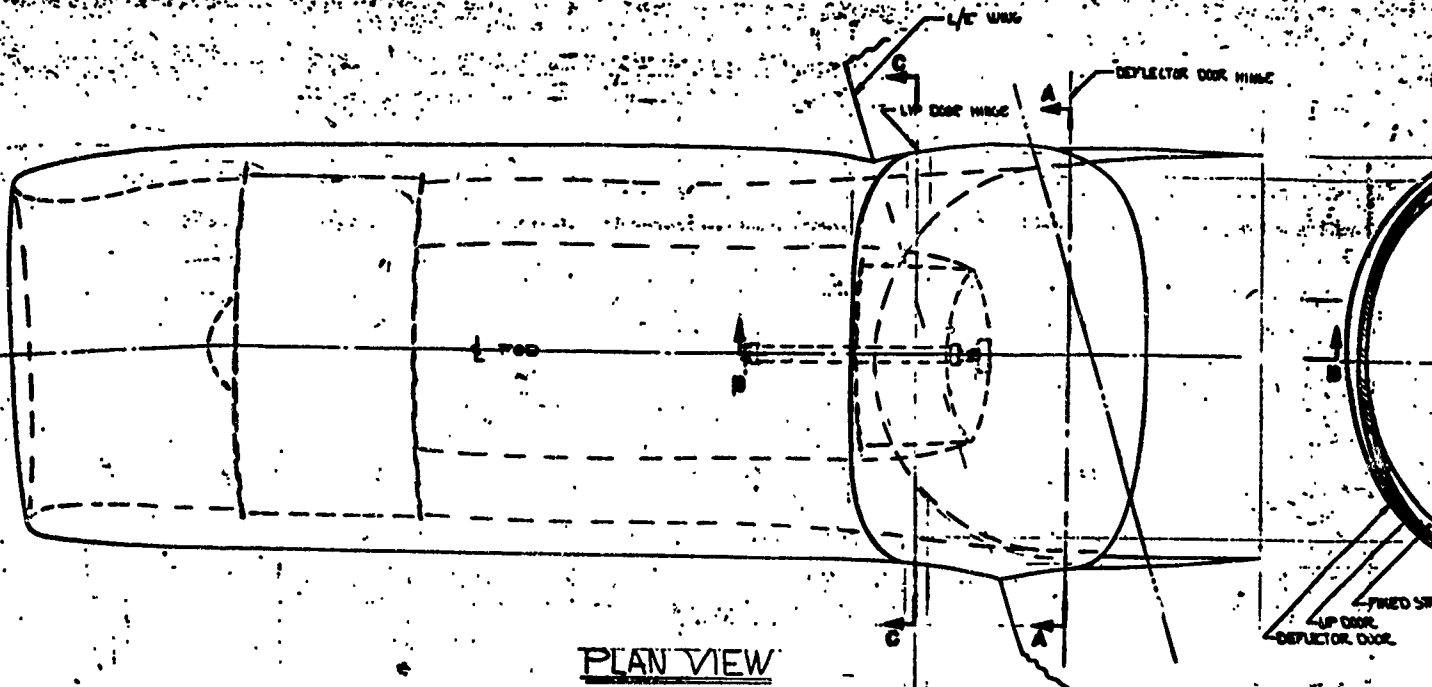
In order to obtain effective vectoring performance for upper surface blowing, the engine exhaust flow must be attached to the wing upper surface. This necessitates exhaust nozzle designs that are D-shaped (aspect ratio of approximately 3.0) and a highly integrated wing and nacelle design. Boeing studies of such nacelle configurations show that the mixed flow engine concept shown in Figure 46 and 47 offers good reverser performance, minimum weight, and good mechanical design relative to other nacelle concepts. The unmixed flow concept shown in Figure 45 would not be an acceptable installation for upper surface blowing because of the requirements cited above.

2.1.5 Fan Cascade Thrust Reverser Detailed Design

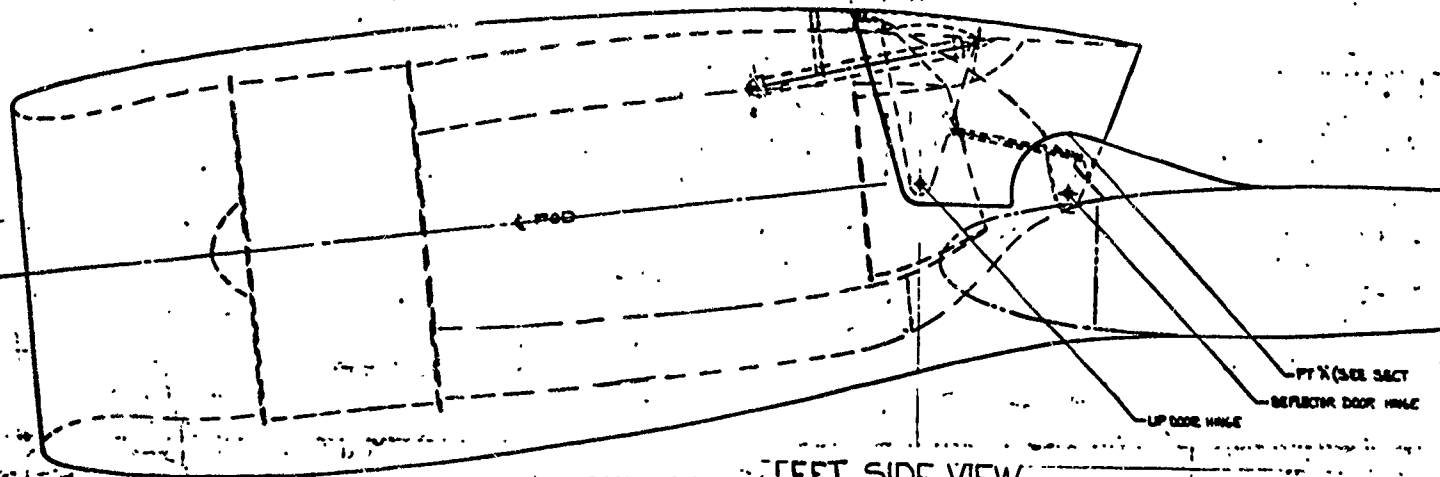
The objective of the detailed design study was to demonstrate the feasibility of the fan cascade thrust reverser concept used for the EBF and MF+VT engine installation. The problems of exhaust flow control, mechanization, and actuation were examined in more detail.

Current high bypass flow engines reverse the fan air through openings provided in portions of their full 360° circumference. This allows them to use relatively short cascade assemblies and single hinged, one piece, blocker doors. To avoid the re-ingestion and ground impingement problems of current cascade designs, the reverser exhaust must be directed through openings in the upper 180° segment of the nacelle. This necessitates the installation of cascade panels approximately twice as long as those in current use. The blocker door mechanism and proper sealing of the cascade openings becomes a major design problem. The use of bi-fold panels or a similar design, is required to block the fan flow during reverser operation and also provide coverage of the cascades during cruise.

Analysis of the fan cascade thrust reverser concepts discussed in Section 2.1.4 disclosed several deficiencies. First, the translating sleeve concept, Figure 28, would require high actuation loads because of the large segment of cowl structure in motion and the fast deployment time required. This would require large size actuators and corresponding structure to carry the loads which would result in higher weight. Also, it was recognized that the blocker door mechanism envisioned was not feasible because of the long cascade length and the resulting sealing problems during the cruise mode. The reverser concept shown in Figure 36 is not feasible because the



PLAN VIEW



LEFT SIDE VIEW

A

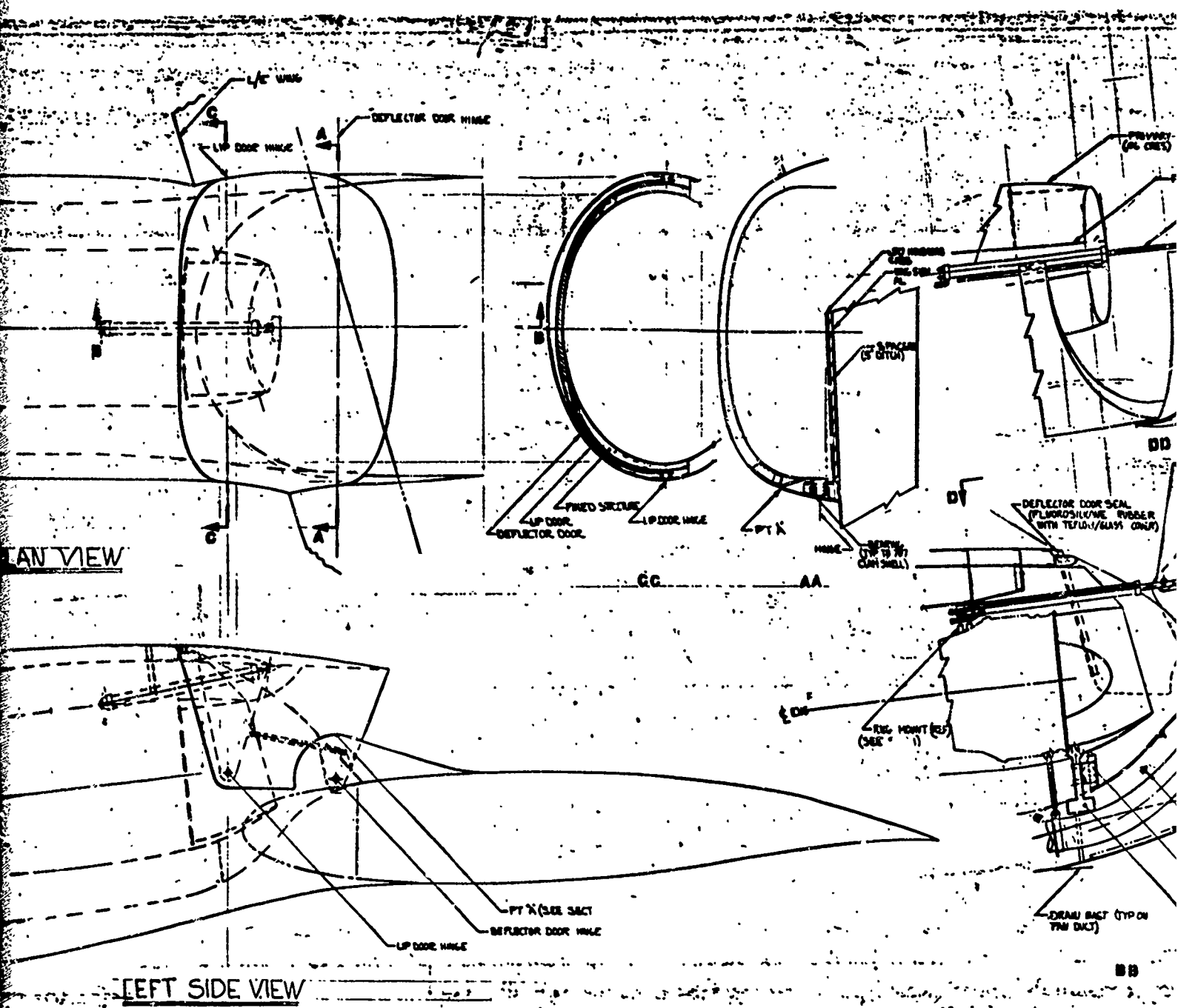


Figure 47: OVERWING

external doors would experience high loads during deployment. The resulting weight penalties for the actuation system and structure would not be acceptable. Therefore, a reverser design was conceived that eliminated the deficiencies of the other concepts.

The revised fan cascade thrust reverser concept is shown in Figure 48. The design utilizes cascade panels and deflector doors located in the upper 180° segment of the nacelle. The cascades have an airfoil cross section with a leading angle of approximately 50° at the blade throat. The cascades solidity, c/l , was selected as 1.40 based on Model 747 thrust reverser development tests. The blocker doors form a smooth surface for the fan duct in the cruise position and with an actuator stroke of 4", the cascades are fully exposed as the doors block the fan exhaust for thrust reversing. The air-flow area match during reverser deployment is shown in Figure 49. The outer doors are oriented in a stream-wise direction for possible in-flight deployment. Their opening angle is intended to prevent possible cross-reingestion on adjacent engines during reverser operation. Interconnecting linkages are used to operate the outer doors with a single hydraulic actuator for each side of the nacelle.

Various blocker door design concepts were examined in trying to develop a satisfactory thrust reverser design. Two of the concepts are shown in Figures 50 and 51. The design in Figure 50 utilized a bi-fold door arrangement mounted to a track. Although the design provides excellent internal geometry for the reverser exhaust, the airflow area match during reverser deployment is poor. When the blocker door is at approximately one-half of its full cycle, the fan duct is totally blocked and only 50 percent of the cascade area is exposed. The concept shown in Figure 51 corrected the area match problem; however, it has an open area between the blocker doors and the track while in the cruise mode. The open area could not be easily sealed without added mechanism and, therefore, added complexity to the reverser system. The concept shown in Figure 48 corrects the airflow match and sealing problems encountered with the previous designs.

Various locations for the blocker door actuator were studied before selecting the placement shown in Section A-A of Figure 48. Early studies placed the actuator at the forward end of the blocker door between the outer fan duct wall and the outside of the nacelle. This location required a separate link between the door and actuator, approximately 10" long, which would follow the blocker door into the blocked position and be exposed to the reverser gases along with a portion of the actuator ram. The required stroke of this actuator would be 18" and its body length would be approximately 26" long. This

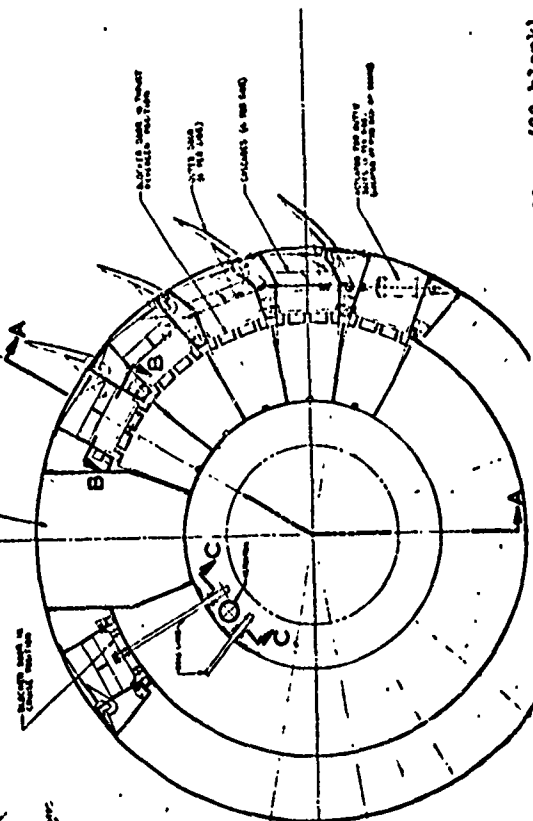
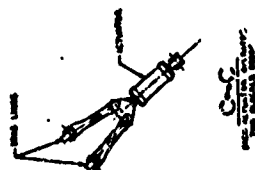
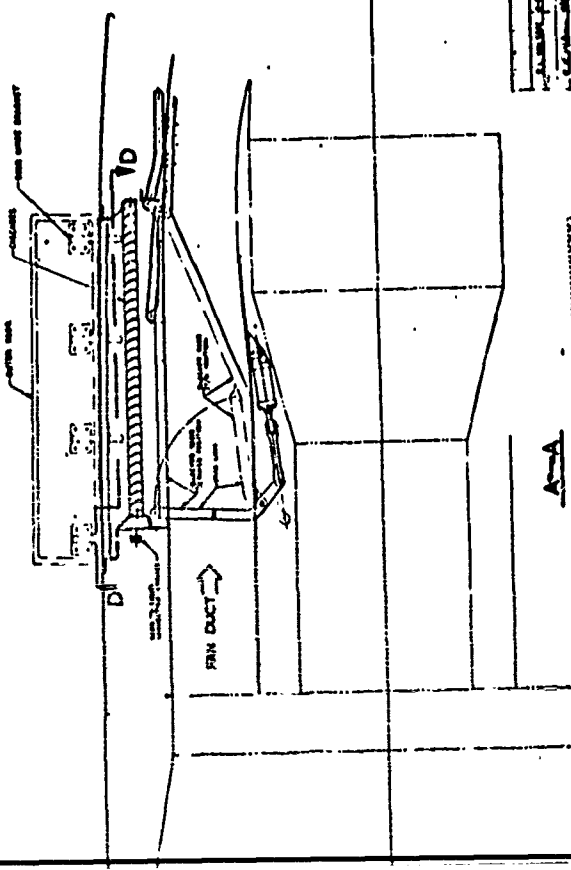
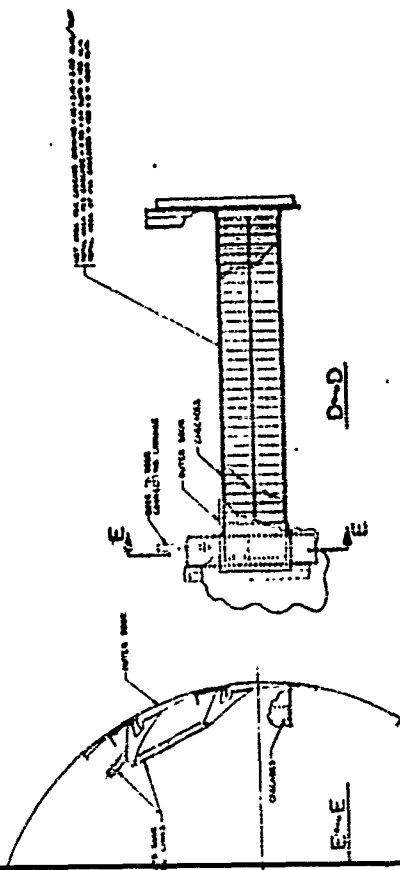
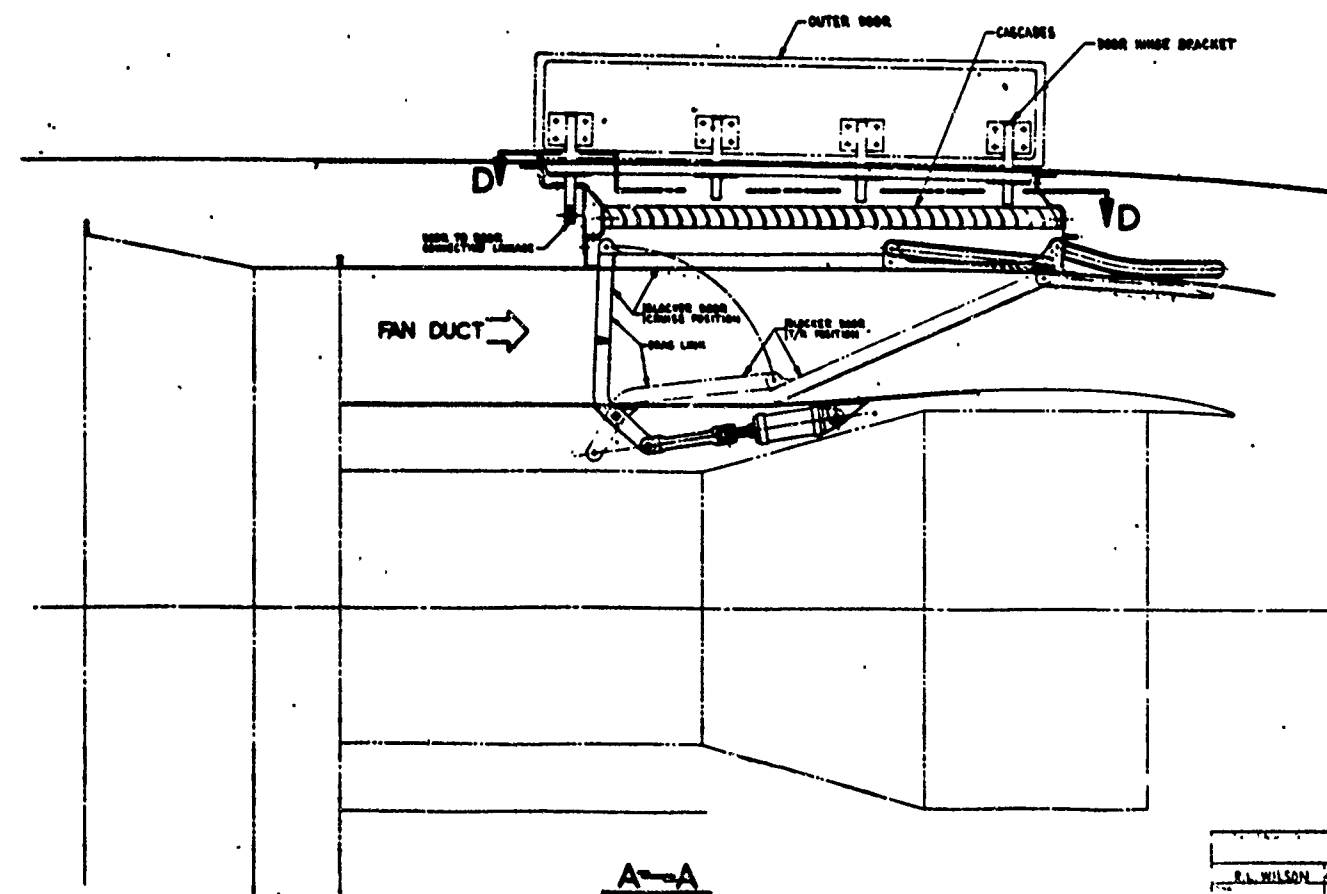
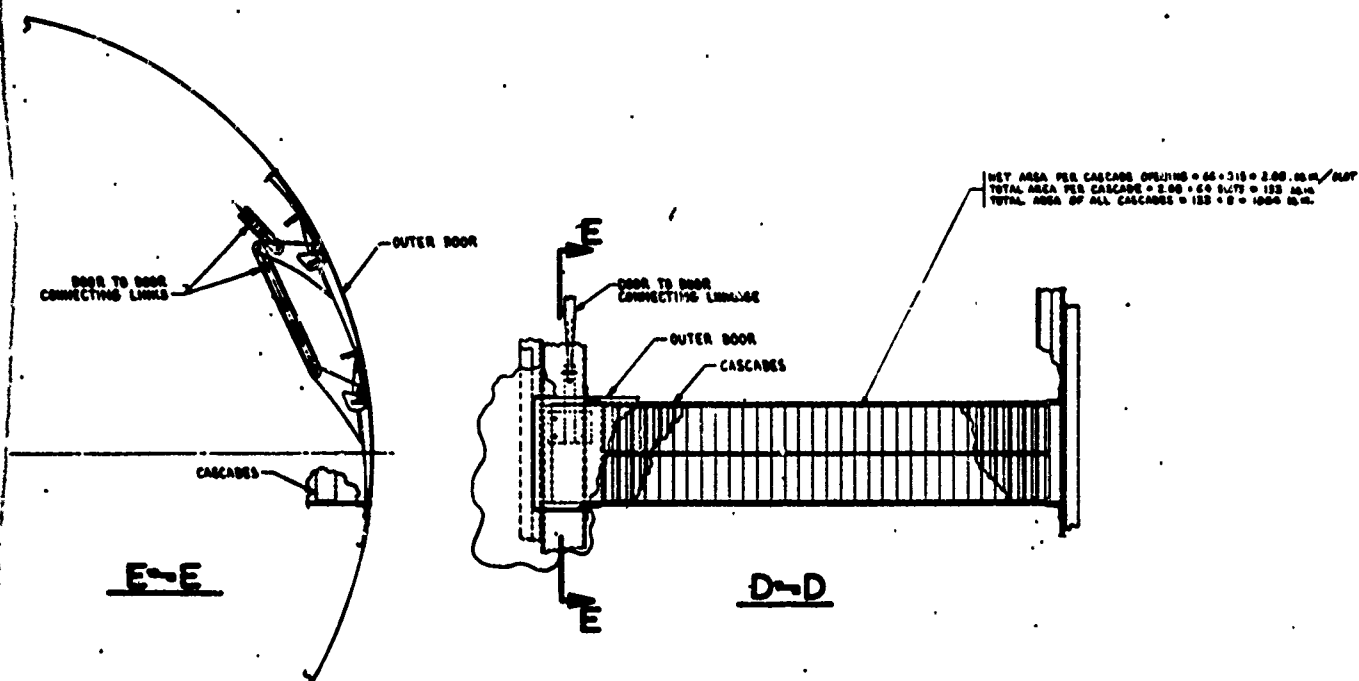


Figure 48: FAN REVERSE -- UPPER 180° QUADRANT.
BPR 6 ENGINE, MIXED FLOW

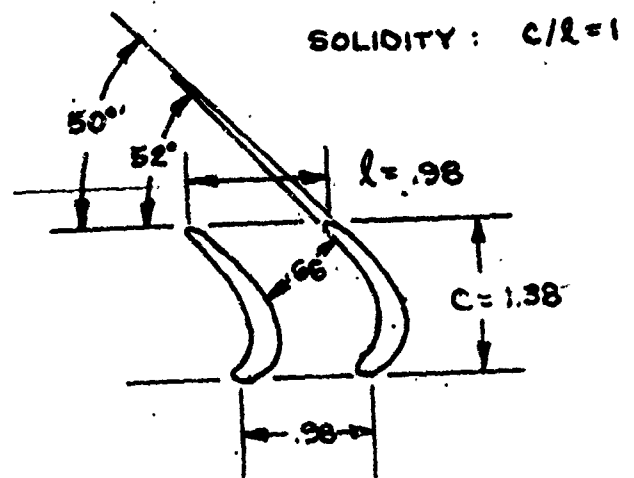


See the following pages
for greater detail.

SEARCHED	INDEXED	SERIALIZED	FILED
FAN REVERSER — UPPER MO' QUADRANT, BPR & ENGINE, MIXED FLOW			
J 8205 TR/TV-PP-17			

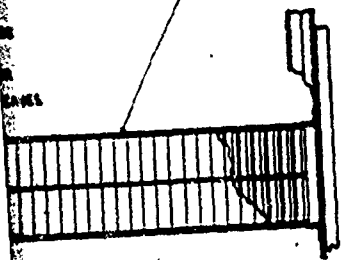


R.L. WILSON 2-4-72		FAN REV
J. R. MASON 4/2/72		UPPER II
J. R. MASON 4/2/72		BPR 6 E
J. R. MASON 4/2/72		J 81205
PRODUCTION DESIGN		1/5

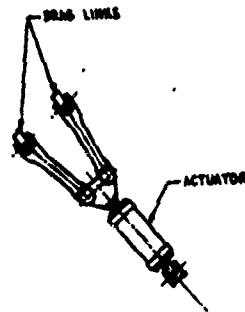
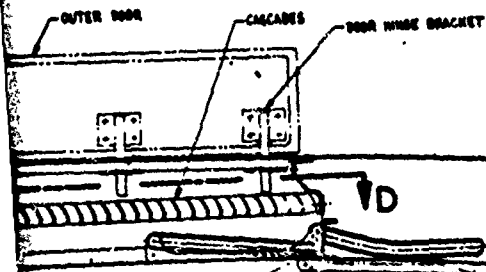


CASCAD BLADE SCHEMATIC

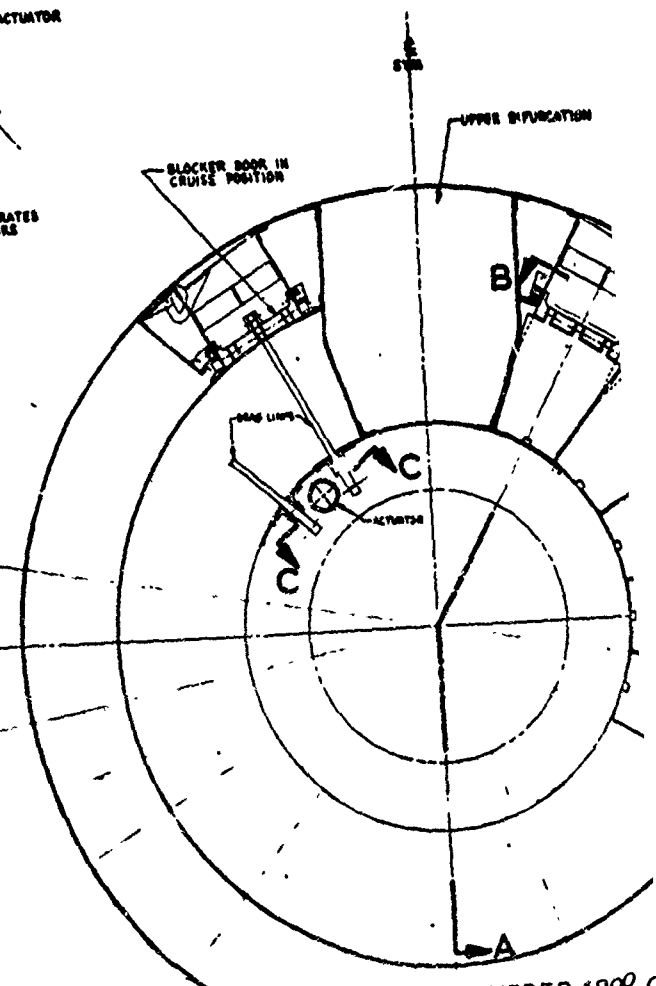
NET AREA PER CASCAD OPENING = $66 \times 310 = 20,460 \text{ sq. in.}$
 TOTAL AREA PER CASCAD = $2,046 \times 6.6 \text{ sq. ft.} = 13,500 \text{ sq. ft.}$
 TOTAL AREA OF ALL CASCADS = $13,500 \times 8 = 108,000 \text{ sq. ft.}$



D-D

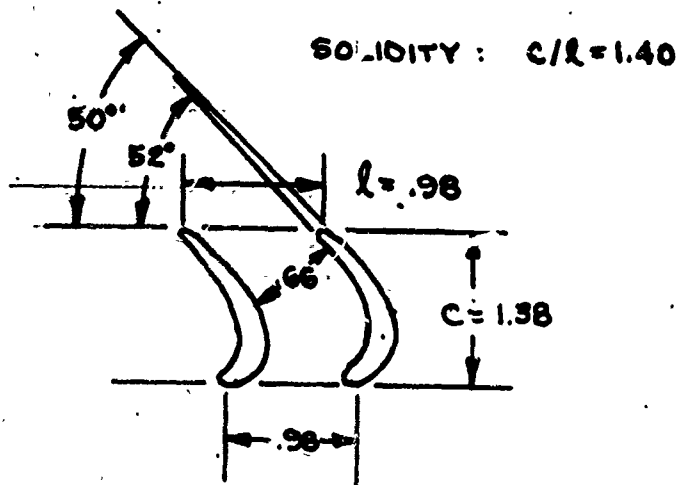


C-C
 EACH ACTUATOR OPERATES TWO BLOCKER DOORS

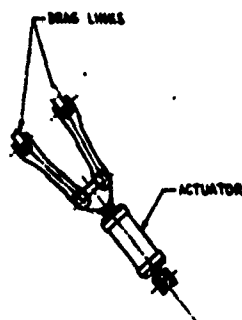


1st. Revision	
R. J. WILSON	4-5-72
FAN REVERSER —	
UPPER 180° QUADRANT,	
BPR 6 ENGINE, MIXED FLOW	
J 81205 TR/TV-PP-17	
PRODUCTION DESIGN	

Figure 48: FAN REVERSER — UPPER 180° C
 BPR 6 ENGINE MIXED FLOW



CASCADE BLADE SCHEMATIC



C-C
EACH ACTUATOR OPERATES
TWO BLOCKER DOORS

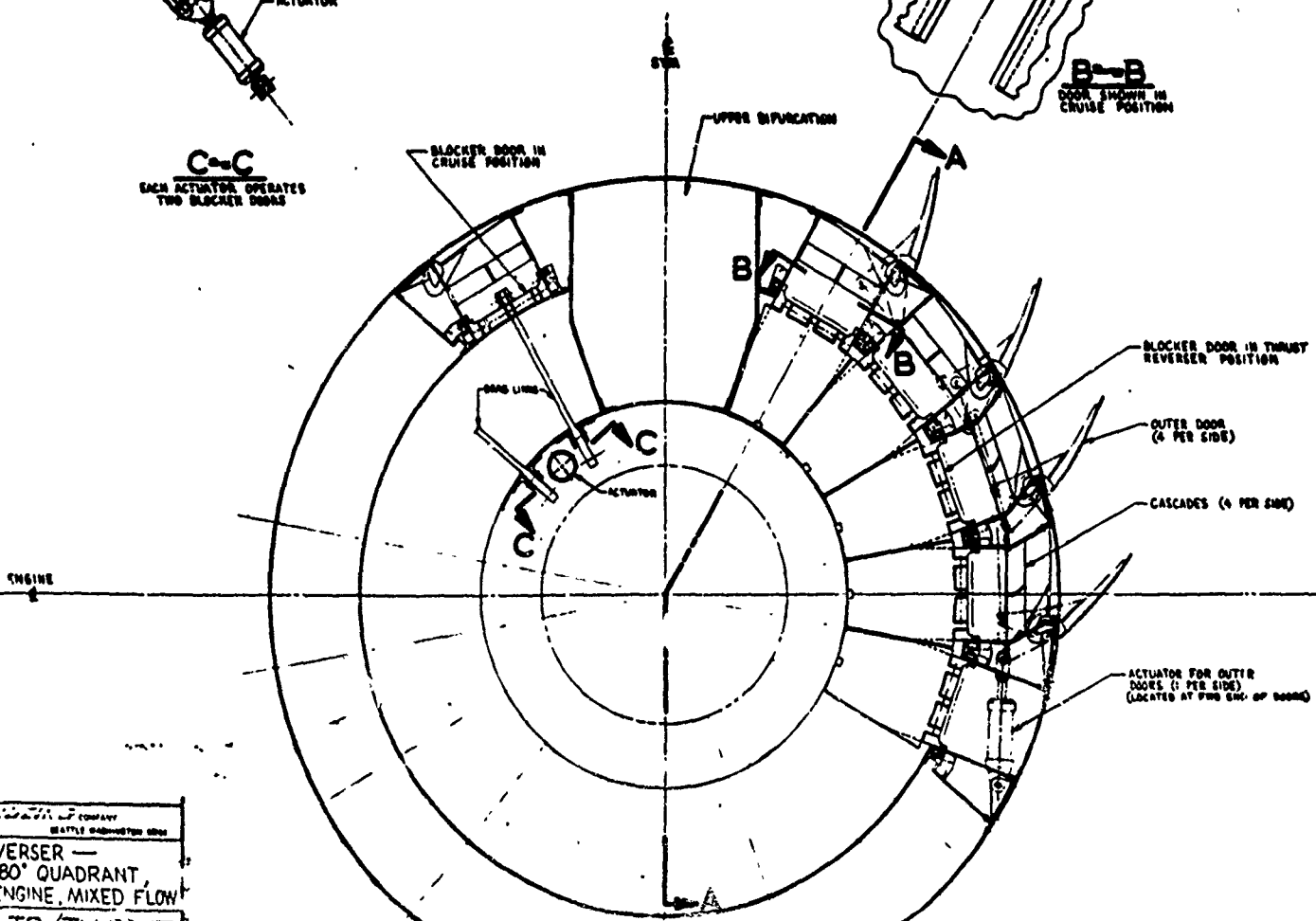
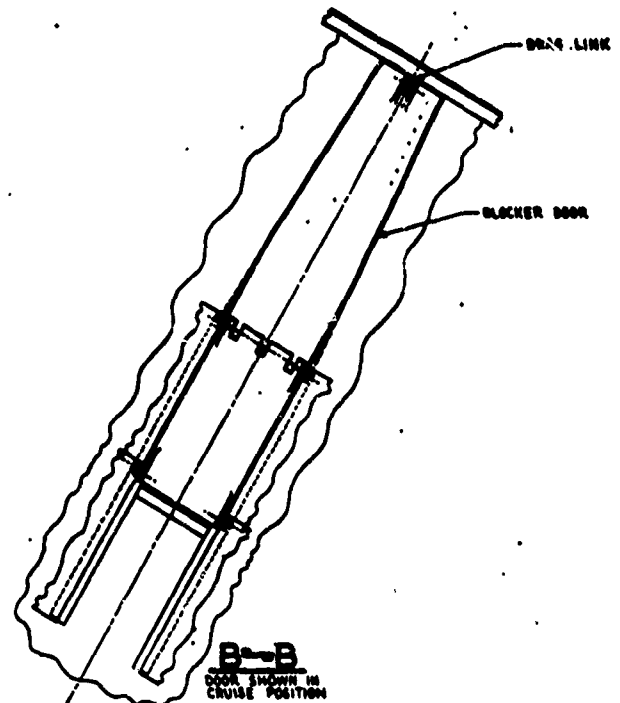


Figure 48: FAN REVERSER - UPPER 180° QUADRANT,
RPR 6 ENGINE, MIXED FLOW

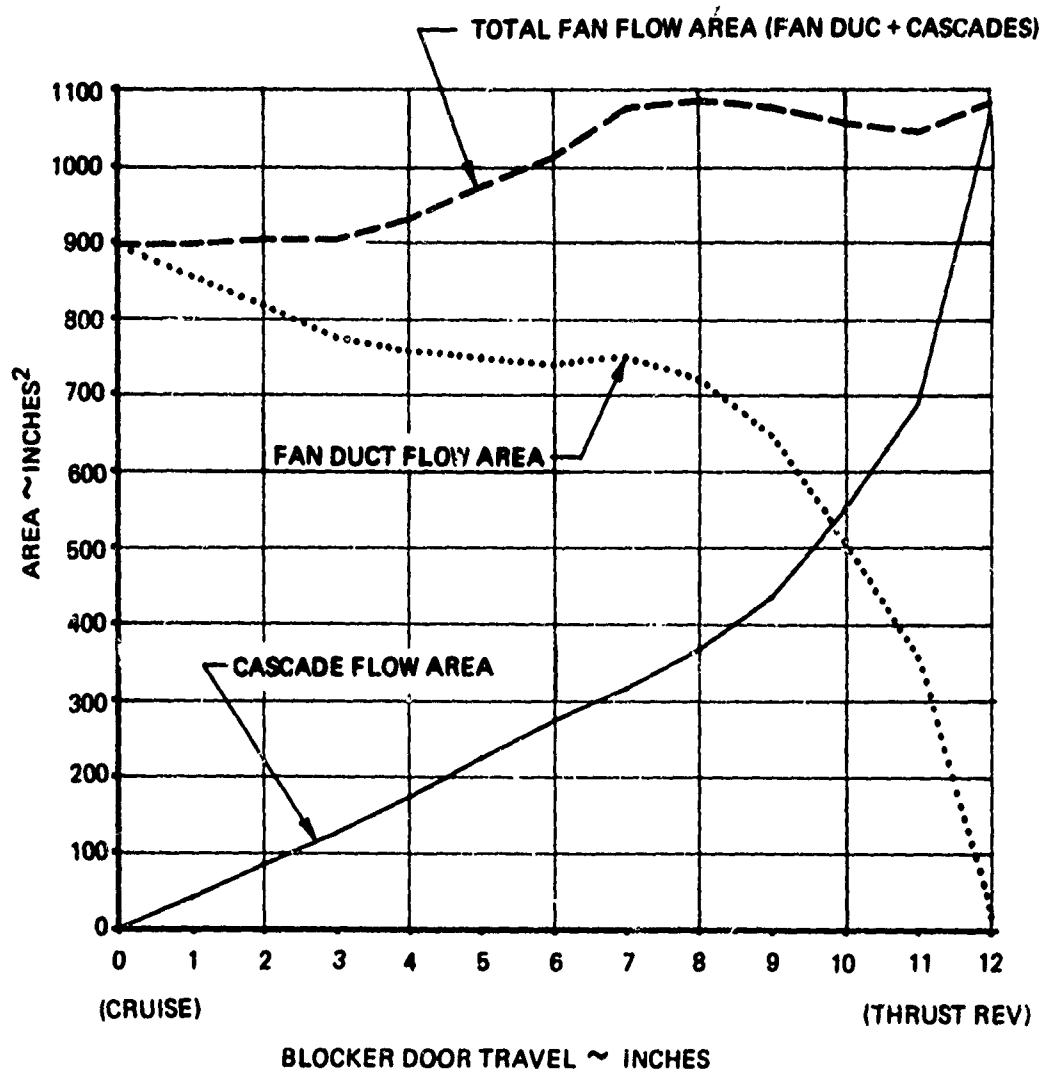


Figure 49: AREA PLOT – FAN DUCT AND/OR CASCADES VS BLOCKER DOOR OPENING

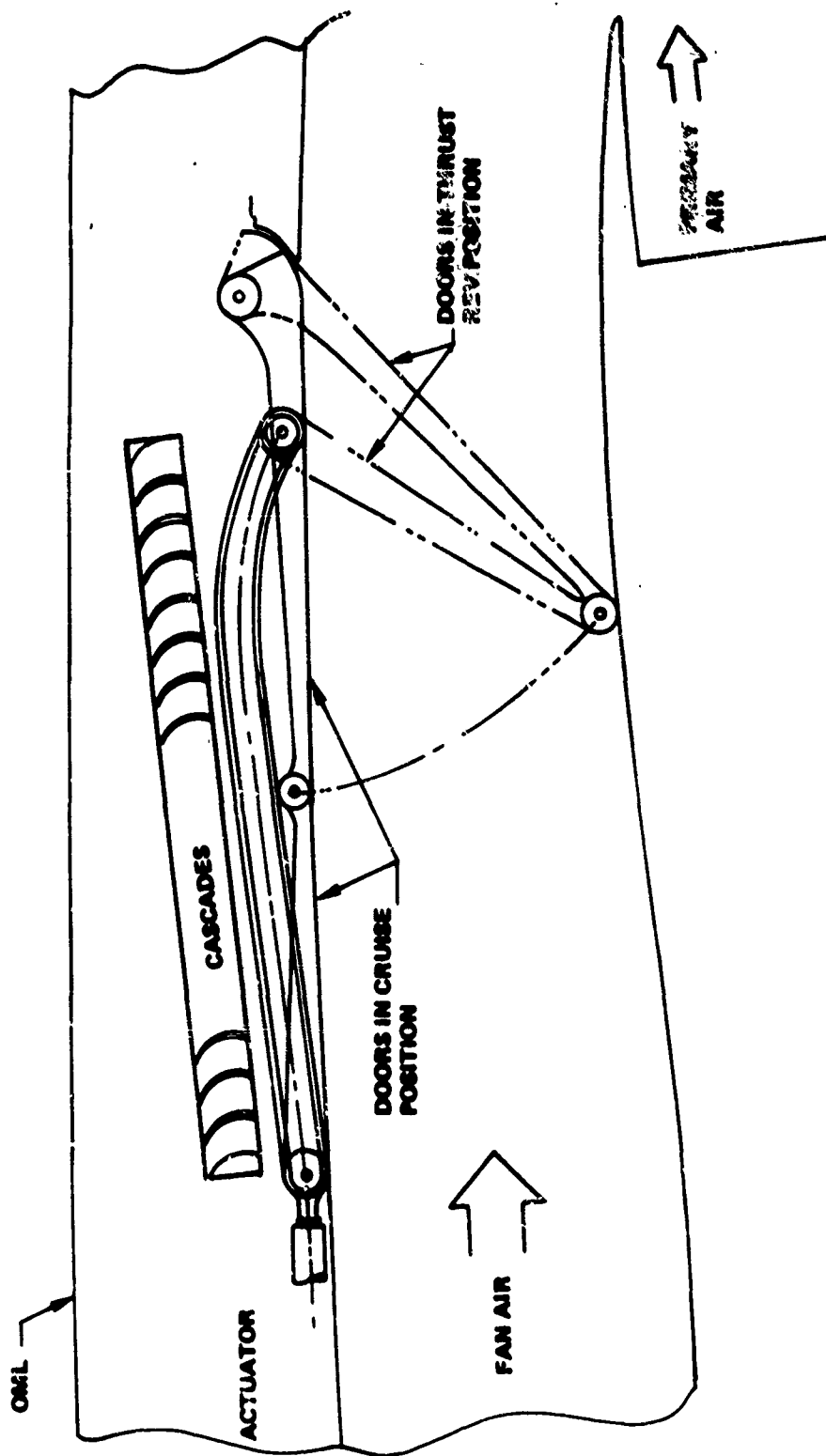


Figure 50: BIFOLD DOOR CONCEPT

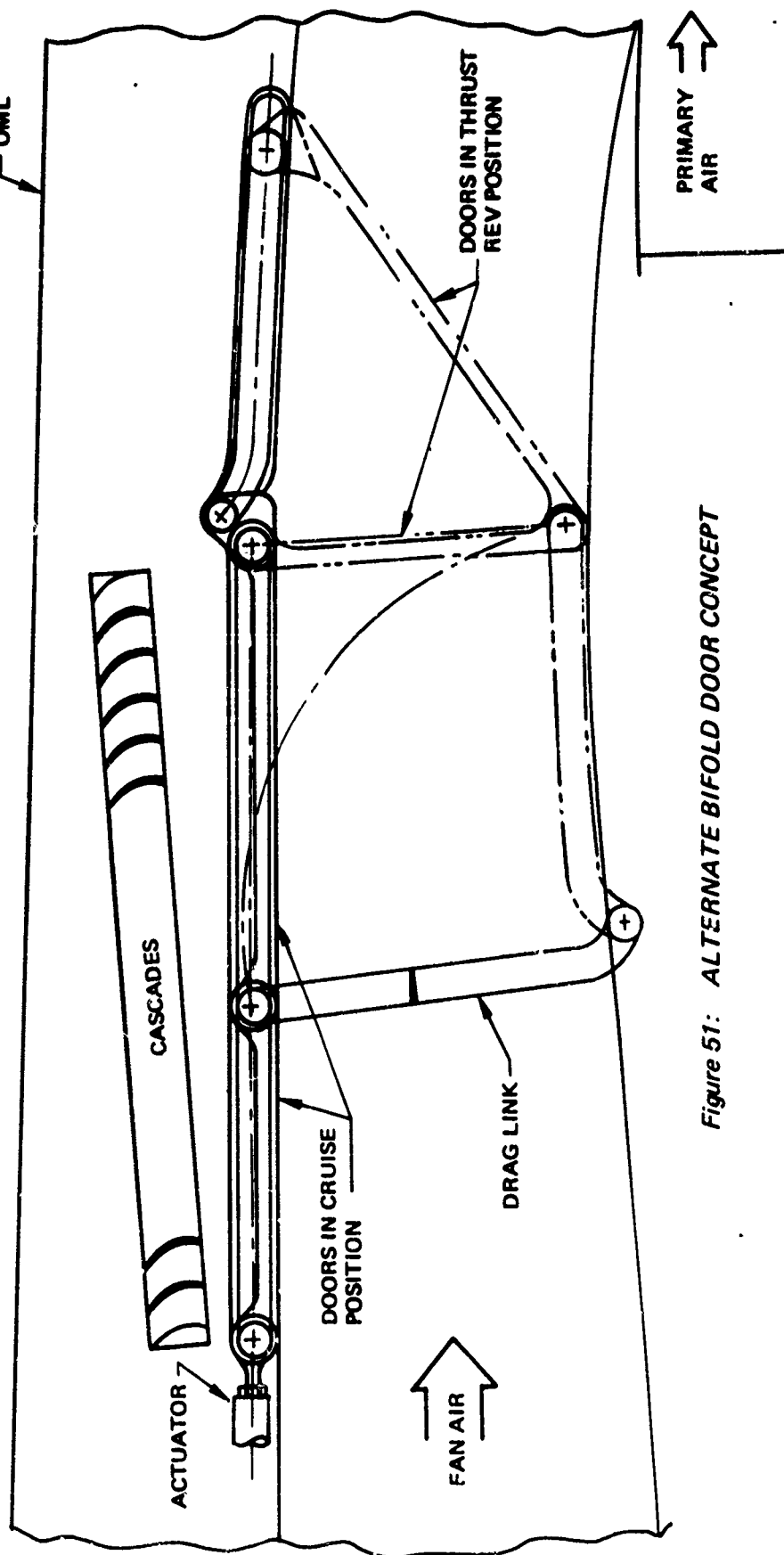
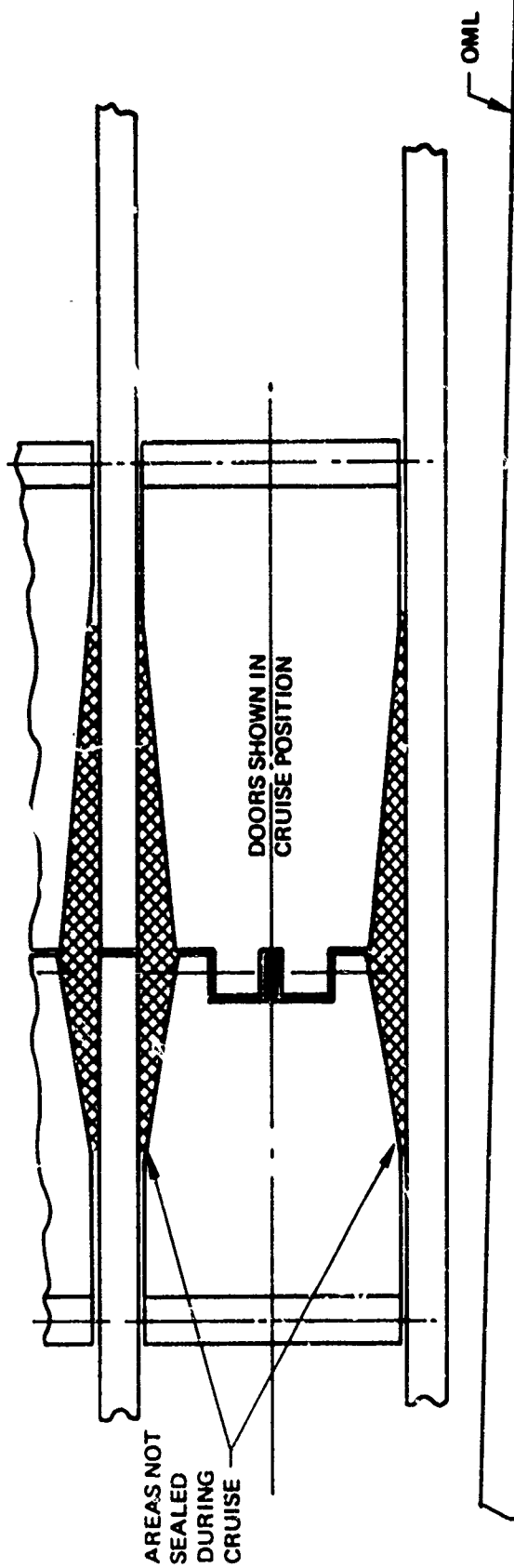


Figure 51: ALTERNATE BIFOLD DOOR CONCEPT

length would place the actuator attach point at the forward flange of the engine fan case. This location is considered unacceptable because of the various engine accessories and service lines on the fan case. To alleviate this problem and still actuate the door from this location, the entire engine nacelle would have to be lengthened approximately 18" with the cascades moved aft by this same amount. The actuator and its connecting linkage could then be positioned aft of the fan case rear flange. Also, the engine strut would have to be lengthened in order to keep the reverser gases forward of the wing leading edge. This potential increase in weight of the strut and nacelle resulted in the decision to place the actuator as shown in Figure 48. The temperature in this location would be an estimated 300° - 400°F. The desirability to keep hydraulic fluid away from the engine would indicate that an air operated actuator be used rather than a hydraulic device. However, if shrouded lines were discretely employed, hydraulic fluid should not become a decisive safety factor and either a hydraulic or pneumatic actuator could be used.

2.2 Task 2.2 --- Analyze Performance of TR/TV Systems

The design study conducted during Task 2.1 included thrust reverser (TR) and thrust vectoring (TV) systems applicable to three high lift systems for STOL tactical transports including:

1. externally blown flaps
2. mechanical flap and vectored thrust
3. upper surface blowing

The TR/TV concepts were evaluated on the basis of TR and TV performance and weight with the objective of obtaining the best TR/TV performance for the lightest weight system. Also, the impact of the TR/TV concept on the airplane aerodynamic characteristics was included in the evaluation. The purpose of the evaluation was to determine the most promising configurations for model tests during Part 1C.

Internal performance for the cruise nozzles, vectoring nozzles, vectoring nozzles, and thrust reversers was computed using the empirical prediction methods developed during Part 1A, Task 1.1 of the program. Detailed descriptions of the methods are provided in Volume I of this report. Weight estimates were made using Class I estimating methods, considering the size, materials, and actuation systems of the nacelle and TR/TV system installation. The weight accuracy is estimated to be ± 10 percent. This does not include weight that would be needed for a "quiet" nacelle, or flutter. The range of weights for the nacelle configurations is shown in Figure 52.

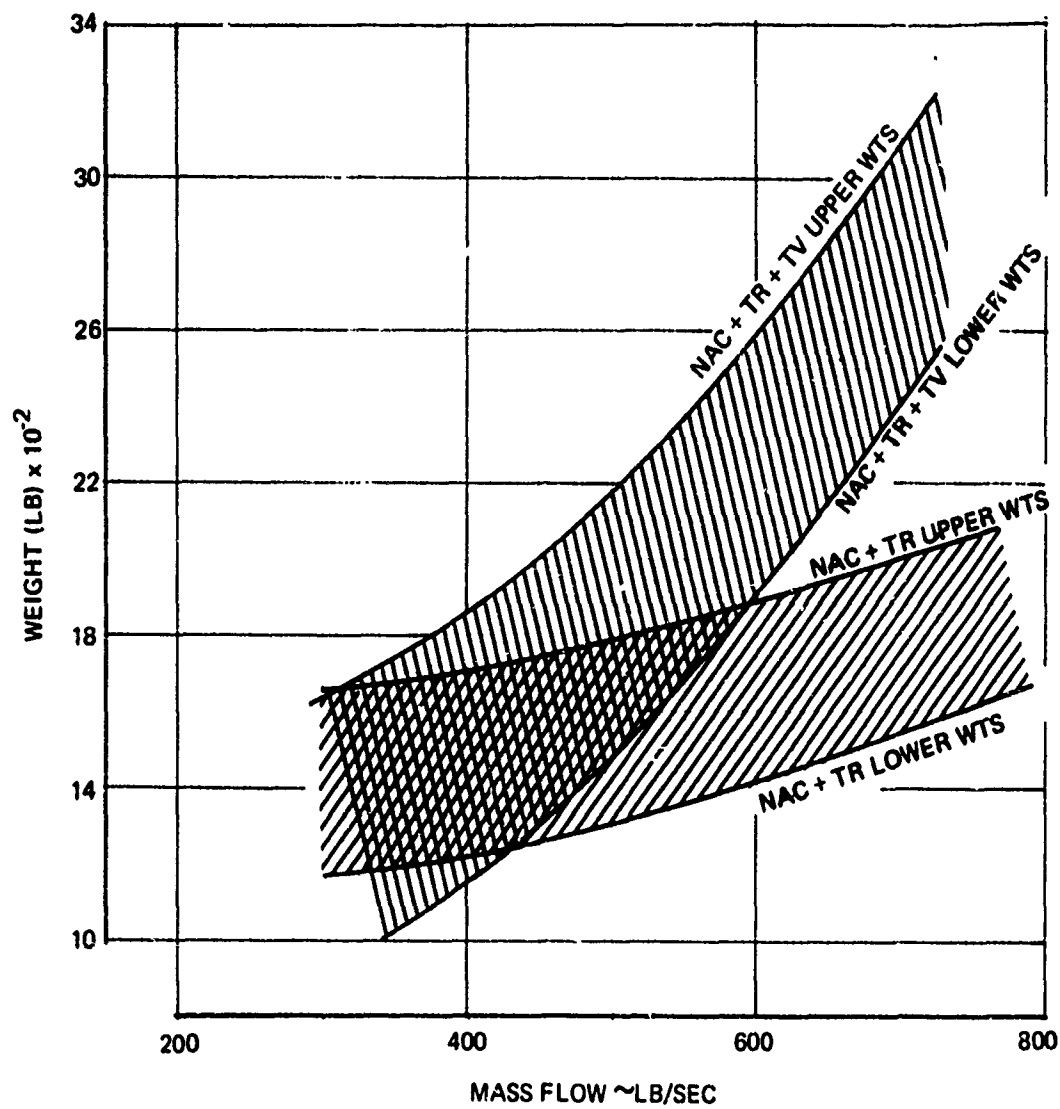


Figure 52: TR/TV NACELLE WEIGHT VS MASS FLOW

2.2.1 Externally Blown Flap Lift Systems

The thrust reverser concepts evaluated for an EBF propulsion system installation are shown in Figures 28 through 31. Table VII compares the predicted performance and weight for each concept. As shown in the Table, concept -16, (Figure 31) has the highest reverser performance, but the total propulsion installation is 500 lb/installation heavier than the other feasible concepts. Concepts -02 and -03 (Figures 28 and 29 respectively) have essentially the same installed weight, but concept -02, a fan cascade and mechanical primary spoiler, has better reverser performance. Concept -03 utilizes a fan cascade and "cycle spoiling" of the primary thrust during thrust reversing.

These thrust reverser concepts will cause no adverse effect on engine operation due to the mechanical design of the reverser. The detailed design study, Section 2.1.5, showed that the blocker door mechanism can be designed to maintain airflow match can be maintained for the translating sleeve and cascade TR system (concept -16). However, exhausting the reverser flow from the upper 180° sector of the nacelle could distort the internal flow which could affect engine operation. This is especially true for the fan cascade thrust reverser concepts (-02 and -03). The degree of this problem is dependent on the proximity of the reverser to the fan exit.

On the basis of Table VII, concept -02 has the best overall system performance and weight. The reverser performance is acceptable to achieve STOL landing field length, and it has essentially the same weight as the lowest weight concept (1570 vs. 1550 lb). One disadvantage of the concept is that the exhaust flow from the mechanical primary thrust spoiler would be directed to each side of the nacelle, resulting in impingement of the exhaust flow on the airplane fuselage (inboard nacelle) and on the adjacent nacelle. This could result in higher reverser cutoff speeds due to possible surface heating and re-ingestion problems.


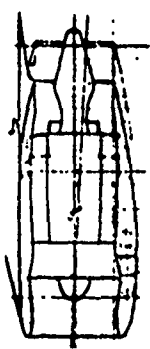

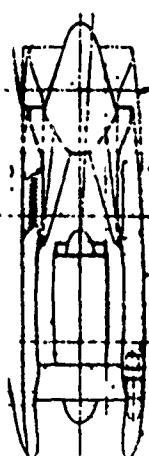
2.2.2 Mechanical Flap and Vectored Thrust Lift Systems

The evaluation of MF+VT vectoring concepts emphasized the thrust vectoring performance and propulsion system weight. Thrust reverser performance was considered for those systems with equivalent thrust vectoring performance and weight. Table VIII compares the predicted performance and weight for each concept.

Mixed Flow Engines --- Single Pod

As shown in Table VIII, concepts -06, -07, -13, and -19 (Figures 36, 38, 37, and 34) have essentially the same weight (within 100 lb) and vectoring performance. Concepts -13 and -19 have

Table VII: THRUST REVERSER CONCEPTS FOR EXTERNALLY BLOWN FLAP LIFT SYSTEMS

DESIGNATION NUMBER	THRUST REVERSER CONCEPT	INTERNAL PERFORMANCE				WEIGHT*			BASELINE INSTALL**				
		BYPASS RATIO	CRUISE		REVERSE η_R	Φ	NACELLE	STRUCT	CRUISE PERF		ΔW	TOTAL	
			C_V	C_D					ΔC_V	ΔC_D			
TR/TV-PP-02	 CASCADE FAN THRUST REVERSER PRIMARY SPOILER	6.0 UN- MIXED FLOW	FAN .968 PRI .968	FAN .948 PRI .949	.35	1.065	1330	240	FAN 0 PRI 0	FAN 0 PRI -.039	530	200	730
TR/TV-PP-03	 CASCADE FAN THRUST REVERSER CYCLE SPOILING OF PRIMARY THRUST	6.0 MIXED FLOW	.967	.984	.32	1.027	1310	240	0	0	710	220	930
TR/TV-PP-14	 CASCADE THRUST REVERSER CLAMSHELL BLOCKER DOOR	6.0 MIXED FLOW	.991	.954	.50	1.145	1690	270	+0.024	+0.030	710	220	930
TR/TV-PP-16	 CASCADE THRUST REVERSER TRANS SLEEVE, PLUG BLOCKER	6.0 MIXED FLOW	.959	.990	.50	.968	1790	280	-.092	+0.006	710	220	930

* WEIGHT OF ENGINE NOT INCLUDED

** $\Delta C_V = C_V - (C_V)$ BASELINE
 $\Delta C_D = C_D - (C_D)$ BASELINE
 $\Delta W = W - (W)$ BASELINE

* WEIGHT OF ENGINE NOT INCLUDED

** $\Delta C_V = C_V - (C_V)$ BASELINE

$\Delta C_D = C_D - (C_D)$ BASELINE

$\Delta W = W - (W)$ BASELINE

the highest thrust reverser performance which makes these concepts attractive for a mixed flow engine installation. However, the under area air flow match characteristic of concept -13 suggests that a variable area nozzle will be required for that concept to maintain air flow match during reverse mode. This will result in a weight increase. As noted in Section 2.1.4, applications of concept -13 will probably be limited to aircraft with one engine under each wing because of the possibility of cross-ingestion and ground impingement during reverse mode. Concept -06 has potentially greater reverse thrust than concept -07 because of the length of the multibearing nozzle duct. It is possible that the longer duct length would cause higher spoiling of the primary flow.

Since concepts -06 and -19 require cruise nozzle area variation during the vectoring mode (and concept -19 reverse mode) engine area control will be an important consideration during the steady state and transient conditions. It is believed that engine airflow match will be possible but will require a reliable control system that senses engine power demand, nozzle area and deflector position.

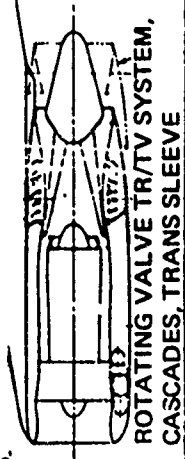

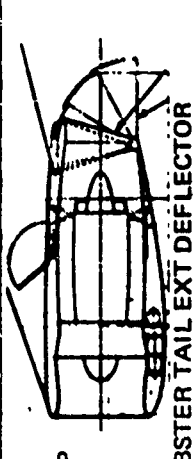
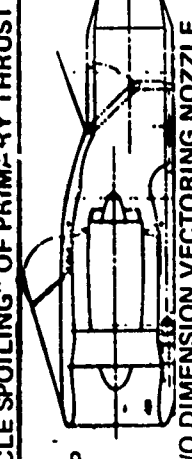
Therefore, it appears that the best overall vectoring system concept of those studied for mixed flow engines on four-engine aircraft could be either the multibearing concept (concept -06 Figure 36) or the combined thrust vectoring/reverser external deflector concept (concept -19, Figure 34). Concept -13 would be best suited for airplane configurations with one engine under each wing. Although these concepts were drawn for a BPR 6.0 engine, only concepts -19 and -13 would be suitable for BPR 3.0. The "cycle spoiling" feature of concept -06 would be unsuitable for engines with $BPR < 6.0$.

Unmixed Flow Engines --- Single Pod

The rotating nozzle concept (Figure 40) offers a technique to vector and reverse the thrust of bypass ratio 6.0 or less unmixed flow engines. This concept was the only system evaluated for BPR 3.0 and 6.0 engines. Vectoring performance is high because the nozzle geometry is virtually the same as the cruise and vectored positions and additional pressure losses during vectoring or reversing would be minimal. It should be noted, however, that cruise nozzle performance will be affected by the bifurcated fan and primary ducts.

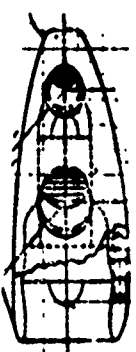


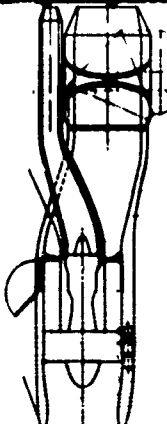
As shown in Tabel VIII the concepts evaluated for BPR 12.0 unmixed flow engines have poor weight characteristics. It was concluded from the evaluation that thrust vectoring systems for BPR 12.0 size engines are probably not feasible primarily due to excessive weight.

Table VIII: THRUST REVERSER/VECTORIZING CONCEPTS FOR MECHANICAL FLAP AND VECTORED THRUST LIFT SYSTEMS

DESIGNATION NUMBER	THRUST VECTORIZING/REVERSER CONCEPT	ENGINE BPR	INTERNAL PERFORMANCE						WEIGHT*			BASELINE INSTALL **			
			CRUISE			REVERSE			NACELLE	STRUCT	TOTAL	CRUISE PERF		WEIGHT	
			C _V	C _D	η _R	Φ	η _V	Φ				C _V	C _D	ΔW NACELLE	ΔW STRUCT TOTAL
TR/TV-PP-05		3.0 MIXED FLOW	.963	.975	.50	1.09	.857	1.02	1750	290	2040	-.009	-.006	+1140	+80
TR/TV-PP-06		6.0 MIXED FLOW	.983	.941	.32	1.06	.957	.922	1500	290	1790	+.016	-.043	+790	+70
TR/TV-PP-07		6.0 MIXED FLOW	.991	.954	.32	1.06	.955	.90	1500	300	1800	+.024	-.030	+720	+80
TR/TV-PP-08		6.0 MIXED FLOW	.969	.900	.32	1.36	.974	.993	2080	320	2400	+.002	-.088	+1370	+100

* WEIGHT OF ENGINE NOT INCLUDED
 ** ΔC_V = C_V - (C_V) BASELINE
 ΔC_D = C_D - (C_D) BASELINE
 ΔW = W - (W) BASELINE

Table VIII: THRUST REVERSER/VECTORIZING CONCEPTS FOR MECHANICAL FLAP AND VECTORED THRUST LIFT SYSTEMS (Continued)

DESIGNATION NUMBER	THRUST REVERSER/VECTORIZING CONCEPT	ENGINE BPR	INTERNAL PERFORMANCE						WEIGHT*			BASELINE INSTALLATION**			
			CRUISE		REVERSE		VECTOR		NACELLE	STRUCT	TOTAL	CRUISE PERF		WEIGHT	
			C _V	C _D	η _R	φ	η _V	φ				C _V	C _D	ΔW NACELLE	ΔW STRUCT
TR/TV-PP-10		6.0 UN- MIXED FLOW	FAN .980 PRI .973	FAN .935 PRI .938	.53	.98	.98	1.00	1710	280	1990	FAN +0.012 PRI +0.005	FAN -0.014 PRI -0.041	+80	+1260
TR/TV-PP-13		6.0 MIXED FLOW	.969	.948	.45	.88	.954	.928	1400	300	1700	+0.002	-0.036	+80	+770
TR/TV-pp-19		6.0 MIXED FLOW	.980	.970	.44	1.10	.950	.900	1430	290	1720	+0.013	-0.014	+70	+720
TR/TV-PP-09		12.0 UN- MIXED FLOW	FAN .951 PRI .959	FAN .979 PRI .991	.43	1.02	.913 (FAN ONLY)	.883	3180	500	3680	FAN +0.011 PRI 0	FAN -0.0; 0 PRI 0	260	2680

*** WEIGHT OF ENGINE NOT INCLUDED

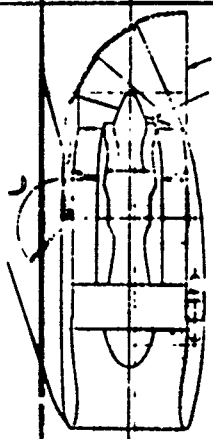

** ΔC_V = C_V(C_V) BASELINE

ΔC_D = C_D - (C_D) BASELINE

ΔW = W - (W) BASELINE

WEIGHT OF ENGINE NOT INCLUDED
 $\Delta C_V = C_V(C_V)$ BASELINE
 $\Delta C_D = C_D - (C_D)$ BASELINE
 $\Delta W = W - (W)$ BASELINE

Table VIII: THRUST REVERSER/VECTORIZING CONCEPTS FOR MECHANICAL FLAP AND VECTORED THRUST LIFT SYSTEMS (Concluded)

DESIGNATION NUMBER	THRUST REVERSER/VECTORIZING CONCEPT	ENGINE BPR	INTERNAL PERFORMANCE					WEIGHT*			BASELINE INSTALLATION**					
			CRUISE		REVERSE		VECTOR	NACELLE	STRUCT	TOTAL	C _V	C _D	WEIGHT		TOTAL	
			C _V	C _D	η _R	φ	η _V						φ	ΔW		ΔW
TR/TV-PP-12		12.0 UN- MIXED FLOW	FAN .951 PRI .959	FAN .979 PRI .991	.43	1.019	.980	.822	2490	350	2840	FAN +0.11 PRI 0	FAN -0.10 PRI 0	1790	110	1900
TR/TV-PP-15 DUAL POD		3.0 MIXED FLOW	.970	.944	.44	1.10	.950	.900	2000	430	2430	-0.002	-0.037	740	90	830

* WEIGHT OF ENGINE NOT INCLUDED

**** $\Delta C_V = C_V - (C_V)$ BASELINE WEIGHT OF ENGINE NOT IN**

$$\Delta C_D = C_D - (C_D) \text{ BASELINE}$$
$$\Delta W = W - (W) \text{ BASELINE}$$

Mixed Flow --- Dual Pods

As shown in Table VIII the external deflector/target thrust vectoring/reverser systems offer good performance and weight characteristics for BPR 3.0 dual pod installations.

Aerodynamic Stability and Control Considerations

The effective thrust vector of a mechanical flap and vectored thrust lift system rarely acts through the airplane center of gravity. Therefore, the resulting thrust pitching moment must be considered when balancing a vectored thrust airplane. Acceptable engine locations must be defined to avoid adverse effects on the stability and control of the aircraft. Figure 53 illustrates how four stability and control balancing requirements are used to define the envelope of acceptable engine locations. These criteria are for takeoff rotation, longitudinal control power, static tip up, and static longitudinal stability. Of the four boundaries the forward boundary of the envelope, static longitudinal stability is the most critical. Placing the thrust vector forward of the envelope means that the airplane will be unstable because of the horizontal tail size cannot compensate for the adverse pitching moment.

As shown in Figure 53 concepts -06, -07, and -13 are within the acceptable thrust vector location envelope, and concepts -10 and -19 are outside the boundary. Therefore, rebalancing of the airplane configuration is required for concepts -10 and -19. This could require either resizing the horizontal tail or relocating the wing further aft toward the c.g., or both, with corresponding possible weight penalties. Rebalancing the airplane to accommodate concept -10 will be more difficult than for concept -19 because the pitching moment is greater. It should be noted that the pitching moment problem exists for those systems that combine the function of the thrust reverser and thrust vectoring systems and directs the reverser exhaust forward of the wing leading edge. Concepts that separate the thrust vectoring and thrust reverser systems do not have pitching moment problems.

2.2.3 Upper Surface Blowing Lift Systems

Evaluation of upper surface blowing concepts was based primarily on the reverser performance and weight comparisons. It was assumed that the thrust reverser concept would not influence the performance of the vectoring system. Table IX compares the performance and weight characteristics for the two thrust reverser concepts for upper surface blowing lift systems. Concept -18 (Figures 46 and 47) provides the required exhaust flow characteristics for optimum USB performance, and also offers good reverser performance and weight characteristics. This concept has been successfully applied to STOL configurations currently under study at Boeing.

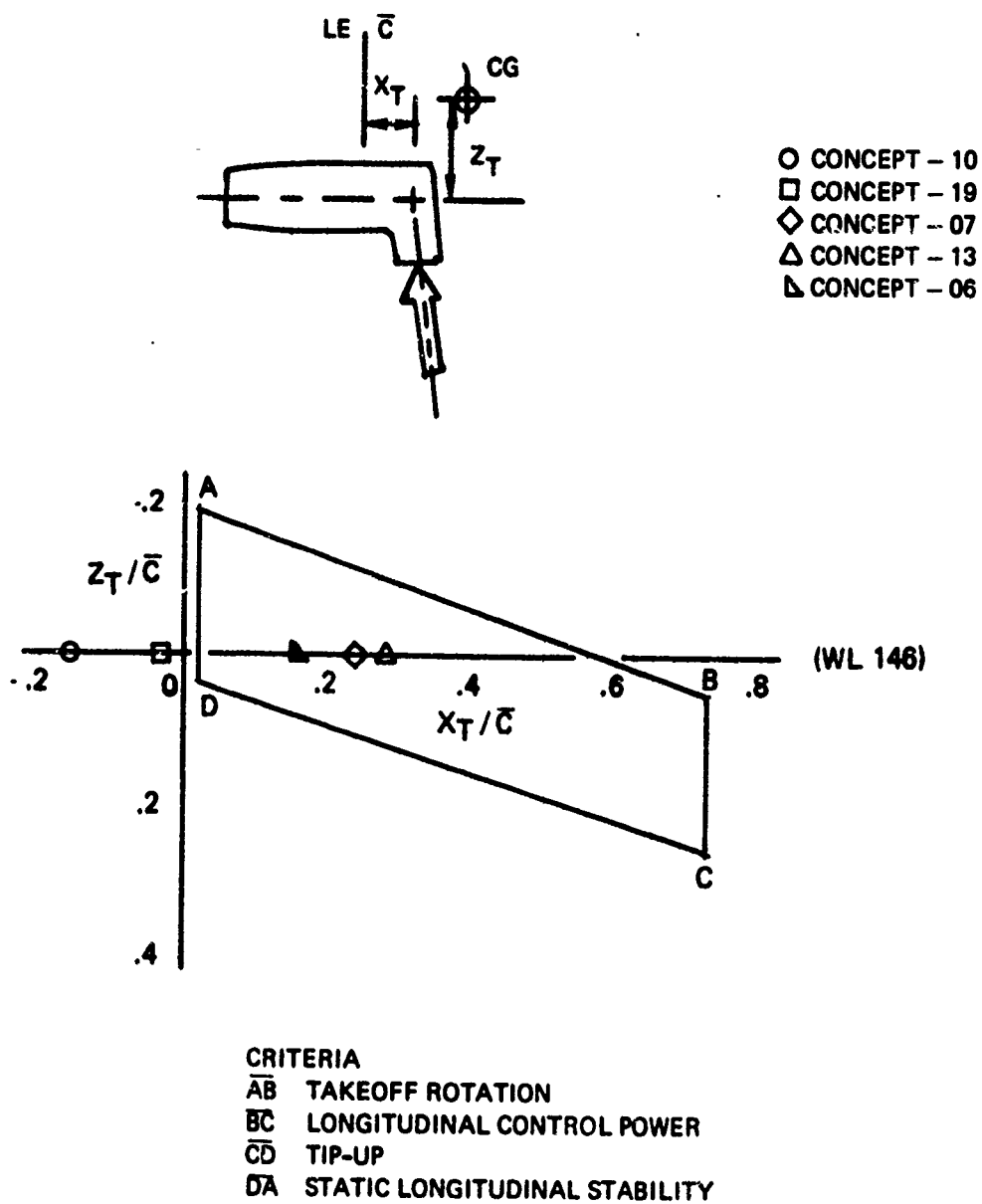
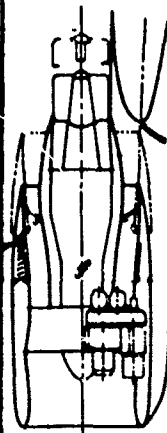



Figure 53: STABILITY AND CONTROL ENGINE LOCATION ENVELOPE

Table IX: THRUST REVERSER CONCEPTS FOR UPPER SURFACE FLOWING LIFT SYSTEMS

DESIGNATION NUMBER	THRUST REVERSER	INTERNAL PERFORMANCE						WEIGHT*			BASELINE INSTALL**			
		ENGINE BPR	CRUISE		REVERSE		NACELLE	STRUCT	TOTAL	CRUISE PERFORM		WEIGHT		
			C _V	C _D	η _R	Φ				C _V	C _D	ΔW NACELLE	ΔW STRUCT	ΔW TOTAL
TR/TV-PP-04	 CASCADE FAN THRUST REVERSER PRIMARY THRUST SPOILER	6.0 UN- MIXED FLOW	FAN .968	FAN .969	.35	1.06		240	1570	0	0		+40	+840
			PRI .968	PRI .969			1330			0	-0.35	+800		
TR/TV-PP-18	 EXTERNAL TARGET THRUST REVERSER	6.0 MIXED FLOW	.966	.984	.50	.95	1280	270	1550	-0.02	0	+570	+50	+620

* WEIGHT OF ENGINE NOT INCLUDED

** ΔC_V = C_V - (C_V)_{BASELINE}

ΔC_D = C_D - (C_D)_{BASELINE}

ΔW = W - (W)_{BASELINE}

* WEIGHT OF ENGINE NOT INCLUDED

** ΔC_V = C_V - (C_V) BASELINE

ΔC_D = C_D - (C_D) BASELINE

ΔW = W - (W) BASELINE

2.2.4 Conclusions

The results of the TR/TV concept evaluations are summarized in Table K. The following conclusions can be made based on the evaluation results:

1. The thrust reverser system for externally blown flap lift systems will probably involve the use of a fan cascade thrust reverser.
2. Mechanical flap and vectored thrust lift systems could use either
 - a. rotating nozzles
 - b. multibearing vectoring nozzles
 - c. external deflector/target thrust vectoring/reversing systems

depending on the type of engine cycle (mixed or unmixed flow).

The rotating nozzle vectoring system would be used for unmixed flow engines and would present airplane balancing problems due to the thrust vector location and the resulting adverse pitching moment. The external deflector/target TR/TV system would also pose balancing difficulties but to a lesser degree. Multibearing vectoring nozzle installations would present no airplane balancing problems.

3. Upper surface blowing lift systems will utilize an external target thrust reverser system installed with a mixed flow engine.

2.3 Task 2.3 Select Designs for Part 1C

On the basis of the evaluations, the following TR/TV systems representing various lift systems for STOL tactical transports were considered for Part 1C static tests and future low speed wind tunnel tests:

1. A fan cascade thrust reverser system that exhausts the fan flow through cascades installed in the upper 180° sector of the nacelle (EBF, MF + VT).
2. An external deflector/target TR/TV system that combines the functions of thrust vectoring and reversing into a single mechanism. (MF + VT)
3. A multibearing vectoring nozzle (MF + VT).
4. An external target thrust reverser for an overwing installation (USB).

Table X: EVALUATION SUMMARY

LIFT SYSTEM	ENGINE TYPE	DESCRIPTION	TR/TV CONCEPT
EXTERNALLY BLOWN FLAP	BPR 6.0 UNMIXED	FAN CASCADE THRUST REVERSER AND PRIMARY THRUST SPOILER	TR/TV-PP-02
	BPR 12.0 UNMIXED	FAN CASCADE THRUST REVERSER	TR/TV-PP-02 SCALED TO BPR 12.0 NO PRIMARY SPOILER
MECH FLAP AND VECTORED THRUST	BPR 6.0 UNMIXED	ROTATING FAN AND PRIMARY NOZZLES	TR/TV-PP-10
	BPR 6.0 MIXED	MULTIBEARING VECTORED NOZZLE TR/TV SYSTEM ($\sigma = 120^\circ$)	TR/TV-PP-13
		EXTERNAL DEFLECTOR/TARGET TR/TV SYSTEM	TR/TV-PP-19
		MULTIBEARING VECTORED NOZZLE FAN CASCADE THRUST REVERSER AND PRIMARY "CYCLE SPOILING"	TR/TV-PP-03
	BPR 3.0 UNMIXED	ROTATING FAN AND PRIMARY NOZZLES	TR/TV-PP-10 SCALED TO BPR 3.0 SIZE
	BPR 3.0 MIXED	MULTIBEARING VECTORED NOZZLE TR/TV SYSTEM ($\sigma = 120^\circ$)	TR/TV-PP-13 SCALED TO BPR 3.0 SIZE
	BPR 12.0 UNMIXED	EXTERNAL DEFLECTOR/TARGET TR/TV SYSTEM	TR/TV-PP-19 SCALED TO BPR 3.0 SIZE
		NO VECTORED SYSTEM FEASIBLE IN THIS BYPASS RATIO ENGINE	
	BPR 3.0 MIXED DUAL POD	EXTERNAL DEFLECTOR/TARGET TR/TV SYSTEM	TR/TV-PP-15
UPPER SURFACE BLOWING	BPR 6.0 MIXED	EXTERNAL TARGET THRUST REVERSER SYSTEM	TR/TV-PP-18
	BPR 3.0 MIXED FLOW SINGLE OR DUAL POD	EXTERNAL TARGET THRUST REVERSER SYSTEM	TR/TV-PP-18 SCALED TO BPR 3.0 SIZE

Parametric test data are available that are applicable to the multibearing nozzle and the external target thrust reverser concepts. Multibearing nozzle data was obtained during Part 1A of the program (Reference 8). A wide range of geometry variations were tested that is adequate to define the vectoring and reversing performance of multibearing nozzles. The multibearing nozzle test results are reviewed in Volume I of this report. Data for the external target thrust reverser for the USB lift system was obtained from a Boeing sponsored static test program (Reference 9). The results have been made available to the STOL Transport TR/TV Program and are reviewed in Section IV.

Because of the existence of data for the multibearing nozzle and external target thrust reverser concepts further testing of these concepts was considered unnecessary. Therefore, the fan cascade thrust reverser system and the external deflector/target TR/TV system concepts were selected for Part 1C static testing.

2.4 Task 2.4 - Test Plan Preparation

Test plans were developed for Part 1C static tests for the thrust reverser and thrust vectoring concepts selected during Task 2.3. The purpose of the tests was to obtain parametric performance data as a function of geometric variables and engine power setting. The test plans (Reference 10) provide definition and descriptions of the test objectives, methodology, models, facility requirements, conditions, procedures, and data acquisition requirements. The test plans were submitted to the Air Force Project Engineer for approval on 31 March 1972 and were approved on 26 May 1972.

2.5 Task 2.5 - Fabricate Hardware for Part 1C

Test model design and fabrication was initiated immediately following approval of the Air Force Project Engineer to proceed. Model fabrication was initiated on 17 June and was completed on 27 July 1972. Detailed descriptions of the test model hardware are contained in Section IV.

SECTION III

PART IC - MODEL TESTING

3.1 Task 3.1 - Conduct Static Performance Test

The objective of Task 3.1 was to obtain parametric performance data for the promising thrust reverser and thrust vectoring concepts developed during Part IB design studies. Static performance data as a function of fundamental geometric variables and engine power setting was required.

As discussed in Section III, a fan cascade thrust reverser system and an external deflector target TR/TV system were selected for static testing. The tests were conducted at the Boeing Propulsion/Noise Laboratories during July and August 1972. The test results are summarized here-in. Detailed results are contained in a test report (Reference 11) submitted to the Air Force Project Engineer in October 1972.

3.1.1 Fan Cascade Thrust Reverser Model Test

A proposed method to minimize thrust reverser exhaust gas reingestion and aerodynamic interference on STOL tactical aircraft is to direct the exhaust flow upward and forward of the wing leading edge. For a fan cascade reverser system, this means the aperture opening of the fan cascade will be limited to the upper 180° sector of the nacelle. The cascade aperture will be longer than conventional cascade designs (i.e., 747, DC-10) as a result of this requirement. There are several problems associated with this design, most notably the potential distortion of the fan duct internal flow during reverser operation vertical directional control of the exhaust flow while providing acceptable reverse thrust performance.

Objectives

The objectives of the static test was to:

- 1) Obtain performance data for a fan cascade thrust reverser designed to exhaust the fan flow from the upper 180° sector of the engine nacelle.
- 2) Investigate the characteristics of the fan duct internal flow during reverser operation.
- 3) Establish design criteria for future wind tunnel models and for full scale hardware design.

Test Model

The test model simulated a fan cascade thrust reverser suitable for either un-mixed flow or mixed flow (with cycle spoiling of primary thrust) high bypass ratio turbofan engines. A schematic of the model is shown in Figure 54. The model consisted of an annular flow duct simulating a fan exhaust duct, with simulated duct bifurcations for the strut (upper) and engine accessory controls (lower), and a cascade reverser located in the upper portion of the nacelle. The annular flow passage was held concentric by three struts located radially 120° apart. Blocker inserts were used to simulate the thrust reverser blocker door geometry. Inserts for 45°, 90°, and 135° were tested. A photograph of the model is shown in Figure 55. Each configuration was tested over the total pressure to ambient pressure range of 1.2 to 2.2.

The cascade reverser used was a model fabricated for Model 747 thrust reverser development testing. The cascade segments were rearranged to provide the desired flow directional control as shown in Figure 56. The cascade vane entrance angle varied depending on the axial location of the vane and the leaving angle of each vane was fixed at 50°.

Details of the model total pressure instrumentation are shown in Figure 54. Three rakes with a total of 33 probes were installed radially 120° apart. The probes are "area-weighted" so that each probe measures the total pressure in an equal-area sector of the flow. The model total pressure was computed using the average of the duct total pressures. Model total temperature was measured by a chromel alumel thermocouple located in the plane of the total pressure probes.

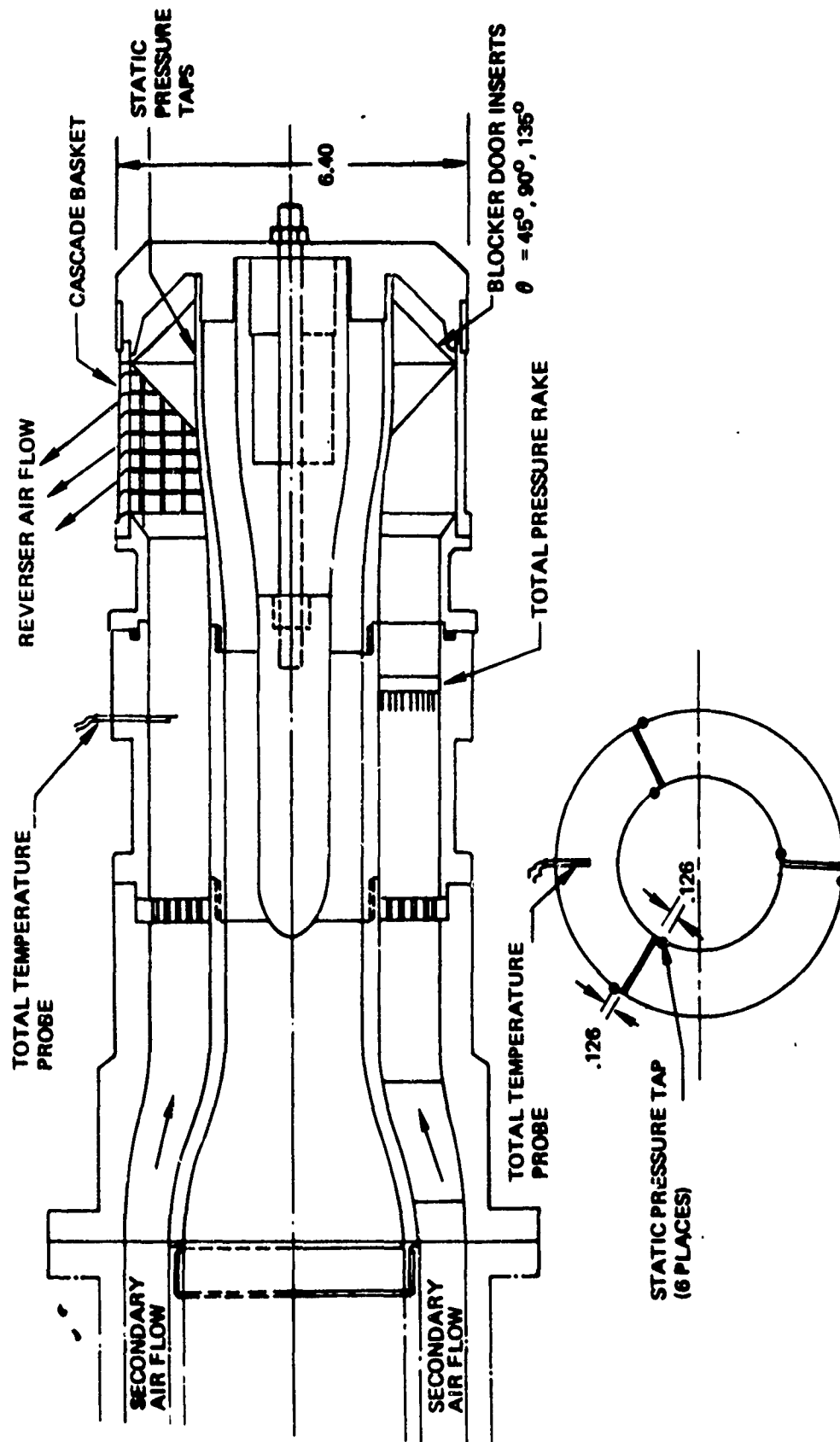
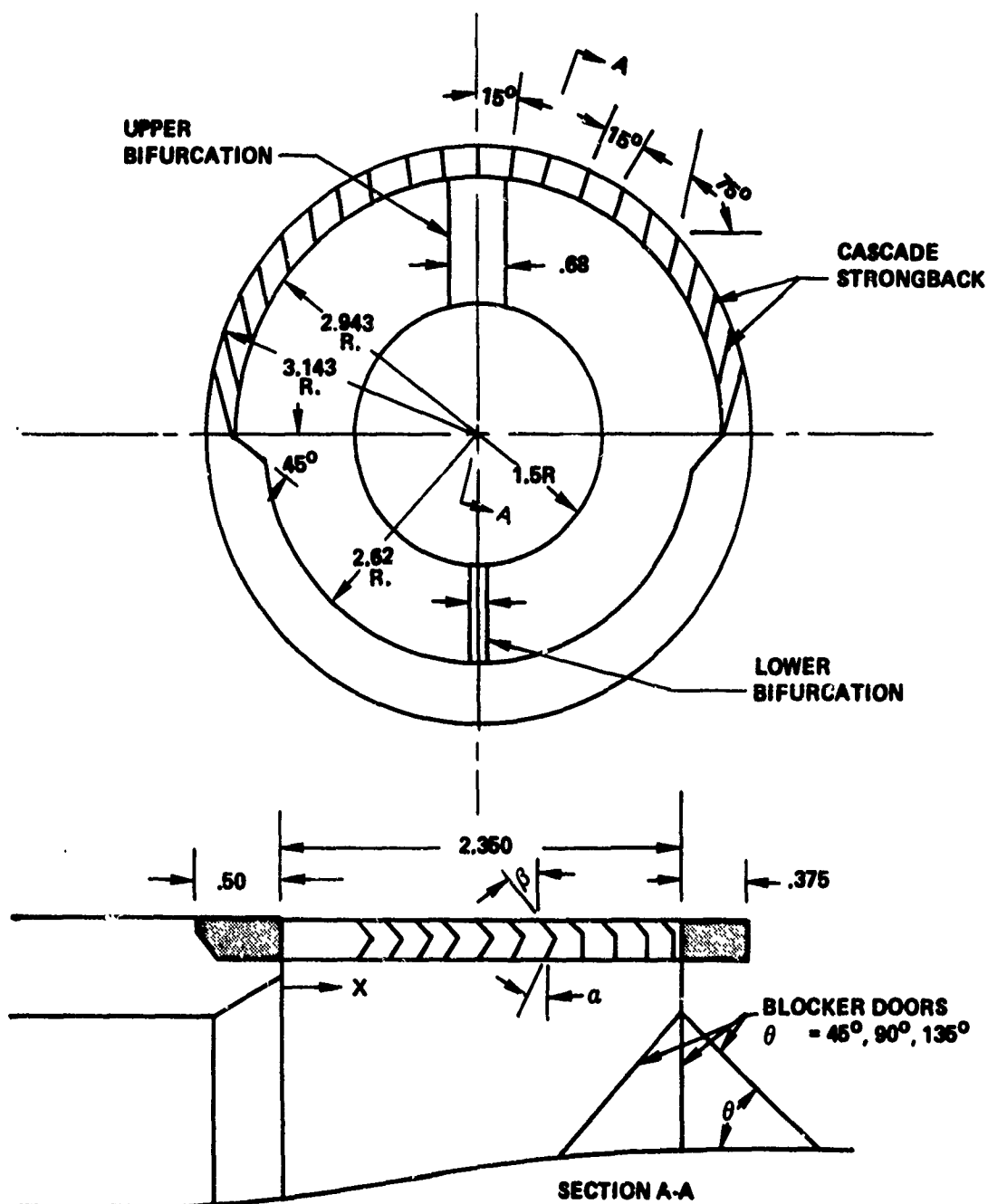


Figure 54: FAN CASCADE THRUST REVERSER INSTALLATION



Figure 55 : FAN CASCADE REVERSER MODEL INSTALLATION



VANE NO.	X	α	β	VANE NO.	X	α	β
1	.440	40°	40°	7	1.500	20°	40°
2	.600	40°	40°	8	1.680	0°	40°
3	.780	40°	40°	9	1.880	0°	40°
4	.950	40°	40°	10	2.080	0°	40°
5	1.130	40°	40°	11	2.240	0°	40°
6	1.320	20°	40°				

Figure 56: Annular Duct and Cascade Geometry

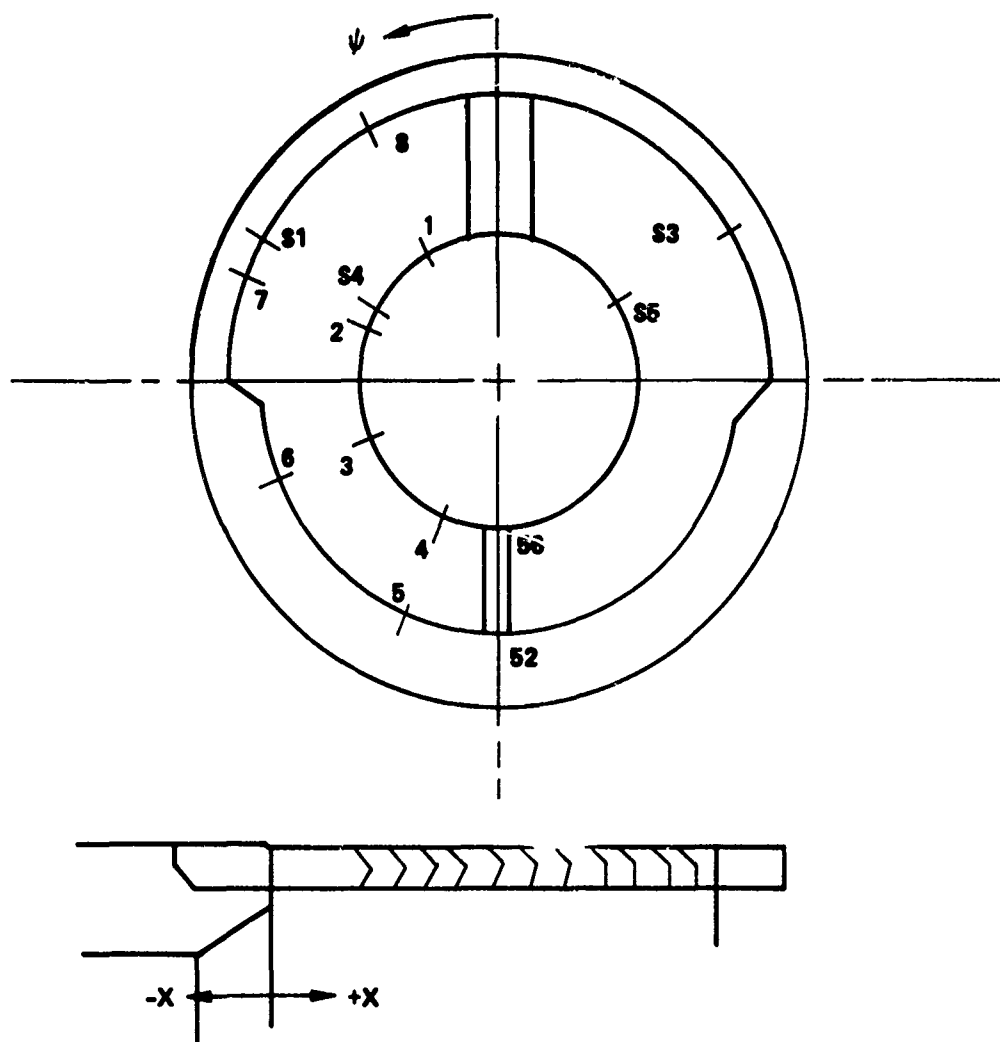
Static pressure taps were installed in the inner and outer wall of the duct as illustrated in Figures 54 and 57. The first static tap in rows 2 and 7 were positioned in the same plane as the total pressure probes. In addition, two static pressure taps were located adjacent to each total pressure rake, one on the inner wall and the other on the outer wall. These static taps were used to evaluate the characteristics of the internal flow during reverser operation.

A total pressure survey of the fan cascade thrust reverser exhaust flow field was conducted using a 12 probe total pressure rake installed at various radial positions as shown in Figure 58 and illustrated in Figure 59. The exit probes were positioned approximately equidistant between each vane except for the first vane where space was sufficient for two probes. Surveys were made for the radial positions and blocker door geometries shown in Figure 59. The rake was always oriented to be parallel to the cascade strongbacks (see Figure 59). The correct angle was verified using an inclinometer.

Test Results

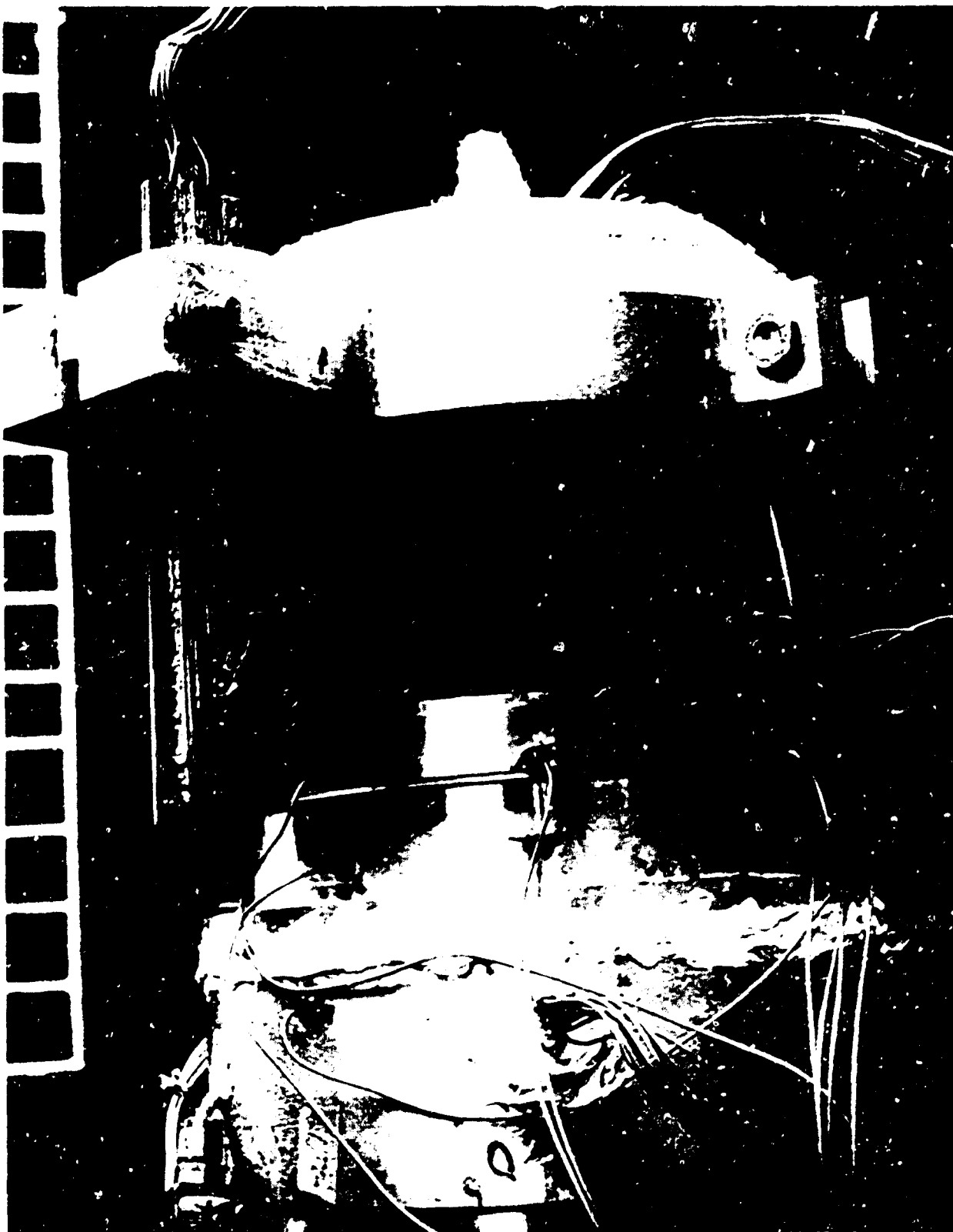
Results of the fan cascade thrust reverser static test are summarized below. Because some of the configurations had nearly equivalent performance, data points are not shown in the performance comparison plots to maintain clarity. Performance data for each configuration is presented in Reference 11.

1. Reverser efficiency of at least 50% is possible for a fan cascade thrust reverser that exhausts all of the fan flow through the upper portion of the nacelle, (Figure 60).
2. The highest reverser performance was obtained when the duct blocker door angle was 135° (Figure 60 and 61).
3. The cascade discharge coefficient was not appreciably affected by the duct blocker door geometry. Air flow match data indicate the reverser was slightly oversized relative to the assumed cruise nozzle flow area (Figure 62).
4. The position of the cascade in the upper 180° segment of the model resulted in internal flow distortion in the annular fan exhaust duct (Figure 63). Static pressure data show that the distortion diminished at approximately $x/h = -3.00$ upstream of the cascade.



ROW	ψ	AXIAL STATION X					
1	27°		-2.45	-1.30	-.50		
2	67°	-3.30	-2.45	-1.30	-.50		
3	113°		-2.45	-1.30	-.50	+.70	+2.50
4	158°		-2.45	-1.30	-.50		
5	158°		-2.45	-1.30	-.50		
6	113°		-2.45	-1.30	-.50	+.70	+2.50
7	67°	-3.30	-2.45	-1.30	-.50		
8	27°		-2.45	-1.30	-.50		
S1	60°	-3.30					
S2	180°	-3.30					
S3	300°	-3.30					
S4	60°	-3.30					
S5	180°	-3.30					
S6	300°	-3.30					

Figure 57: Internal Duct Static Pressure Tap Locations



*Figure 58: FAN CASCADE REVERSER MODEL - EXIT TOTAL
PRESSURE RAKE INSTALLATION*

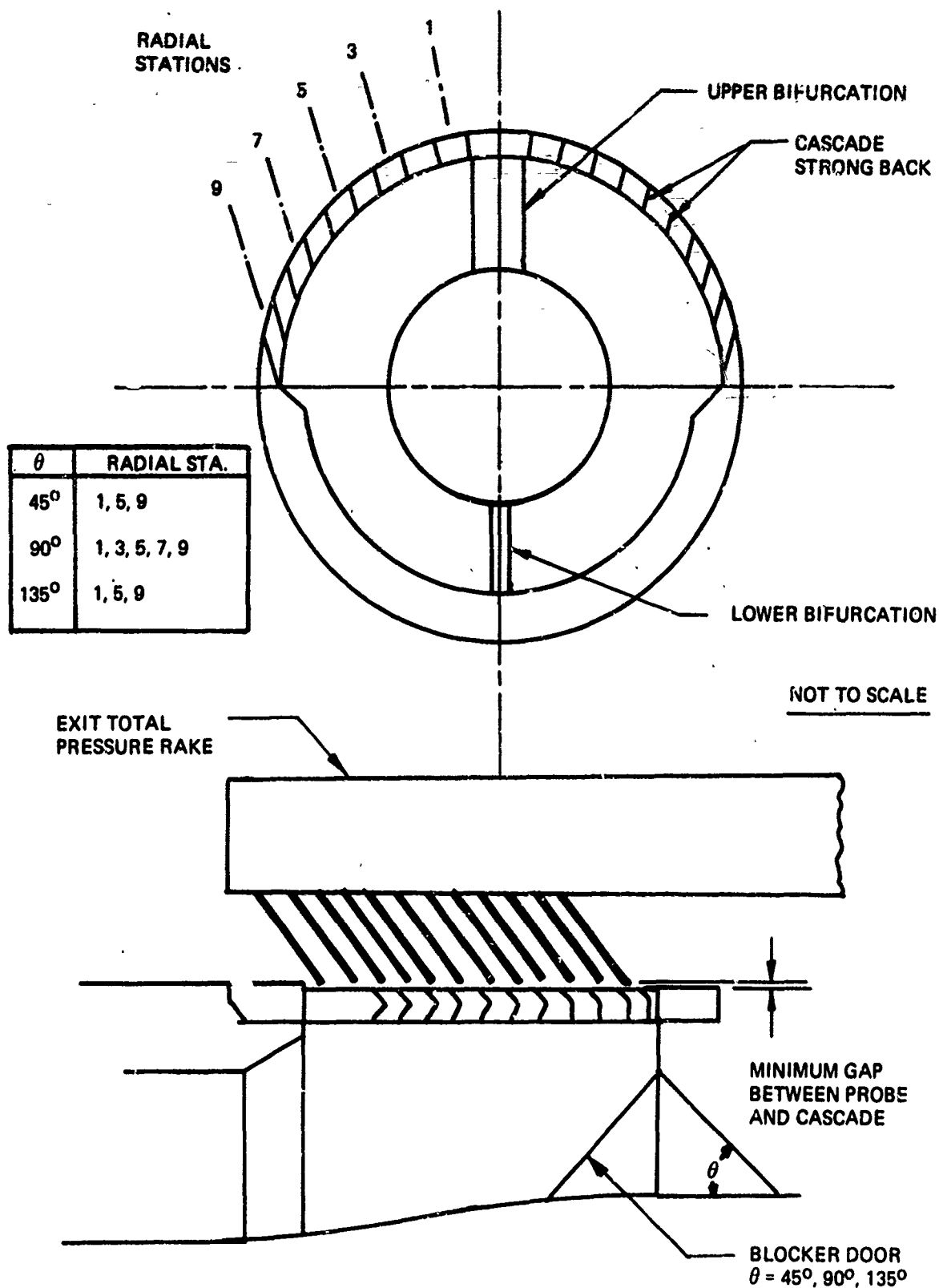


Figure 59: FAN CASCADE THRUST REVERSER EXIT TOTAL PRESSURE RAKE INSTALLATION

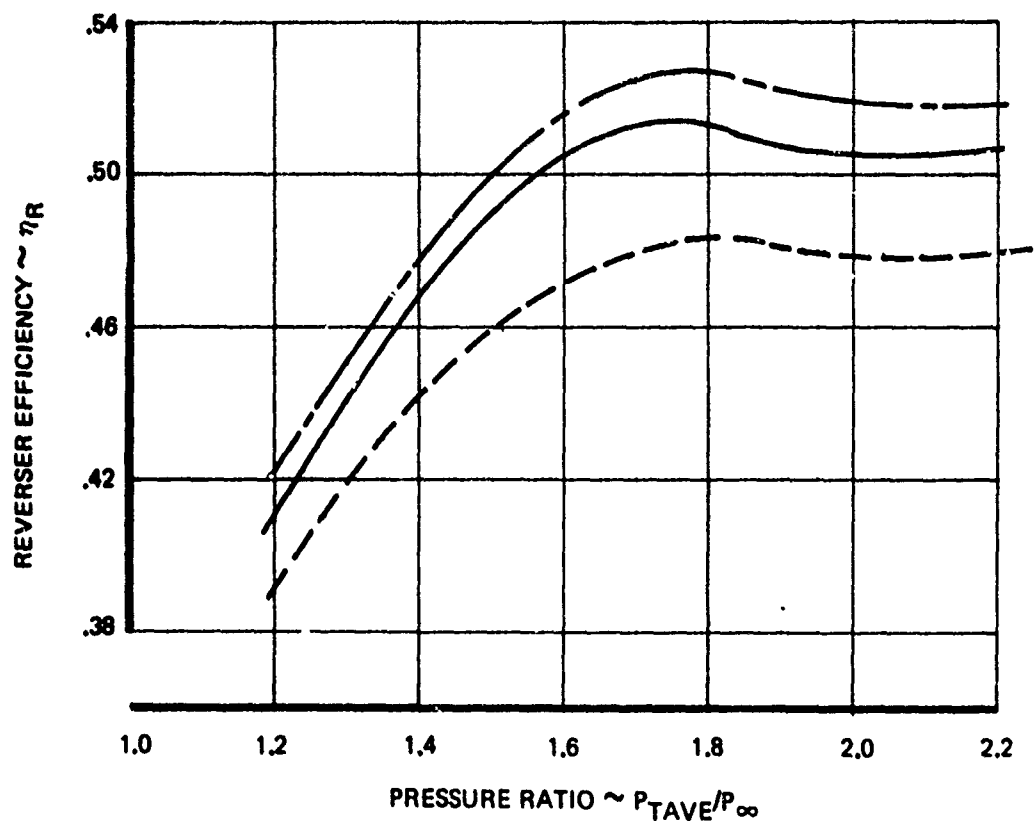
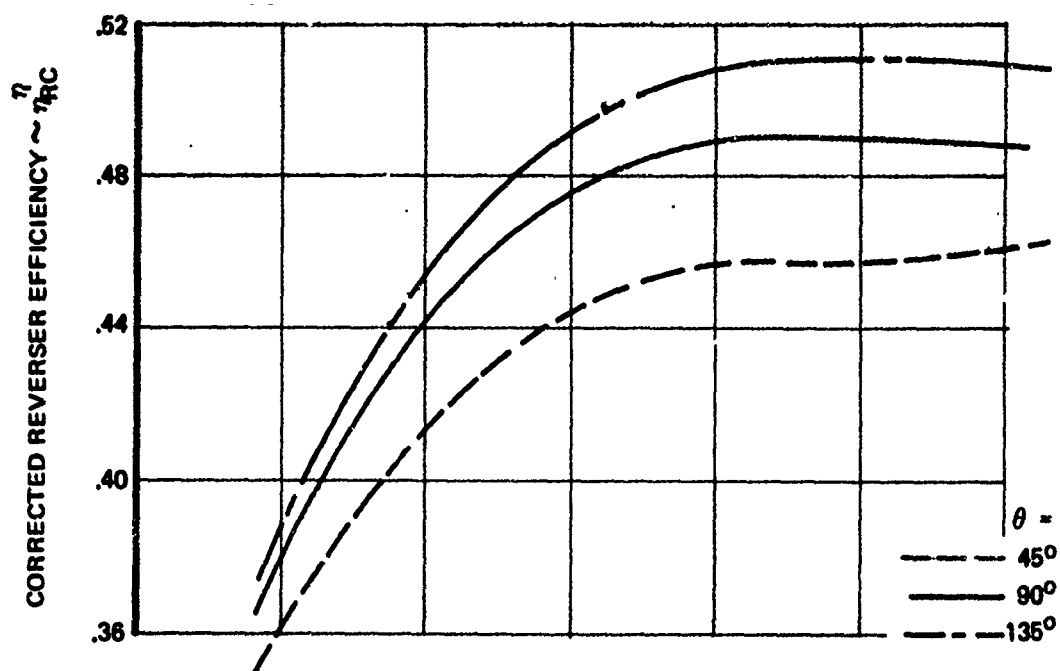


Figure 60: FAN CASCADE THRUST REVERSER
REVERSER EFFICIENCY
CORRECTED REVERSER EFFICIENCY

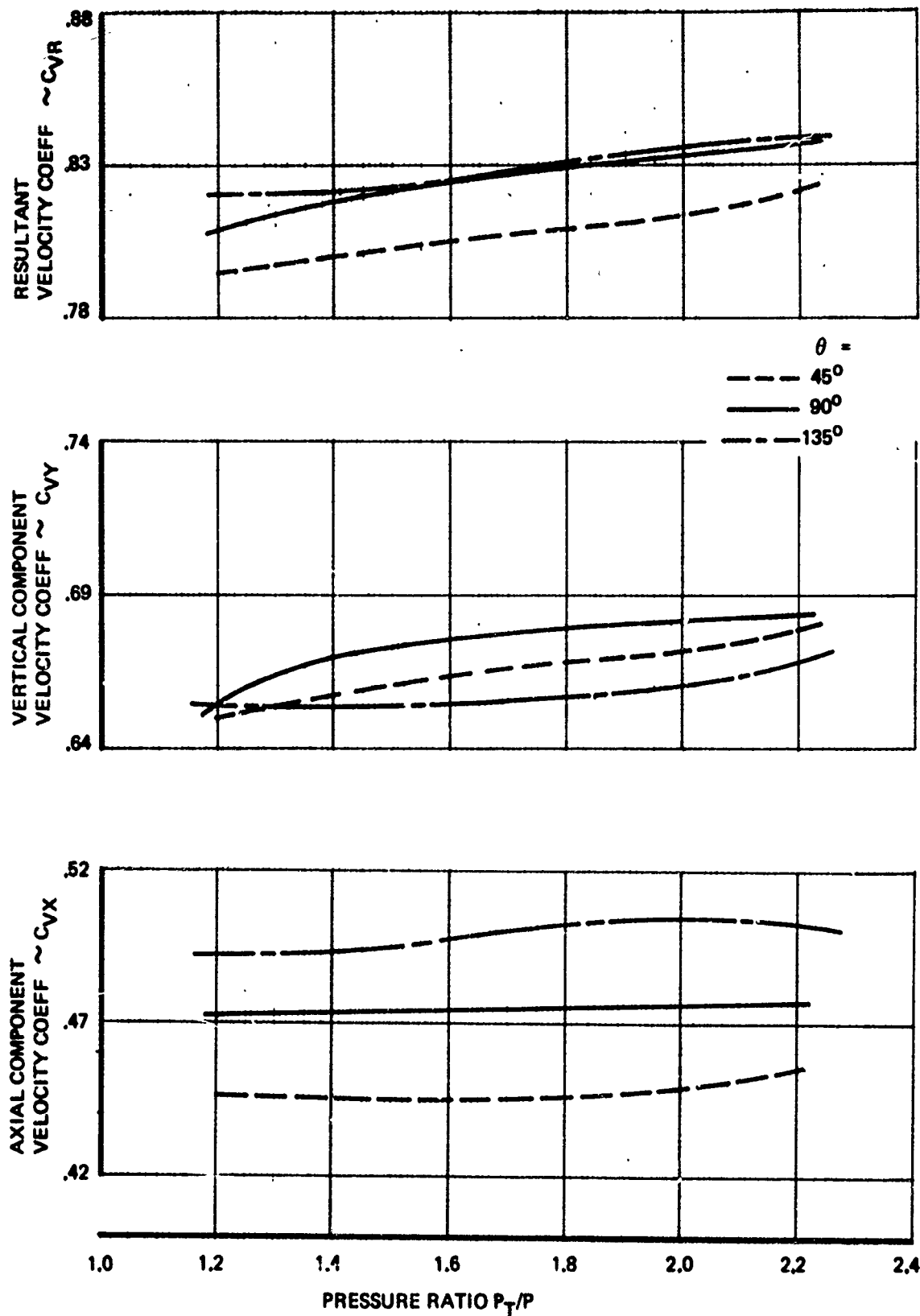


Figure 61: FAN CASCADE THRUST REVERSER
VELOCITY COEFFICIENT

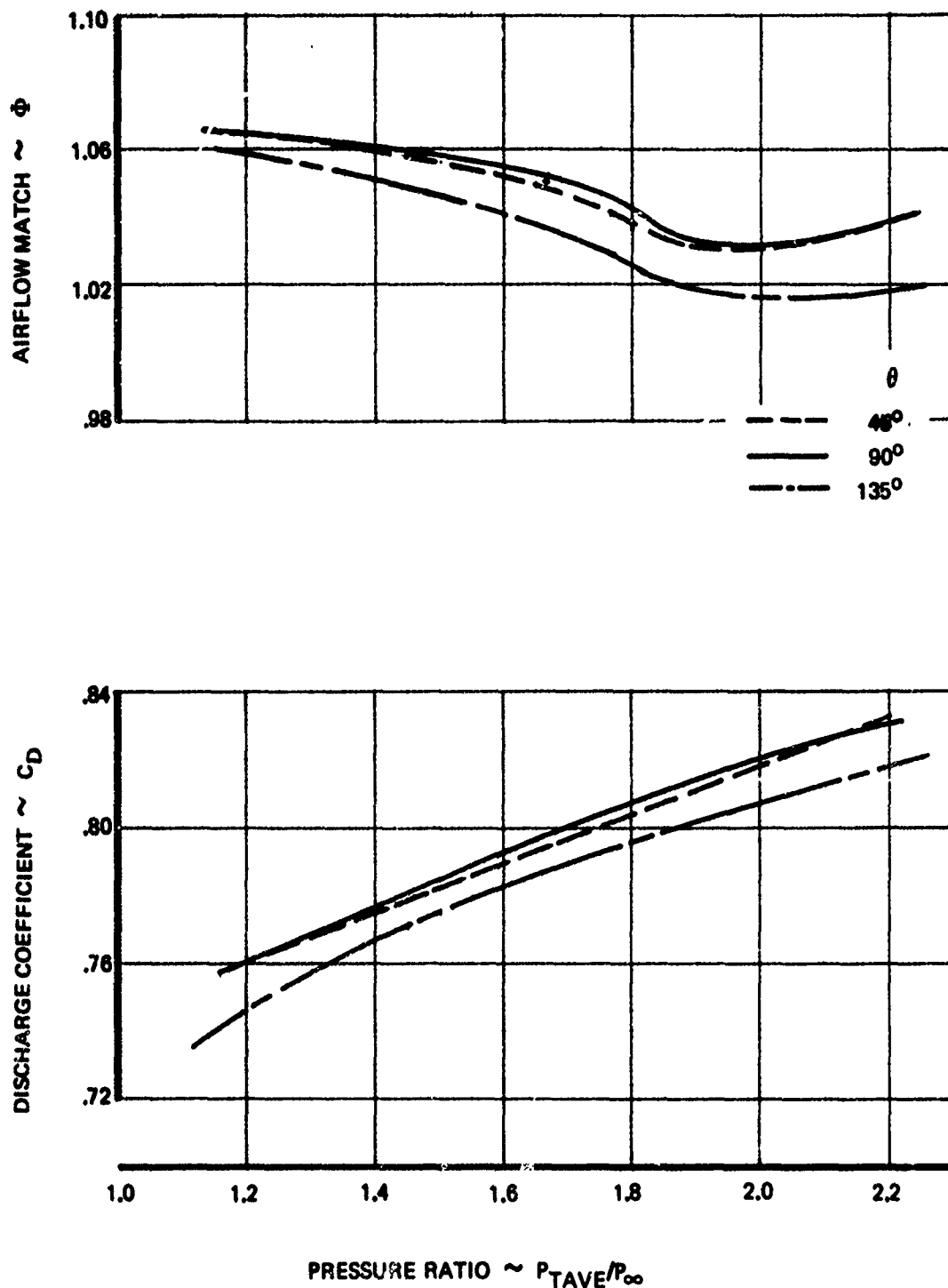


Figure 62: FAN CASCADE THRUST REVERSER
 DISCHARGE COEFFICIENT
 AIRFLOW MATCH

NOTE: FLAGGED SYMBOLS INDICATE
OUTER WALL STATIC TAP

$P_{TAVG}/P_{\infty} = 1.575$
 $P_o = 21.1508 \text{ PSIA}$
 $q_o = 2.0516 \text{ PSIA}$

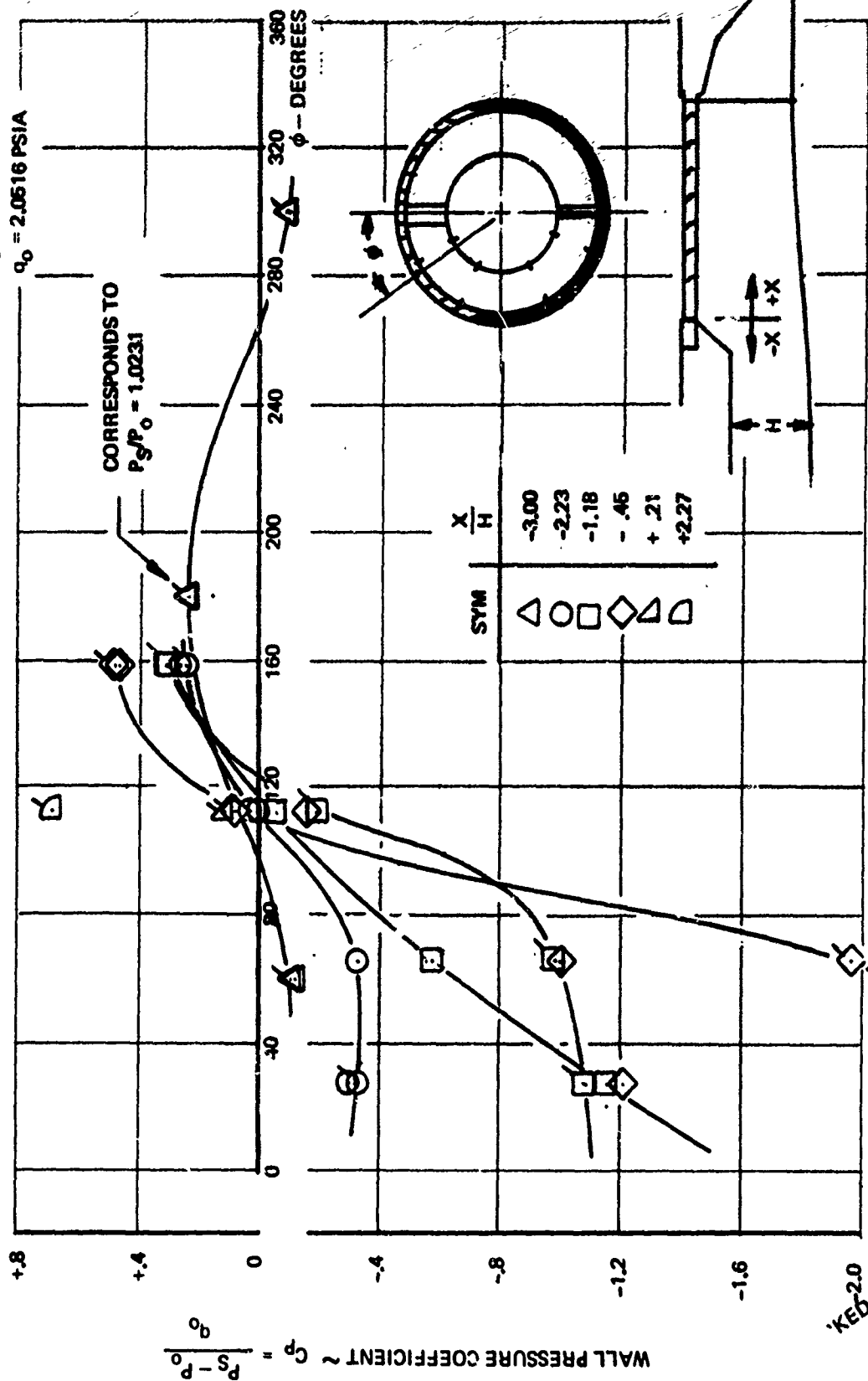


Figure 63: DUCT STATIC PRESSURE DISTRIBUTION $P_{TAVG}/P_{\infty} = 1.575$

5. A survey of the cascade exit total pressure showed that the exhaust flow was fairly uniform except at the cascade rows nearest the top of the model and to the side of the model, (Figure 64). Tailoring of the internal geometry adjacent to the cascade would improve the reverser performance.

Engine Stability Assessment

An analysis of the supply duct internal static pressure data was conducted by Pratt & Whitney Aircraft to assess the duct pressure distortion on engine operation. Fan/compressor back pressure distortions caused by asymmetric thrust reversing is recognized as a potentially significant destabilizing effect. The resulting loss of engine stability margin is a function of magnitude and extent of back pressure distortions and corresponding fan/compressor sensitivities with correlations normally being derived from test data. The test data required to establish these correlations are fan exit total pressure profile measurements. Since velocity distortions are influenced by the presence of a fan and compressor in the system, quantitative predictions of performance change cannot be made. However, velocity distortion measurements are a good indication of flow quality and are useful in evaluating various reverser/deflector schemes relative to upstream flow field effects.

An assessment of the destabilizing effect of a velocity distortion in a clean duct can be made only if the influence of the fan/compressor on the velocity distortion is ignored and percent velocity distortion is assumed equal to percent total pressure distortion. With this in mind, the pressure data was used to calculate the velocity distortion at a location upstream of the reverser, considered representative of the fan exit plane ($x/h = 3.00$). The distortion generated by the reverser and propagated upstream is assumed to be 180° in extent and the data taken in the low and high velocity flow regions is assumed to be representative of the flow within their respective segments.

The reverser test data shows a velocity distortion $\frac{V_{max}-V_{min}}{V_{avg}}$ of 15 percent plus over a range of duct Mach number typically from low to high engine power setting. This is considered to be significant level of distortion.

Reverse has been previously identified as a critical stability operating condition for STOL aircraft engines. For example when all destabilizing effects imposed upon a STOL aircraft engine during reverse operation were taken into account in a recent stability assessment, a back pressure distortion

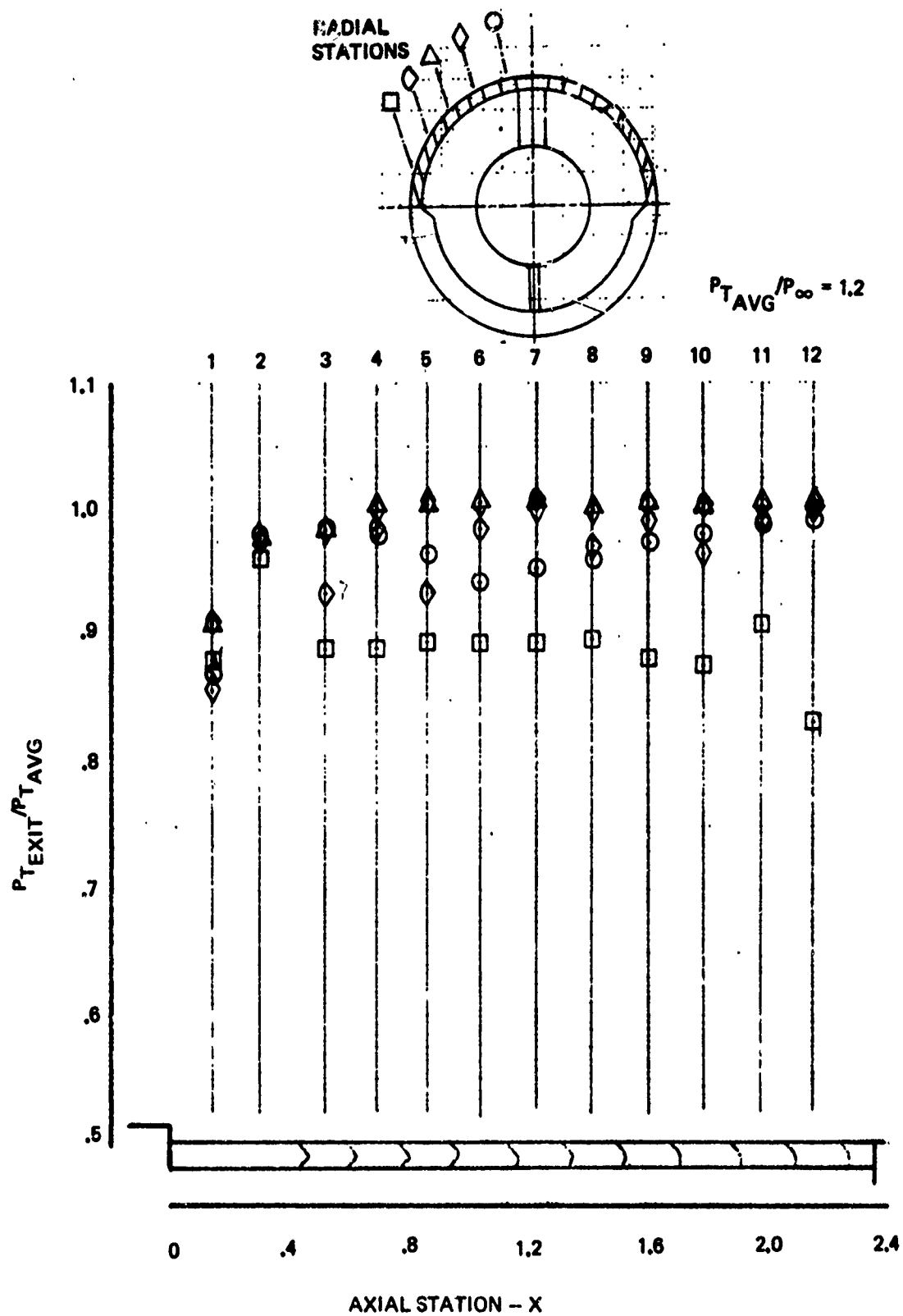


Figure 64: CASCADE EXIT TOTAL PRESSURE SURVEY—
BLOCKER DOOR ANGLE - 90°

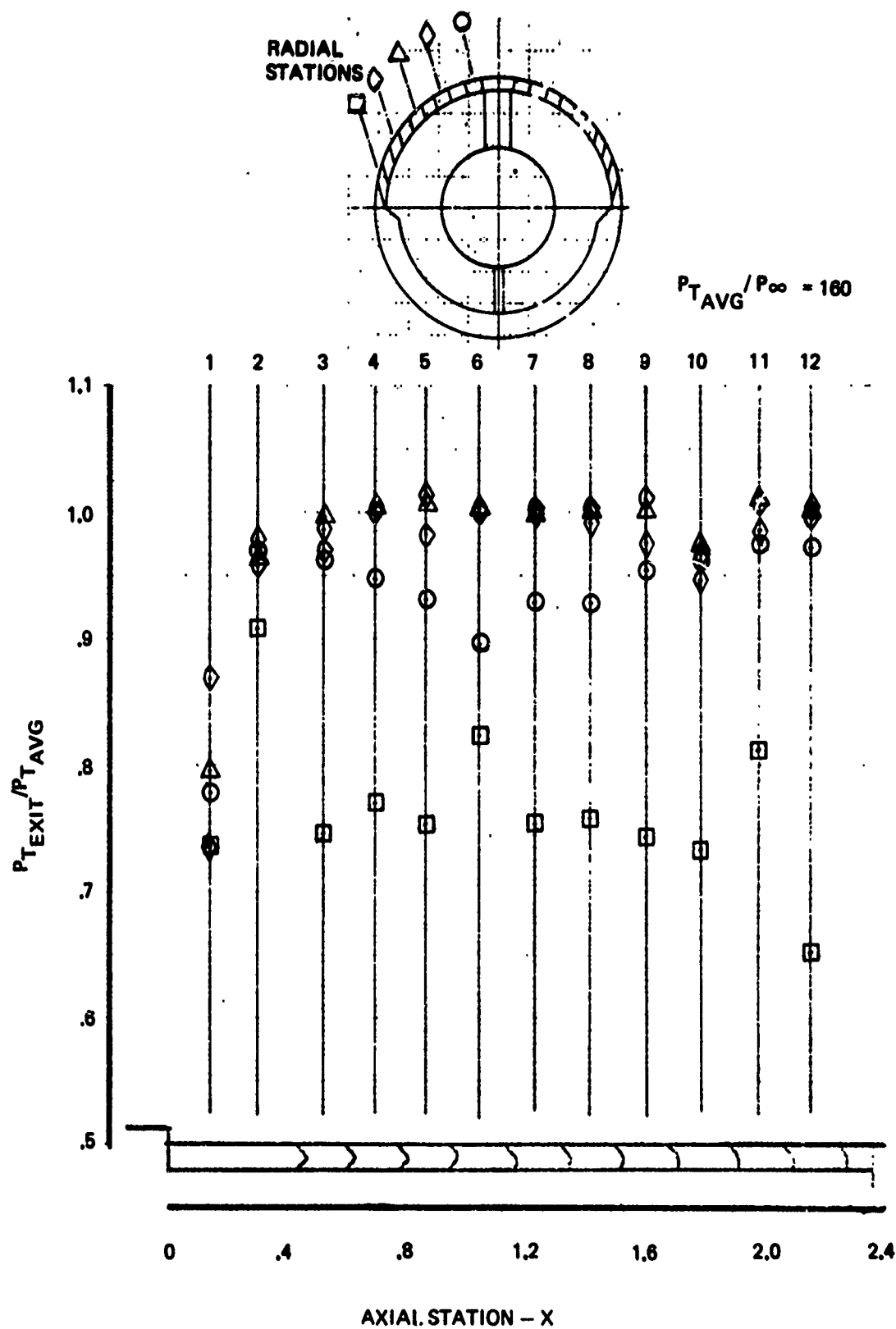


Figure 64: CASCADE EXIT TOTAL PRESSURE SURVEY—
BLOCKER DOOR ANGLE = 90° (Continued)

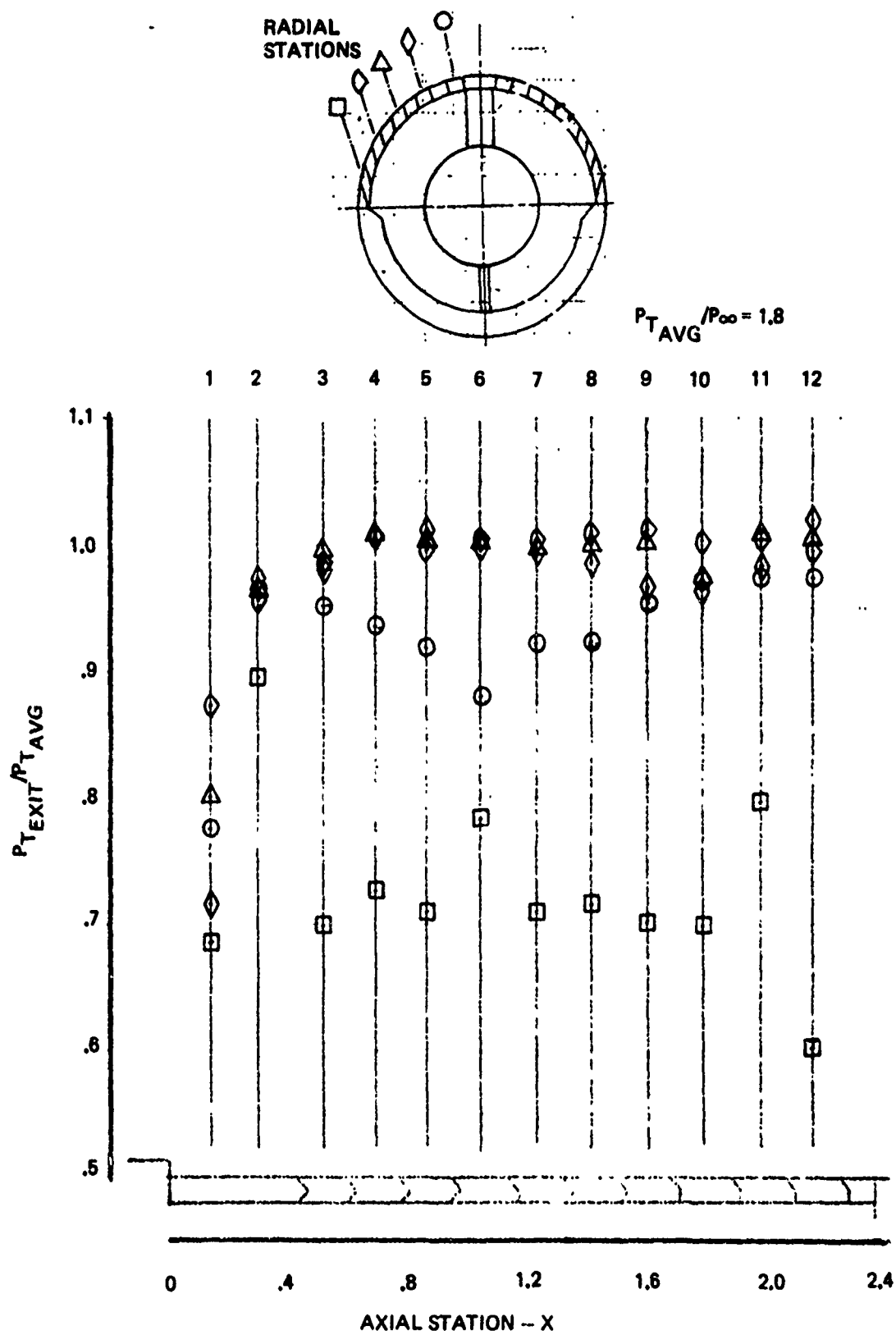


Figure 64: C, SCADE EXIT TOTAL PRESSURE SURVEY--
BLOCKER DOOR ANGLE = 90° (Concluded)

representative of $10\% \Delta P_t/P_t$ was accommodated by oversizing the reverser cascade. Distortion levels greater than 10% cannot be further accommodated without excessive performance penalties, however trades of performance and/or weight penalties (increased duct length for distortion attenuation) for stability can be negotiated.

It has been pointed out that it is not currently possible to quantitatively equate loss in stability margin with measured velocity distortion in a clean duct. This is primarily due to interactive effects of the upstream fan/compressor with the downstream velocity distortion. The velocity distortion amplitude will change and will be exhibited as both a static and total pressure distortion when a compressor characteristic and the magnitude of the distortion and is not currently predictable.

3.1.2 External Deflector/Target TR/TV Model Test

Details of the external deflector/target TR/TV design are shown in Figure 35. The TR/TV system consists of three movable panels with a common hinge. During thrust vectoring, the middle panel is rotated clockwise to deflect the exhaust flow. During thrust reversal, the inner panel rotates to the bottom of the nacelle to block the deflected flow and the outer panel is rotated to expose flow area at the top of the nacelle to block the deflected flow and the outer panel is rotated to expose flow area at the top of the nacelle for the reverser exhaust. The concept may be used for either single pod or dual pod installations.

The optimum deflector design will be a correct combination of deflector setback distance from the nozzle exit and the entrance flow Mach number as determined by the nozzle diameter. Provisions will be required to increase nozzle throat area to reduce the Mach number of the flow entering the deflector during thrust vectoring. Flow control must be maintained at the deflector exit in order to avoid losses associated with high Mach number turning.

Objectives

The objectives of the static test are to:

1. Obtain thrust vectoring performance data as a function of the following parameters:
 - o deflector setback distance

- o turning Mach number
 - o deflection angle
 - o nozzle pressure ratio
2. Evaluate the thrust reverser performance of the model geometry corresponding to the optimum geometry for thrust vectoring.
 3. Establish design criteria for future wind tunnel models and for full scale hardware design.

Test Models

A schematic of the external deflector/target TR/TV model installation is shown in Figure 65. A total of 25 external deflector configurations were tested. Table XI lists the configurations and their respective geometric variations as defined by Figures 66, 67, and 68.

The external deflector model was tested in three basic modes:

1. cruise mode
2. thrust vectoring mode
3. thrust reversing mode

over the nozzle total to ambient pressure ratio range of 1.2 to 2.2. The cruise nozzle configuration, $D_n/D = 1.0$, established the baseline thrust and mass flow characteristics of the model used to compute thrust vectoring efficiency, thrust reverser efficiency, and airflow match for the vectoring and reversing model configurations.

The initial thrust vectoring mode runs tested the model in the fully deflected position to determine the effect of deflector setback distance, S , and entrance Mach number on vectoring performance and to determine the required setback distance corresponding to the maximum effective vector angle and airflow match conditions. The setback distance was held constant for the remaining vectoring mode runs, while deflector position was varied to determine vectoring performance at intermediate deflector positions. Also, the nozzle diameter was varied to determine the required schedule of nozzle diameter versus deflector position. Photographs of the vectoring model are shown in Figures 69 and 70. The reverser model, shown in Figure 71 was tested at the setback distance corresponding to optimum performance for the vectoring model.

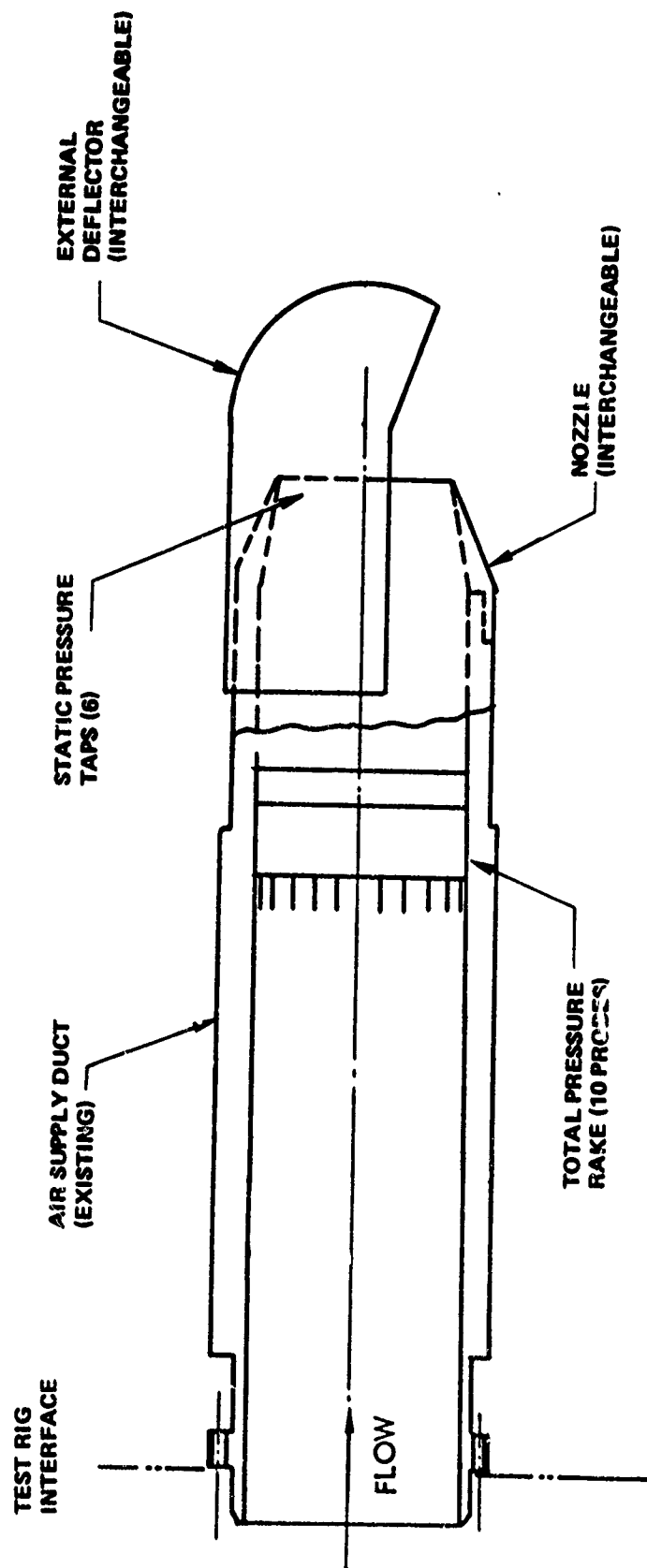
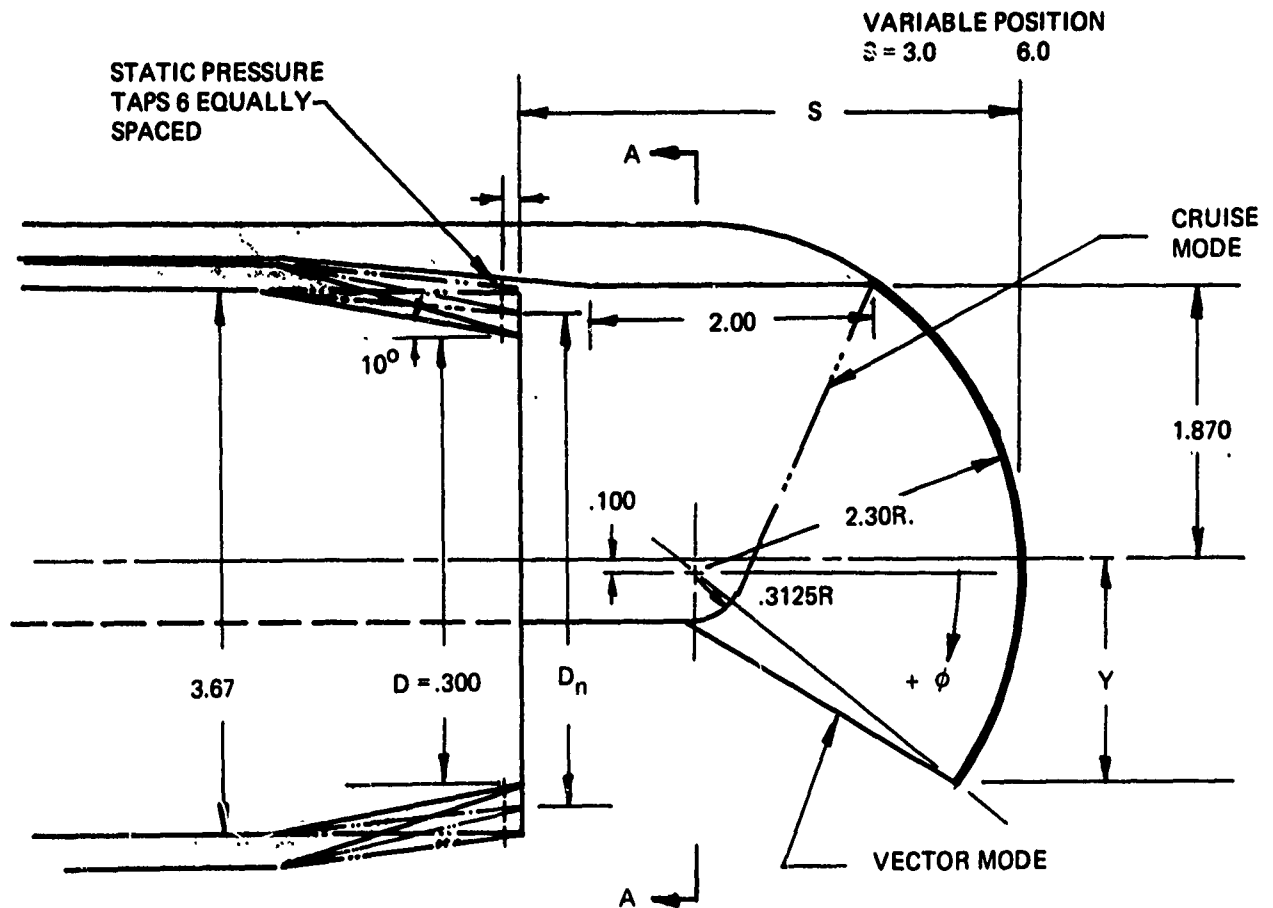


Figure 65: EXTERNAL DEFLECTOR TR/TV MODEL INSTALLATION SCHEMATIC

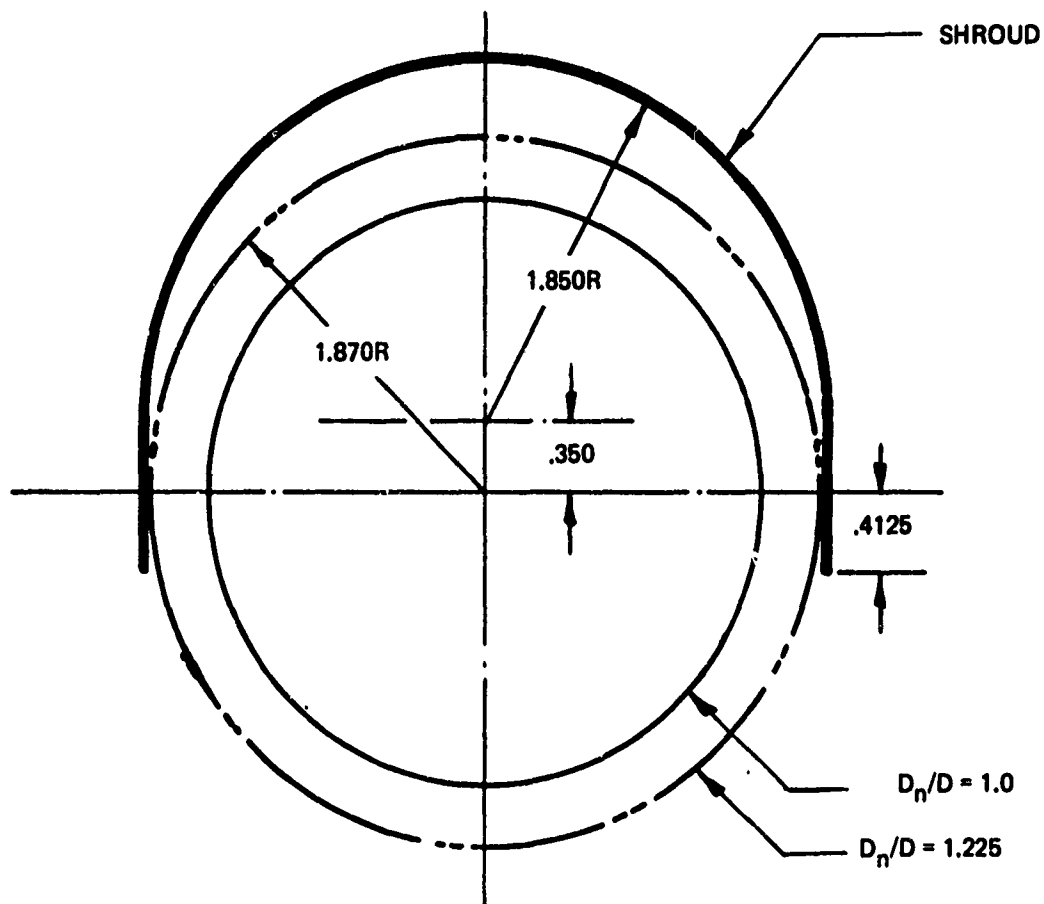
Table XI: EXTERNAL DEFLECTOR MODEL TEST CONFIGURATIONS

CONFIGURATION	Dn/D	S/D	Y/D	θ	REMARKS
Cruise Nozzle	1.0	-	-	-	Baseline Thrust and Mass Flow
Cruise Nozzle	1.0	1.20	-.623	-60°	Effect of Cruise Shroud
Thrust Vectoring Model	1.00	1.33	.500	36°	Effect of Setback Distance
		1.50			
		1.80			
		2.00			
	1.225	1.33			
		1.00			
		1.10			
Thrust Reverser Model		1.20			Effect of Deflector Position And Nozzle Diameter
	1.225	1.03	.500	36°	
			.181	10°	
	1.15	1.03	.137	7°	
			.500	36°	
			.181	10°	
	1.00	1.03	.137	7°	
Thrust Reverser Model					Effect of Nozzle Diameter
	1.225	1.03	-	-	
	1.15				
	1.00				
Cruise Nozzle					Effect of Modified Lip
	1.225	1.03			
	1.15				
	1.00				
Cruise Nozzle	1.00	-	-	-	Long Term Repeatability



CONFIGURATION	ϕ	Y/D	D_n/D	S/D
CRUISE	-60°	-.623	1.0	1.20
VECTOR	$+ 7^\circ$	+.136	1.0, 1.15, 1.225	1.030
	$+10^\circ$	+.187	1.0, 1.15, 1.225	1.030
	$+36^\circ$	+.500	1.0, 1.15, 1.225	1.0 \rightarrow 2.0

Figure 66: EXTERNAL DEFLECTOR GEOMETRY
VECTOR MODE



SECTION A-A

Figure 67: EXTERNAL DEFLECTOR GEOMETRY -SECTION A-A

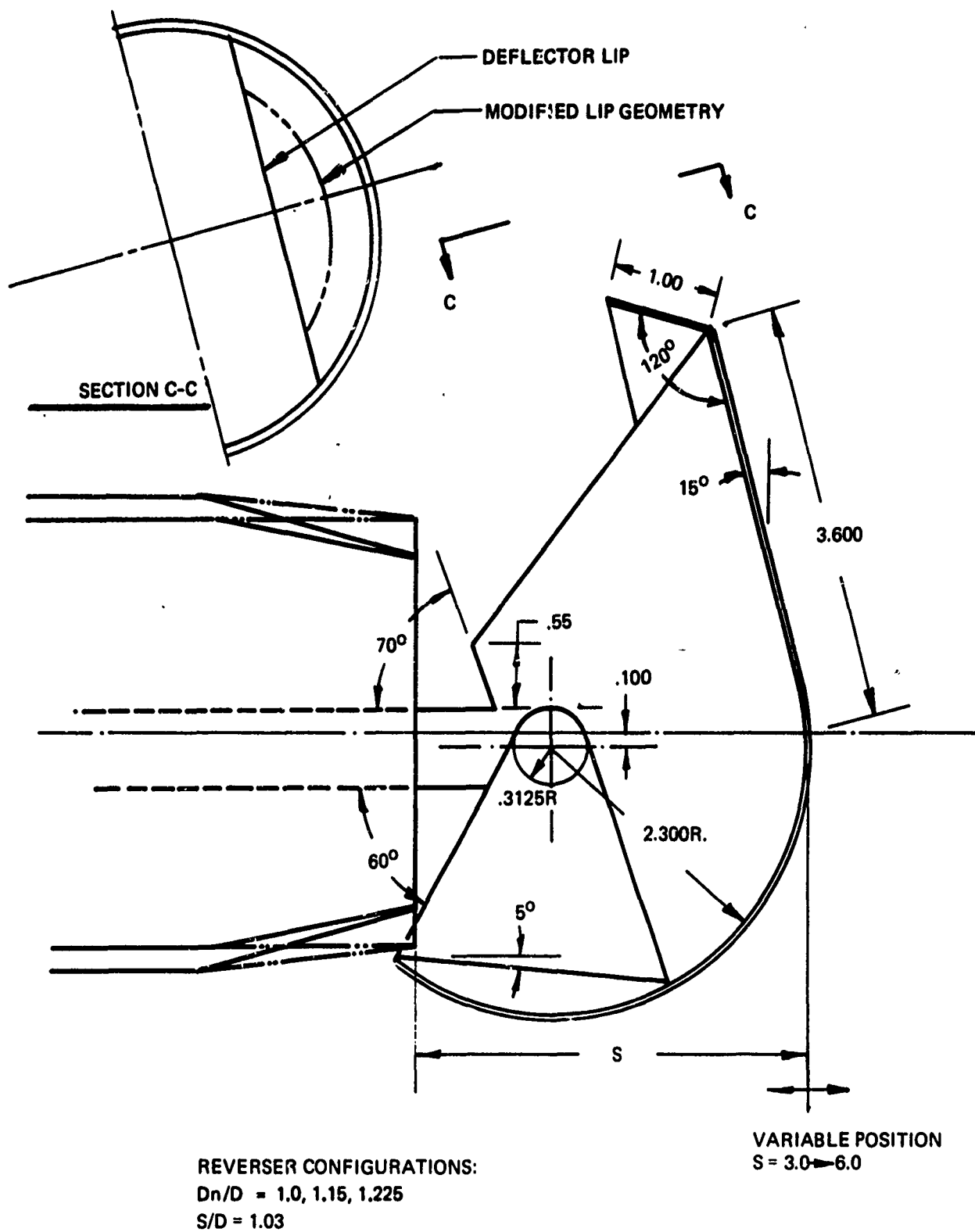


Figure 68 EXTERNAL DEFLECTOR GEOMETRY—REVERSE MODE

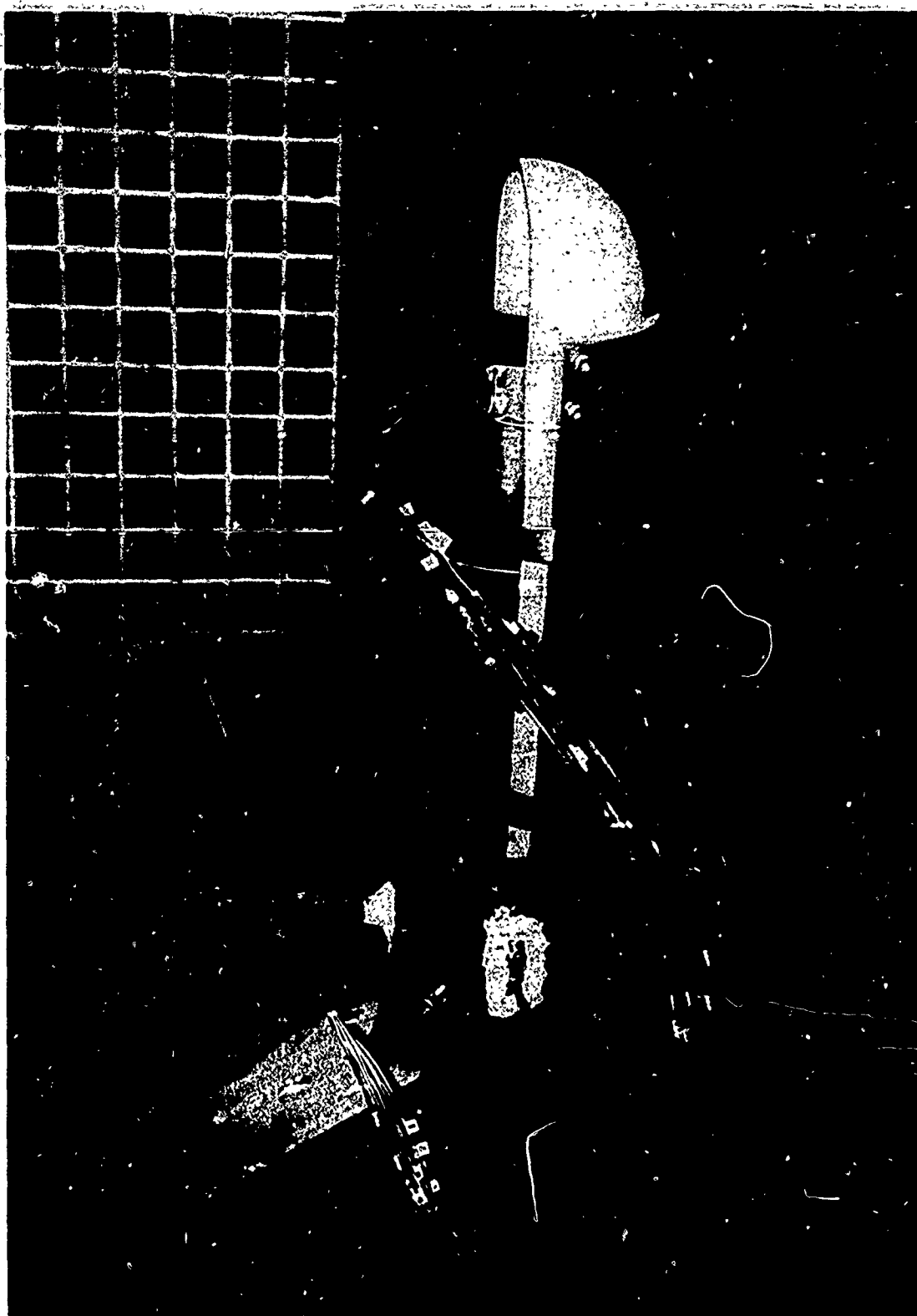


Figure 69: EXTERNAL DEFLECTOR TR/TV MODEL ($S/D = 1.03$ $\phi = 7^\circ$)



Figure 70: EXTERNAL DEFLECTOR TR/TV MODEL ($S/D = 1.03$ $\phi = 36^\circ$)

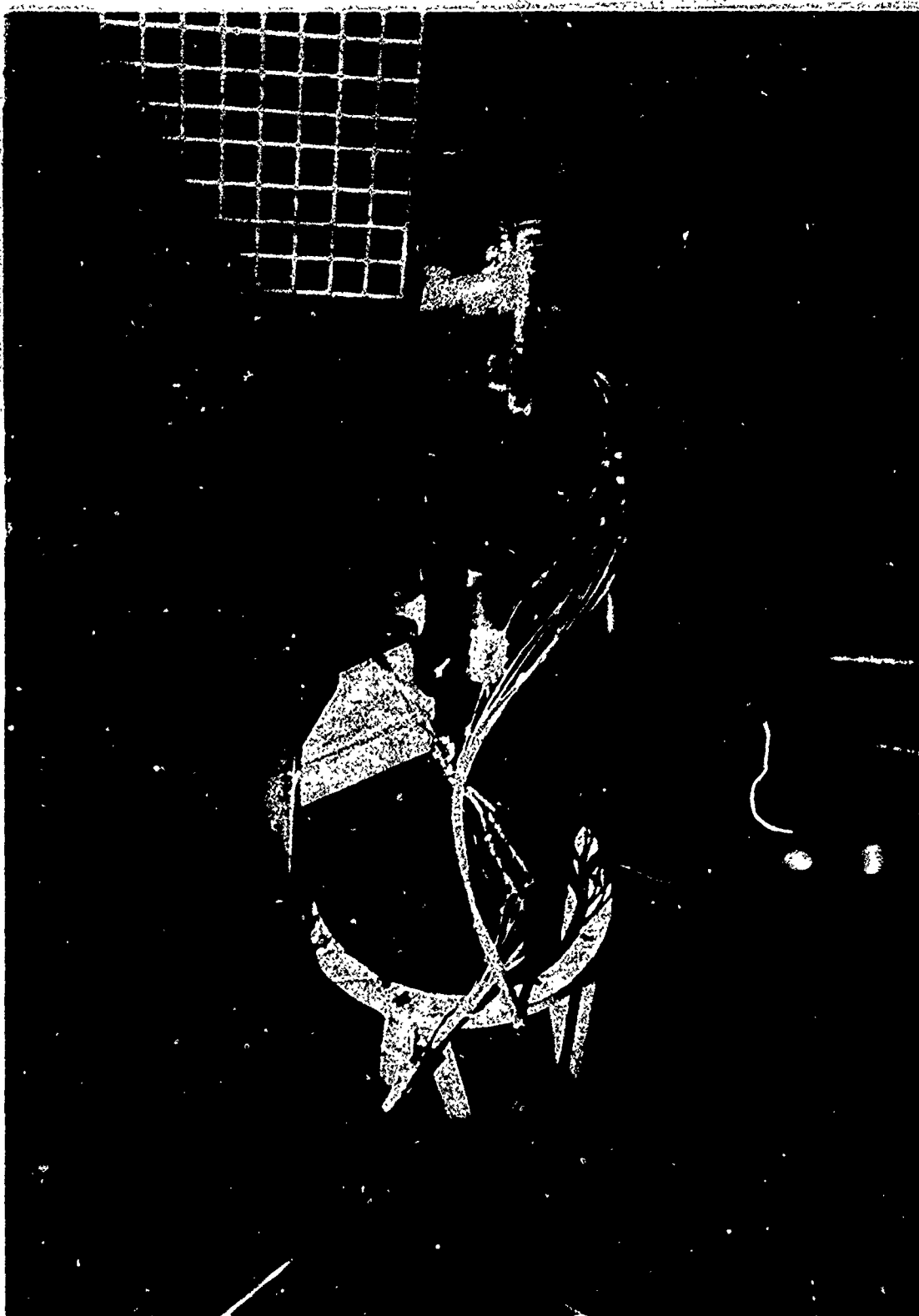


Figure 71: EXTERNAL DEFLECTOR THRUST REVERSER MODEL

Model total pressure was measured using a 10 probe "area-weighted" total pressure rake located in the air supply duct upstream of the test model. A chromel alumel thermocouple installed in the duct adjacent to, and in the same plane as the total pressure probe monitored model flow total temperature. Static pressure taps were installed near the throat of the test nozzles as shown in Figure 66. These pressures were used to determine the flow Mach number entering the deflector.

Test Results

Results of the external deflector/target TR/TV model test are summarized below. Detailed results are contained in Reference 11.

1. Vectoring performance was very sensitive to nozzle pressure and deflector geometry. Small changes in pressure ratio setting (Figure 72) and in the deflector setback distance and deflector rotation position had significant effects on the vectoring efficiency and airflow match characteristics. (Figure 73, 74, 75, 76, 77, 78)
2. Optimum vectoring efficiency at $P_T/P_\infty = 1.6$ was $\eta_V = 0.88$ with an effective vector angle $\sigma_{eff} = 66^\circ$ at airflow match conditions. The vectoring performance was lower than the performance goal of $\eta_V = .90$ and $\sigma_{eff} = 75^\circ$ indicating that the deflector design should be revised.
3. Optimum vectoring performance occurred when the flow Mach number at the entrance of the deflector was approximately $M_{ENT} = 0.45$ (Figure 79).
4. The thrust reverser performance evaluation showed that the reverser efficiency and airflow match were also sensitive to nozzle pressure ratio (Figure 80). Reverser efficiency at $P_T/P_\infty = 1.60$ varied between 34 to 41% depending on the nozzle diameter. Airflow match data indicated the reverser was significantly under area and that modifications to the deflector geometry would be required to improve the reverser airflow match characteristics (Figure 81).

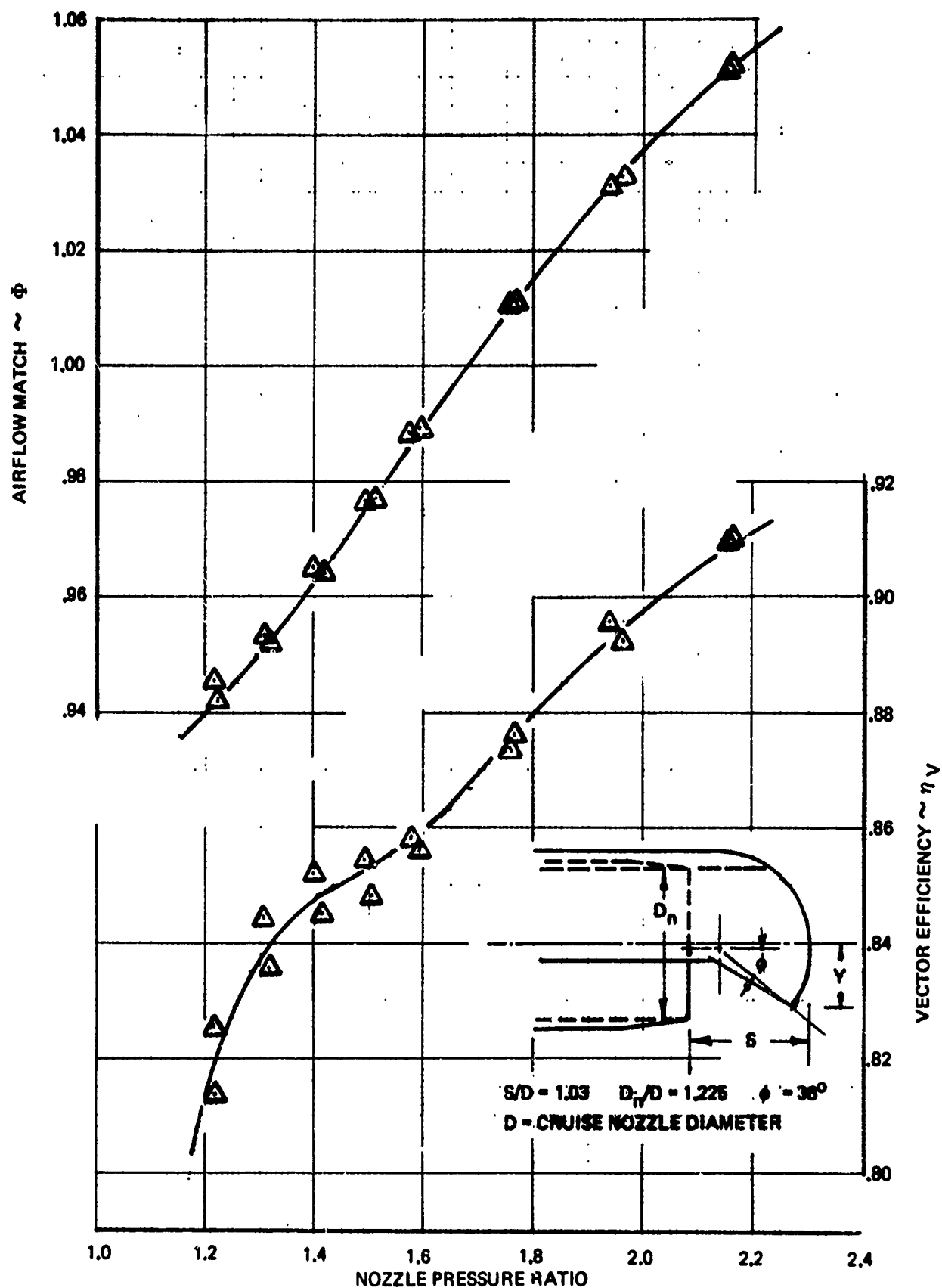


Figure 72: VECTOR EFFICIENCY (η_v) AIRFLOW MATCH (Φ)
 $D_n/D = 1.225$ $S/D = 1.033$ $Y/D = .50$

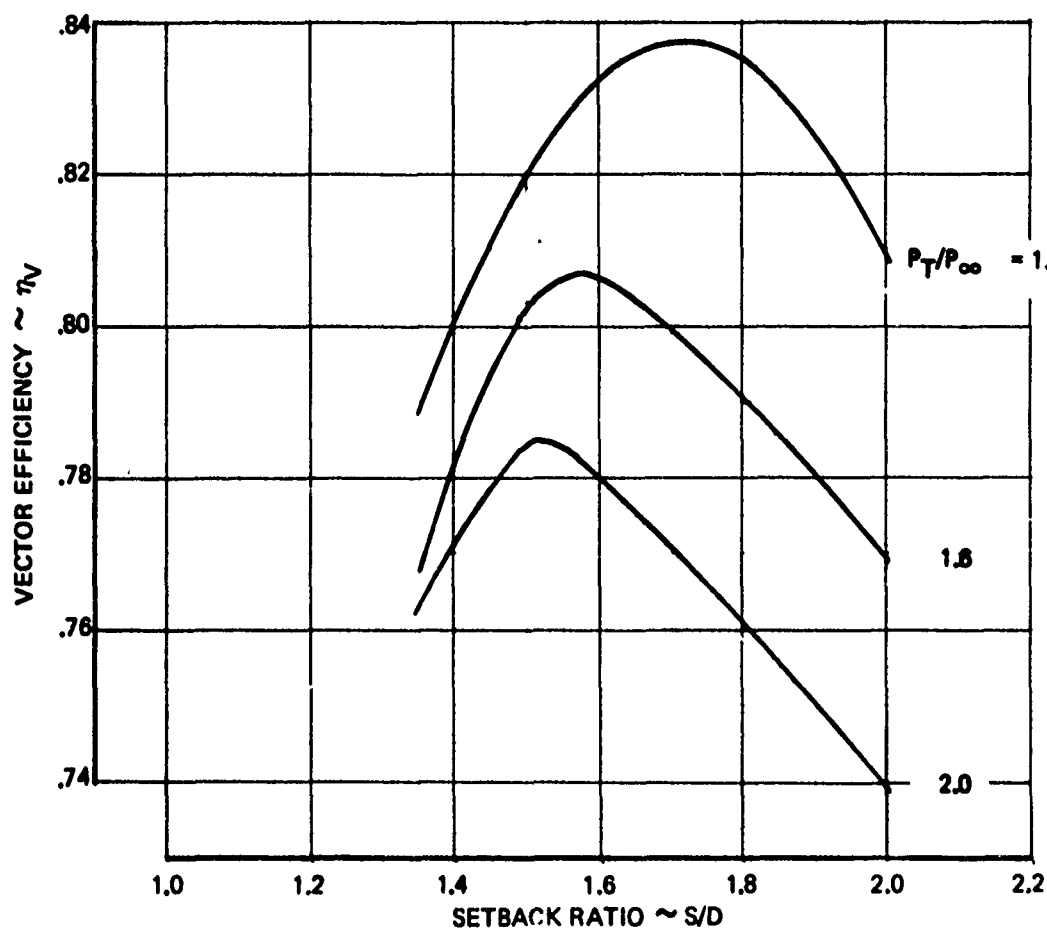
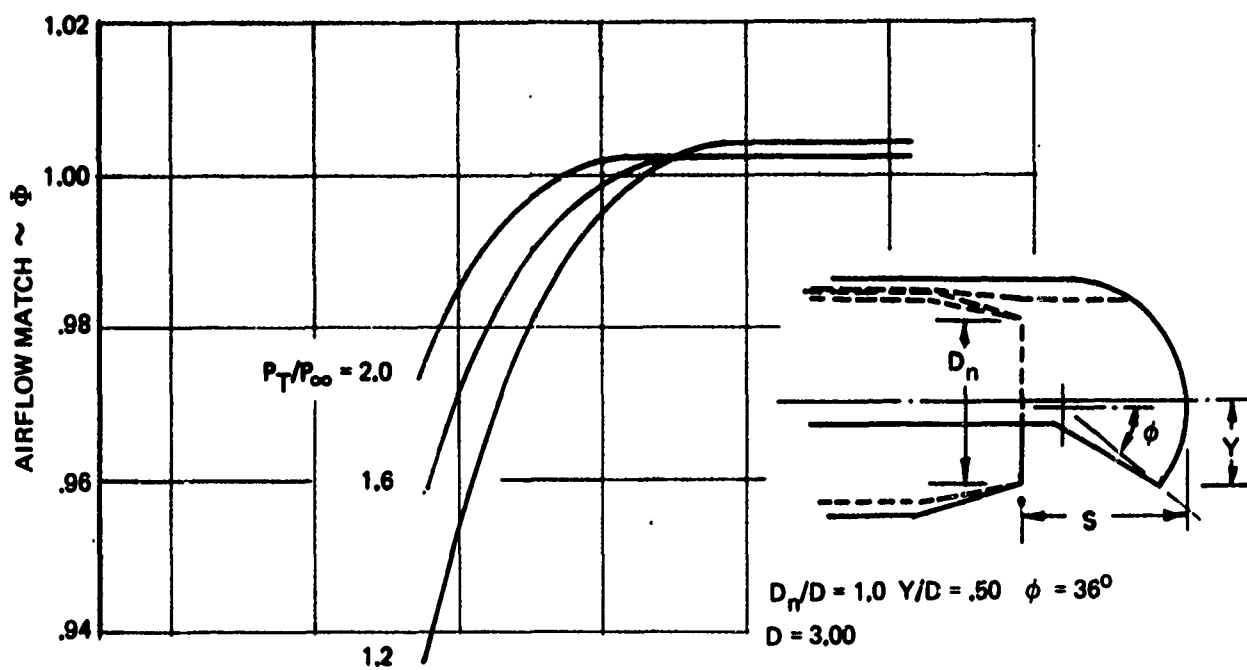


Figure 73: EFFECT OF SETBACK RATIO ON VECTOR EFFICIENCY AND AIRFLOW MATCH $D_n/D = 1.0$

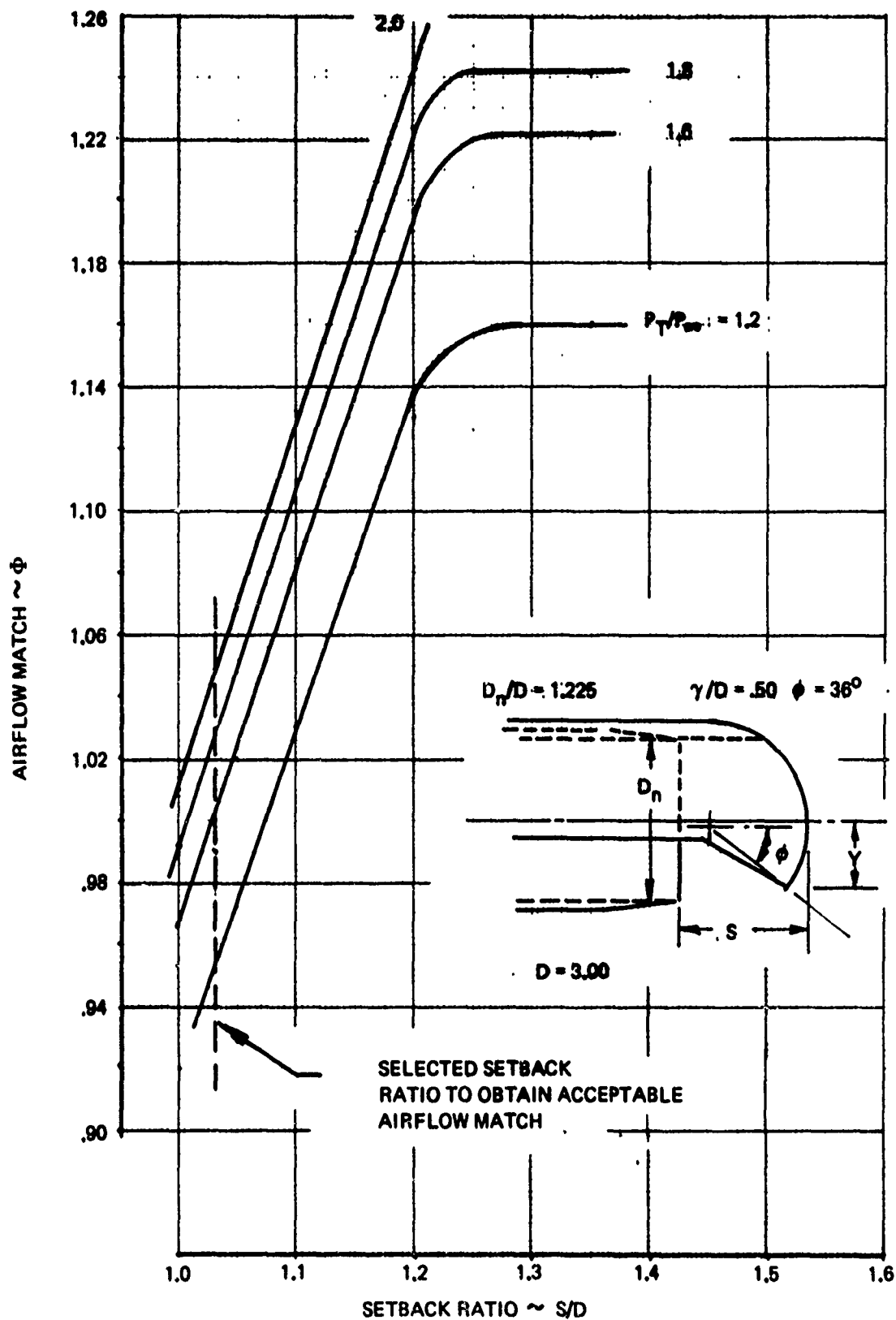


Figure 74: EFFECT OF SETBACK RATIO ON AIRFLOW MATCH
 $D_n/D = 1.225$ $\gamma/D = .50$

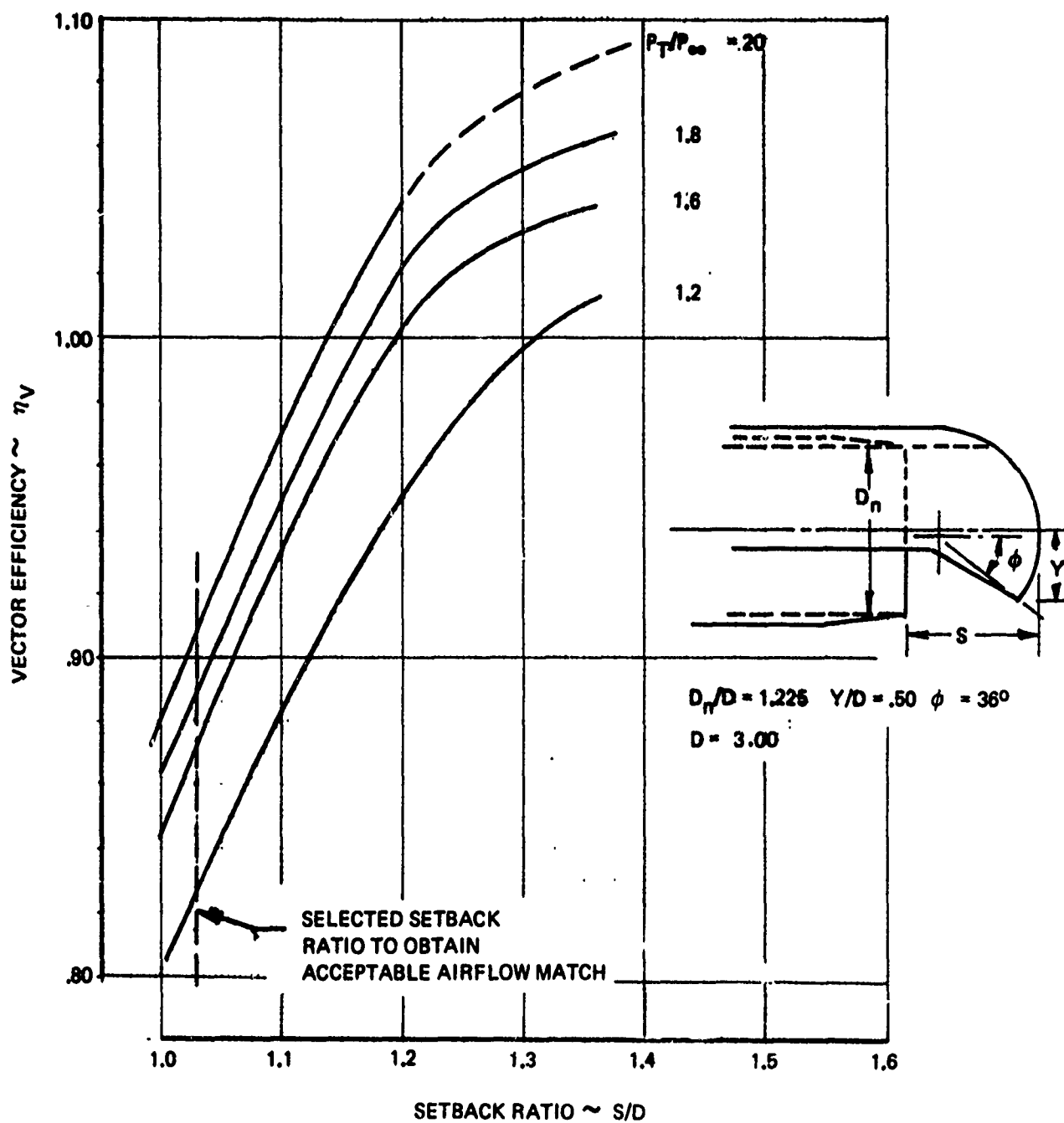


Figure 75: EFFECT OF SETBACK RATIO ON VECTOR EFFICIENCY
 $D_n/D = 1.225$ $Y/D = .50$

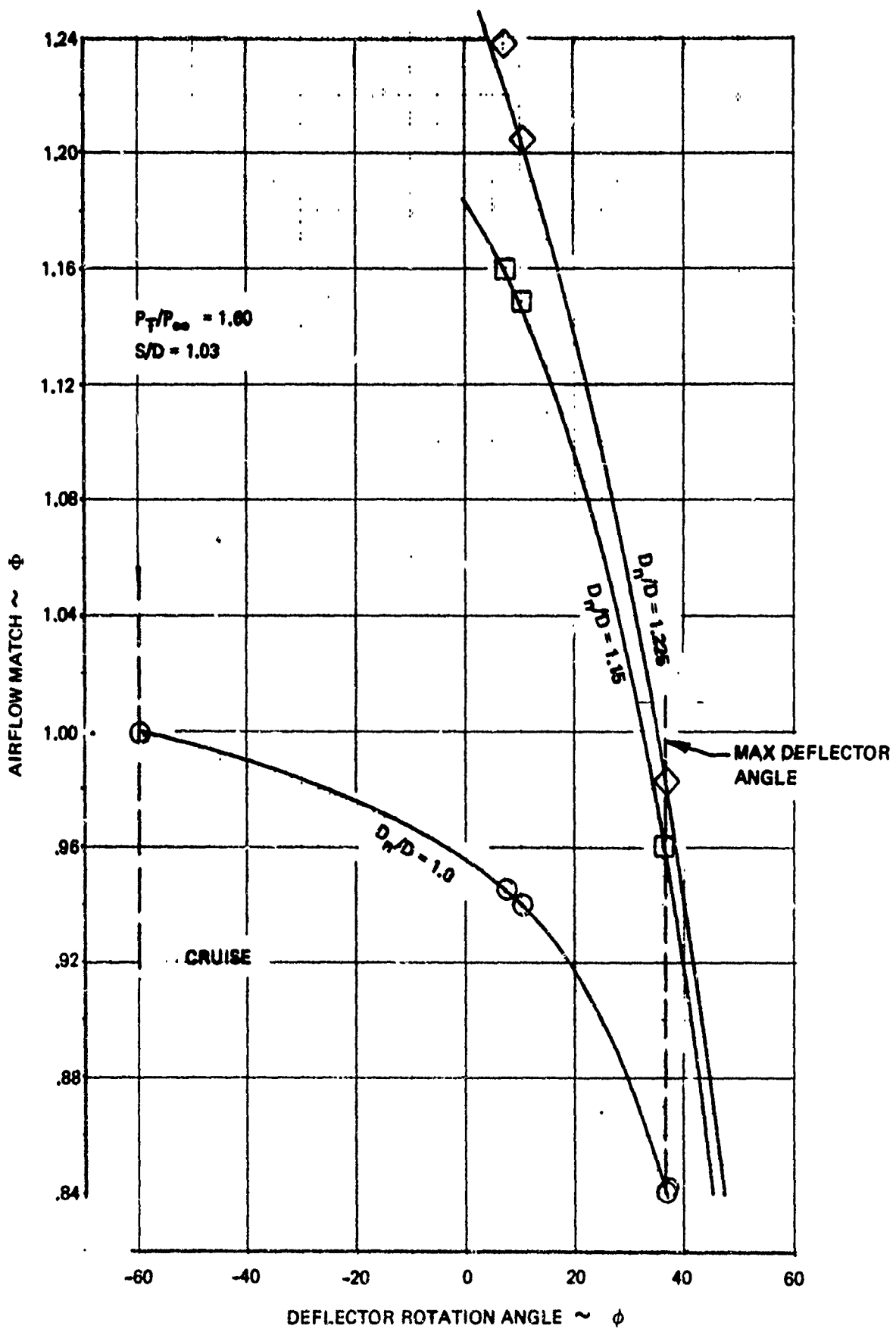


Figure 76: EFFECT OF DEFLECTOR POSITION ON AIRFLOW MATCH, $P_T/P_\infty = 1.60$

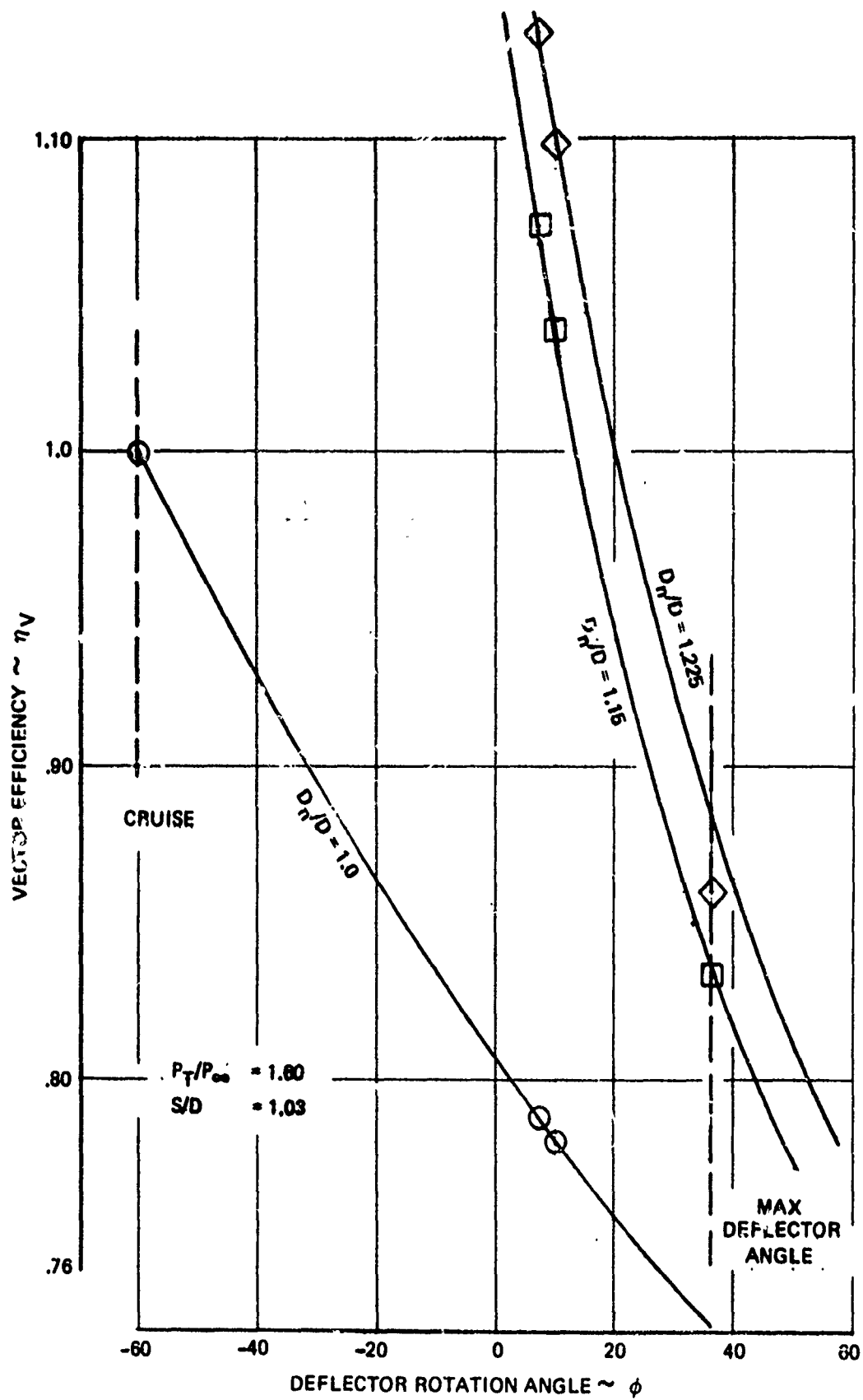


Figure 77: EFFECT OF DEFLECTOR POSITION ON VECTOR EFFICIENCY, $P_T/P_\infty = 1.60$

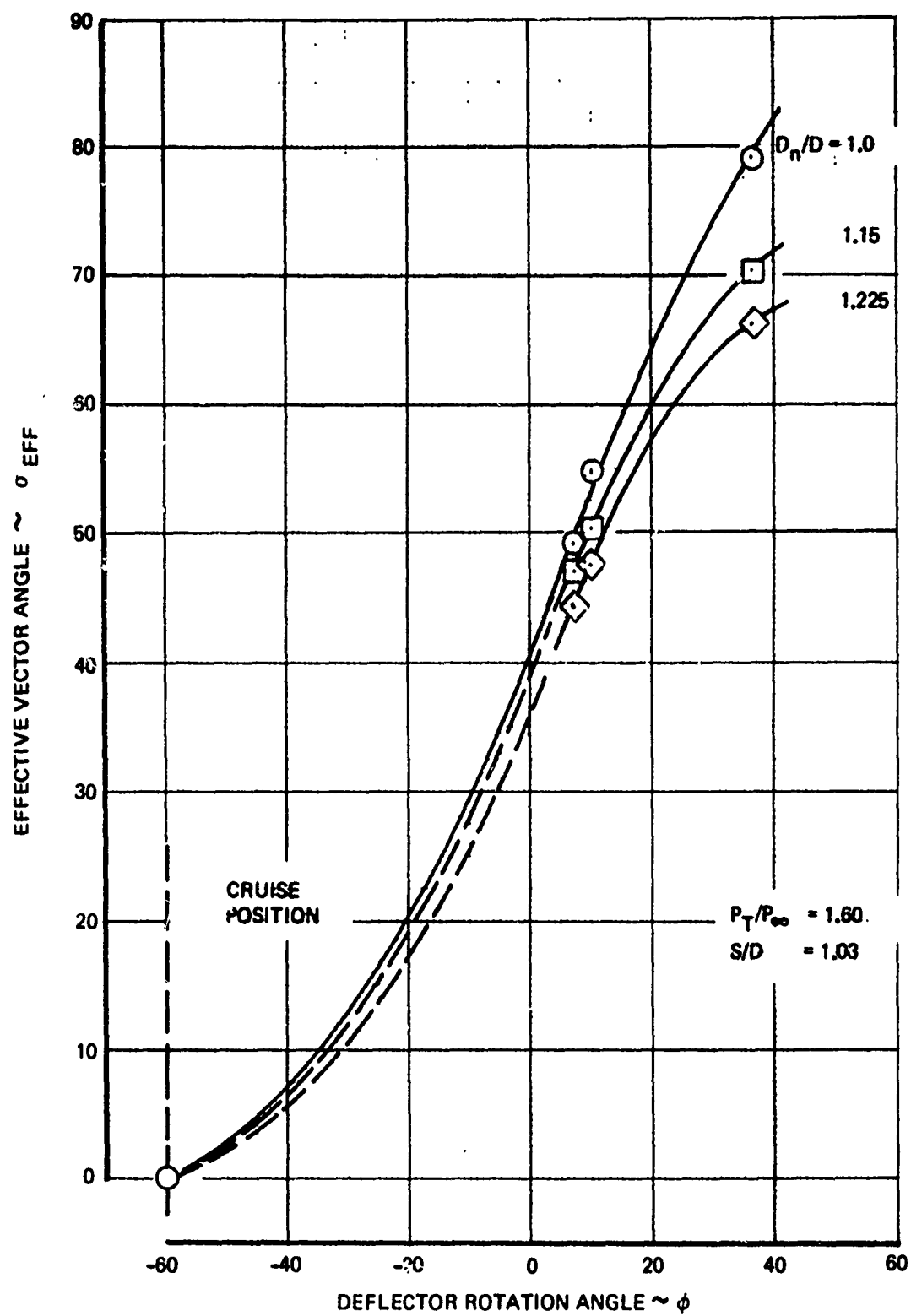


Figure 78: EFFECT OF DEFLECTOR POSITION ON EFFECTIVE VECTOR ANGLE

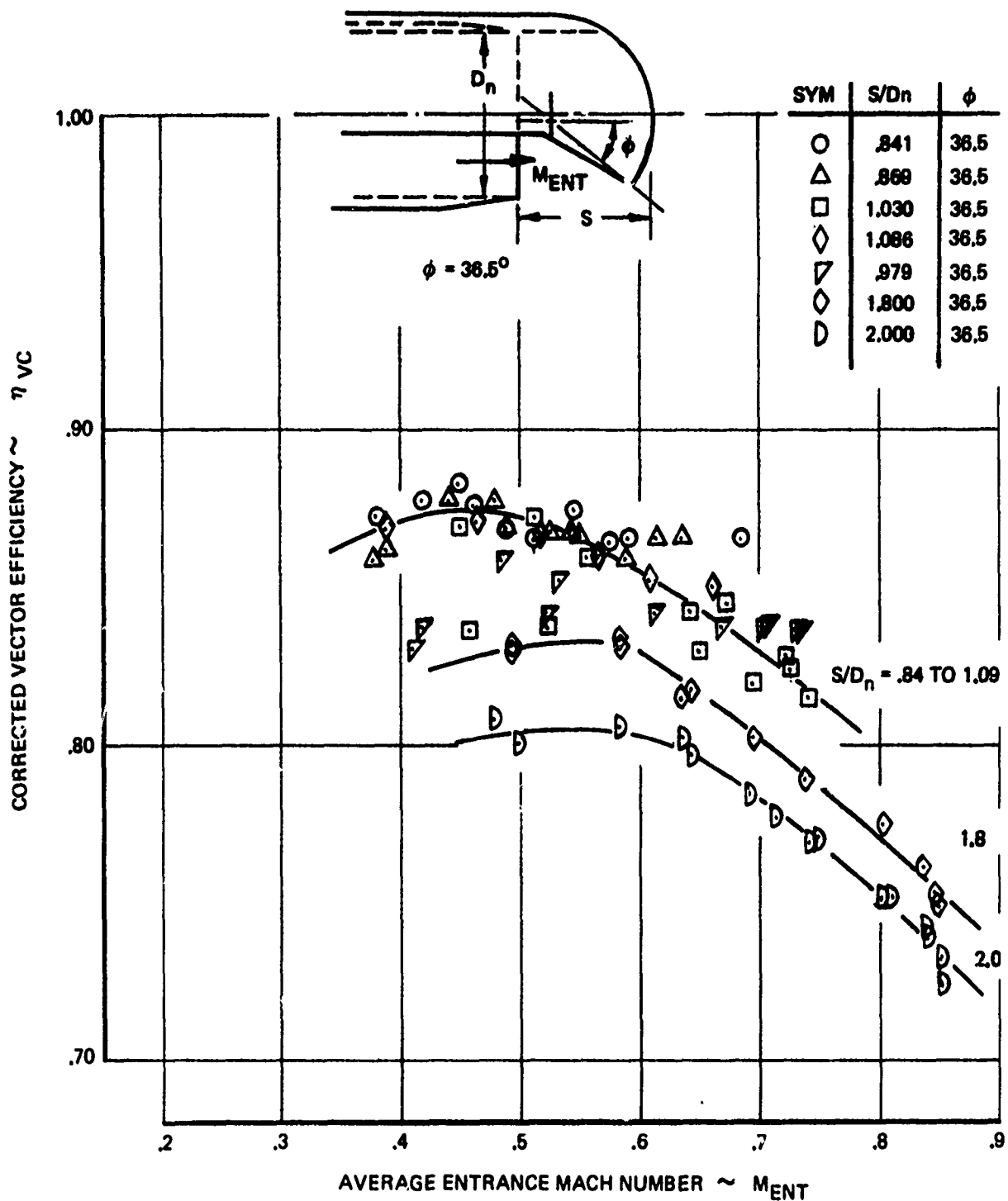


Figure 79: EFFECT OF ENTRANCE MACH NUMBER ON CORRECTED VECTOR EFFICIENCY

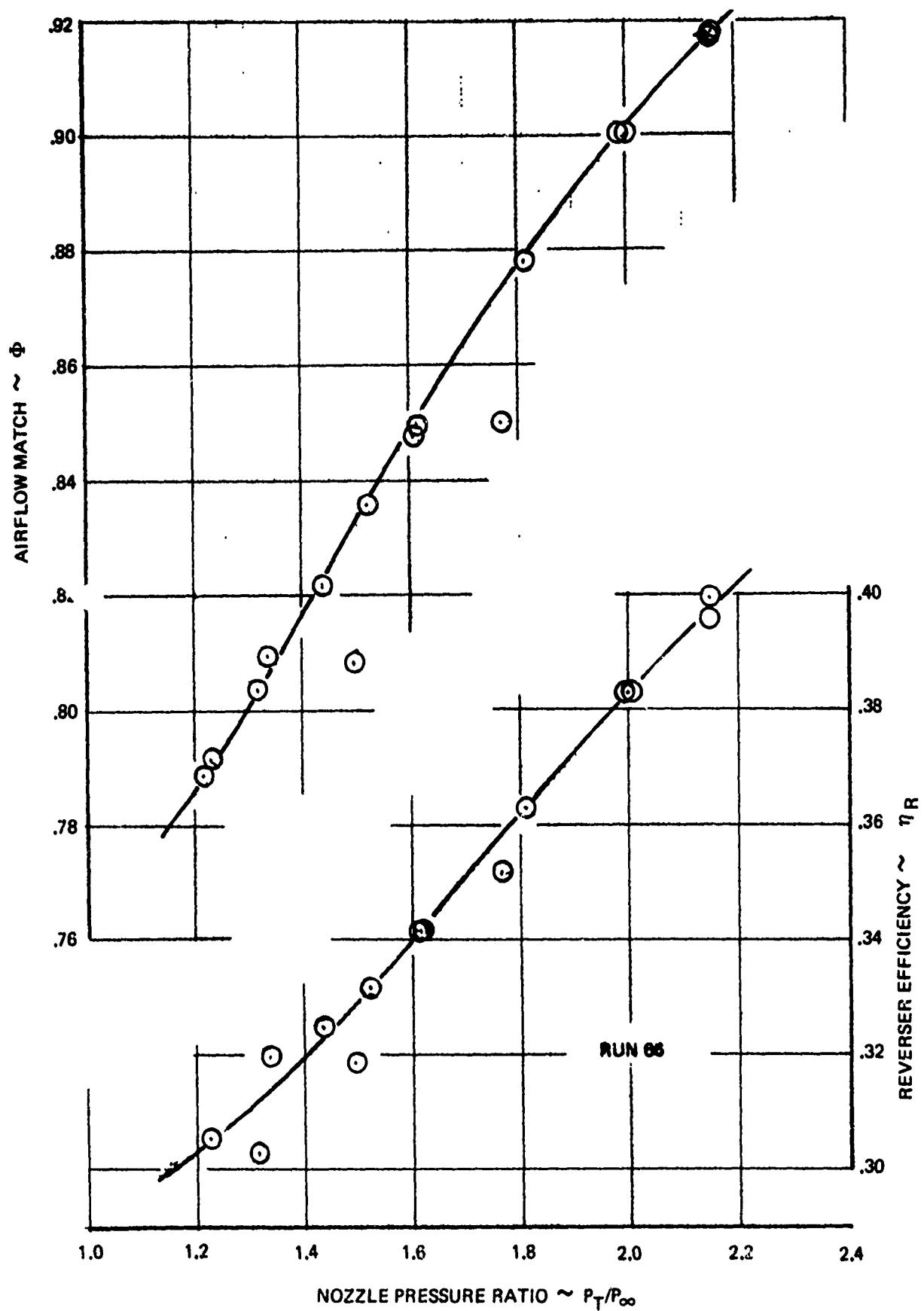


Figure 80: REVERSER EFFICIENCY (η_R) AIRFLOW MATCH (Φ)
 $D_n/D = 1.225$ $S/D = 1.03$

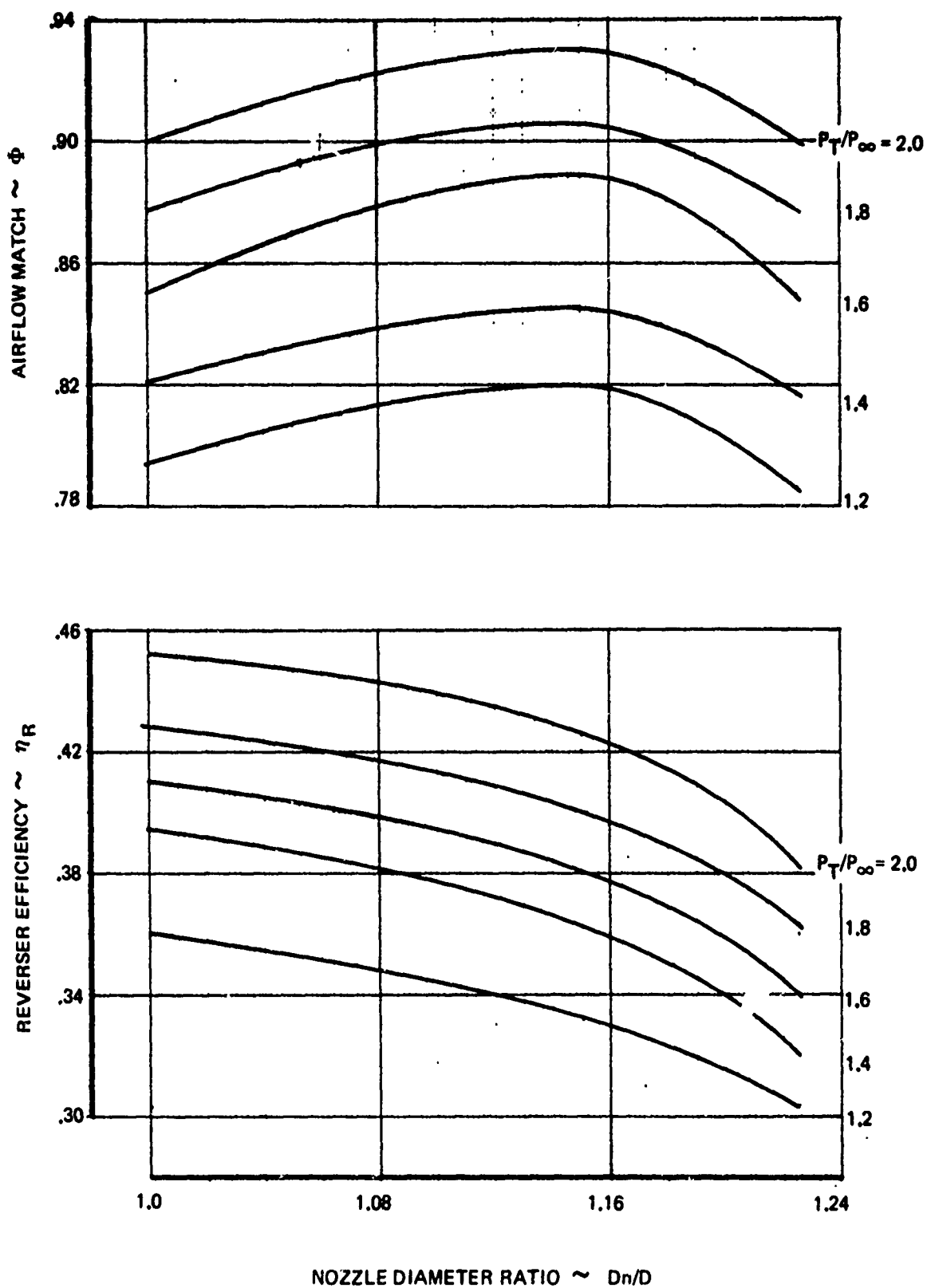


Figure 81: THRUST REVERSER PERFORMANCE CHARACTERISTICS

Further details of the test models and installation, instrumentation, procedure, and results of the fan cascade thrust reverser model and external deflector/target TR/TV model static tests are presented in Reference 5.

3.1.3 Overwing Target Thrust Reverser Data Review

Static performance for an overwing target thrust reverser design were obtained during a Boeing sponsored static test program. Thrust reverser efficiency and airflow match characteristics were investigated with a small scale model on the Boeing Thrust Vectoring Test Rig. Figure 82 shows a schematic of the reverser model and photographs showing the model installed on the test rig are presented in Figures 83 and 84. The model was tested with separate fan and primary mass flows and pressure ratios simulating a high bypass ratio turbofan engine. Geometric parameters investigated during the test included door length, lip length, door angle, reverser door setback distance, and duct shape. Data correlations for reverser efficiency and airflow match for the reverser model are discussed in the following paragraphs.

Reverser efficiency data corresponding to the engine take-off power setting are summarized in Figure 85. As discussed in Volume I, a parameter that provides satisfactory correlations of target thrust reversers performance is $\phi - \theta$, the difference between the reverser door blockage angle, ϕ , and the reverser door angle, θ (see Figure 82). This parameter was successfully used to correlate annular target thrust reverser performance and was applied to the overwing external target thrust reverser data.

The correlation shown in Figure 85 indicates that the reverser geometry should provide for a net angle $\phi - \theta$ of approximately -25° to achieve 50 percent reverser efficiency. It should be noted that the correlation seems to provide best agreement when the door angle is constant and the lip geometry and setback distance are varied to establish the blockage angle. The door angles for doors 10 and 11 were 93° while the other configurations had a door angle of 78° . This characteristic was also noted for annular target thrust reverser correlations presented in Volume I.

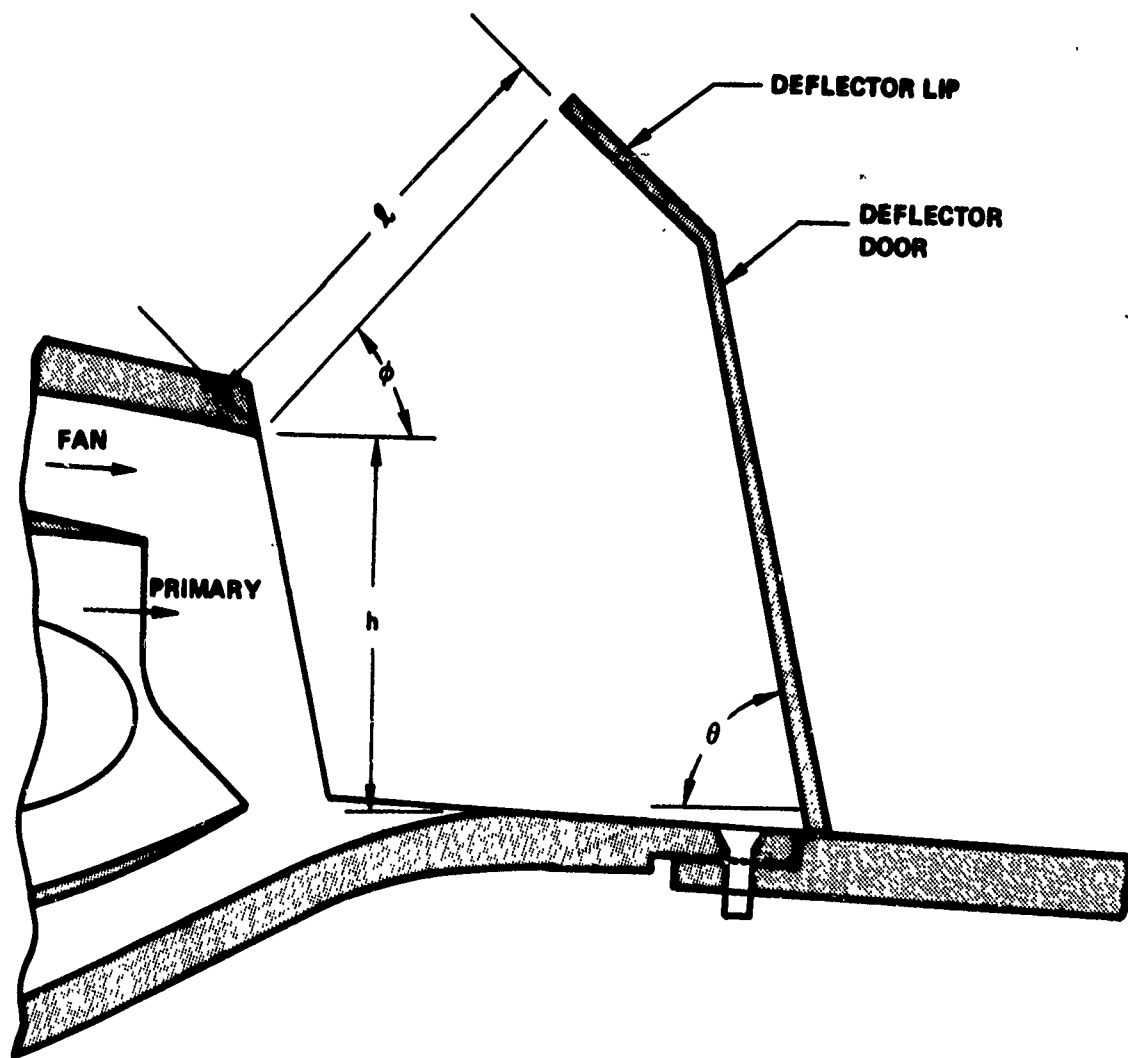


Figure 82: Overwing Target Thrust Reverser Model Schematic

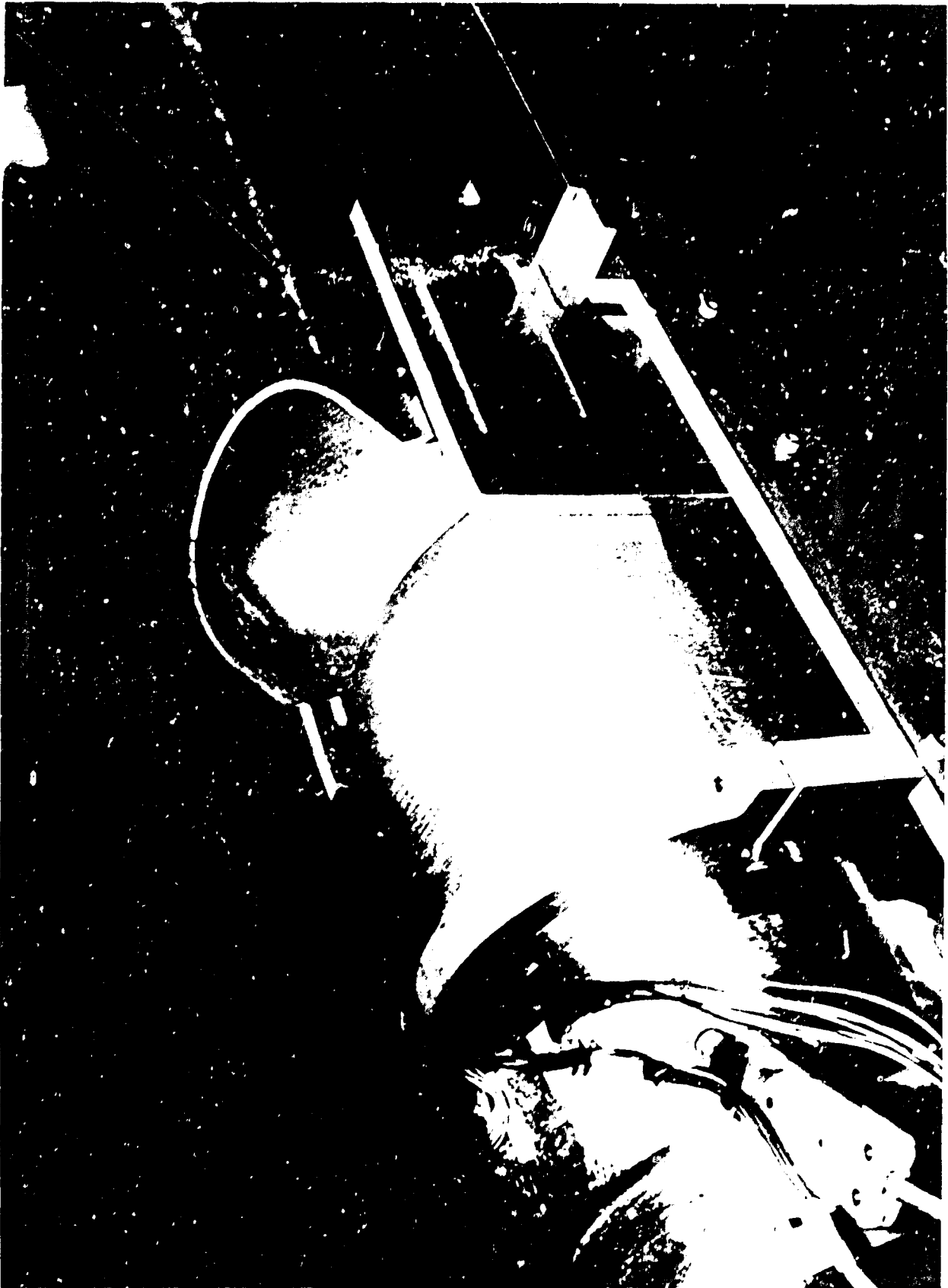


Figure 83: TARGET THRUST REVERSER MODEL - FRONT VIEW



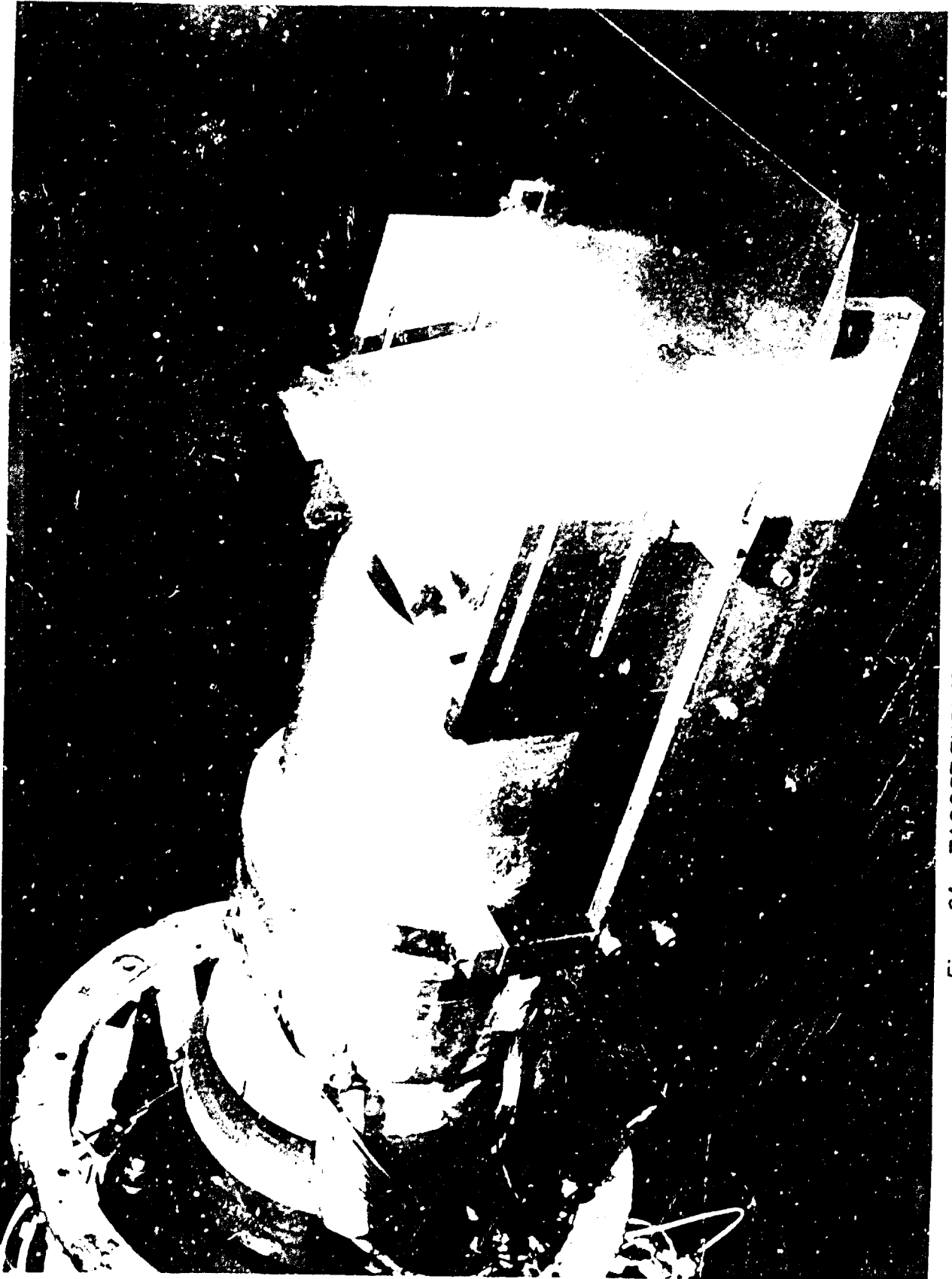


Figure 84: TARGET THRUST REVERSER MODEL - AFT VIEW

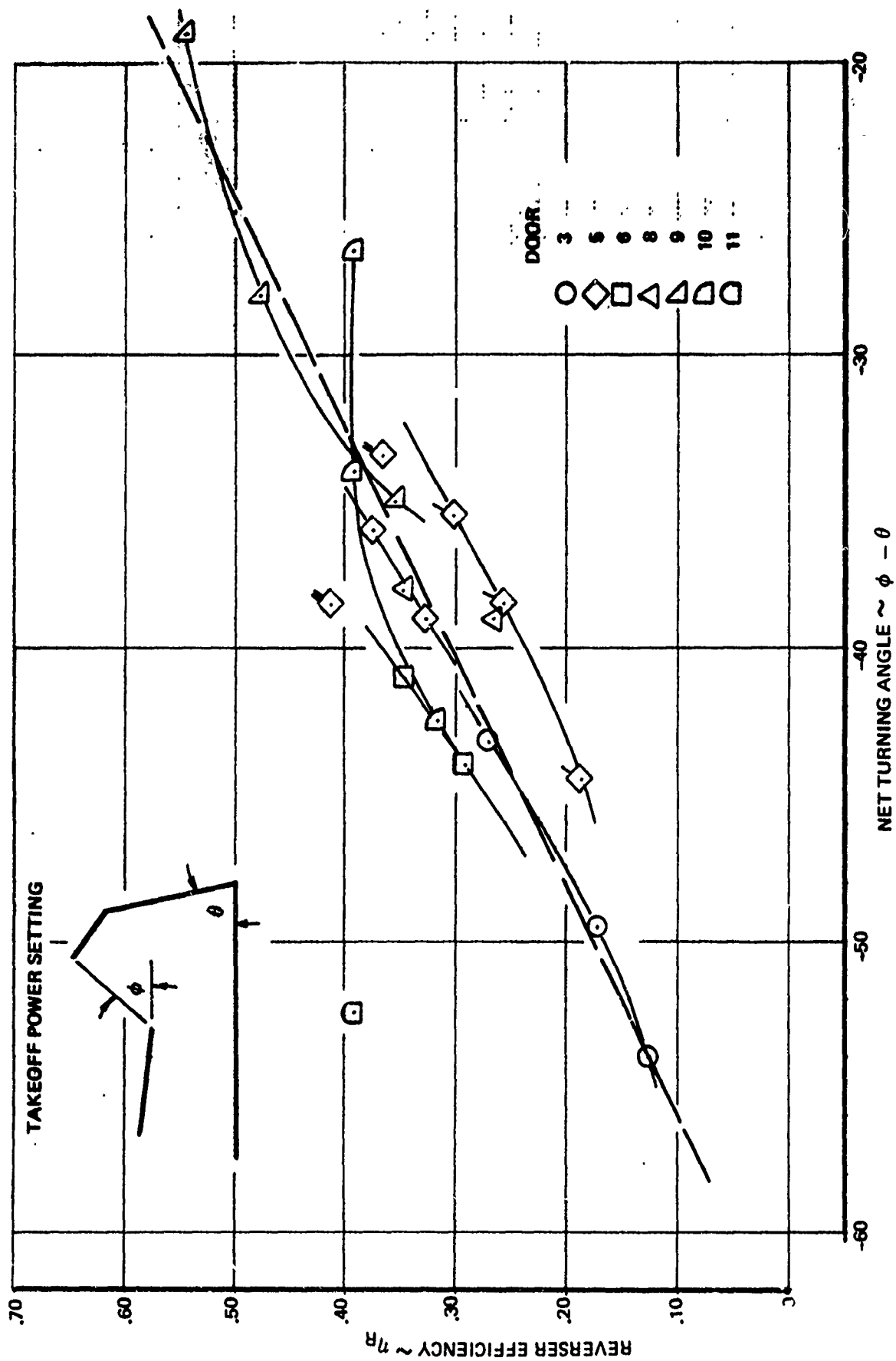


Figure 85: REVERSER EFFICIENCY CORRELATION

Experience with the annular target thrust reverser showed that the parameter, $\theta - \theta$, did not satisfactorily correlate airflow match data. Similar results were obtained for the overwing target thrust reverser model as shown in Figure 86 for the primary nozzle flow data. Considerable data scatter occurred that was dependent on the reverser door geometry. However, modifying the airflow match data by the ratio of the nozzle height, h , and door opening, l , considerably reduced the data scatter as shown in Figure 87. A similar correlation of fan airflow match data is shown in Figure 88.

As noted for the reverser efficiency correlation, the airflow match correlation seems to work best when the door angle is constant. The door 5 data with single flags are for a door geometry with a longer lip than the other configurations. This data would indicate that a correlating parameter that includes the lip geometry might provide a better correlating parameter.

3.2 -- Task 3.2 Correct Data to Full Scale Performance

The objective of Task 3.2 was to correct the scale model performance data obtained during Task 3.1 using scaling relationships to predict full scale performance. A brief review was conducted of the literature collected during Part 1A of the program and other existing data. Only two significant references were found that pertain to scaling nozzle performance, Reference 12 and 13. The first report describes an analytical method to scale nozzle velocity and discharge coefficients. The method employs the turbulent, compressible boundary layer analysis of Stratford (Reference 14). By assuming the losses are due entirely to skin friction and are a function of Reynolds number and geometry (at a given nozzle pressure ratio) the influence of Reynolds number on velocity coefficient is given by the following equation:

$$C_{VFS} = \frac{1 - 2 \left(\frac{Re_{FS}}{Re_{MS}} \right)^{-1/5} \left[\frac{(1 - C_{VMS})(N+1)}{\left(\frac{2N+2}{N+2} - C_{VMS} \right)(N+2)} \right]}{1 - 2 \left(\frac{Re_{FS}}{Re_{MS}} \right)^{-1/5} \left[\frac{1 - C_{VMS}}{2 \left(\frac{2N+2}{N+2} - C_{VMS} \right)} \right]}$$

where N is the turbulent boundary layer exponent (typically $N = 7$ for a turbulent boundary layer), and the subscripts MS and FS refer to model scale and full scale. The influence of Reynolds number on discharge coefficient is given by the following equation:

$$C_{DFS} = 1 - \left(\frac{Re_{FS}}{Re_{MS}} \right)^{-1/5} (1 - C_{OMS})$$

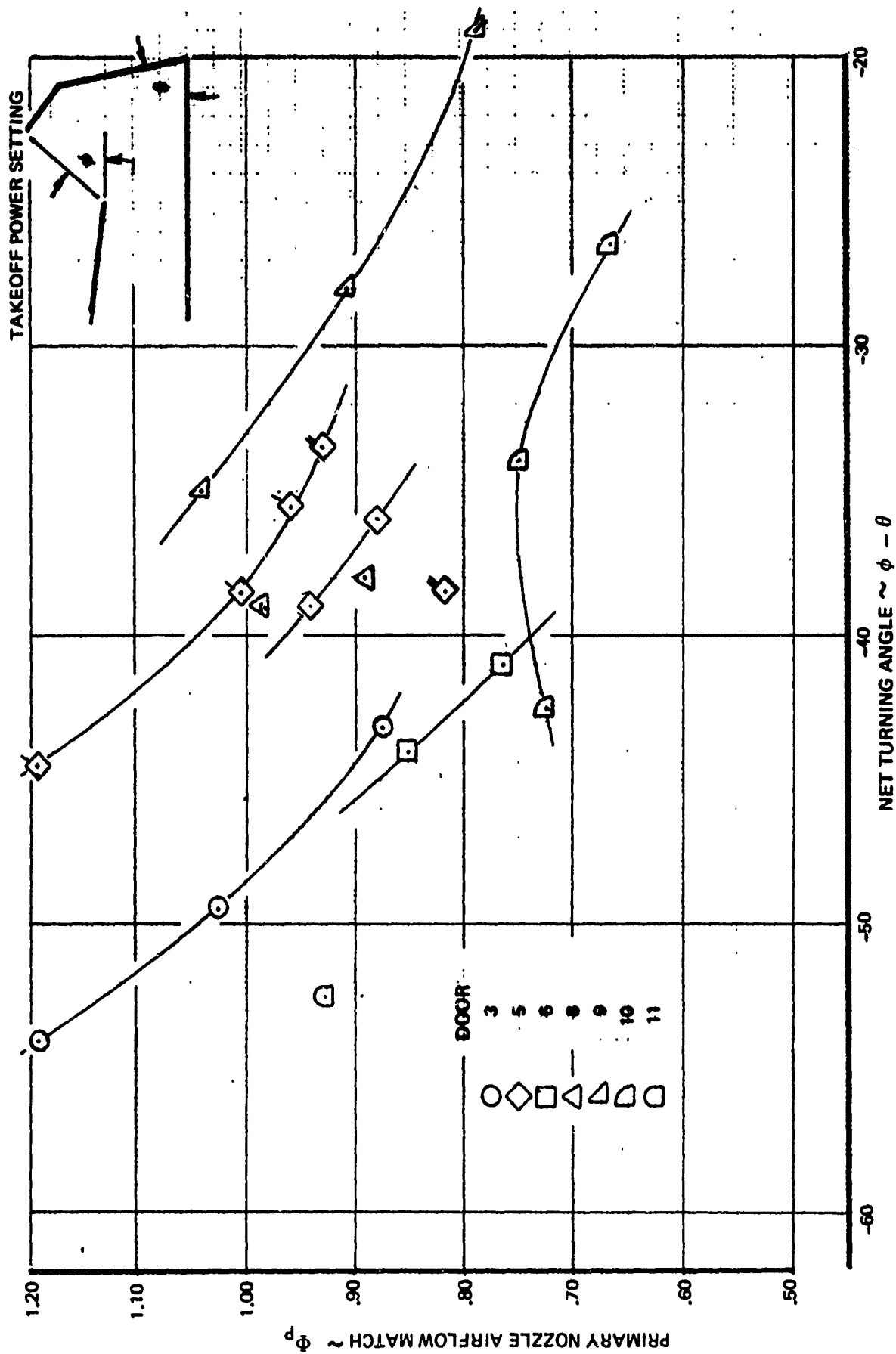


Figure 86: PRIMARY NOZZLE AIRFLOW MATCH DATA

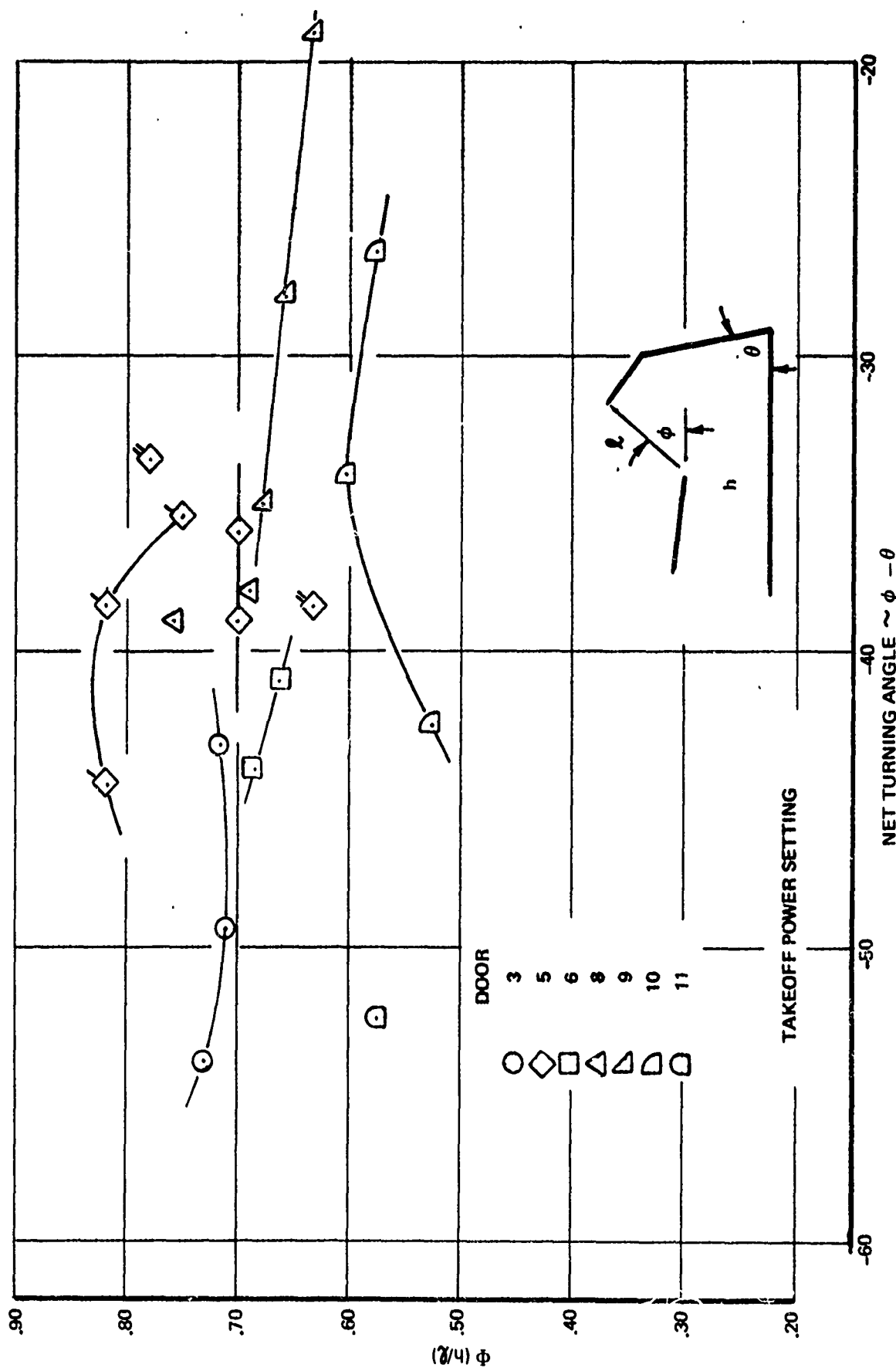


Figure 87: PRIMARY NOZZLE AIRFLOW MATCH CORRELATION

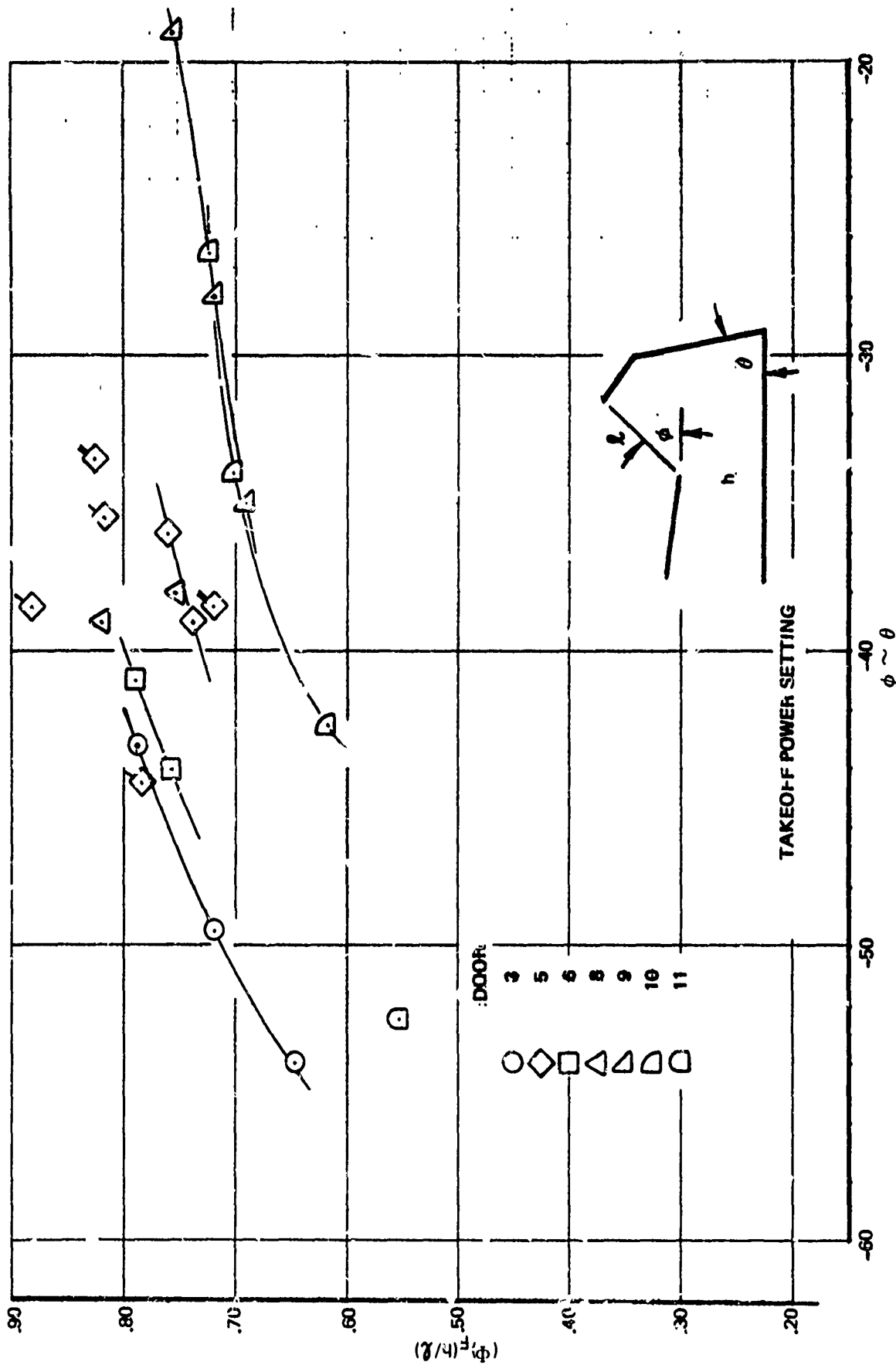


Figure 88: FAN AIRFLOW MATCH CORRELATION

The effect of Reynolds number on velocity coefficient is shown graphically in Figure 89. Nozzles with high velocity coefficient are affected less by Reynolds number than nozzles having low velocity coefficients. Since the full scale Reynolds number, Re_{FS} , is usually greater than Re_{MS} , the full scale velocity coefficient is usually greater than the model scale C_v .

A comparison of theoretical and experimental velocity coefficients at several Reynolds numbers is shown in Figure 90. The solid lines were calculated from Equation (1) by matching the C_v at a Reynolds number ratio of 1.0.

Reference 14 presents test data illustrating Reynolds number effects on nozzle performance coefficients. These data were compared to predictions made using Equations (1) and (2) with favorable results. For example, the effect of Reynolds number on ASME nozzle discharge coefficient is shown in Figure 91.

Several references were found containing comparisons between model and full scale TR and TV performance parameters (Reference 15 to 23). Comparisons for corrected reverser efficiency are shown in Figures 92 to 96. In most cases the model scale efficiency is greater than full scale. The difference in performance is usually attributed to exhaust gas leakage through full scale tail pipe gaps and thrust reverser seals. Model scale test hardware frequently does not scale gaps and seals accurately. In some cases differences between model and full scale values were due to geometric differences. For example, data taken for the full scale target reverser shown in Figure 96 was obtained with a greater setback than for model scale.

The existing data indicates that scaling of thrust reverser airflow match characteristics is not always successful. For example, differences were not found between the Model 737 target thrust reverser model and full scale primary and fan airflow match characteristics. Full scale airflow match showed an apparent increase in fan flow and decrease in primary flow during reverse operation.

Comparisons between combined fan and primary airflow (Figure 97) indicates that model scale data predicts full scale airflow match only within $\pm 2\%$. Final tailoring of airflow match in reverse thrust must be done at full scale. However the model data are useful in predicting large mismatch characteristics.

A comparison of model and full scale performance for a hinged spherical deflector nozzle in the cruise mode is shown in Figure 98. Nonuniform exit flow conditions for the full scale nozzle degraded predictions of nozzle coefficients and contributed to the observed discrepancies.

BOUNDARY LAYER EXPONENT = $N = 7$

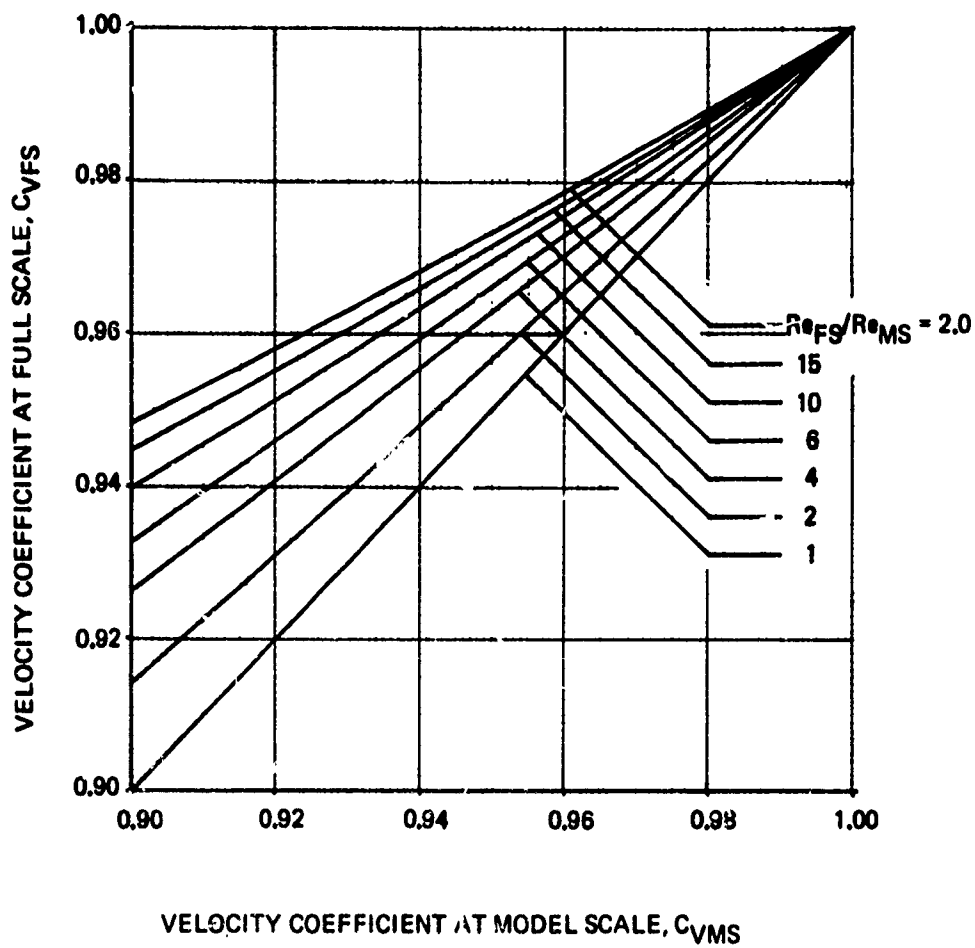


Figure 89: SCALING EFFECTS OF REYNOLDS NUMBER ON VELOCITY COEFFICIENT

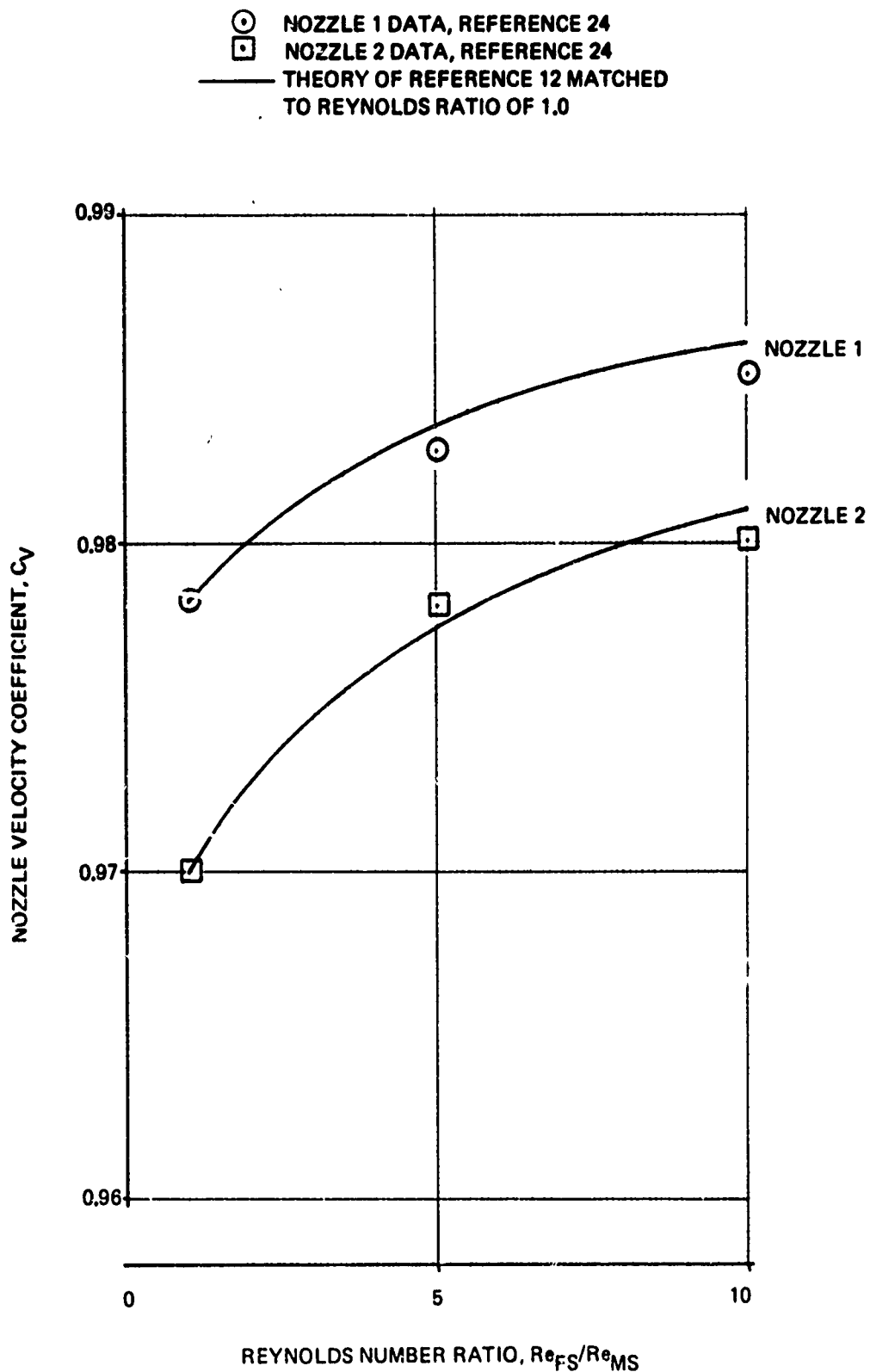


Figure 90: COMPARISON OF THEORETICAL AND EXPERIMENTAL EFFECTS OF REYNOLDS NUMBER ON VELOCITY COEFFICIENT

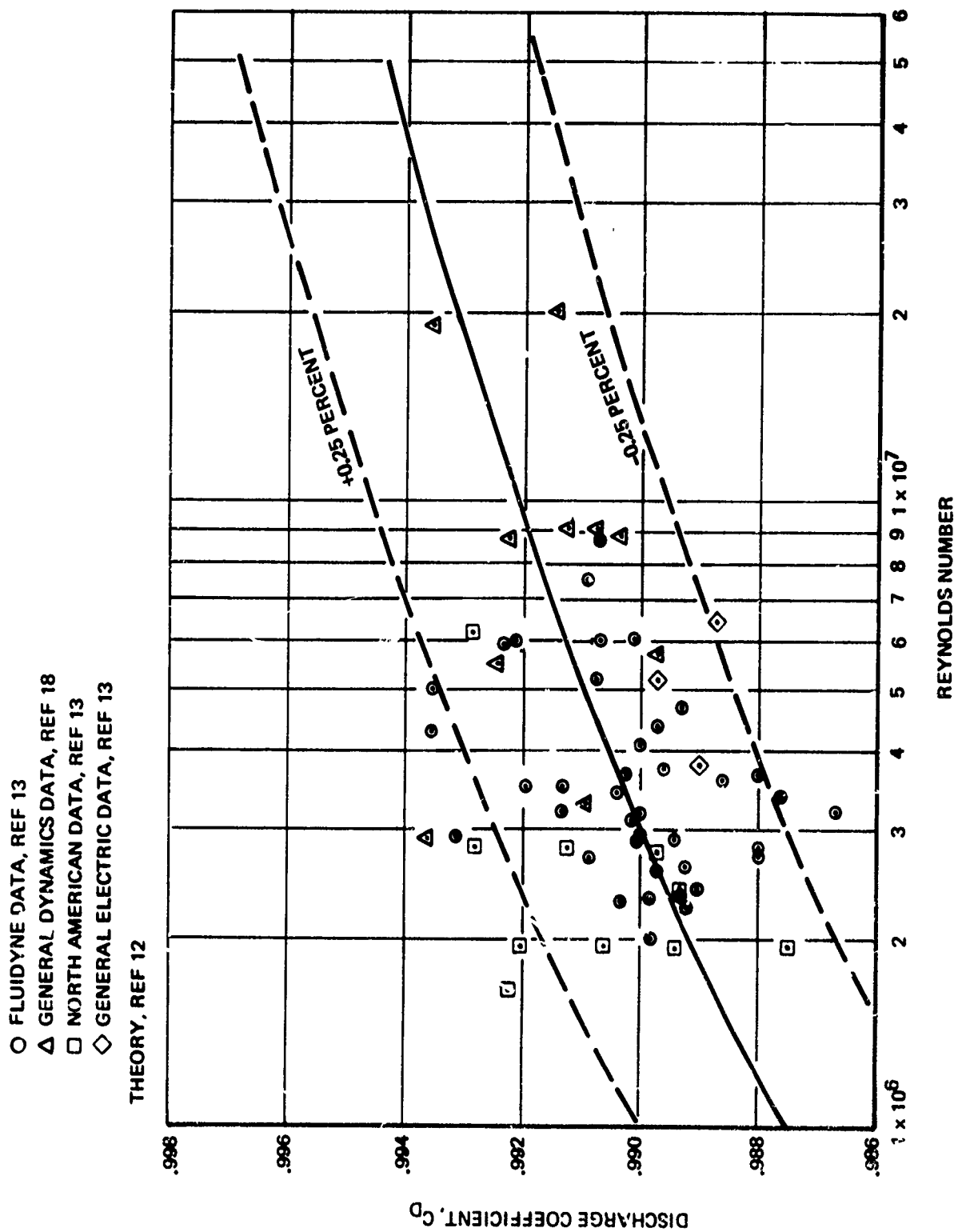


Figure 91: ASME DISCHARGE COEFFICIENT VS THROAT REYNOLDS NUMBER

REFERENCE 19

— MODEL SCALE (0.3)
- - - FULL SCALE

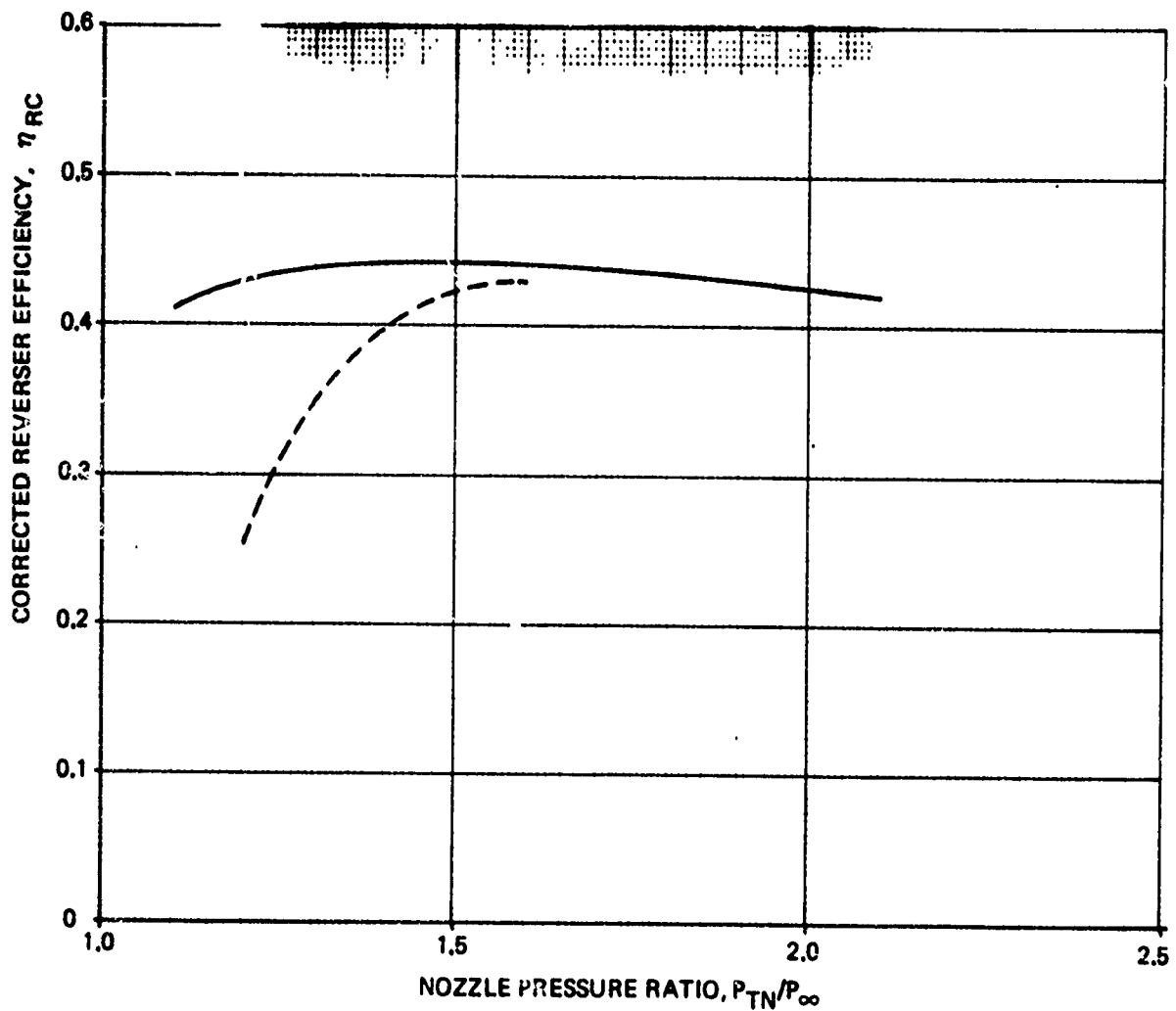
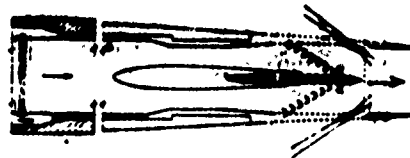
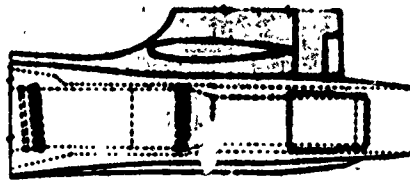
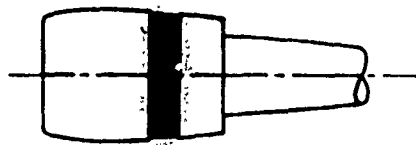
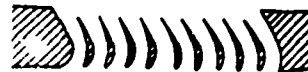


Figure 92: COMPARISON OF MODEL AND FULL SCALE
CORRECTED REVERSER EFFICIENCY DATA
FOR A CASCADE THRUST REVERSER

— MODEL SCALE (0.067), REFERENCE 17
 - - - FULL SCALE, REFERENCE 16



THRUST REVERSER INSTALLATION



CASCADE DETAILS

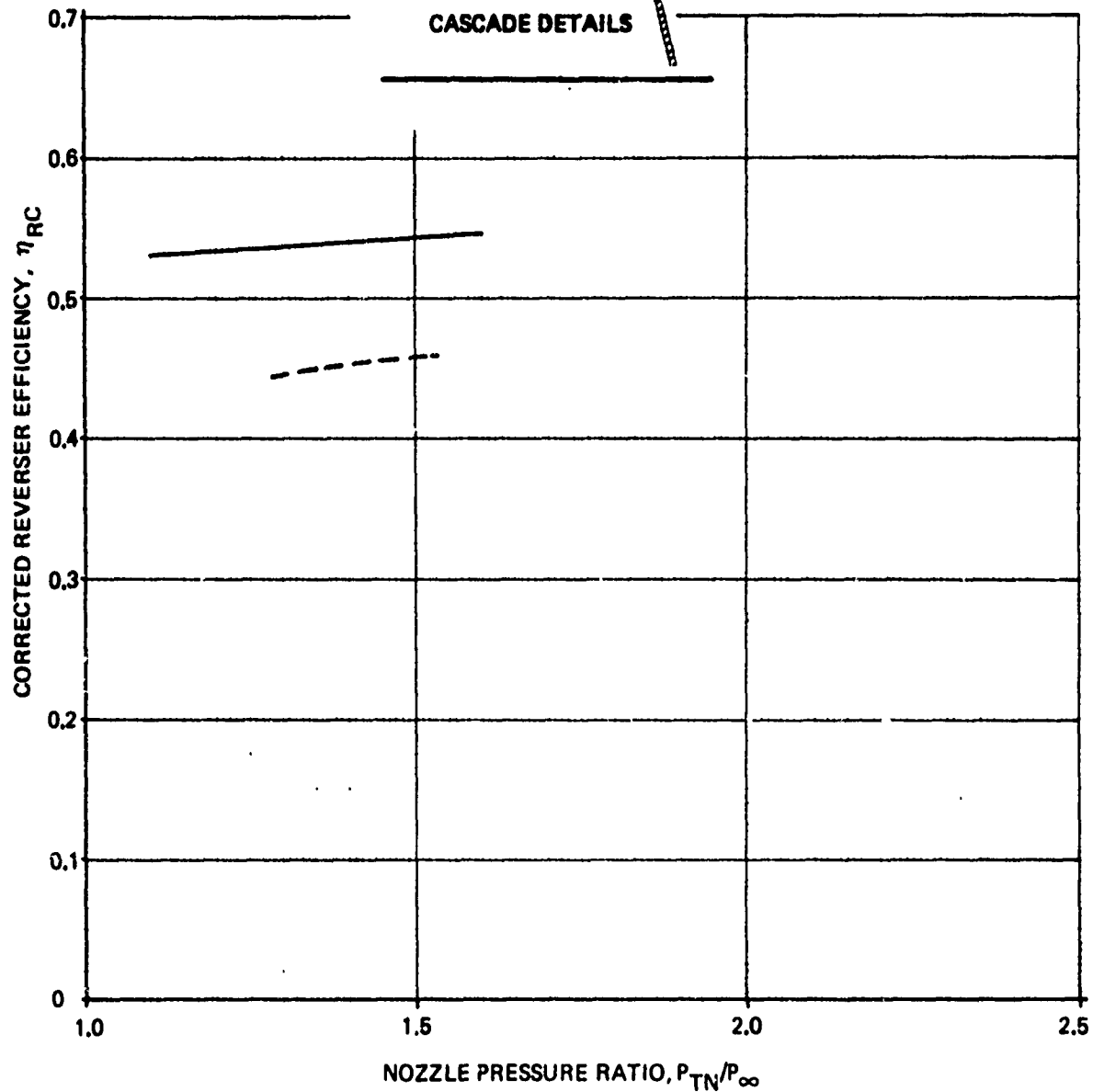


Figure 93: COMPARISON OF MODEL AND FULL SCALE
 CORRECTED REVERSER EFFICIENCY DATA
 FOR THE C-5A FAN CASCADE REVERSER

REFERENCE 18

— MODEL SCALE (0.25)

- - - FULL SCALE

$l/d_n = 0.621$

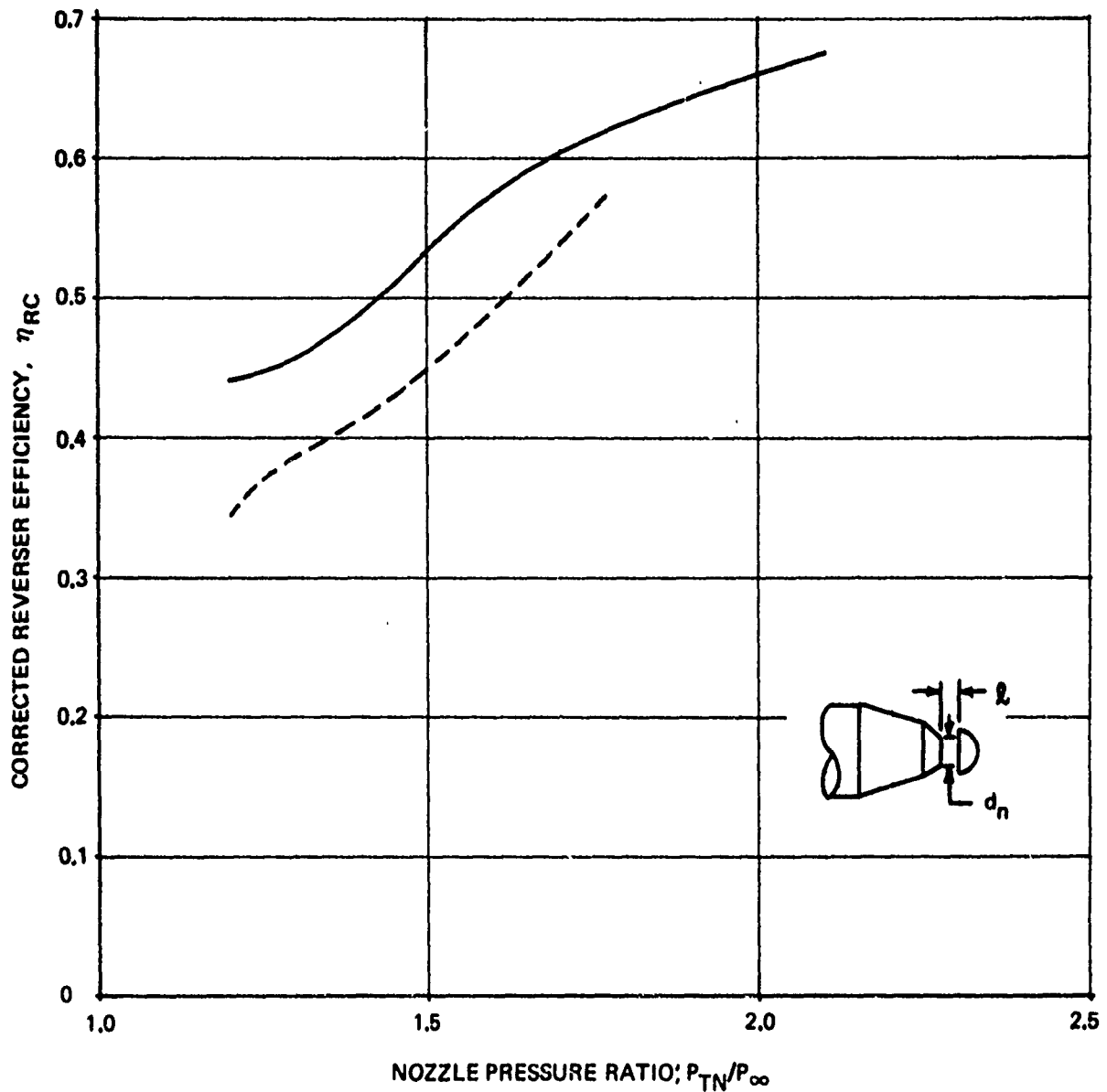
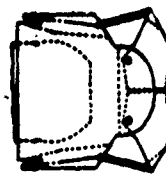
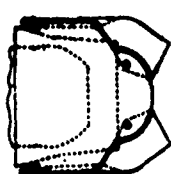


Figure 94: COMPARISON OF MODEL AND FULL SCALE CORRECTED REVERSER EFFICIENCY DATA FOR A HEMISPHERICAL TARGET REVERSER

REFERENCE 20

———— MODEL SCALE (0.154)

----- FULL SCALE



FORWARD THRUST POSITION

REVERSE THRUST POSITION

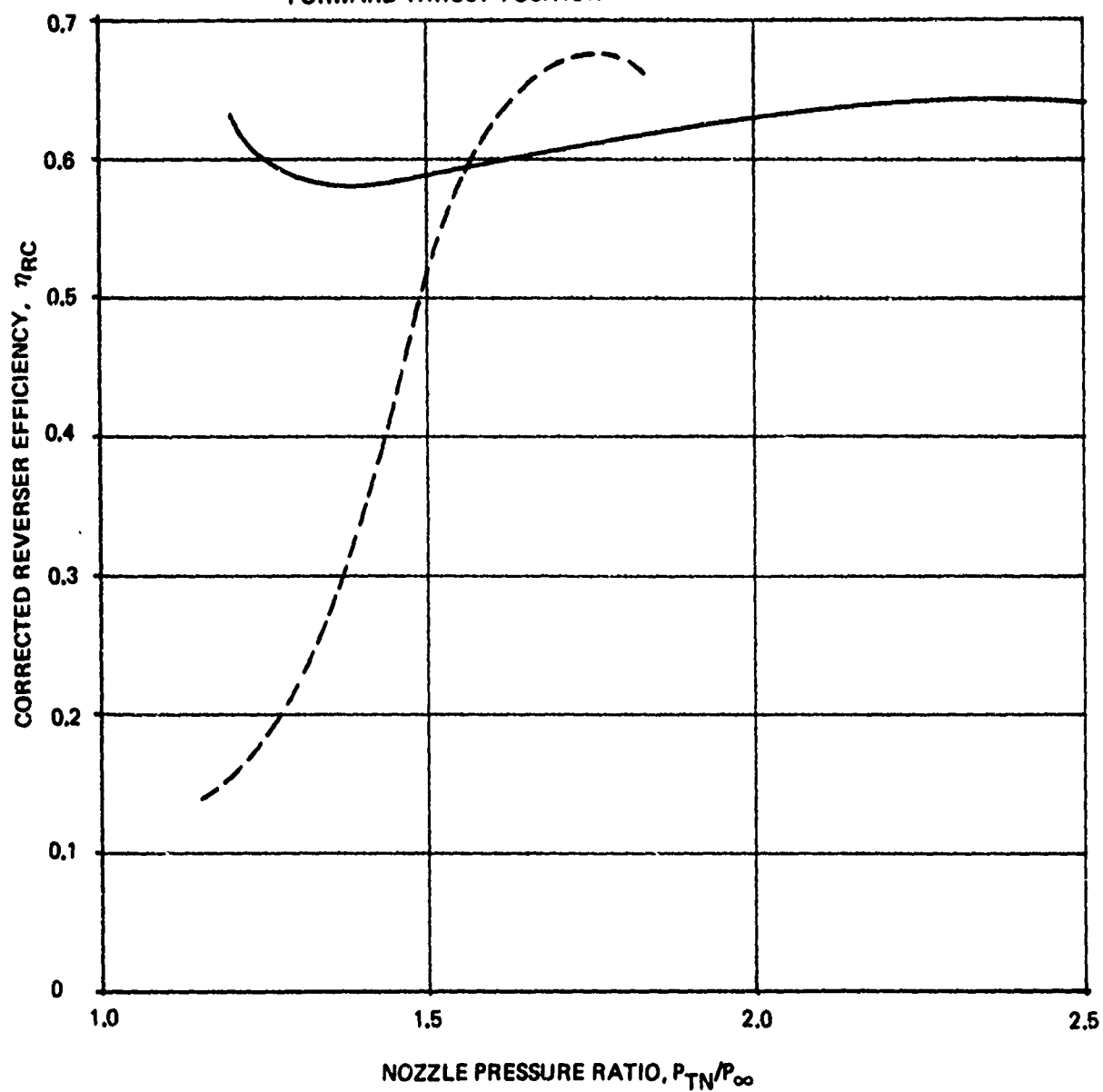


Figure 95: COMPARISON OF MODEL AND FULL SCALE CORRECTED REVERSER EFFICIENCY DATA FOR A TARGET THRUST REVERSER

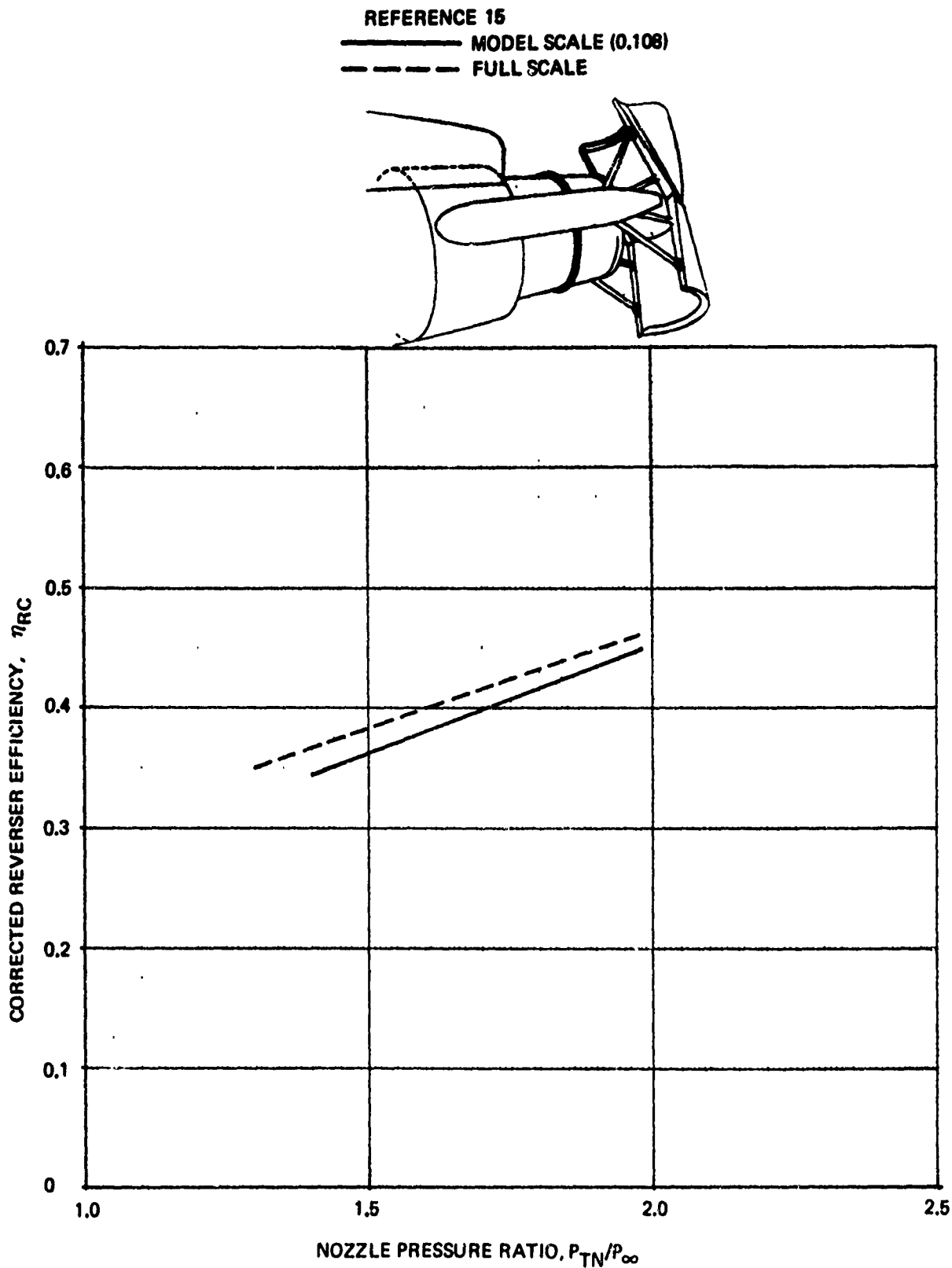


Figure 96: COMPARISON OF MODEL AND FULL SCALE
CORRECTED REVERSER EFFICIENCY DATA
FOR THE 737 TARGET THRUST REVERSER

REFERENCE 15

— MODEL SCALE (0.108)

- - - FULL SCALE

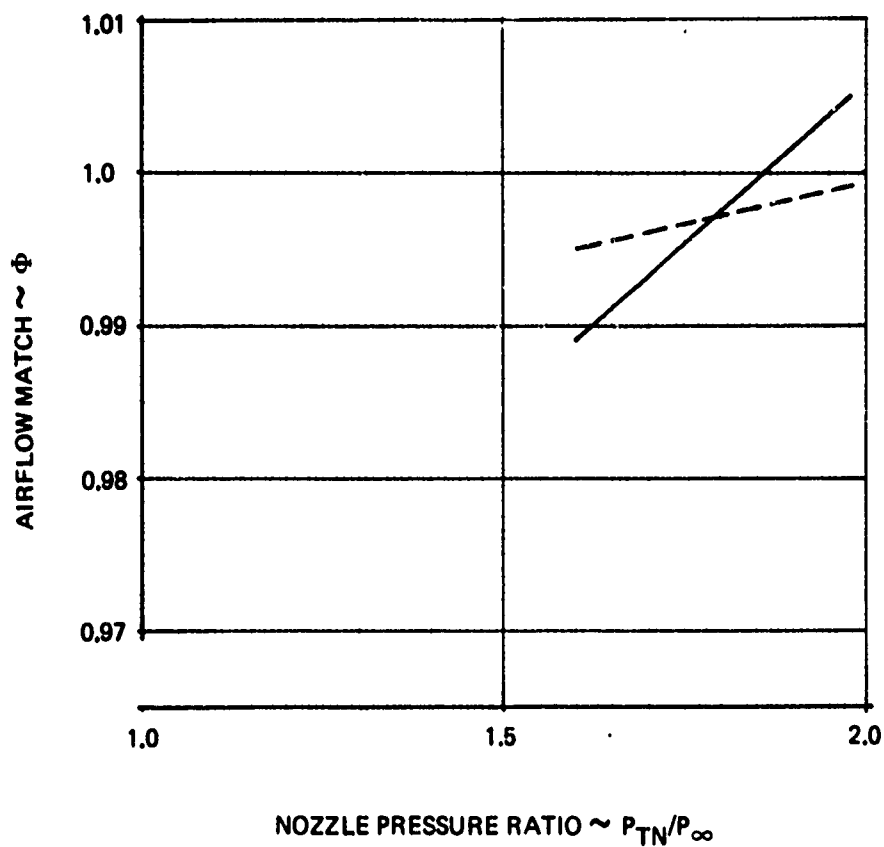
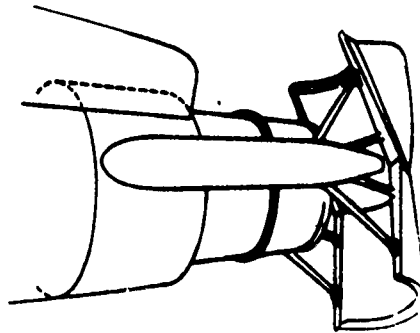


Figure 97: COMPARISON OF MODEL AND FULL SCALE AIRFLOW MATCH DATA FOR THE MODEL 737 TARGET THRUST REVERSER

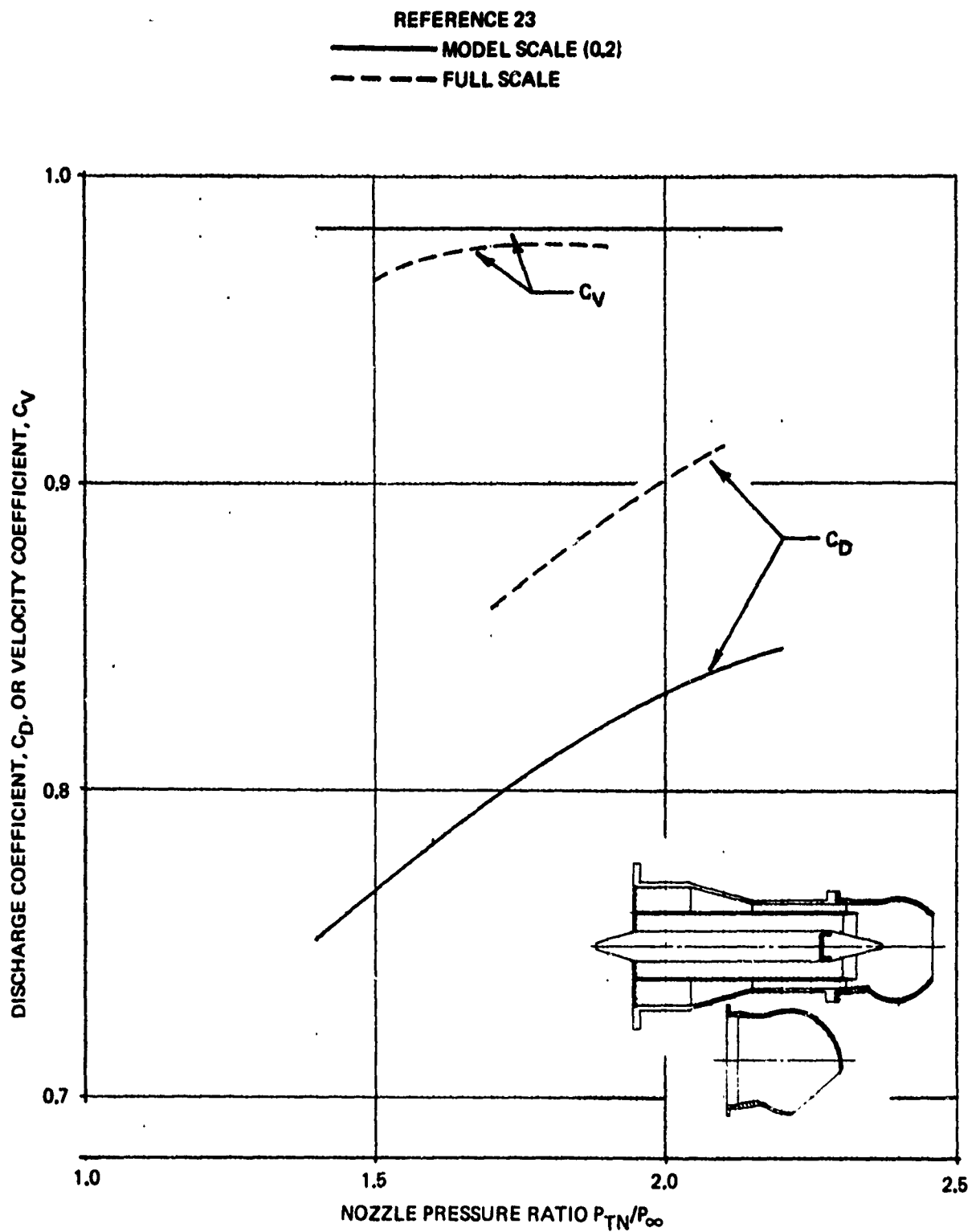


Figure 98. COMPARISON OF MODEL AND FULL SCALE PERFORMANCE FOR A SPHERICAL EYEBALL NOZZLE

Unfortunately, none of the reports noted above generalized scale effects to predict thrust reverser or thrust vectoring nozzle performance parameters, i.e., reverser efficiency, η_R , vectoring efficiency, η_V , or airflow match, ϕ . Therefore, the following approach was taken to satisfy the objectives of Task 3.2. The scaling relationships for C_V and C_D given Equations (1) and (2) were programmed into the TR and TV System Performance Program (TEM-357) developed during Part 1A. Scale corrections are made (at the users discretion) to the following types of nozzles:

- (1) Cruise nozzles
 - a) Conical
 - b) Annular
 - c) Irregular shaped nozzle
- (2) Thrust vectoring nozzles
 - a) Single bearing
 - b) Three bearing
 - c) Spherical eyeball
 - d) Lobstertail

The changes in program input required for scale corrections will be discussed in the Final Report.

3.3 -- Task 3.3 Correlate with Existing Model Data

The objective of Task 3.3 was to correlate the data obtained during Task 3.1 with the data developed during Part 1A of the program. The approach taken to fulfill this objective was to analyze the data and incorporate the significant data correlations into the Internal Performance Module of TEM-357. As noted in Volume I existing external deflector data were found inadequate to predict effects of setback and door length ratio. Theoretical results were shown illustrating the effects of external deflector geometric parameters. However, the theoretical results showed considerable disagreement with test data and were therefore not included in the subroutine used to predict external deflector performance. Instead, two specific sets of data were used to predict external deflector performance, one for flat plate and the other for curved deflectors.

In order to assess the effects of deflector setback, experimental data obtained from the hinged external deflector test were analyzed and correlated in terms of simple geometric parameters. A correlation for discharge coefficient ratio as a function of setback ratio is shown in Figures 99 to 101. Seventeen TV and three TR configurations correlated using the setback ratio parameter. Correlations attempted in terms of other geometric parameters resulted in greater data scatter.

A correlation for corrected vector efficiency is shown in Figures 102 to 104. For setback ratios $X/D > 1.0$, the different configurations correlate on a single line. For setback ratios $X/D < 1.0$, however, the data correlation branches into two curves, an upper curve for deflection angles of approximately 10 degrees and a lower curve for deflection angles of 30 degrees.

Efforts to develop a general data correlation for the three types of external deflectors (flat, curved, and hinged) were not successful. For example, discharge coefficient ratio correlations are compared on Figure 105 for annular target thrust reversers, the hinged external deflector and theory for a flat plate deflector. Because of the lack of correlation between different types of TR and TV configurations, the hinged deflector data correlations were incorporated into the external deflector subroutine of TEM-357 as a separate option. It is believed that the effects of setback ratio are adequately covered by the hinged deflector data correlations.

NOZZLE PRESSURE RATIO = 1.2

○ THRUST VECTORING NOZZLE CONFIGURATIONS

◇ THRUST REVERSER CONFIGURATIONS

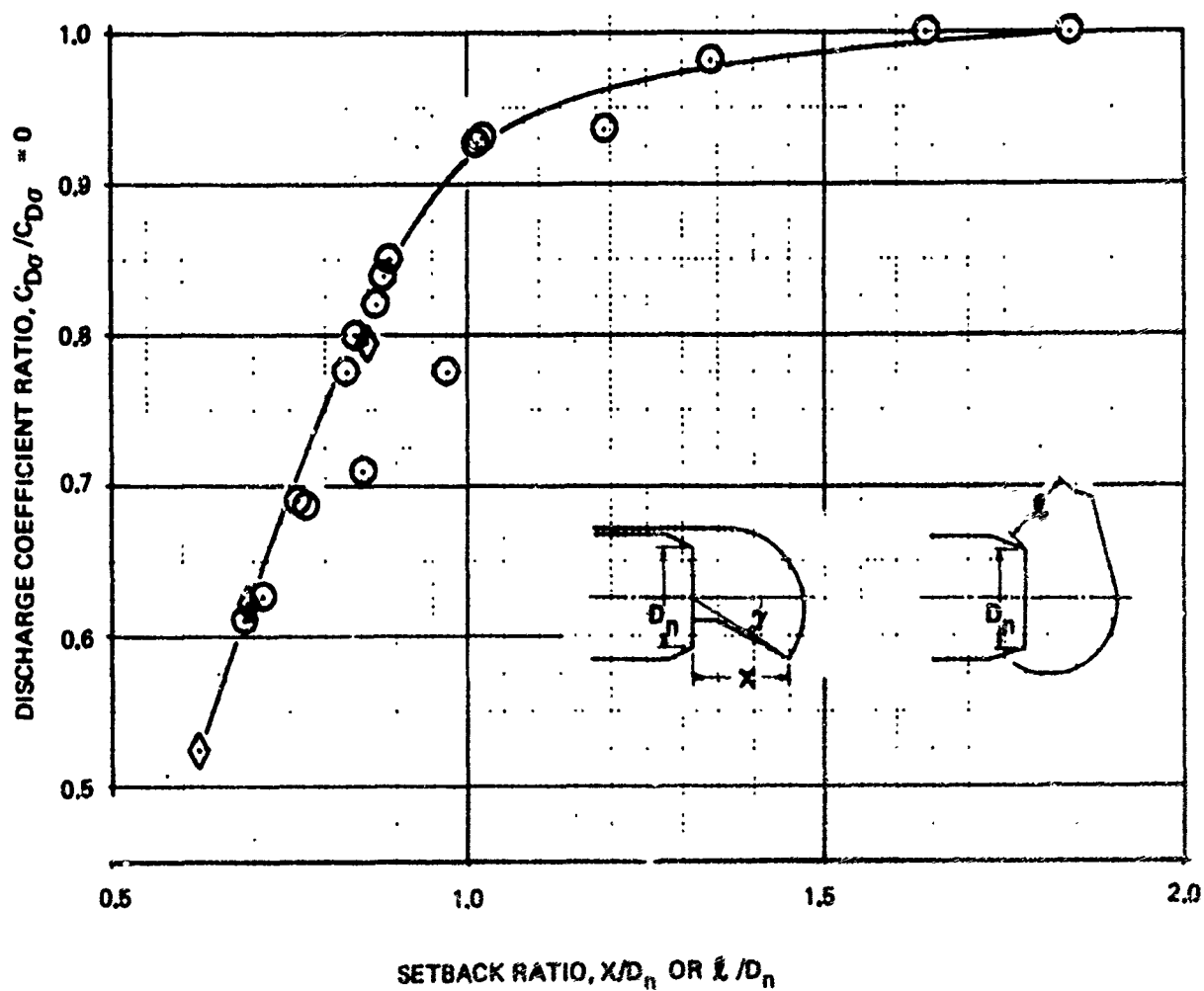


Figure 99: DISCHARGE COEFFICIENT CORRELATION FOR HINGED EXTERNAL DEFLECTOR, $P_T/P_\infty = 1.2$

NOZZLE PRESSURE RATIO = 1.6

- THRUST VECTORING NOZZLE CONFIGURATIONS
- ◇ THRUST REVERSER NOZZLE CONFIGURATIONS

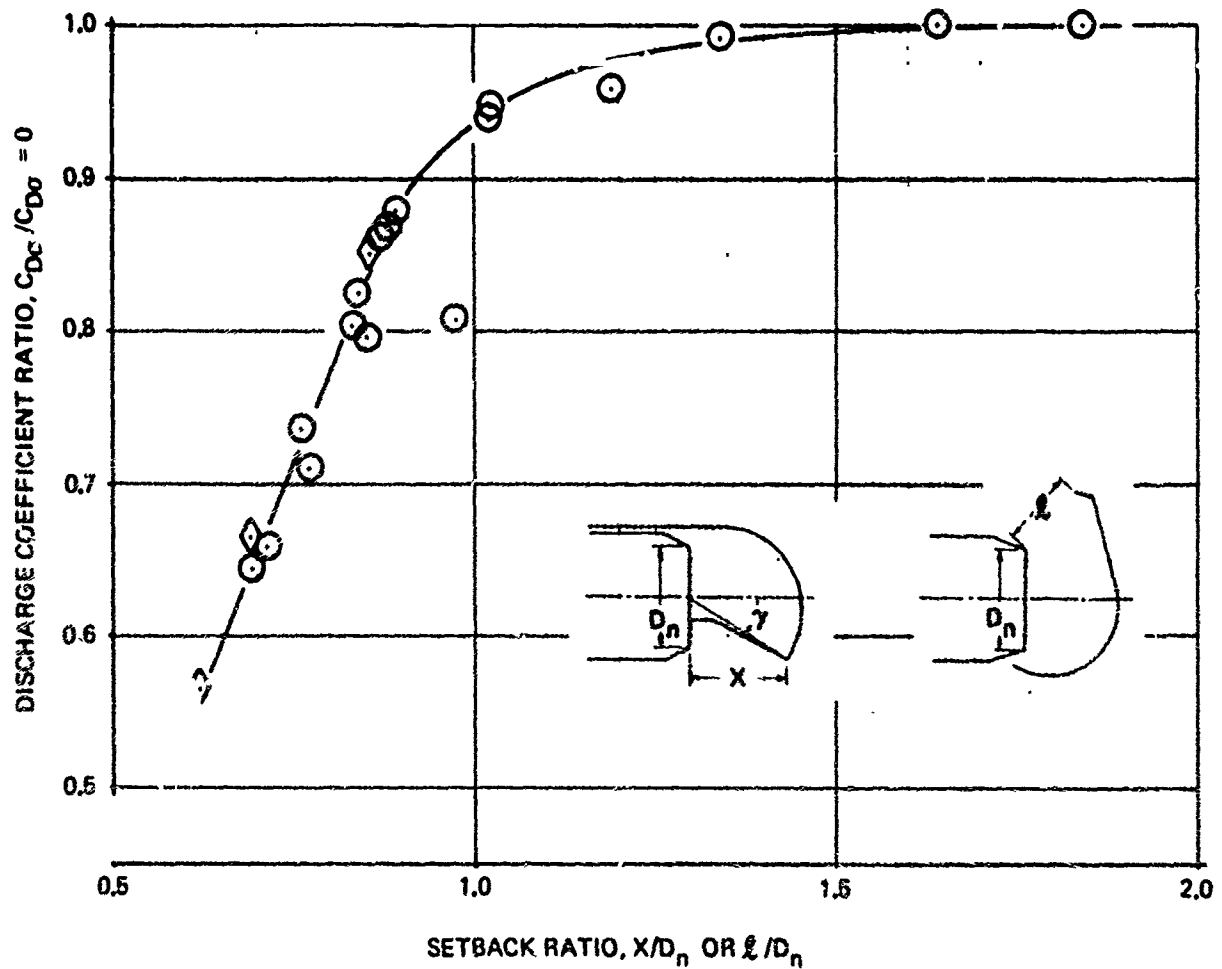


Figure 100: DISCHARGE COEFFICIENT CORRELATION FOR HINGED EXTERNAL DEFLECTOR NOZZLE, $P_T/P_\infty = 1.6$

NOZZLE PRESSURE RATIO = 2.2

○ THRUST VECTORING NOZZLE CONFIGURATION

◇ THRUST REVERSER NOZZLE CONFIGURATIONS

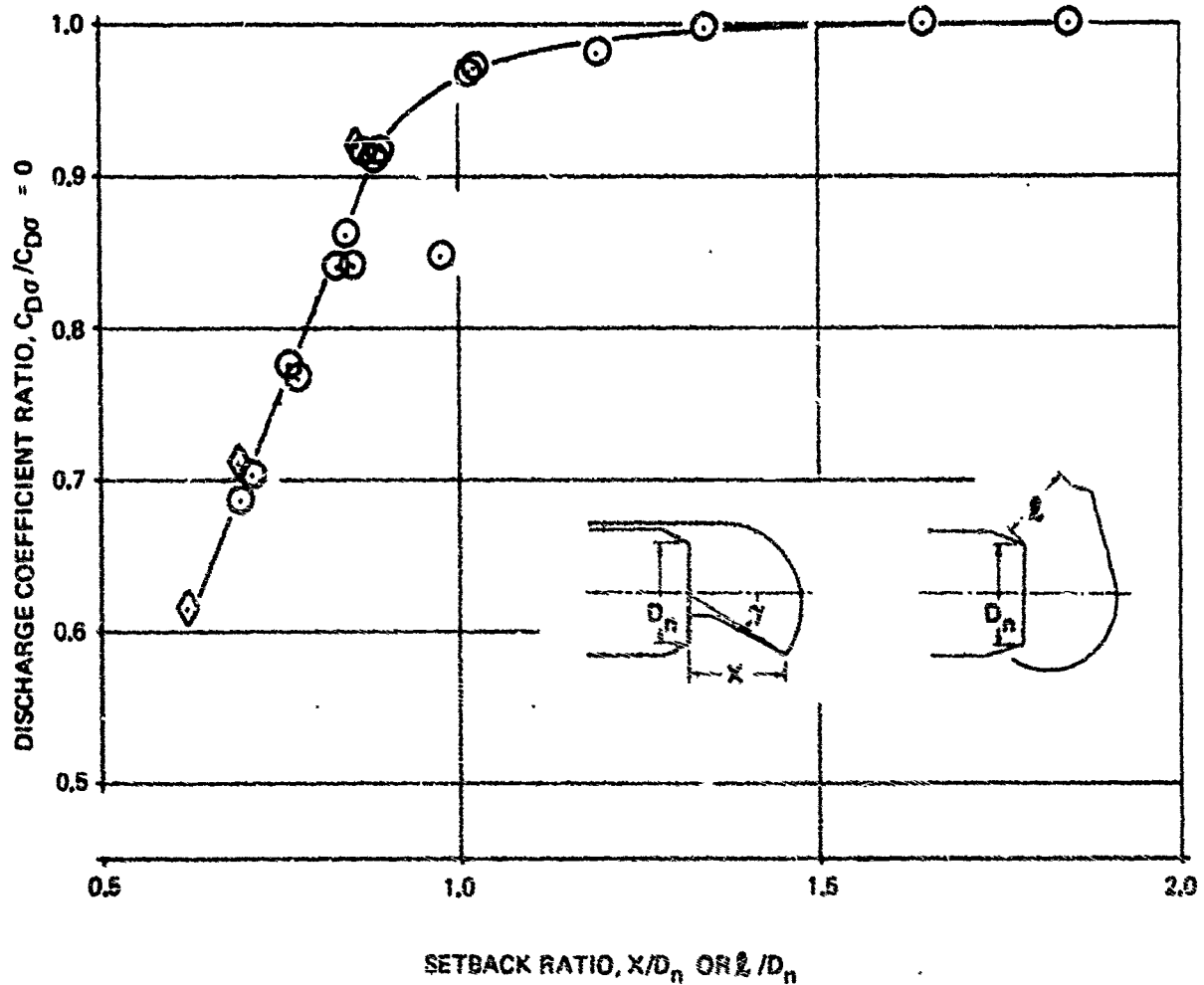


Figure 101: DISCHARGE COEFFICIENT CORRELATION FOR HINGED EXTERNAL DEFLECTOR NOZZLE, $P_T/P_\infty = 2.2$

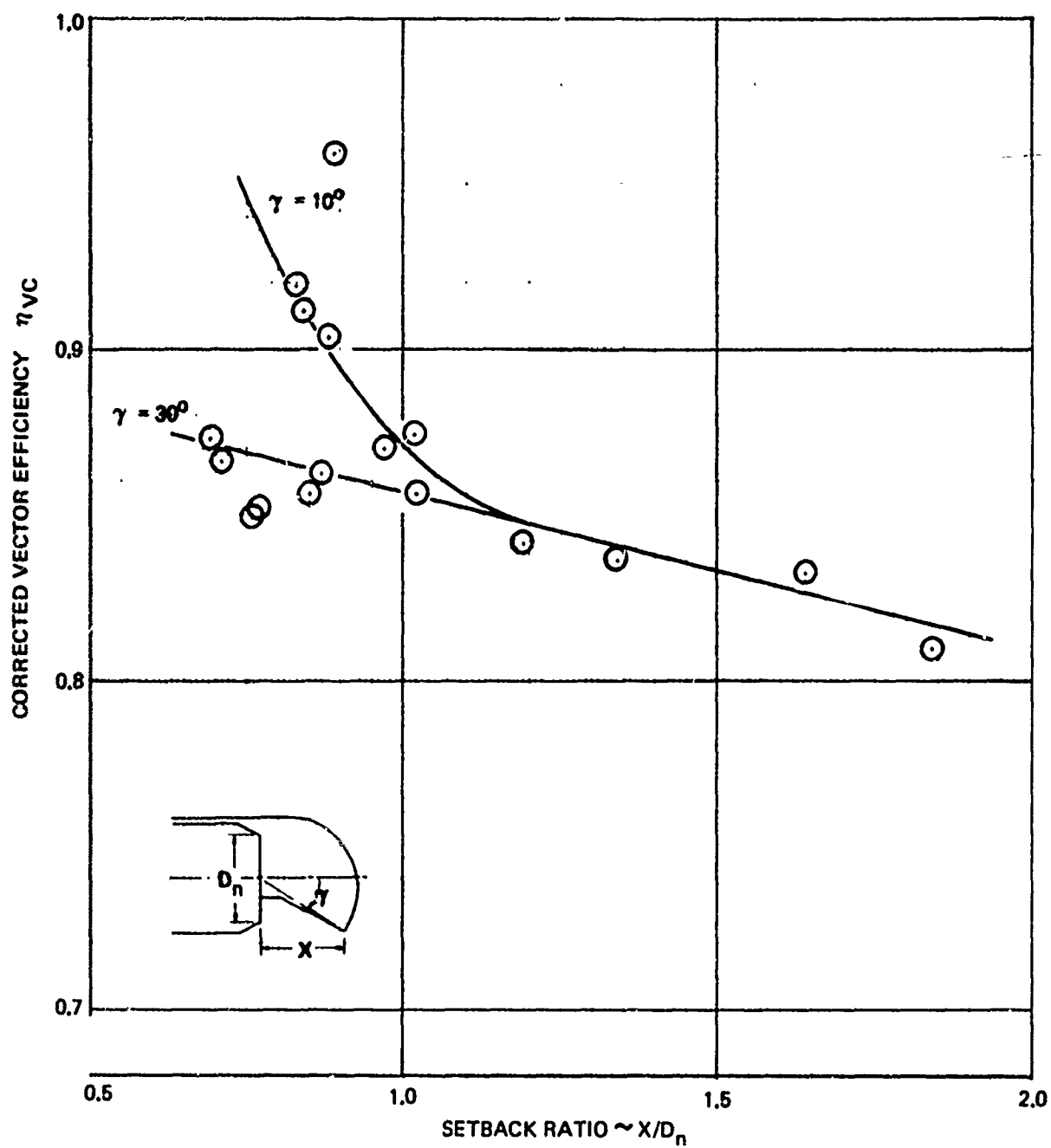


Figure 102: CORRECTED VECTOR EFFICIENCY CORRELATION
FOR HINGED EXTERNAL DEFLECTOR NOZZLES $P_T/P_\infty = 1.2$

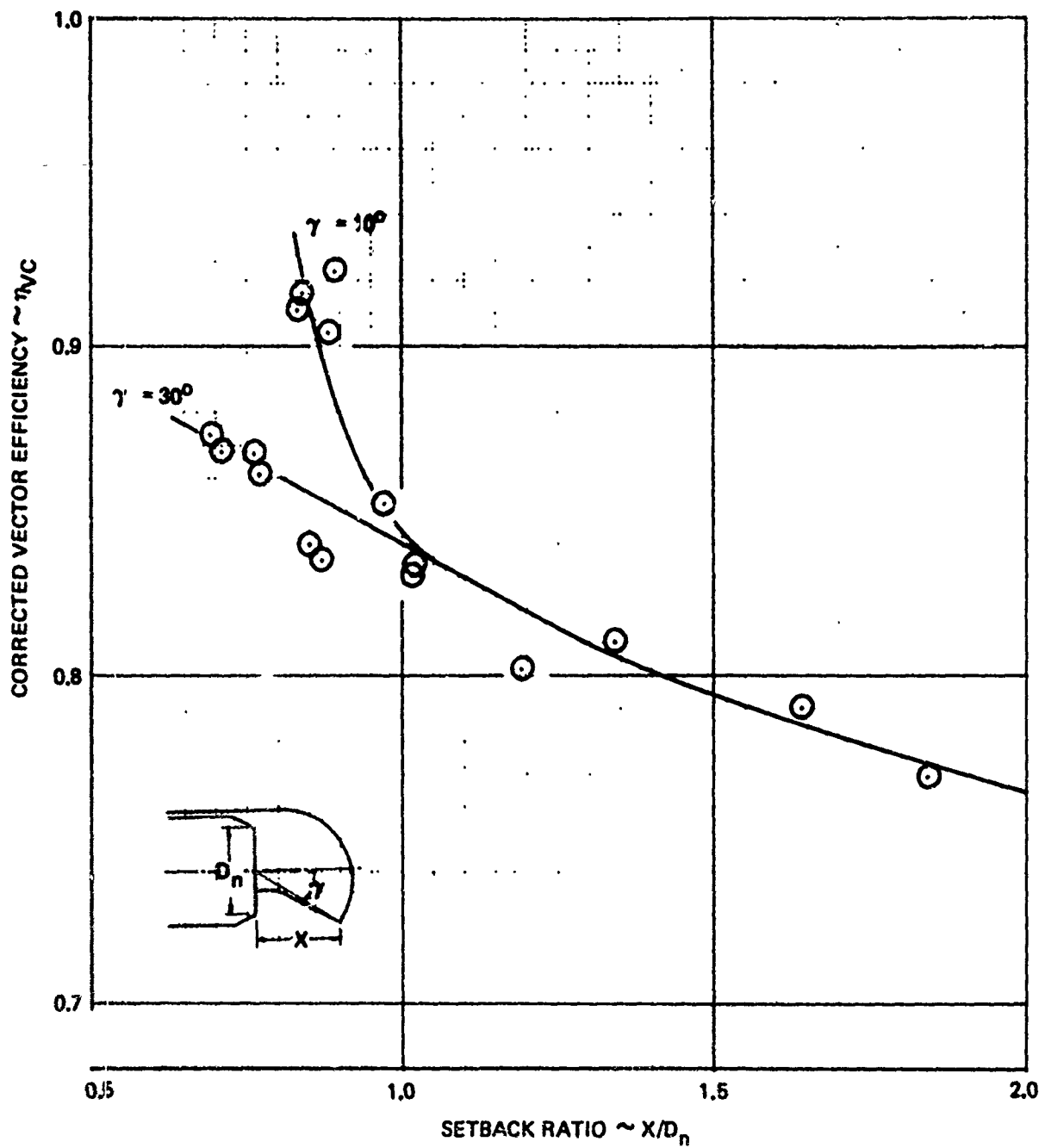


Figure 103: CORRECTED VECTOR EFFICIENCY CORRELATION
FOR HINGED EXTERNAL DEFLECTOR NOZZLES, $P_T/P_\infty = 1.6$

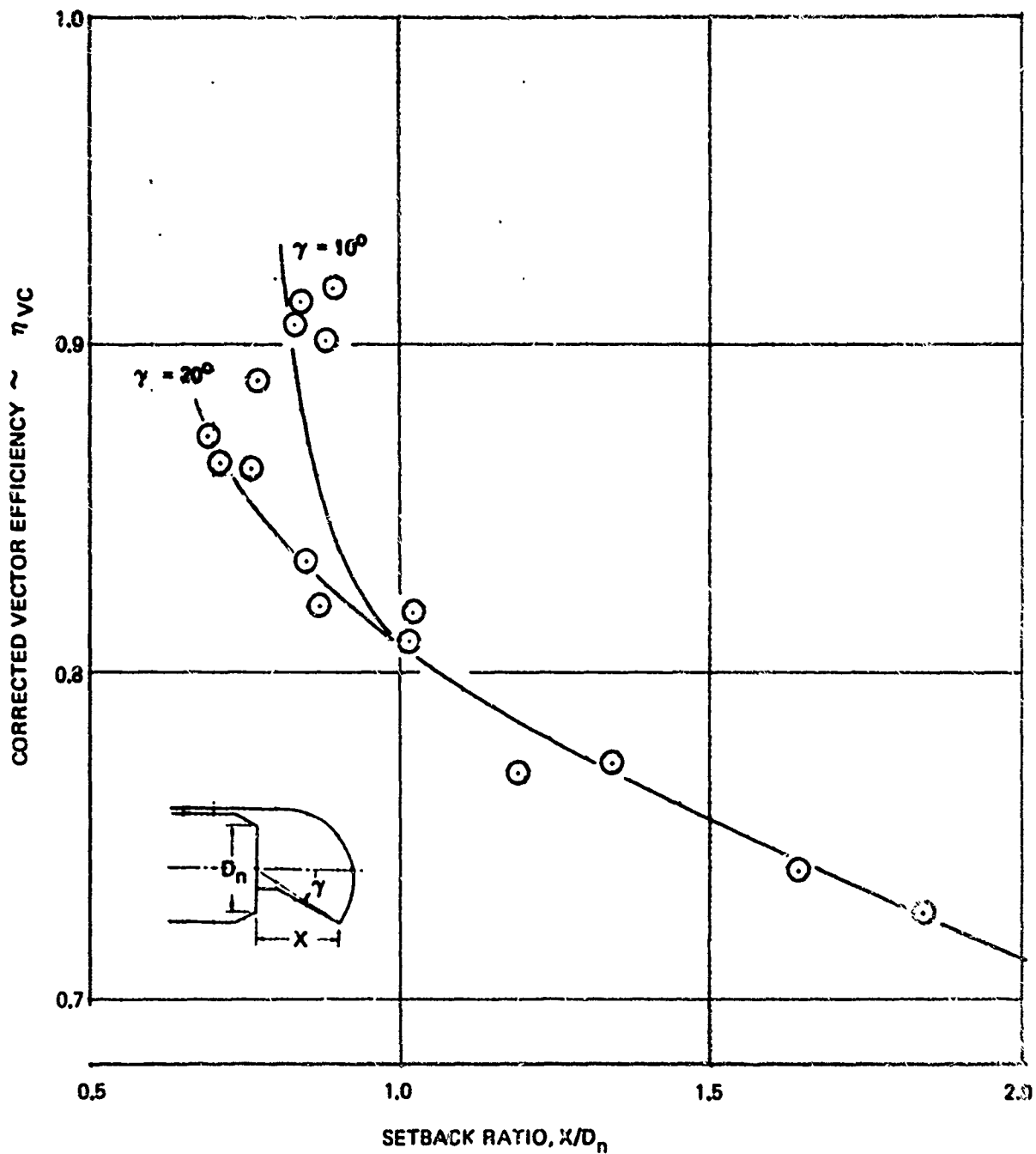
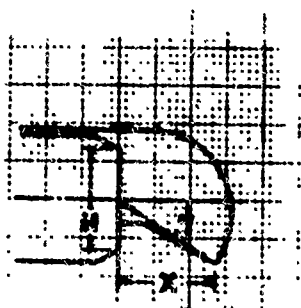
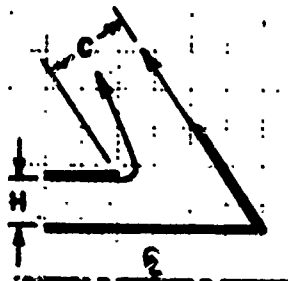


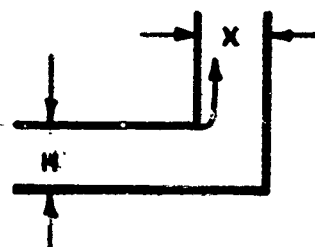
Figure 104: CORRECTED VECTOR EFFICIENCY CORRELATION FOR HINGED EXTERNAL DEFLECTOR NOZZLES, $P_T/P_\infty = 2.2$



DATA REF 11
"HINGED EXTERNAL
DEFLECTOR"



DATA VOL I
"ANNULAR TARGET
THRUST REVERSER"



THEORY, VOL I
"90° MITRE BEND"

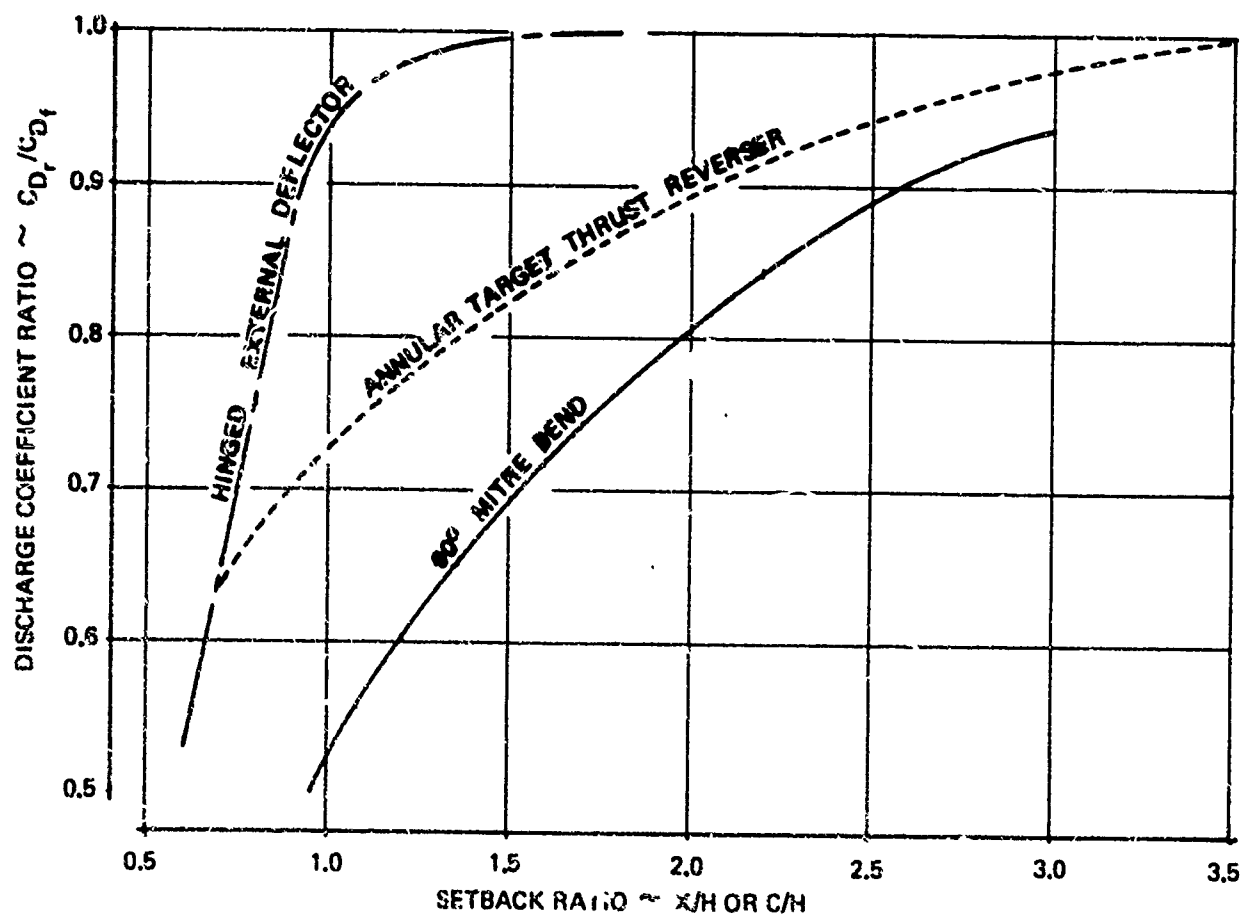


Figure 105: COMPARISON OF DISCHARGE COEFFICIENT RATIO
DATA CORRELATIONS

SECTION IV

CONCLUSIONS AND RECOMMENDATIONS

4.1 Part IB - Design

The design tasks conducted during this study have produced several thrust reverser and thrust vectoring concepts applicable to the high lift systems likely to be used on STOL tactical transport aircraft:

1. Externally blown flap (EBF)
2. Mechanical flap and vectored thrust (MF + VT)
3. Upper surface blowing (USB)

In addition, a detailed design for a fan cascade thrust reverser system that meets the requirements of airflow match, performance, and flow directional control to minimize exhaust flow reingestion and aerodynamic interference effects was completed. The various TR and TV concepts were evaluated on the basis of internal performance, weight, and aerodynamic stability and control characteristics to select test models for static performance tests conducted during Part IC. The primary conclusions to be drawn from the design study include the following:

1. The aircraft high lift system has a significant impact on the thrust reverser or thrust vectoring system. Each high lift system has unique propulsion system installation requirements that affect the thrust reverser or thrust vectoring system design.
2. To avoid the problems of reingestion and foreign object damage during the stopping ground roll, the reverser system must have the capability of controlling the direction of the exhaust flow. There are few regions in which the reverser exhaust can be directed:
 - a) Upward and forward above the nacelle forward of the wing leading edge
 - b) Outboard of outboard nacelle
 - c) Above the wing aft of leading edge
 - d) Aft of wing trailing edge

Of these four regions, the best solution consistent with a practical reverser design is to direct the flow upward and forward above the nacelle forward of the wing leading edge.

3. Thrust reverser systems for unmixed flow engines may or may not use a primary thrust spoiler depending on the engine bypass ratio. The following general guidelines were established:
 - a) Bypass ratio 3.0 unmixed flow engines require thrust reversers for both the fan and primary flows.
 - b) A mechanical spoiler may be used to spoil the primary thrust of bypass ratio 6.0 unmixed flow engines.
 - c) A mechanical spoiler is recommended to spoil the primary thrust of bypass 12.0 unmixed flow engines. The spoiler may be eliminated provided the fan reverser efficiency is at least 50%.
4. "Cycle spoiling" of the primary thrust could provide a simple and lightweight reverser system for a mixed flow engine, and appears to be an attractive installation when combined with a thrust vectoring system. However, the overall reverser effectiveness is dependent on the engine bypass ratio, and the controlling area of the primary flow during reverse operation. The over area condition of the primary flow determines the primary thrust spoiling effect. "Cycle" spoiling would require interstage bleed for fan-high-low compressor engine configurations because of loss in low pressure compressor surge margin.
5. Landing field length studies conducted during the program showed that the reverser delay time and the reverser cutoff velocity are the significant parameters that determine the landing roll distance. The field length studies also showed that an optimum reverser system for a STOL tactical transport would have a zero delay time, less than 20-knot cutoff speed, and reverser effectiveness greater than 35%.
6. Combining the thrust reverser system and thrust vectoring system for a mechanical flap + vectored thrust lift system is a difficult design task. The options available to the designer are either to 1) combine the functions of thrust reversing and thrust vectoring into a single mechanism or 2) separate the thrust reversing and vectoring functions and provide a complete design for each system. The first option is perhaps the most desirable because of potential weight savings and reduced support systems required, but is complicated by increased mechanical complexity, by the reverser exhaust directional control requirements, and by aerodynamic interference effects. For example, a combined thrust reverser/vectoring system must place the reverser exhaust forward of the wing leading edge to obtain the desired flow directional control. However, the requirements mean that the thrust vector is forward of the airplane center

gravity while directional control of the fan reverser exhaust can be achieved.

7. The following conclusions were made based on performance and weight evaluation results:

- a) The thrust reverser system for externally blown flap lift systems will probably involve the use of a fan cascade thrust reverser.
- b) Mechanical flap and vectored thrust lift systems could use either
 - a. rotating nozzles
 - b. multibearing vectoring nozzles
 - c. external deflector/target thrust vectoring/reversing systems

depending on the type of engine cycle (mixed or unmixed flow). The rotating nozzle vectoring system would be used for unmixed flow engines and would present airplane balancing problems due to the thrust vector location and a resulting adverse pitching moment. The external deflector/target TR/TV system would also pose balancing difficulties but to a lesser degree. Multibearing vectoring nozzle installations would present no airplane balancing problems.

- c) Upper surface blowing lift systems will utilize an external target thrust reverser system installed with a mixed flow engine.

8. Static performance tests and future wind tunnel investigations should include the following thrust reverser and thrust vectoring systems:

- a) fan cascade thrust reverser systems (EBF, MF + VT)
- b) external deflector/target TR/TV system (MF + VT)
- c) multibearing vectoring nozzle (MF + VT)
- d) external target thrust reverser (USB)

Recommendations related to thrust reverser and thrust vectoring system design include the following:

- 1. Future studies of TR and TV systems should include detailed design studies of the thrust reverser and thrust vectoring systems considered during Part IB. The design studies would be based on the results of the Part IB design results and would emphasize the system mechanical design requirements,

structural life requirements, and safety and reliability requirements.

2. Future design studies should include trade studies of:

a) TR/TV subsystems including

- 1) controls - manual vs. automatic pneumatic vs. hydraulic
- 2) interlocks - engine, flight controls, landing gear
- 3) failsafe - redundancy, interlocks

b) Noise suppression vs. no noise suppression.

4.2 Part IC - Model Test

The model static performance tests conducted during Part IC of the program have resulted in parametric test data for a fan cascade thrust reverser system and an external deflector/target combined thrust vectoring and reversing system. These data plus existing data for multibearing nozzles and an external target thrust reverser will be useful to define the performance characteristics of these TR/TV systems and provide guidance for future wind tunnel model and full-scale design criteria. The primary conclusions of the model tested conducted during Part IC include:

1. Reverser efficiency of at least 50% is possible for a fan cascade thrust reverser that exhausts all of the flow through the upper portion of the nacelle. The highest reverser performance was obtained when the duct blocker door angle was 135°.
2. Internal flow distortion can be expected when the fan reverser is located in the upper 180° segment of the nacelle that could effect the fan surge margin during reverser operation depending on the spacing between the fan exit and the reverser. The reverser should be located at least three times the fan exhaust duct height downstream of the fan exit.
3. Careful tailoring of the internal duct geometry adjacent to the fan cascade reverser would probably improve the reverser efficiency.
4. The external deflector/target TR/TV performance was very sensitive to small changes in nozzle pressure ratio setting, and deflector geometry.
5. The external deflector/target TR/TV system design must be revised to improve vectoring performance and to increase the effective vector angle. Also, the design must be revised

to improve the airflow match characteristics during reverse thrust mode. The impact of the design modifications on the total system design including weight, and mechanical complexity must be considered.

6. Optimum vectoring performance occurs when the controlling area is located at the deflector exit and the entrance Mach number of the flow entering the deflector is Mach .45.

Recommendations for future static performance and wind tunnel models include the following:

1. Future static performance tests of fan thrust reversers should provide a degree of simulation of the fan exhaust velocity profiles to assess the effect of the internal flow distortion on the fan performance.
2. Future test model geometry should reflect the results of the detailed design work recommended in Section 5.1.

REFERENCES

- 1 "Medium STOL Transport, A Feasibility Study for a Prototype Development Program," D162-10052-1, The Boeing Company, June 1971.
- 2 "Preliminary Performance Estimates of Commercial STOL Transport Turbofan Engines, STF 342 Series," TDM-2177, Pratt & Whitney Aircraft, April 1969.
- 3 "Preliminary Performance Estimates of STF 344 Turbofan Engine," TDM-2190, Pratt & Whitney Aircraft, October 1969.
- 4 Hatley, J. P., "A Simplified Method for Rapid Calculation of Off-Design Performance of Turbojet or Turbofan Engines at Subsonic Flight Conditions" (TEM-022), D6-5423, Part I, The Boeing Company, 1962.
- 5 Mount, J. S. and Lawson, D. W. R., "Developing, Qualifying, and Operating Business Jet Thrust Reversers", SAE Paper 690311, March 1969.
- 6 Cecil, D. J., "Program Usage Instructions for Computer Program TEM 36D, Landing Roll Study", AMEP-M-354A. The Boeing Company, April 1972.
- 7 Wood, S. K. and McCoy, J., "Design and Control of the 747 Exhaust Reverser Systems", SAE Paper 690409, April 1969.
- 8 Petit, J. E., "STOL Transport Thrust Reverser/Vectoring Program Supplemental Test Report," D180-14801-1, The Boeing Company, 1972.
- 9 AMST Technical Data - Propulsion, D162-10069-4, Vol. 2, The Boeing Company, May 1972.
- 10 Petit, J. E., "STOL Transport Thrust Reverser/Vectoring Program, Part 1C Test Plan," D180-14970-1, The Boeing Company, April 1972.

REFERENCES

- 11 Petit, J. E., "STOL Transport Thrust Reverser/Vectoring Program, Part IC Test Report," D180-15194-1, The Boeing Company, October 1972.
- 12 Hiatt, D. L., The Analytical Velocity Coefficient Calculation of an Annular Nozzle, and The Effect of Reynolds Number on Velocity Coefficient, D6-20355TN, The Boeing Company, November 1967.
- 13 Wear, D. E., Reynolds Number Effects on Nozzle Performance, General Electric Coordination Memo No. B-70-11, August 1970.
- 14 Stratford, B. S., The Calculation of the Discharge Coefficient of a Choked Nozzle and the Optimum Profile for Absolute Airflow Measurement, Journal of the Royal Aeronautical Society, Vol. 68, April 1964.
- 15 Neal, B., Comparison of Model and Full Scale Test Data Obtained During the Development of a Target Thrust Reverser for the 737 Airplane, The Boeing Company Coordination Sheet No. 737-PPU-928, February 1968.
- 16 Preliminary Study Data Thrust Vectoring and Thrust Reverser System, General Electric Report R70AEG336, August 1970.
- 17 Poland, D. T., The Aerodynamics of Thrust Reverser for High Bypass Turbofan, AIAA Paper 67-418, July 1967.
- 18 Kohl, R. C., Performance and Operational Studies of a Full Scale Jet Engine Thrust Reverser, NACA TN 3665, April 1956.
- 19 Kohl, R. C. and Algranti, J. S., Investigation of a Full Scale, Cascade Type Thrust Reverser, NACA TN 3975, April 1957.
- 20 Hawk, G. W., Summary of the Development of Mechanical Type Thrust Reversers, WADC Technical Report 57-17, May 1957.
- 21 McDermott, J. F. Jr., Summary of the Development of Aerodynamic Type Thrust Reversers, WADC Technical Report 57-18, May 1957.

- 22 Pickered, J. C., Selection and Design of Thrust
Reversers for Jet Aircraft, IAS Paper No. 60-77,
June 1960.
- 23 Carlson, N. G., Development of Flight Weight Deflection
Device and Actuation System for the TR30-P-8 Engine,
Final Report, Pratt & Whitney Aircraft Report PWA-3266,
December 1967.
- 24 Schloemer, J., Test Results of Reynolds Number Effects
on Plug Nozzle Performance Coefficients, General
Electric Technical Brief, 70016.